

Sodium chloride damage to porous building materials

PROEFSCHRIFT

ter verkrijging van de graad van doctor
aan de Technische Universiteit Delft,
op gezag van de Rector Magnificus prof. dr. ir. J.T. Fokkema,
voorzitter van het College voor Promoties,
in het openbaar te verdedigen
op vrijdag 10 maart 2006 om 10.30 uur

door

Barbara Antonietta LUBELLI

Dottore in Architettura, Politecnico di Milano

geboren te Milaan, Italië

Dit proefschrift is goedgekeurd door de promotoren:

Prof. ir. R.P.J. van Hees

en

Prof. dr. ir. K. van Breugel

Toegevoegd promotor: Dr. ir. C.J.W.P. Groot

Samenstelling promotiecommissie:

Rector Magnificus, voorzitter

Prof. ir. R.P.J. van Hees, Technische Universiteit Delft, promotor

Prof. dr. ir. K. van Breugel, Technische Universiteit Delft, promotor

Dr. ir. C.J.W.P. Groot, Technische Universiteit Delft, toegevoegd promotor

Prof. L. Binda, M.Sc., Polytechnic Milaan, Italië

Prof. dr. C. Price, M.A., University College London

Prof. dr. ir. K. Kopinga, Technische Universiteit Eindhoven

Prof. dr. ir. J.M.J. Coenen, Technische Universiteit Delft

Prof. dr. ir. J.G. Rots, Technische Universiteit Delft

ISBN 90-9020343-5

Cover design: Bert Mathlener, TNO Bouw, Delft

Cover picture: Caterina Lubelli

Printed by: Print Partners Ipskamp, Enschede

The work described in this thesis has been partially carried out within the EU projects:

Contract no. EVK4-CT-2000-00023, ASSET (Assessment of suitable products for the conservative treatment of sea-salt decay) and Contract no. EVK4-CT-2001-0047-DGXII, COMPASS (Compatibility of plasters and renders with salt loaded substrates in historic buildings) and was sponsored by TNO Building and Construction Research

Table of contents

1. Introduction	1
1.1 Definition and relevance of the problem	1
1.2 Objectives of the research	2
1.3 Outline of this thesis	3
2. Damage due to sodium chloride: a literature overview	5
2.1 Introduction	5
2.2 Behaviour of the salt-water system	5
2.2.1 Dissolution	6
2.2.2 Crystallization	7
2.2.3 Hydration state change	9
2.2.4 Deliquescence	9
2.3 Salt solution transport	9
2.3.1 Moisture transport	9
2.3.2 Salt transport	12
2.4 Damage mechanisms	13
2.4.1 Crystallization pressure	13
2.4.2 Other mechanisms	17
2.4.3 Combined damage processes	20
2.5 Location of salt in pores	21
2.6 Crystal habits	22
2.7 Discussion and conclusions	23
3. Sodium chloride damage in practice: results of case studies	25
3.1 Introduction	25
3.2 Effect of material properties on salt damage	26
3.3 Sodium chloride sources	33
3.4 Sources of moisture for salt damage	35
3.5 Effect of environmental conditions on salt damage	37
3.6 Evaluation of risk factors for salt damage	38

3.7	Inputs to the development of an effective weathering test	41
3.8	Discussion and conclusions	42
4.	Effect of RH changes on NaCl damage: monitoring of a case study	45
4.1	Introduction	45
4.2	Notes on the history of the building and of the renovations	45
4.3	Description of the damage	46
4.4	Sampling	47
4.5	Laboratory investigation	49
4.5.1	Determination of moisture load and sources	49
4.5.2	Determination of salt type and distribution	49
4.5.3	Assessment of material properties	51
4.6	Monitoring of the damage and of the environmental conditions	56
4.7	Discussion and conclusions	61
5.	Towards an effective weathering test: effect of environmental conditions on damage	63
5.1	Introduction	63
5.2	Literature overview on salt weathering tests	64
5.3	Materials	66
5.3.1	Composition and preparation	66
5.3.2	Physical properties	68
5.4	Effect of accelerated drying on sodium chloride damage	72
5.4.1	Test procedure	72
5.4.2	Results	74
5.4.2.1	Effect of the environmental conditions on the drying behaviour	74
5.4.2.2	Effect of the environmental conditions on the salt distribution	76
5.4.2.3	Effect of the environmental conditions on the damage	77
5.4.2.4	Location of salt in pores	81
5.4.2.5	ESEM investigations	83
5.4.3	Inputs to the development of an accelerated test	85
5.5	Effect of RH cycles on sodium chloride damage	86
5.5.1	Test procedure	86
5.5.2	Results	87
5.5.2.1	Effect of RH cycles on the damage	87
5.5.2.2	ESEM investigations	90
5.5.3	Inputs to the development of an accelerated test	95
5.6	Accelerated weathering test	96
5.6.1	Test procedure	96
5.6.2	Results	97
5.6.2.1	Effect of the temperature and RH cycles on the damage	97
5.6.2.2	ESEM investigations	99

5.6.3 Assessment of the test procedure	100
5.6.3.1 Rate of development of the damage	101
5.6.3.2 Degree of realism	103
5.6.3.3 Factors limiting the effectiveness of the test	104
5.7 Discussion and conclusions	105
6. Dilation due to NaCl crystallization: a hypothesis on the damage mechanism	107
6.1 Introduction	107
6.2 Materials and methods	108
6.3 Results	110
6.3.1 Hygric behaviour of NaCl contaminated specimen	110
6.3.2 Hygric behaviour of NaCl contaminated specimen	111
6.3.3 Effect of absorption of NaCl solution on dilation	114
6.3.4 Hygric behaviour of NaNO ₃ and KCl contaminated specimens	115
6.3.5 Effect of pH on the dilation behaviour	117
6.3.6 Hygric behaviour of NaCl contaminated specimens in the presence of a crystallization inhibitor	117
6.3.7 Hygric behaviour of Na ₂ SO ₄ contaminated specimen	119
6.3.8 Hygric behaviour of blank and NaCl contaminated specimens at 40 °C	120
6.4 ESEM investigations	122
6.5 Discussion and conclusions	126
7. Conclusions	129
7.1 Results of the research	129
7.2 Practical application of the results	131
7.3 Outlook	132
References	135
Appendix 1: Properties of NaCl solution	145
Appendix 2: List of case studies	149
Appendix 3: Method for the assessment of moisture and salt distribution	155
Summary	159
Samenvatting	161
Acknowledgments	165
Curriculum vitae	167

Chapter 1

Introduction

1.1 Definition and relevance of the problem

Weathering of materials due to the presence of salts has been known since the antiquity. Herodotus refers to the phenomenon occurring in the Nile valley: “*salt exudes from the soil to such an extent it damages even the pyramids*”¹. However, it is only in the 19th century that salt weathering becomes the subject of serious studies and investigations. Starting from the second half of the 20th century the interest in salt damage has increased and a series of hypotheses and models on the possible damage mechanism have been formulated.

The interest in the phenomenon has been probably stimulated by the spread of the salt damage hazard on a large scale during the last decades. The rise of the ground-water table (due e.g. irrigation and vegetation clearance), the increase in the salinity of ground water (caused e.g. by incursion of seawater), and the introduction of new sources of salts (originating e.g. by the use of de-icing salt and atmospheric pollution) are the main causes of the enhanced risk of salt damage.

Among the salts commonly found in buildings, sodium chloride (NaCl) is one of the most abundant and ubiquitous. It can be present in weathered rocks and construction materials in a wide range of environments: from hot [Cha 80] and cold [Pre67] arid regions to humid coastal areas. Sodium chloride found in buildings may be originally present in the materials (like mortars prepared using not-washed sand from the sea) or may have penetrated later in the walls from external sources (like rising of ground water, sea-salt spray, sea-flooding etc). Nowadays in European countries the use of materials containing NaCl is not common and more often NaCl reaches the buildings after their construction. In the Netherlands, partially located beneath the sea level, sea-flooding has often constituted an important source of salts, enriching both the ground and the walls of buildings located in the flooding area with a huge amount of NaCl. Besides, the presence of sea-salt spray in the coastal areas and the use of de-

¹ Erodoto, Le Istorie, Vol.1, Edizioni Scientifiche Italiane, Napoli (1947)

icing salts (sodium and calcium chloride) contribute to NaCl being one of the most common salts in buildings.

Ancient monuments are, more often than new constructions, threatened by salt decay because of the large amount of salt accumulated in the course of time, the frequent lack of maintenance and, sometimes, the occurrence of calamities in the past. Limiting the salt decay is therefore necessary in order to preserve our architectural heritage. A better understanding of the salt damage mechanism would not only help to prevent the decay of the existing buildings but also to develop more durable materials and to design adequate combinations of materials.

In spite of the fact that several theories on salt damage have been developed, no unanimous opinion exists on the mechanism causing the decay [Gou97, Cha00a, Dut03]. The experimental verification of the theories has been mainly delayed by the difficulty of measuring some of the variables included in the models. At the moment it is still difficult to forecast the susceptibility of materials to salt decay on the mere basis of their properties. Moreover, a building is usually made up of several materials (e.g brick/mortar/plaster), each having different properties. The interaction between the materials is crucial when determining the risk of salt damage. Because of the above-mentioned reasons, accelerated crystallization tests are still, in most of the cases, the best way to assess the susceptibility of materials (and combinations of materials) to salt decay.

1.2 Objectives of the research

The research described in this thesis has two main aims, strictly related to each other: i) to gain a better understanding of the mechanism of damage occurring in traditional building materials in the presence of sodium chloride and ii) to develop an effective crystallization test. These objectives are pursued by combining in-situ observations with laboratory experiments.

The interest for the investigation of the damage mechanism due to sodium chloride crystallization originates from the fact that this matter is particularly controversial. Crystallization pressure as described in [Sch99] may explain damage only in pores in the nanometer range [Fla02, Rij04], sizes usually absent in most of the traditional building materials. New theories have been recently proposed, mentioning the possibility that a non equilibrium situation, for example produced by fast evaporation or by wet-dry cycles, may result in high transient crystallization pressure even in larger pores [Sch04, Ste05]. Next to the most accepted models, supposing crystallization pressure generated by salt filling the pores, a completely different hypothesis on salt damage exists, proposed by Puhlinger already 20 years ago [Puh83]: this suggests that damage is generated by modifications in the structure of the salt adhering to the material due to the changes in local and ambient environmental conditions.

The difficulty of NaCl in reaching high supersaturation, together with the absence of hydration at temperatures higher than 0.1 °C [Wil81] and the very limited influence of temperature on this salt solubility and RH of equilibrium, have been usually referred to for explaining the little harmfulness of NaCl in laboratory tests. Nevertheless, sodium chloride is known to cause

severe damage in practice and therefore, as Goudie and Viles state [Gou97], “further experimental simulations need to be developed to address this issue”. From this consideration arises the second objective of this research, i.e. the definition of an effective test, able to reproduce, in laboratory and in a short time, the decay observed in practice in NaCl contaminated building materials.

1.3 Outline of this thesis

This thesis starts with a short introduction into the behaviour of salt-water systems and salt solution transport in porous materials. Then the mechanisms most often addressed as causes of the damage are critically discussed with respect to the decay due to sodium chloride (chapter 2). The literature review identifies the still unsolved questions, points out the limits of the most diffused theories and indicates the hypotheses that need to be further studied: it constitutes therefore the starting point of the research developed in this work.

From the literature review, the necessity of verifying the theories in practice emerges. For this reason, an approach starting from the study of the salt decay in the field is adopted in this research.

The investigation of several case-studies (chapter 3) points out the parameters influencing the type and the severity of the decay due to NaCl and evaluates their relative importance. This leads to the identification of the factors of risk for the occurrence of the decay in different circumstances, and sets therefore the basis for a correct intervention.

The relevance of the environmental conditions, and in particular of the RH changes, for the development of damage due to NaCl is demonstrated. A case study is presented in which the combined monitoring of the damage (quantified as debris falling from a wall) and of the environmental conditions (temperature and RH) allows explaining the damage process (chapter 4).

The results obtained from the in-situ investigation give indications on the parameters to be adopted in the laboratory crystallization test and on their realistic range of variation. Chapter 5 deals with the development of an accelerated crystallization test for sodium chloride. At first the effects of the environmental conditions (high temperature, low RH, air flow and cycles of temperature and RH) on the damage are investigated. The obtained results are then applied in the set up of an accelerated crystallization test. The new developed procedure is tested on three materials and its reliability and degree of acceleration are evaluated with respect to both existing weathering tests and practice situations.

In chapter 6 the damage mechanism due to NaCl crystallization is investigated. The effects of the presence of NaCl on the hygric and hydric behaviour and on the related dilation of a lime-cement mortar are studied in detail. The hypothesis that damage may develop from the differential dilation of salt contaminated and not contaminated areas of a material is considered. Systematic experiments are performed in order to definitively assert the relevance

of this mechanism for the occurrence of the damage. The behaviour of specimens contaminated with different salts (NaCl, NaNO₃, KCl and Na₂SO₄) is investigated to define whether this phenomenon is restricted to NaCl or common to more salts. On the basis of the results of the dilation experiments and the outcomes of the ESEM observations on cross sections of the specimens, a new hypothesis on the damage mechanism is proposed.

Chapter 2

Damage due to sodium chloride: a literature overview

2.1 Introduction

Porous building materials are known to be susceptible to damage when contaminated with salts. Salts may enter and be transported within the porous materials only if dissolved in water. Knowledge of the phase changes in the salt-water system is, therefore, of primary importance. In section 2.2 the phase changes (dissolution, crystallization, hydration and deliquescence) of salt-water systems are described, with particular attention to the behaviour of NaCl solution. Once dissolved, the salts may move into the pore network of the material because of gradients in moisture and ions concentration. Salt creeping in the pore network, as postulated by Puhlinger [Puh83], is also considered as a possible mechanism of salt transport. Moisture and salt transport are shortly described in section 2.3.

Notwithstanding the fact that all sources agree on the salt weathering hazard, there is not yet an unanimously accepted hypothesis on the mechanism(s) responsible for the decay of salt contaminated materials [Cha00a]. In the particular case of sodium chloride, the question on the damage mechanism is even more controversial. In section 2.4 the mechanisms most often addressed as causes of the damage are critically discussed with respect to the decay due to sodium chloride.

2.2 Behaviour of salt-water system

The phase transitions undergone by salts in ambient conditions (crystallization, deliquescence, dissolution and alteration of hydration state) normally comprise two components: the salt and water. Transition phases of salt alone, such as sublimation or melting, does not commonly occur. The thermodynamics of a phase transition are concerned with the energy difference between the initial and final phases. For a spontaneous (without the input of energy) phase transition to occur, the resultant phase must be the one having the lowest free energy. The effect of pressure and temperature on the system has to be considered too, since they influence

the free energy, and thus the spontaneity of the phase transition. Since atmospheric pressure is usually constant, it is mainly the temperature that influences the phase transition.

2.2.1 Dissolution

When an ionic solid dissolves in water, bonds within the crystal lattice are broken and formed between the liberated ions and water molecules. For most salts the solubility increases with increasing temperature. By contrast the solubility of sodium chloride is almost independent of temperature (figure 2.1).

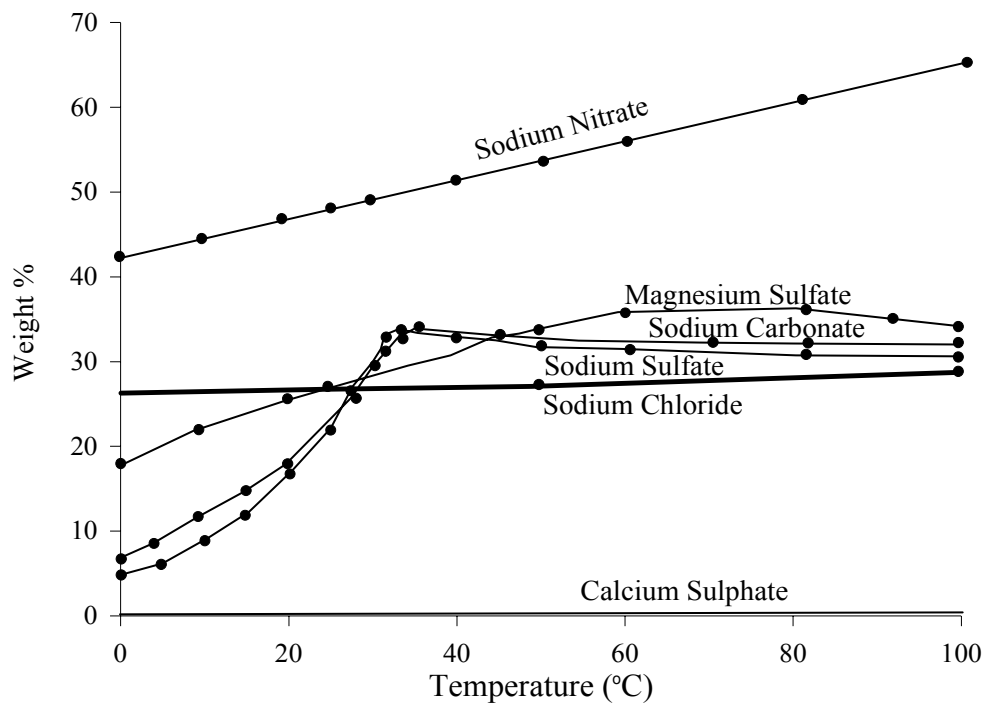


Figure 2.1 Solubility of different salts in relation to solution temperature [Gou97]

The solubility of the salt depends on the change in free energy of the solution. The free energy G of a solution can be written as:

$$G = G_0 + RT \ln a \quad (2.1)$$

where:

G_0 [J/mol] = free energy of pure water

R [J/mol K] = gas constant

T [K] = absolute temperature

a [-] = activity of dissolved salt

The activity depends on concentration and temperature. For dilute solution it can be calculated (Debye-Hückels law [Atk78]). For concentrated solutions it is only to be found empirically.

However, at equilibrium, the activity of the solution equals the activity of the water vapour in the ambient air. The water vapour activity is by definition equal to the relative humidity (RH). The relation between RH and the molality of a salt solution is given by the Robinson-Stokes equation [Lar99]:

$$\ln \varphi = -n \phi M_w m \quad (2.2)$$

where:

φ [-] = RH

n [-] = number of ions in the salt

ϕ [l/kg] = osmotic coefficient

M_w [kg/mol] = mole weight of water

m [mol/l] = molality of the solution

The osmotic coefficient expresses the deviation of the electrolyte solution from ideality and has to be found empirically. Knowing the osmotic coefficient, Eq (2.2) gives a functional relationship between the molality of a solution and the RH of the ambient air. The water vapour activities and the osmotic coefficients for sodium chloride at different molality at 25 °C are reported in Appendix 1 [Rob&Sto59].

A saturated salt solution is in equilibrium with a certain RH of the air: this value of RH is called RH of equilibrium (RH_{equ}) and is different for each salt. For $RH_{air} > RH_{equ}$ the solution will become more and more diluted; for $RH_{air} < RH_{equ}$ the water will evaporate and the salt will start crystallizing.

The RH_{equ} of a salt solution is dependent on the temperature, if also the solubility of that salt is. Therefore, in case of NaCl, since the solubility is not strongly dependent on temperature, also the RH_{equ} remains about the same in a large temperature range (Table 2.1). A saturated solution of NaCl at 20 °C is in equilibrium with a RH of 75.5%.

Solubility is not only dependent on temperature, but also on pressure. According to Riecke's principle [Rie94], a crystal under linear pressure has a higher solubility than an unpressed crystal. The measured solubility of NaCl solution under pressure is reported in Appendix 1 [Kau71]. Most of the theories on crystallization pressure are developed starting from the Riecke principle.

Table 2.1 RH_{equ} of NaCl at different temperatures [Arn90]

T (°C)	0°C	5°C	10°C	15°C	20°C	25°C	30°C
RH_{equ} (%)	75.5	75.7	75.7	75.6	75.5	75.3	75.1

2.2.2 Crystallization

When the ambient RH is lower than the RH_{equ} of a saline solution, water evaporates and the salt concentration rises, ultimately leading to saturation and crystallization. The process of

crystallization within a solution occurs by a step growth mechanism. The solute breaks its bonds with the solvent and forms new bonds with the growing crystal [Cab58].

Saline solution reaching saturation will normally start crystallizing. Crystallization starts with the formation of stable nuclei. At concentrations around saturation, nuclei can fall apart easily again. Higher level of supersaturation increases the possibility of formation of stable nuclei, thus the crystallization process starts. Crystallization is thermodynamically possible only if the solution is supersaturated, but it is very slow when the solution does not exceed the critical supersaturation concentration. In this meta-stable region, although crystallization is slow, it can occur in the presence of an external or foreign nucleus (this phenomenon is called heterogeneous nucleation, the foreign nuclei serving as catalysts in the crystallization process).

In general, crystallization can occur (figure 2.2) either if the temperature of the solution decreases without changes in the solution concentration (line A-B), if water evaporates leading to an increase in the solution concentration (line A-C) or if a combination of these two situations occurs (line A-D). In case of sodium chloride, since the solubility is not strongly depending on temperature, crystallization mainly occurs because of evaporation of the solvent (line A-C) until a sufficient supersaturation is reached.

The degree of supersaturation at which finally crystallization occurs affects the growth rate of the crystal. Higher supersaturations result in faster growth rate of the crystal. The growth rate determines the morphology of the crystals [Sun81]: crystals with equilibrium shapes (cubic for NaCl) grow at low supersaturation, whereas dendritic crystals are observed precipitating from highly supersaturated solution [Rod02].

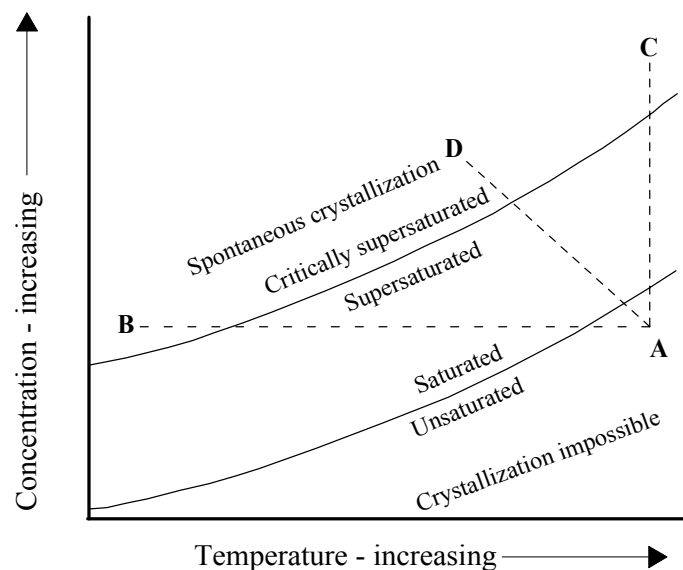


Figure 2.2 Temperature – solute concentration plot [Win94]

2.2.3 Hydration state changes

Several salts can exist, depending on temperature and RH conditions, in different hydration states, i.e. with a different number of water molecules combined with the salt. Hydration state changes are alterations of the number of these water molecules.

NaCl hydrates only at temperatures lower than 0.1 °C to form NaCl · 2H₂O [Wil81]; above this temperature only the anhydrous form exists: NaCl. For this reason in the present work hydration state change is not relevant.

2.2.4 Deliquescence

This term refers to the interaction between the crystal surface of a salt in its highest hydrated state, and molecules of water vapour. Because of the hygroscopicity of the salt, water is absorbed by the crystal and forms hydrogen bonds with the salt ions. When the amount of absorbed water will be sufficient, the crystal will dissolve to form a saturated solution. Deliquescence occurs when the ambient RH is higher than the RH_{equ} of the salt. Alternatively, if the ambient RH is lower than the RH_{equ}, evaporation will occur and the salt may crystallize. In materials having pores in the nanometer range, deliquescence of salt can start at a RH lower than the RH_{equ}, due to the combined effect of hygroscopicity of the salt and fine porosity of the material causing capillary condensation [Rij04].

2.3 Salt solution transport

Salt can enter and move through porous materials only when dissolved in water. Therefore, understanding the movement of moisture in material is of primary importance. In the following sections a short overview of moisture and salt movement in porous material is given.

2.3.1 Moisture transport

Water can enter a porous material either as liquid or vapour. In the liquid state water can enter a material by capillarity and/or infiltration.

Capillarity, which is the mechanism governing rising damp in a wall, is a consequence of surface tension. Because of the attraction between the liquid and the capillary walls, the liquid rises in a capillary and a meniscus is formed. This curvature implies that the pressure just beneath the meniscus is less than the atmospheric pressure by approximately $2 \gamma \cos \theta / r$, where γ is the surface tension of the water, θ the contact angle between the edge of the meniscus and the pore wall, r the radius of the capillary (we assume a meniscus with a hemispherical surface).

This pressure difference presses the liquid up in the capillary until hydrostatic equilibrium (equal pressure at equal depths) is reached. Since the pressure p exerted by a column of water of mass density ρ_w and height h is given by:

$$p = \rho_w g h \tag{2.3}$$

where:

ρ_w [kg/m³] = density of water

g [m/s²] = gravity acceleration

The height of capillary rise at equilibrium can be calculated equating $2 \gamma \cos \theta / r$ and $\rho_w g h$, which gives:

$$h = (2 \gamma / r \rho_w g) \cos \theta \quad (2.4)$$

where:

γ [N/m] = surface tension

r [m] = radius of the pore

θ [°] = contact angle between the liquid and the pore wall

The contact angle θ is determined by the balance of the forces at the contact between liquid and pore wall (figure 2.3). If the pore wall - air, pore wall - water and water - air surface tensions are denoted γ_{sg} , γ_{sl} , and γ_{g} respectively, than the vertical forces are in balance if:

$$\gamma_{sg} = \gamma_{sl} + \gamma_{g} \cos \theta \quad (2.5)$$

This expression solves to:

$$\cos \theta = (\gamma_{sg} - \gamma_{sl}) / \gamma_{g} \quad (2.6)$$

In most porous materials the contact angle is 0° for pure water, therefore the term $\cos \theta$ is equal to 1.

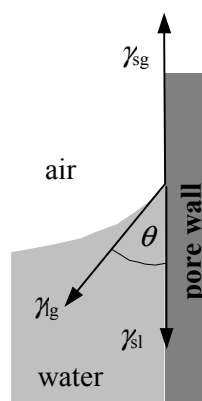


Figure 2.3 The balance of forces resulting in a contact angle θ

The calculated height is valid only in theory, since in reality the maximum height is limited by irregularity present in the pore section. Besides, in case of very small pores, absorption is

extremely slow. Laboratory tests shows that capillaries smaller than 0.1 μm are practically ineffective in absorbing water [Win94].

Liquid water can enter a material also by infiltration. Penetration of rain-water in a material when it is flowing over its surface depends upon climatic factors, in addition to the nature of the material. Penetration into capillaries and pores is only possible when the cavity surface is covered with a layer of water, as it usually occurs in humid climate [Cam98].

In the vapour state water can enter a material through molecular adsorption and capillary condensation.

Molecular adsorption is a mechanism by which the water molecules of the air are adsorbed by the material. Because of the adhesion forces between the porous material and water, molecules of water adhere to the pore walls, forming a layer that at low RH is monomolecular and becomes multi-molecular at higher RH. Molecular adsorption depends on the nature of the material and is predominant in pores smaller than 2 nm having a relatively high specific pore surface area. Besides, this mechanism has importance at low RH, since, as the RH rises, the water film becomes thicker and capillary condensation starts taking place in narrow pores. The two mechanisms overlap each other but, at high RH, the capillary condensation becomes dominant.

Capillary condensation occurs in the material, in pores of size smaller than 0.1 μm , at high RH. This mechanism is explained by the dependence of the saturation water vapour pressure on the curvature of the meniscus. The saturation pressure in equilibrium with a concave or convex meniscus was calculated by Thomson, Lord Kelvin [Tam80]:

$$p' = p'' \exp \left(\frac{-2\gamma}{r \rho R T} \right) \quad (2.7)$$

where:

p' [Pa] = maximum vapour pressure

p'' [Pa] = maximum vapour pressure over a meniscus of a capillary pore

r [m] = radius of the meniscus

R [J/(kg K)] = constant of gas

T [K] = absolute temperature

γ [J/m²] = surface tension

ρ [Kg/m³] = density of water

Water vapour can condense also on the outer surface of a material. Surface condensation occurs when the temperature drops below the dew point. Dew point is defined as the temperature to which moist air must be cooled at constant pressure and constant water vapour pressure in order to make saturation occur. This can easily happen, in Mediterranean countries, at the beginning of the spring when air becomes warmer and rich in moisture, on thick walls with high heat capacity and large thermal inertia whose temperature keeps a memory of the past cold season [Cam98].

Once water has entered a porous material it will move inside it either in liquid form or in the form of water vapour, depending on the moisture content in the material. During the period in which the water filled capillaries are interconnected, liquid water will move by capillarity, under the influence of gradient in moisture content and/or in temperature. When the moisture content decreases, at a certain point, the capillaries filled with water will not be interconnected anymore. From that moment on moisture transport will mainly occur through water vapour diffusion. The moisture content corresponding to this moment is called critical moisture content. Therefore two phases can be distinguished in the drying of an initially saturated porous material: in the first phase, when the moisture content is high and the surface of the material is wet, moisture transport to the surface is occurring by liquid flow; later, when the moisture content decreases and becomes less than the critical moisture content, the drying front enters the material and drying occurs mainly by vapour diffusion. Since liquid flow is a much more effective mechanism of moisture transport than vapour diffusion, the drying speed abruptly decreases for moisture contents lower than the critical moisture content.

The different mechanisms of moisture transport effective at the different pore sizes are summarized in figure 2.4.

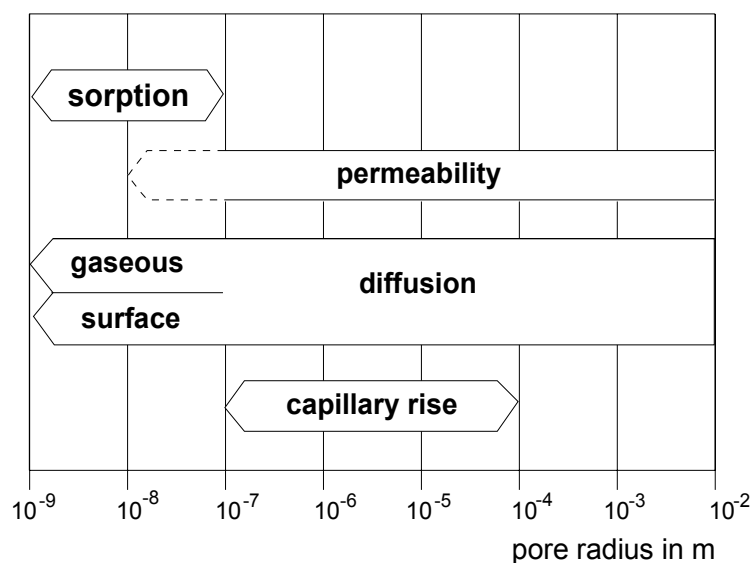


Figure 2.4 Size ranges of relevance for different transport phenomena [Men92]

2.3.2 Salt transport

Salt can move in porous material only when dissolved in water. Once in solution, the ions can be transported through the porous network by liquid flow or ion diffusion.

In case of liquid flow, salt ions are transported in solution within the porous network because of gradients in moisture content and temperature, as described in subsection 2.3.1. The salt may crystallize whenever the concentration of the solution exceeds the solubility of the salt.

Salt solution transport is usually modelled as pure water transport, in spite of the fact that the salt may affect the properties of both the water and the material. In fact surface tension, density and viscosity of a solution increase [Kau71] [Appendix 1] with increasing salt concentration with the result that the rate of capillary flow decreases as the salt concentration increases. Besides, some salts, as for example NaCl, can affect the presence of a receding drying front: it has been shown [Pel04] that materials having a receding drying front when drying after saturation with water, may not show any drying front when saturated with sodium chloride. The authors have explained this behaviour by the wetting properties of NaCl, retaining a solution film on the surface of the crystal, and this has obviously important consequences for the moisture and salt transport in the material.

Ion diffusion occurs only at high moisture content, when ions can move freely in the water filled porous system. Diffusion is driven by a gradient in the ion concentration, as it happens for example in case of chloride migration into concrete constructions submerged in seawater [Tah 98]. Diffusion coefficients for different salts have been calculated and are used to model ion diffusion [Kau71].

The transport of ions during drying of initially saturated porous material depends therefore on these two mechanisms: liquid flow that transports the ions towards the evaporation surface (advection) accumulating them, and ion diffusion that levels off any accumulation. The distribution of salt at the end of the drying process will depend on the competition between advection and diffusion [Pel02].

Another mechanism of salt transport is creeping. Creeping can be observed e.g. in salts crystallizing on glass walls above the surface of a solution and it has been postulated by Puhlinger [Puh83] as a model for the salt movement within a porous structure. Salt crystallizes at the edge of the film of solution and forms a micro-porous structure; this enhances capillary flow towards the edge of the film, making the crystallizing front advance. As Puhlinger [Puh83] states, it is “the salt which transports the liquid”. Because of the continuous changes occurring in the porous salt structure, no model can describe this transport mechanism.

2.4 Damage mechanism

In spite of the fact that the presence of salts in building materials is recognized as a cause of damage, no unanimous opinion exists on the mechanism causing the decay. Several theories have been formulated, without the existence of a unique mechanism leading to damage being objectively demonstrated. A critical analysis of the existing theories and their applicability in the particular case of sodium chloride damage is reported in the following sections.

2.4.1 Crystallization pressure

The most diffused and accepted theory considers the pressure exerted by crystallization of salt responsible for the damage. The salt is supposed to fill the pores of the material and to generate pressure on the pore walls. These stresses are considered sufficient to exceed the tensile strength (usually very low) of the material and to damage it.

One of the first studies to explain crystallization pressure starting from thermodynamic considerations is the work by Thomson [Tho62]: he states what is usually referred to as the Riecke principle: “under linear pressure a crystal has a higher solubility than an unstressed crystal” [Rie94]. This means that in aqueous solution a crystal under pressure is in equilibrium with a solution that would be supersaturated for a crystal not subject to pressure. Starting from this consideration, Correns [Cor49] formulated his well-known theory that relates the pressure produced by crystallization to the level of supersaturation of the solution:

$$\Delta p_{\text{cryst}} = R (T / V_m) \ln(C / C_s) \quad (2.8)$$

where:

Δp_{cryst} [atm] = crystallization pressure (difference between the pressure on the loaded phase and the ambient pressure)

R [l atm/K mol] = gas constant

T [K] = absolute temperature

V_m [l/mol] = molar volume of the solid phase

C/C_s [-] = supersaturation ratio of the solution in contact with the growing crystal

and

C [mol/l] = concentration of the solution in contact with the growing crystal

C_s [mol/l] = concentration of the saturated solution

Correns also adds further conditions to his theory: no “unpressed” crystals should be present in solution (otherwise they would remove the supersaturation) and the interfacial energy (Correns calls it phase boundary force) between the crystal and the pore wall (γ_{cs}) has to be greater than the sum of the interfacial energy between solution and pore wall (γ_s) and between crystal and solution (γ_{cl}).

$$\gamma_{cs} > \gamma_s + \gamma_{cl} \quad (2.9)$$

It is only when the energy of the pore wall-crystal interface is greater than the sum of the interfacial energy of the pore wall-liquid and of the crystal-liquid that it is possible for solution to enter between crystal and the pore wall and for the crystal to grow.

Winckler and Singer [Win72] apply Correns equation to calculate the value of crystallization pressure for different salts at different supersaturation ratios and different temperatures. The theoretical crystallization pressures for sodium chloride are reported in table 2.

The possibility of reaching a high supersaturation, and therefore a high crystallization pressure, in a narrow pore system where several nucleation sites are present, has been questioned by several authors [Price in Gou97, Sne97].

Table 2 Crystallization pressure for NaCl (after [Win&Sing72])

Crystallization pressure [atm]					
C / Cs = 2		C / Cs = 10		C / Cs = 50	
T = 0°C	T = 50°C	T = 0°C	T = 50°C	T = 0°C	T = 50°C
554	654	1845	2190	3135	3737

The approach described until now, as well as the ones based upon it (e.g. [Wey59]) do not directly relate the pore size distribution of the material to the crystallization pressure that can be developed. Other approaches, deriving from the theories of Honeyborne and Harris [Hon58] and Everett [Eve61] on frost damage, try to relate crystallization pressure, and consequently damage, to the pore size distribution of building materials.

Considering the differences in the chemical potential of small and larger crystals, Everett [Eve61] obtained the following expression for the pressure difference of the two crystals:

$$\Delta p_{\text{cryst}} = \gamma dA / dV \quad (2.10)$$

where:

A [cm²] = surface of the crystal

V [cm³] = volume of the crystal

γ [dyn/cm] = interfacial energy of the crystal

Assuming a spherical geometry for the crystal, Everett [Eve61] derived the following expression:

$$\Delta p_{\text{cryst}} = 2\gamma(1/r - 1/R) \quad (2.11)$$

where:

Δp_{cryst} [dyn/cm²] = crystallization pressure

r [cm] = radii of the small crystal

R [cm] = radii of the large crystal

γ [dyn/cm] = interfacial energy

This equation gives the crystallization pressure that can be exerted by a crystal in a large pore (of radius R) due to the fact that the growth of a smaller crystal in an adjacent small pore (of radius r) is thermodynamically not favourable. Hence, the large crystal continues to grow and builds up pressure until its chemical potential equals that of the small crystal.

Since the pore size is a parameter that can be measured, whereas supersaturation level in pores have to be estimated, Eq. 2.11 was preferred to Eq. 2.8 by several authors, especially when they aimed to check the theory with the experimental results of crystallization tests.

Fitzner and Snethlage [Fit82] used Eq. 2.11 to calculate the crystallization pressures developed in stone of known pore size distribution. The theoretical values showed to be not in accordance with the experimental results (similar pressures were calculated for materials showing different severity of the damage), and Eq.2.11 was modified by introducing correction factors increasing the importance of smaller pores. Following the same approach, Rossi Menaresi and Tucci [Ros89] calculated the crystallization pressure that may be developed in stone of different pore size distributions. It resulted that stones having a large number of small pores connected to larger pores develop the highest crystallization pressure. When the amount of small pores is lower, surface hardening will occur instead of disintegration. No comparison between the calculated values and actual experimental results is reported in their work.

More recently some authors have combined Correns' and Everett's approaches, recognizing that they are actually equivalent, i.e supersaturation is also limiting the maximum pressure in Everett's model [Sch99, Fla02]. In all these models an equilibrium situation is supposed, in which the unloaded tips of a growing cylindrical crystal, because of their curvature, are subjected to the same pressure, and have therefore the same solubility increase, as the loaded side surfaces of the crystal.

The growing crystal exerts a radial stress on the pore wall. The radial stress is accompanied by a tensile hoop stress in the pore wall, and it is this tensile stress that can cause damage to the material (in most materials tensile strength is lower than compressive strength, so damage will occur when their tensile strength is overcome). Scherer [Sch99] adds that damage is not caused by crystallization in a single pore, but growth of crystals through a region of the body comparable in size to the strength-controlling flow is required.

Calculations on the basis of the Scherer's model have shown that relevant pressures will be developed only in very small pores, usually absent in most of the traditional building materials (brick, stone and mortar). Besides, if pressure is developed in partially saturated material, as it is usually the case in practice, the tensile stress developed by the crystallization will be partially compensated by the compression generated by the liquid partially filling the pore [Rij04]. This implies that for an equal crystallization pressure, much smaller pores are needed in a partially saturated material than in a saturated one.

On the basis of Scherer's theory it has been calculated [Fla02] that sodium chloride crystallization can generate significant pressures only in pores of 4 nanometers or smaller. Similar results are reported in [Rij04] showing the inability for sodium chloride to generate pressures in materials with large pores.

Very recently, Scherer [Sch04] explains the occurrence of crystallization damage in stone-like materials by considering the possibility that, due to evaporation, solution is trapped between the crystal and the pore walls whereas the free ends of the crystals are not in contact with the solution. In this situation, that according to Scherer is likely to happen during wet-dry cycles, formation of isolated pockets of salt is likely to occur and pressure of relevant entity might be developed even in large pores.

Steiger [Ste05a] emphasizes the necessity of considering the evolution of crystallization pressure in a porous material as a dynamic process, a non equilibrium situation that is

controlled by kinetic influences such as evaporation and cooling rates, presence of unloaded crystal surfaces etc. According to Steiger, high pressures occur transitorily and high crystallization pressures may be developed because of rapid evaporation or cooling [Ste05a]. An objection made against Scherer's theory regards the type of damage due to salt crystallization [Cha00b]. In [Sch99] ice and salt growth mechanisms are explained in a similar way and are therefore expected to generate similar type of damage whereas, according to [Cha00b], in practice salt damage mostly appears as powdering or scaling of the surface layer of the material and frost damage occurs as cracking and spalling of large pieces of the material. Scherer [Sch00] replies explaining that salt accumulation near the surface driven by evaporation, is the reason of the different damage type observed.

In the particular case of sodium chloride, the question on the damage mechanism is even more controversial: several experiments [Rod99a, Cha00b, Pel02, Rij04, Ste05a] seem to confirm the low tendency of NaCl to reach a high supersaturation and therefore to develop crystallization pressure high enough to produce damage. A maximum supersaturation ratio of 2.2 was obtained in levitated droplets [Ste05a], thus the occurrence of higher supersaturation in pore solution is unlikely.

Besides, sodium chloride has a tendency to nucleate heterogeneously [Ben04], i.e. it uses foreign nuclei (like the pore walls) for the nucleation of the salt crystal. Therefore crystallization is more likely to occur at supersaturation levels lower than for other salts that tend to nucleate homogeneously from solution, like sodium sulphate. Moreover, crystallization of NaCl is likely to occur at the surface of the stone, giving rise preferably to not dangerous efflorescences, whereas other salts, like sodium sulphate, precipitate mainly in the stone as harmful crypto-florescences: these differences are explained by [Rod99a, Ben04] by the faster capillary rise and the slower evaporation of NaCl solution compared to Na₂SO₄ solution.

In spite of the above-mentioned factors, serious decay occurs in reality in sodium chloride contaminated materials, leaving still open the question whether crystallization pressure can explain the damage in case of NaCl, or other mechanisms need to be taken into account.

2.4.2 Other mechanisms

Apart from crystallization pressure, other mechanisms have been proposed as being responsible for salt damage. In the following sections the mechanisms possibly involved in the decay due sodium chloride are critically discussed.

Hydration pressure

Hydration pressure is the pressure developed by the increase of volume occurring during hydration of a salt. Like crystallization pressure, also hydration pressure has been questioned and uncertainties still remain on the relevance of this mechanism for the damage.

In literature several studies concerning the hydration and de-hydration of sodium sulfate, one of the most common and damaging salts found in buildings, are reported. Doehne [Doe94] showed, by means of experiments performed in the ESEM, that large crystals of anhydrous sodium sulfate (thenardite), when exposed to water vapour, initially form a skin of sodium

sulfate decahydrate (mirabilite) that prevents the complete hydration of the crystal until sufficient liquid is present to dissolve the skin. During de-hydration mirabilite is observed to break down to form sub-micron aggregates of thenardite. Provided that the mirabilite is not dissolved by excess liquid water, subsequent hydration-de-hydration cycles result in a highly porous salt structure that occupies similar volume in both states. This suggests that cycling the RH may not play as important role in the deterioration of the stone due to of sodium sulfate as the rapid crystallization of mirabilite from solution.

Rodriguez-Navarro and co-authors [Rod00] studied the process of hydration of sodium sulfate. They show, by means of ESEM experiments, that hydration of thenardite to mirabilite does not occur in the solid state (from the crystal lattice absorbing water vapour and altering from one hydration state to another), but through dissolution of thenardite followed by re-precipitation of mirabilite.

From these considerations it emerges that only if enough water is present to produce dissolution and re-precipitation of the salt in a higher hydrated state, serious damage can occur.

Further, since NaCl does not hydrate at temperatures higher than 0.1°C [Wil81], this damage mechanism is not relevant in the present work and will not be further discussed.

Differential thermal expansion of salt

Differential thermal expansion has been proposed by Cooke and Smalley [Coo68] as possible damage mechanism. According to them, damage in porous building materials may originate, during temperature changes, from the fact that certain salts, like for example NaCl, have a higher coefficient of thermal expansion than the material in whose pores they occur.

Some studies seem to validate this theory [Joa82, Lar90, Coo93] whereas some others show the thermal expansion to be ineffective in producing damage [Gou74]. In case of sodium chloride, the thermal expansion of the salt, upon temperature increase from freezing to 60°C, is 0.5%, whereas the expansion of granite is less than 0.2% [Win94]: this difference is quite small, yet a contribution of this mechanism to sodium chloride damage cannot be completely excluded. However, since serious decay occurs even at constant temperature (see chapters 5 and 6), differential thermal expansion is not likely to be the main cause of damage.

Differential hygric dilation

Another possible mechanism of damage in the presence of NaCl has been proposed in [Wen92, Sne97] for sandstone containing reactive clay. They proved that the hygric behaviour of a sandstone containing reactive clay is irreversibly modified by the presence of soluble salts (sodium chloride, magnesium sulfate and calcium nitrate). During RH cycles the salt contaminated material expanded at low RH and shrunk at high RH, whereas the not contaminated material showed an opposite behaviour; moreover, the expansion of salt contaminated specimens appeared to be irreversible and to increase with the number of cycles. The observed shrinkage has been explained by the authors by the effect ions have in modifying the thickness of the double layer formed on the surface of the clay minerals, whereas no definitive explanation has been given for the expansion measured during drying. The possible consequence of this modified hygric behaviour is clear: whenever zones rich in salt are present while neighbouring zones are free of salt (as it usually occurs in weathered

materials where salt concentrates at the evaporation surface) shear forces are generated between these zones during climate changes. These stresses can damage the material: we can imagine the damage as a detachment of the salt-rich part of the material from the not contaminated one, therefore in the form of scaling or spalling of the surface. More recently similar experiments have been performed on fired-clay bricks rich in NaCl [Wen02]: these have confirmed the behaviour observed in the sandstone [Wen92, Sne97], even in absence of reactive clay.

From the above reported literature, it emerges that the effect of NaCl on the hygric behaviour needs to be further studied, since both systematic experiments and theoretical explanations are missing. An extensive experimental study on the hygric behaviour of lime-cement mortar has been performed in this research work and is reported in chapter 6.

Puhringer's model

The model of salt damage proposed by Puhringer [Puh83] is quite different from any of the models on crystallization pressure described in section 2.4.1. He starts from the observation that porous materials suffering of salt damage in most of the cases do not show pores completely filled with salts (as required by the most diffused and accepted theories on salt crystallization damage) and proposes a model in which damage is caused by repeated uptake and release of moisture producing volumetric changes in the porous salt structure adhering to the material. Puhringer [Puh96] states that, since the volume of water-salt in solution is smaller than the volume of water and salt considered separately, integration of water in a salt-water system leads to a reduction in volume, whereas separation of water from the salt-water system leads to increase in volume. Changes in concentration of salt-water systems, due to variation of the temperature or of the RH, result in volumetric changes. These volumetric changes will cause shear stresses in the material that modifies neither its structure nor its dimension. These stresses may result in damage.

Puhringer's theory does not need the pores to be filled with salts, but, on the contrary, requires that enough pore space is left free: "...salt must form and changes in spaces which permit a certain instability in the moisture content above and in the salt formation. This implies that the quantity of salt must in addition be so small that fixation of moisture in the salt does not result in a stable moisture content in the pore system" [Puh83].

Puhringer's model has been often referred to in order to describe situations that the most accepted crystallization theories cannot explain: for example the case in which scales detach from the surface of decayed materials but not enough salt is present underneath them to press them off [Fra98a], or the case in which an irreversible dilation is observed during NaCl crystallization [Sne97, chapter 6 of this thesis].

One of the limits of Puhringer's theory is the lack of any mathematical model that could allow the calculation of the stresses developed by the salt and therefore the experimental verification of his theory. As Duttlinger and Knofel [Dut03] pointed out, in general crystals are not adherent to the pore wall or support but are separated by a thin solution film; therefore adherence to the pore would be excluded. However, Correns and Steinborn [Cor39] observed that some faces of alum crystals were strongly attached to the support while other did not

adhere to it. The adherence of the crystal to the support depends on the interfacial energies; these are different depending on the face of the crystal and on the material constituting the support. The adherence of salt crystal to the pore wall indicates that the pore/crystal interfacial energy is lower than the pore/solution interfacial energy.

According to Charola [Cha00a] the adherence of the salt crystal to the substrate would not be enough to produce stresses able to damage the material. Since, to our knowledge, any quantification of the developed stresses is missing, the possibility that salt adhering to the pore wall may develop stresses and cause damage in weak materials, cannot be fully excluded.

Chemical weathering

The presence of salt may increase the weathering of building materials by interacting chemically in several ways with the components of the substrate.

Sodium chloride may cause damage indirectly, by enhancing decay processes started by other salts, as it occurs in the case of the reaction between H_2SO_4 and CaCO_3 leading to the formation of gypsum in limestone. This reaction, which would normally stop after a while because of the formation of a gypsum layer on the calcite, goes on for a longer time in presence of NaCl. In fact this salt leads to the formation of hydrochloric acid that keeps the surface of the calcite free from gypsum and allows the reaction to proceed further [Lau27].

Besides NaCl modifies the solubility and phase changes of other salts present in solution. The effects of sodium chloride on quartz [Lie60], sodium sulphate [Obi89] and gypsum solubility [Boc61, Fur68, Zen93, Cam96] are known.

In some of the case studies analysed in chapter 3 the catalyst effect of NaCl on decay processes initiated by another salt has been observed.

2.4.3 Combined damage processes

Salt damage may be present together with other damage processes leading to enhanced effects. With respect to the present research, which is mainly focussed on the study of sea-salt decay in the Netherlands, the effect of salt in combination with biological growth and frost damage may be of interest.

Biological growth has been recognised as effective weathering agent only in recent years. However, there has been little consideration on how salt and biological weathering processes might interact, apart from the recognition that many micro-organisms can precipitate sulphates and oxalates, and thus may be active in creating salts which subsequently cause damage to rocks and building materials. It should be reminded that organisms can also have an indirect effect on weathering of material surfaces, by altering the environmental conditions by retaining water, by reducing the porosity at the surface, or by altering the colour and thus the thermal response of the substrate. These modifications may have a positive or negative effect on the salt damage mechanism.

The interactions that may be developed in the presence of salt and frost are extensively reviewed by William and Robinson in [Wil81]. The authors experimentally studied the effect

of the combined salt crystallization-frost mechanism on the damage. They found that the damage in NaCl contaminated specimens considerably increased when crystallization occurred at low temperatures. They explain the difference between the little damage obtained in the crystallization test and the very serious decay observed after a freeze-thaw test on NaCl contaminated specimens by the following reasons:

- NaCl considerably lowers the temperature of freezing. This implies that a slower freezing of the solution occurs, resulting in the growth of bigger crystals. These larger crystals are more damaging than the thin crystals formed during fast freezing.
- NaCl hydrates at 0.1 °C [Wil81] causing an increase of volume additional to the one produced by freezing of water.

However, the increased damage observed for NaCl when crystallizing at low temperature was not observed for other salts like Na₂SO₄ [Wil81].

Mc Greevy studied the effect of salt solution concentration on the damage due to the combined salt crystallization-frost mechanism [Gre82]. His results show that the type and the concentration of solution affect the amount of ice formed and therefore influence the severity of the damage.

From the above reported literature it can be concluded that the combination of frost and salt weathering is a much more complex phenomenon than each of these two processes operating independently, and that more experiments are needed to elucidate this subject.

2.5 Location of salt in pores

The pore size in which salts preferentially crystallize is still subject of discussion. According to thermodynamic considerations, since any system tends to reduce the area of its interface to a minimum, in a system containing crystals in equilibrium with a saturated solution, larger crystals will grow at the expense of the smaller. According to this approach [Wel65, Wel68, Fit82], the larger crystals in the larger pores will grow first at the expense of the small crystals in the smaller pores. This approach has been criticized by Rodriguez Navarro and Doehne [Rod99a]: according to them, the thermodynamic approach does not take into account that, when evaporation progresses, because of capillary pressures, the saturated solution will move from the larger to the smaller pores, where it will concentrate. Therefore crystallization is more likely to occur in the smaller pores.

Scherer [Sch04] considers thermodynamic equilibrium as well as capillary pressure in his approach. He describes the case of a material with a broad range of pore sizes, like it usually occurs for porous building materials. During drying it is likely that areas, connected to the porous network by small pore entries, remain longer wet; when these areas start drying, the solution becomes supersaturated and the salt crystallizes on nucleation sites provided by the pore wall. This heterogeneous nucleation does not depend on the pore size. When salts have nucleated in the small and in the large pores, the solution in equilibrium with the crystal in the large pores has a lower concentration than the solution in the small pores. Because of this difference in concentration, the salt ions will diffuse from the small to the large pores: the concentration in the smaller pores will decrease leading to dissolution of the crystal, whereas the concentration in the larger pores will rise and the crystal will keep growing.

The experimental work carried out until now has not been able to definitely answer the question of the location of salt in pores. On the basis of SEM observations, Arnold and Zehnder [Arn90] conclude that crystals start growing in pores between 1 and 10 μm , whereas smaller as well as larger pores remain empty. Crystallization in large pores has been also observed for NaCl by [The97] and [Lar90]. According to other experimental studies [Rod99a], sodium chloride seems to crystallize mainly in smaller pores where the solution concentrates during drying.

The main difficulty that precludes giving a definitive answer to this question is the detection limit of the instruments used for the analyses. Pores sizes that, according to the crystallization theory, would be involved in the damage are in the nanometer range; this pore size cannot easily be investigated, even by the use of most advanced instruments.

In chapter 5 of this thesis ESEM and MIP studies aiming at identifying the location of NaCl crystallization in pores of different materials are reported.

2.6 Crystal habits

The shape of the crystals crystallizing from solution is related to the supersaturation ratio at which crystallization occurs: crystals growing at high supersaturation have shapes far from the equilibrium shape of the salt [Sun81]. Extensive experimental studies have been carried out on NaCl crystallization in the presence of crystallization inhibitors, proving the effect of supersaturation on NaCl growth morphology [Rod&al02].

The shape of salt crystallizing in/on a porous material depends on material properties (thin crystals grow on dense substrates, thicker crystals on substrates having large pores), solution supply (very low solution supply gives rise to whisker shaped crystals, high supply to salt crust), evaporation rate and water content in the substrate (salt crusts are formed on wet substrates, whisker like crystals on less humid material) [Arn85b]. The shape of salt crystals may vary also with ageing: fresh saline whisker efflorescences evolving towards more isometric crystals [Arn85a]. Moreover, the salt seems to keep a memory of the phase changes (hydration, dissolution and crystallization) undergone, so that the crystal habit is also influenced by the “history” of the crystal: this is shown for NaCl [Cha02] as well as for other salts [Cha92].

The size of the crystal is influenced by the evaporation rate: faster evaporation rates lead to a large number of nucleation sites, resulting into crystals of smaller size [Bin85].

Regarding the crystallization habits of NaCl in porous materials, SEM studies show this salt crystallizing in various shapes, from massive and waxy forms to thin wickers [Esw80, Obi89, Rod99a, Cha02, Rod02]. Several ESEM observations performed in this thesis (chapters 5 and 6) on NaCl contaminated materials, confirm the large variety of crystallization habits of NaCl and the relation between the above mentioned parameters and the crystallization habits.

2.7 Discussion and conclusions

From the reported literature review it emerges that no definitive answer has been given yet to the cause of the damage observed in building materials in the presence of salts.

In the recent years the two main approaches to crystallization pressure, one based on solution supersaturation [Cor49], the other on pore size [Eve61], have finally found a unifying theory [Sch99, Fla02, Ste05], but a definitive experimental proof of this theory is still lacking. The difficulty of measuring supersaturation in pore solution is the main obstacle for the verification of these theories. Recently, thanks to the advancement of the NMR technique, the possibility of experimentally assessing these theories seems possible in future [Rij04].

It is worth to notice that in all the damage models mentioned in this chapter little emphasis has been laid on two factors important for the development of salt decay:

- The distribution of salt in a material and therefore the distribution of stresses on a macro-scale during crystallization. It can be expected that the pressures developed by salt crystallizing in pores will depend on the distribution of salt in the material: accumulation or homogenous distribution of salt will result in different stresses and consequently different decay patterns. Moreover, a non homogenous distribution (as it is usually the case because of salt accumulation near the surface due to evaporation) may result in differential dilation of more and less salt-loaded areas and play a fundamental role in damage. This last aspect has been studied in detail in chapter 6 of this thesis.
- The effect of multiple dissolution/crystallization cycles on damage. Salt damage is rarely the result of a single crystallization event, but it is more often the consequence of repeated dissolution and crystallization cycles on the material properties and on the propagation of cracks. The importance of repeated dissolution/crystallization cycles for the damage development is demonstrated for practice as well as for laboratory situations, respectively in chapter 4 and 6.

The literature study points out that, apart from crystallization pressure due to salt filling (or bridging) the pores, other mechanisms may contribute to the damage observed in salt contaminated materials. In particular, the effect of NaCl on the hygric behaviour needs to be studied further, since both systematic experiments and theoretical explanations are missing. An extensive experimental study on the hydric and hygric behaviour of lime-cement mortar has been performed in this research work and is reported in chapter 6.

It should also be stressed that the situations in practice are much more complex than the theory, or even the laboratory experiments, can simulate. Different damage mechanisms may occur simultaneously, leading to a combined (and perhaps enhanced) effect. The observation of the decay patterns in practice and of the relation between damage and boundary conditions is therefore fundamental and should constitute the starting point for each theory and laboratory experiment. For this reason an extensive investigation on case studies affected by salt (NaCl) damage has been introduced in this research (chapter 3).

Chapter 3

Sodium chloride damage in practice: results of case studies

3.1 Introduction

Weathering of building materials due to sea-salts is a well-known phenomenon not only in coastal areas but also in deserts. The type and seriousness of the decay may vary, depending on material properties, moisture and salt source and load, and environmental conditions.

In this chapter the influence of the above-mentioned parameters on salt damage is shown on the basis of investigations performed on several buildings affected by NaCl damage.

The most recurrent decay patterns² observed on different materials are reported and the influence of the material properties on the damage is evaluated (section 3.2). Possible sources, load and distribution of salt (sodium chloride) and moisture are presented using the case studies as examples (section 3.3 and 3.4). The effect of the environmental conditions on the damage is discussed (section 3.5). Finally, the importance of the different variables and of the possible damage mechanisms on the development of the decay is inferred from the studied situations (section 3.6).

Apart from the understanding of the influence of the above mentioned factors on the decay, the analysis of the case studies has another fundamental role in this work: it gives input to the laboratory research and constitutes the framework of comparison of the obtained results. In the development of a laboratory weathering test (chapter 5), knowledge of real situations suggests the most effective testing conditions and gives indications of the possible, realistic range of variation of the selected parameters (moisture and salt load, environmental conditions) (section 3.7). Moreover, the comparison of the results obtained in the laboratory (type of damage, ranking of susceptibility of different materials to salt damage, etc.) with reality constitutes the only way to check the reliability of an accelerated test. In a further stage this comparison should allow to predict the evolution of damage in reality.

² In this thesis the decay patterns are described according to the definitions given in the MDDS [Fra98b, Bal99]

3.2 Effect of material properties on salt damage

The type and the severity of the salt damage are strongly dependent on the material properties (physical, mechanical, chemical and petrographical). Materials exposed to the same environmental conditions may be more or less susceptible to salt damage depending on their properties.

The pore size distribution of a material is considered of paramount importance for the development of salt decay. On the basis of the pore size distribution theories have been developed explaining salt crystallization damage (see chapter 2). Materials having a large number of small pores connected to large pores are considered to be more susceptible to salt damage than materials having only large pores [Wel65, Fit82, Ros91]. According to Scherer [Sch99], it is the presence of small pores that constitutes a factor of risk in the development of salt damage, since higher crystallization pressures may develop in smaller pores.

The influence of the pore size distribution on the occurrence of salt damage has been observed by the author in the case study of the church of Oostkapelle (NL). The west wall of this building, subjected to sea-salt spray, showed the presence of two types of bricks, recognizable by their colour: orange bricks and dark-red bricks. Notwithstanding the fact that both brick types were subjected to the same environmental conditions, the orange bricks were seriously powdered whereas the dark-red bricks were not damaged (figure 3.1). From the analyses performed it was found that the orange bricks had a high open porosity (about 40% vol/vol), constituted by a large number of small pores ($< 2\mu\text{m}$), whereas the dark-red bricks had a lower open porosity and almost no small pores (figure 3.2). The analyses of thin sections of the two types of brick showed that the fine porosity measured in the orange brick is most probably the result of a large carbonate content in the original clay and of the use of too low firing temperatures [Lub05a]. In this case the orange brick has also a higher open porosity than the dark-red brick, resulting in a low mechanical strength.

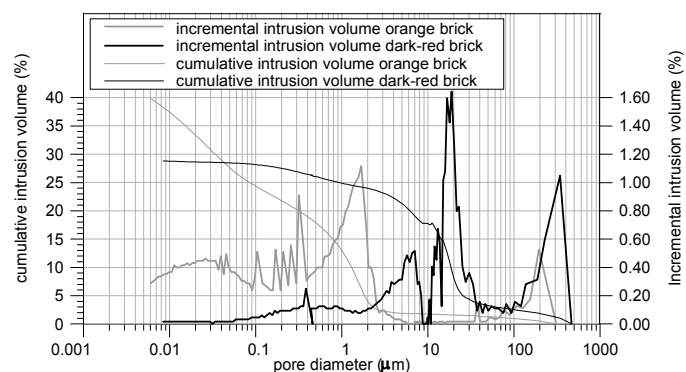


Figure 3.1 (left) Different seriousness of salt damage in bricks exposed to the same environmental conditions (church in Oostkapelle, The Netherlands)

Figure 3.2 (right) Pore size distribution (incremental intrusion volume) and total porosity (cumulative intrusion volume) of orange and dark-red brick

Mechanical strength is another material property considered of fundamental importance for the occurrence of salt damage. Since salt crystallization creates stresses on the pore walls [Sch99], materials having a higher mechanical strength will be more resistant to salt crystallization damage. Therefore the strength is considered as a necessary parameter to evaluate susceptibility to salt damage [Can98] and it is introduced in indexes for durability estimation [Ben04].

Most scientists agree on the fact that pore size distribution and mechanical strength play a primary role in salt damage. Still the possibility of evaluating susceptibility of materials on the basis of mere physical and mechanical parameters is a matter of much discussion. Different physical parameters or combinations of them have been proposed for durability estimation [Fit97, Hon58, Ben04, Ele03], but no final conclusion has been drawn.

Composition of the material itself may also influence the severity of the salt damage: for example the presence of reactive clay in stone has been shown to constitute a factor of risk in the development of decay due to NaCl, because of irreversible dilation generated during crystallization [Sne97].

In the case of bricks, the composition of the original clay may influence the durability: bricks obtained from non calcareous clay have been shown to be more durable because of their lower porosity, higher degree of vitrification and high compressive strength; nevertheless a low percentage of fine grained carbonate may have a positive effect on brick fired at low temperature [Ele03]. Besides clay composition, the production process (mainly the firing temperature) influences the durability: brick fired at too low temperature may not only maintain a dangerously high salt content (mainly sulfates) but will tend to have finer pores than brick fired at higher temperature [Klu93, Fab95]. As mentioned before, the presence of fine pores may enhance the development of salt damage. Moreover, an elevated firing temperature corresponds to an increased degree of vitrification and to a higher mechanical strength resulting in improved durability to salt decay [Klu93, Ele03].

The material properties not only influence the occurrence and severity of the decay, but they may also have an effect on the decay patterns. In particular, the moisture transport properties of a material influence the location of salt accumulation and, consequently, the decay pattern. Salt accumulation in depth may lead to cracks and spalling, salt accumulation near the surface leads often to loss of cohesion in the form of powdering, sanding, scaling or crumbling. Some models have been proposed to forecast the location of salt accumulation, and therefore of damage [Lew90, Sne97]. Unfortunately it is difficult to apply these theoretical models to real situations, at least not quantitatively. Building materials are often not homogenous. Besides, the walls are composed of several materials (brick, stone, mortar and, sometimes, plaster) and the salt solution transport between the different pore systems has to be taken into account [Pet05]. Finally, the presence of salt in the pores significantly alters the moisture transport behaviour of the material [Pel04]. From this discussion it emerges that in practice any prediction on salt accumulation on the basis of a theoretical model is very difficult; an approach starting from the observation of damage in reality becomes therefore an alternative option.

Homogeneous materials show often powdering, sanding, scaling or crumbling; in non homogenous stones preferential weathering, leading to delamination (figure 3.3) or alveolization (figure 3.4), may occur.



Figure 3.3 (left) Preferential weathering showing as delamination in Istria stone (building in Venice, Italy)

Figure 3.4 (right) Preferential weathering leading to alveolization of the Lecce stone (building in Lecce, Italy)

Differences in petrographical structure may lead to delamination of brick. The effect of the internal structure of the material on the salt damage was shown in the case of bricks sampled from the mill of Alkmaar (NL) [Hee03]. The brickwork shows salt damage (mainly sodium sulphate and sodium chloride are present) in the form of delamination of 10-15 mm thick layers (figure 3.5). A Polarized Fluorescent Microscopy (PFM) study of a thin section of the brick (figure 3.6) shows the presence of a laminated structure, with layers having different clay content and porosity. These bricks probably originate from the early beginning of mechanized clay preparation (extrusion). At that time the clay, still having the consistency of soft mud, was driven out of a primitive sort of mouthpiece. Due to friction, differences in flow velocity in the clay column occurred, leading to the laminated structure observed in the brick. These differences in the internal structure may result in differences in moisture transport and hygric behaviour and contribute, in the presence of salt crystallization, to delamination of the brick [Klu05].

Discontinuities in homogenous materials may also be introduced in a later stage, for example by the application of surface treatments like water repellents. These create an outer zone permeable to vapour but not permeable to liquid: the salt, which can be transported only in solution, accumulates under the treated layer, resulting in spalling of the treated part (figure 3.7).

A non homogenous distribution of the damage can not always be clearly attributed to differences in material properties: sometimes damage is not homogeneously distributed, even without obvious differences in the material properties. An example is the peculiar

alveolization of mortar joints in the presence of salts observed in the case study of Heer Abtskerke and Oostkapelle. Holes are visible in the middle of the joints. These holes may be separate (figure 3.8) or connected to form a long groove (figure 3.9). Presence of lime-blowing, or inhomogeneities due to a bad mixing, the application technique or differences in the degree of carbonation, may be at the origin of these peculiar damage patterns.

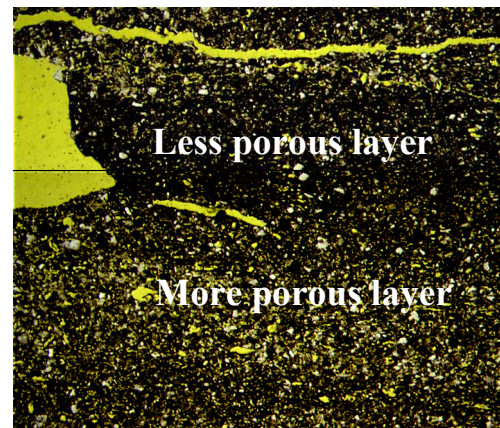
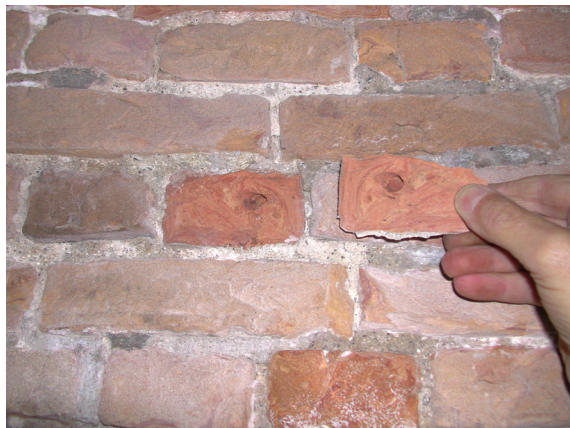


Figure 3.5 (left) Delamination of brick (mill in Alkmaar, The Netherlands)

Figure 3.6 (right) PFM photomicrograph showing the presence of layers of different porosity in the brick from the mill in Alkmaar (25x)



Figure 3.7 (left) Spalling of the treated outer layer of the bricks due to the application of a water repellent (building in Rotterdam, the Netherlands)

Figure 3.8 (middle) Alveolization of mortar joints (church in Heer Abtskerke, The Netherlands)

Figure 3.9 (right) Dissolution of the mortar starting in the middle of the joint (church in Oostkapelle, the Netherlands)

Sometimes differences in properties and damage patterns may be related to the application techniques [Bal05]: this probably happens in the decay of the plaster inside the church of Brouwershaven where the circular decay pattern (figure 3.10) seems to be caused by the shape of the tool and the technique used during the application.



Figure 3.10 Damage pattern originating probably from the application technique (St. Nicholas church in Brouwershaven, the Netherlands)

Beside differences in properties that may occur within a single material, combinations of materials (brick-mortar, wall-plaster) may create a non homogenous system. The behaviour of moisture and salt transport in composite and layered structures has been widely studied in recent years [Bro98, Lub01, Pet05]. Models have been proposed and proved to be effective in determining the location of salt crystallization. These models are based on the principle that, because of differences in capillary pressure, water (or salt solution) will move from coarse to fine pores. In a two-layers system (for example plaster on a substrate) the two situations sketched in figure 3.11 may occur, leading either to salt accumulation at the interface between different pore systems (situation a: coarse plaster over fine substrate) or to salt transport to the surface of the plaster (situation b: fine plaster over coarse substrate) [Pet04, Hui05].

Materials slowing down the evaporation frequently show loss of bond from the underneath material in the presence of salt crystallization. An example is the case of cement re-pointing applied on lime bedding mortar in a brick masonry contaminated with salt. As demonstrated by NMR experiments, the cement pointing used here slows down the drying of the bedding mortar and water evaporates mainly through the bricks (figure 3.12). The presence of cryptofluorescences at the bedding-pointing mortar interface has been observed (figure 3.13) [Lub01]. This can be explained either by a non perfect adhesion between the bedding and the pointing mortar, or by the probably coarse porosity of the pointing mortar, limiting the salt solution transport from the finer porous bedding mortar. The mechanical stresses generated by salt crystallization at the interface lead to loss of bond and finally push out the pointing mortar. A similar type of damage has been observed in practice where a cement re-pointing has been applied on a lime based bedding mortar (figure 3.14).

Not only the re-pointing, but also a whole plaster layer may suffer from loss of adhesion from the under laying material, whenever the conditions for salt crystallization at the substrate/plaster interface are created. This occurs for example in the case of plasters containing a water repellent mixed in the mass. These plasters are usually meant for

accumulating the salt in their inner layer, preventing damage at the surface. If a large quantity of water repellent is added, the liquid transport in the plaster will completely stop and the salt will accumulate at the substrate/plaster interface resulting in loss of adhesion of the complete plaster layer.

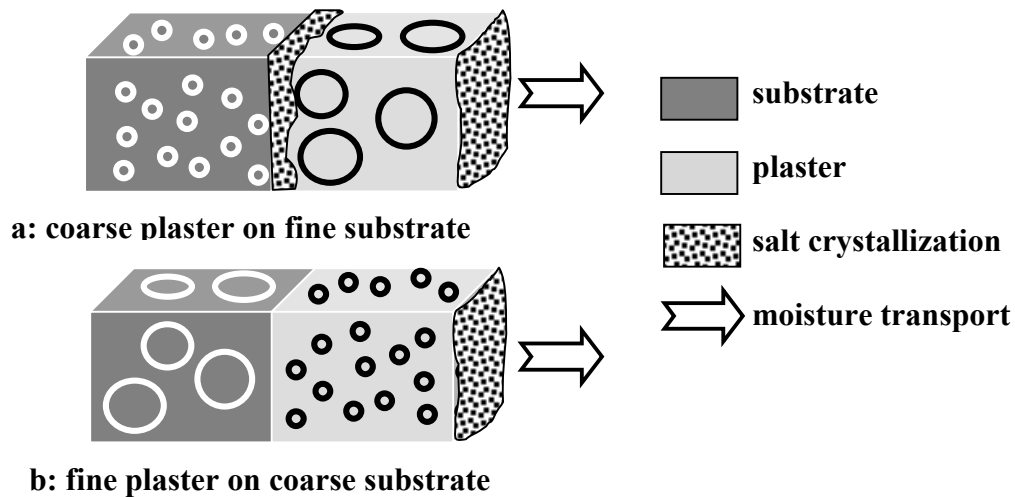


Figure 3.11 Moisture transport during drying of two initially saturated two-layers systems: the arrows indicate the direction of the moisture transport, from the substrate (dark grey) to the plaster (light grey). Depending on the pore size distribution of the plaster/substrate combination, salt accumulation occurs at the interface between the two pore systems (a) or at the surface of the plaster (b)³

Materials enhancing the moisture and salt solution transport from the underneath material to the evaporation surface, more often show loss of cohesion.

From the above discussion it emerges that in restoration interventions, substitution of decayed materials requires particular attention to compatibility [Hee02] between the existing material and the new additions. It is not rare to observe damage to the old existing materials originating from wrong interventions. In fact, since the damage is usually located in a restricted area of the wall, substitution is often limited to the decayed area; if the new material is not compatible with the existing one, damage may appear at the interface.

This has been observed in the plaster of the church of Dreischor. In the lower, decayed, part of the wall the old plaster (probably lime based) has been replaced with a new plaster hindering evaporation. This intervention has increased the level of the rising damp and has enhanced evaporation through the old plaster, resulting in new damage. In figure 3.15 the Moisture Content (MC) and the Hygroscopic Moisture Content (HMC) at 96% RH measured on samples taken along a vertical profile and at different depths in the wall are plotted. The HMC at a certain RH depends on salt content and type; therefore the HMC values give an indication of the presence of hygroscopic salts in walls [Lub04a]. A description of the method for the evaluation of the MC and HMC distribution in buildings is reported in Appendix 3.

³ Model presented by M. de Rooij in the framework of the EU Project COMPASS (Contract no. EVK4-CT-2001-0047-DGXII)

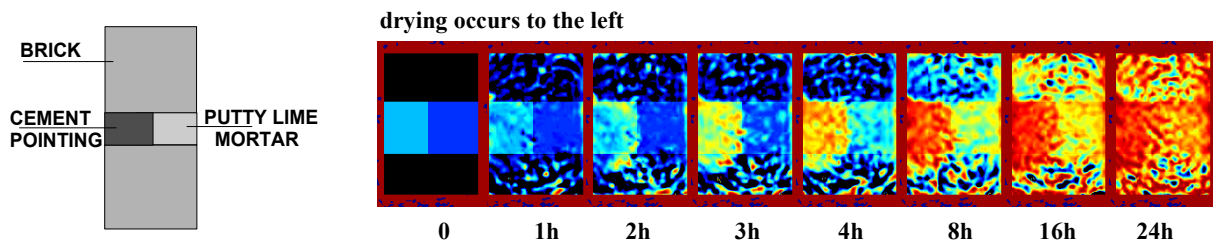


Figure 3.12 The 2D moisture distribution as measured in the system: brick – putty lime bedding mortar – cement pointing during a drying experiment at 0, 1, 2, 3, 4, 8, 16 and 24hours: blue indicates wet areas, red indicates dry areas [Lub01]

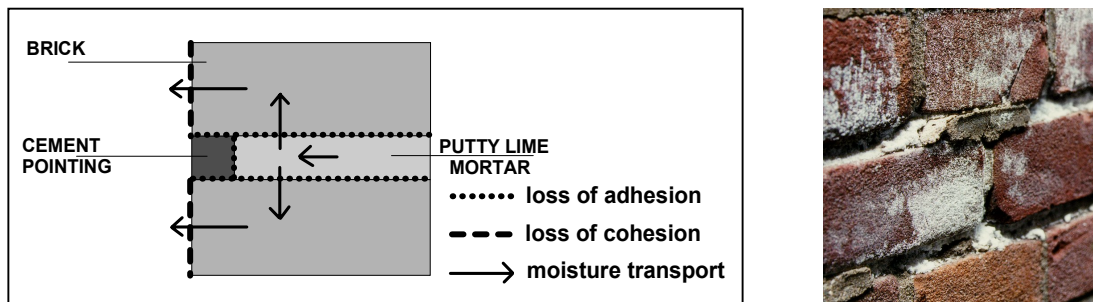


Figure 3.13 (left) Drying behaviour of the system: brick – putty lime bedding mortar – cement pointing mortar: salt accumulation occurs at the interface between the putty lime bedding mortar and the cement pointing resulting in loss of adhesion and push out of the pointing

Figure 3.14 (right) Push out of cement pointing due to salt crystallization (surrounding wall of the church of Harlingen, the Netherlands)

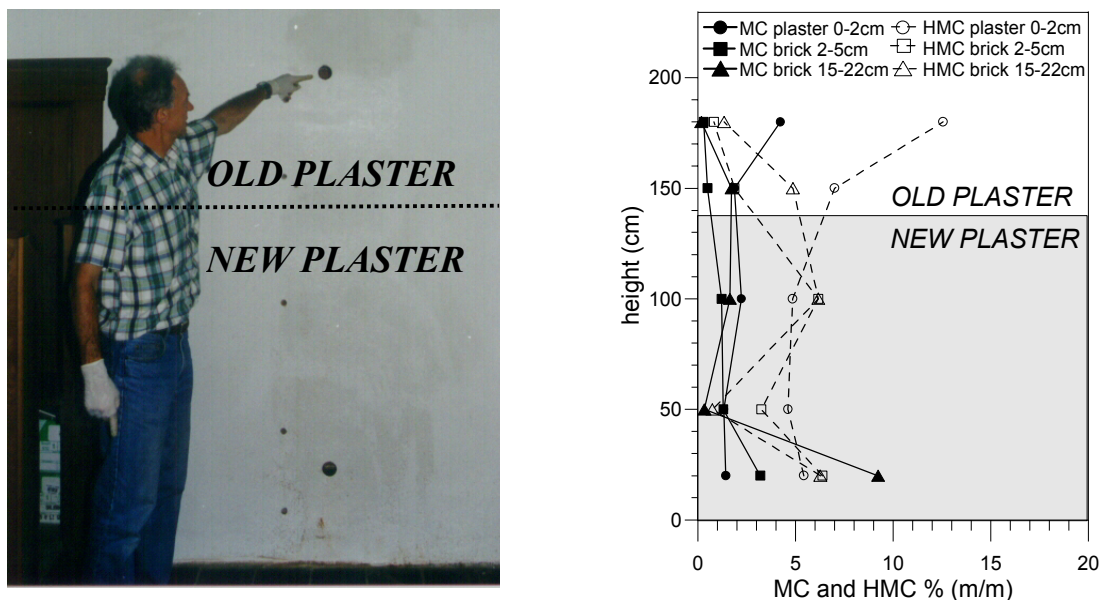


Figure 3.15 Location of the sampling (left) and moisture (MC) and hygroscopic moisture content (HMC) (right): salts concentrate in the old plaster and new damage occurs (church in Dreischor, the Netherlands)

3.3 Sodium chloride sources

Sodium chloride is one of the most abundant and ubiquitous salts found in weathered rocks and construction materials in a wide range of environments: from hot [Cha 80] and cold [Pre67] arid regions to humid coastal areas. Sodium chloride found in buildings may have different sources: it can be originally present in the building materials (as for example in mortars made with non washed sand from the beach) or it may have been introduced later by external sources like ground water, sea-salt spray, de-icing salts, sea-flooding, etc.

Building materials originating from the sea (as e.g. coral stone), as well as the use of non washed sand or seawater in the mortars, may lead to an enormous sodium chloride load in the masonry walls [Hee91]. Nowadays in European countries the use of building materials containing NaCl is not common and more often NaCl reaches the building after its construction.

One of the main sources of salts is water present in the ground, which may penetrate in the wall transported by capillary rise (rising damp). Ground water is a more or less diluted saline solution, and the potential intensity of the salt weathering hazard is basically a function of the height of the groundwater table and of the salinity of the rising water [Jon80, Gou97].

The percentage of NaCl reaching the building by rising damp may be relevant, as it happens for example when the ground has been enriched with salt after a sea-flooding. Several buildings investigated in this research are located in the south-west region of the Netherlands, in areas flooded by the sea about 50 years ago. Even if the buildings were not submerged in the seawater, the ground was enriched with sea-salts and the rising damp transported the salts into the masonry. This is the case for the church of Domburg, in which a high NaCl content is found in the wall, accumulating at the upper level of the capillary rise (figure 3.16), even though the building was never under seawater. The distribution of the salts observed in the masonry is in accordance with the fractionation usually observed in the presence of rising damp [Arn82]: less soluble salts (in this case gypsum) crystallize in the lower part of the wall, more soluble ones (in this case NaCl) are transported to the upper level [Lub04b].

In other case studies, the building itself was partly submerged in seawater: the walls absorbed a considerable amount of NaCl that caused severe damage when the masonry dried out. This is the case for the church of Brouwershaven (see chapter 4) submerged in seawater up to the window sills. The high salt load still present in the masonry contributes to the increasing damage observed in the church over the last five years [Lub05b].

For buildings located near the coast [Win94] sea-salt spray is another possible source of NaCl. Sea-salt particles are removed from the atmosphere by wet deposition (driving rain) and dry deposition (aerosol). The amount of salt deposited is not always relevant in the short term, but continuous accumulation over a long period of time may lead to a high salt amount and to damage. Accumulations found today are representing an integral effect of sea-salt deposition beginning at the time of construction of the building.

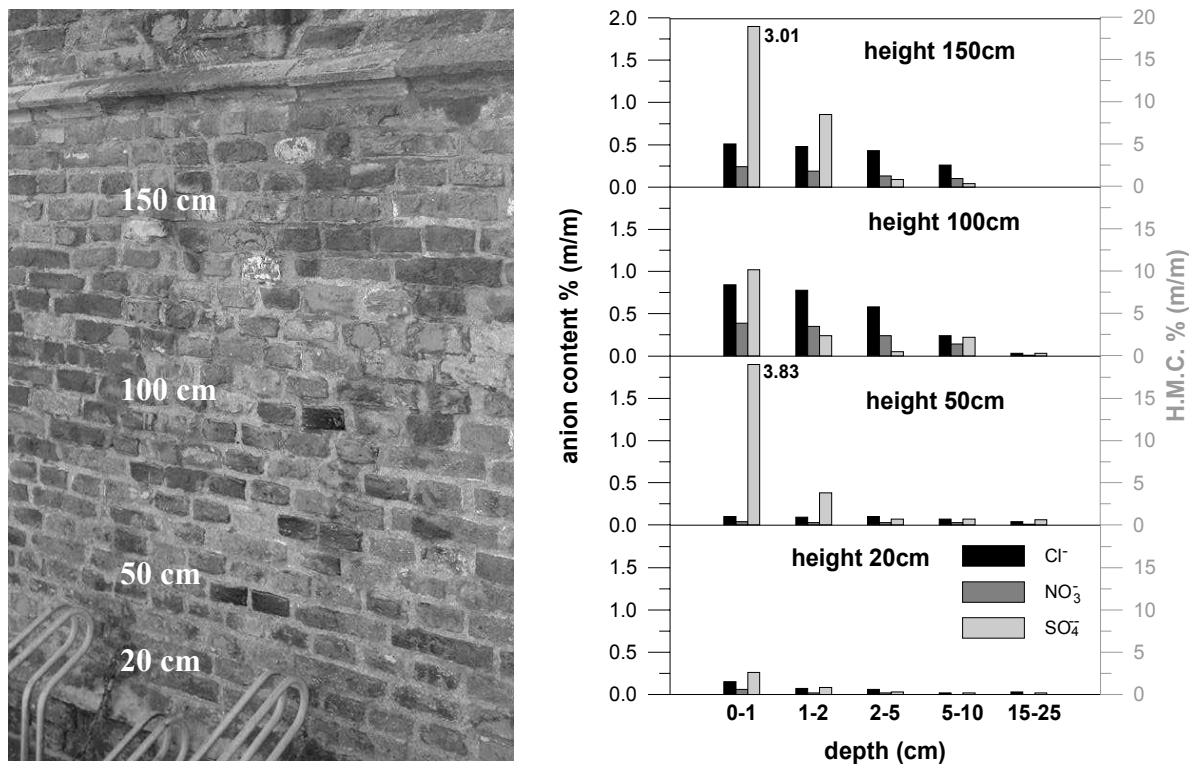


Figure 3.16 Location of sampling (left); anion distribution (measured by ion chromatography) along a vertical profile at different depths (right) (church in Domburg, the Netherlands)

In many of the investigated case studies, damage due to sea-salt spray has been observed in the higher part of the building not reached by rising damp. Damage appears mostly in the form of powdering and sanding of brick, stone and mortar in the upper part of the masonry and it is more serious in the south-west oriented walls, which is the main direction of wind in the Netherlands. The chemical analyses performed on bricks subjected to sea-salt spray in the case studies of Oostkapelle (figure 3.17) and Domburg (figure 3.18) show that chlorides are able to penetrate deep in the material, up to several centimetres, whereas sulfates remain mainly in the outer 1-2 cm. This confirms what is reported in the literature [War00].

In regions with a cold climate the use of de-icing salts (mainly NaCl, CaCl₂ or mixtures) constitutes an important source of chlorides. The amount of salt and the frequency of application depend on the particular climate: in the Netherlands, where the case studies considered in the present research are located, the average amount of salt strewn for example on bridge surfaces is quantified at about 250 grams chloride per square meter per year [Pol00]. Apart from the most common sources of NaCl in masonry mentioned above, occasionally other sources can be present, also in relation to the function of the building over time. For example it is not rare to find buildings used as salt storage in the past, suffering today from serious damage (figure 3.19).

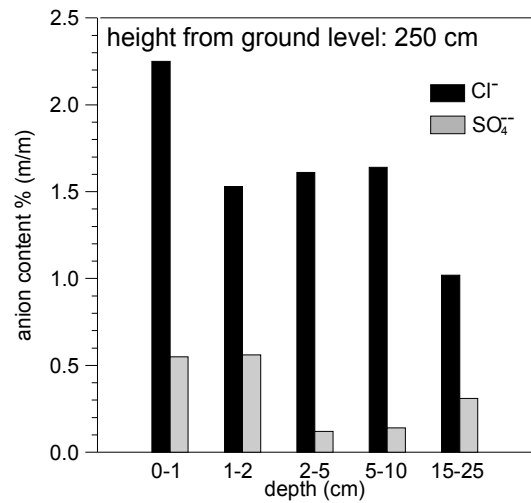
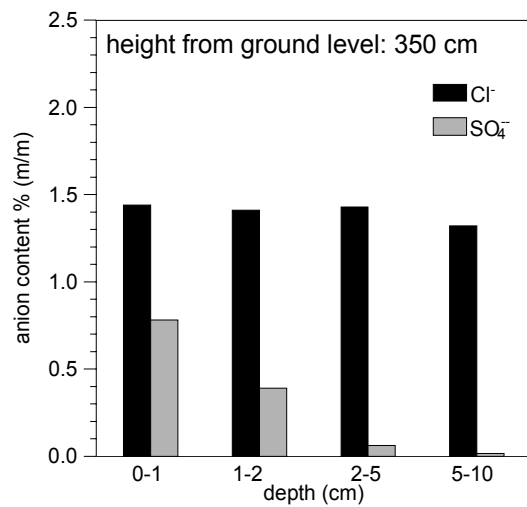


Figure 3.17 (left) Cl^- and SO_4^{2-} content in brick subjected to sea-salt spray (church in Oostkapelle, the Netherlands)

Figure 3.18 (right) Cl^- and SO_4^{2-} content in brick subjected to sea-salt spray (church in Domburg, the Netherlands)



Figure 3.19 Salt damage on the exterior wall of a building used as salt storage in the past (Magazzini del sale, Venezia, Italy)

3.4 Sources of moisture for salt damage

Besides the presence of salt, a moisture source is necessary to mobilize and deposit the salts in pores and cracks and thus causing the damage to progress. In the absence of any source of moisture even a large quantity of salt will not be damaging. On the other hand, little amounts of salt may cause decay if repeated dissolution/crystallization cycles occur.

Moisture sources can be continuous (like rising damp), recurrent (like rain, fog, sea-salt spray, ebb-flood, RH), or occasional (like leakages, flooding).

Rising damp is one of the most common sources of moisture in masonry and also the most dangerous one. Its harmfulness is mainly due to the high moisture load introduced in the masonry and to the fact that often ground water is also a source of salt. The groundwater table and the salinity of the rising water are the main elements determining the salt weathering hazard [Jon80, Gou97]. The moisture absorbed from the ground by capillary suction may saturate the masonry, dissolve even the less soluble salts and make chemical reactions possible. The high danger of rising damp is also related to the difficulties in hindering this moisture source: systems based on the injection of chemical products are not always effective [Hee96] and the use of a mechanical cut is often not possible (due to irregularity of the masonry or stability problems).

Rain penetration is another source of moisture, generally less dangerous than rising damp, since it can be limited by a good re-pointing of the masonry and by sealing of the cracks that may possibly be present. In some buildings anyway rain penetration may play a crucial role in the salt damage. This is for example the case for mills, where due to the movement of the structures, cracks are developed in the masonry through which water penetration may occur. This has been found in the mill of Alkmaar, where a high moisture and salt content have been measured in the south and west walls (figure 3.20), which are the main directions of wind and rain in the Netherlands. On the same walls serious damage was observed.

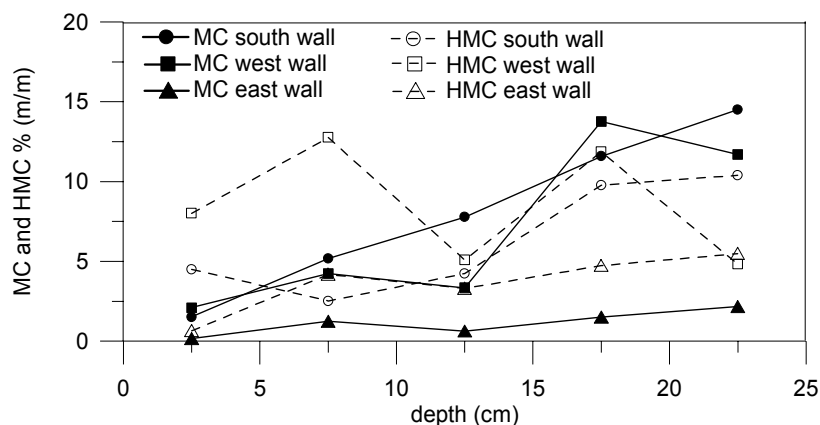


Figure 3.20 Moisture (MC) and hygroscopic moisture content (HMC) on different orientations. The depth is measured from the interior surface (0 cm) (mill in Alkmaar, the Netherlands)

The relative humidity of the air may constitute a source of moisture since it may lead to surface or capillary condensation. Surface condensation occurs when the temperature at the surface drops

below the dew point⁴ of the surrounding air. Capillary condensation may occur, at high RH, in materials having pores smaller than $0.1\mu\text{m}$ (see section 2.3.1).

Moisture adsorption from the air may occur also in presence of hygroscopic salts whenever the RH of the air is higher than the relative humidity of crystallization of the salt or salt mixture present in the wall. The RH changes of the air constitute a moisture source that may cause serious damage in salt contaminated materials. If highly hygroscopic salts like NaCl are present, RH changes of the air through the RH of crystallization of the salt may lead to crystallization/dissolution cycles that can cause damage. Salt accumulating near the surface will have a fast response to the RH changes of the air and several dissolution and crystallization cycles may occur in a short period of time. This is shown in chapter 4 for damage occurring to the plaster in the interior of the church of Brouwershaven.

3.5 Effect of environmental conditions on salt damage

The environmental conditions play a crucial role in determining the location of salt accumulation and therefore in the decay patterns that may develop or even in the occurrence of the decay.

The importance of the environmental conditions for the damage development has been observed in the case of a restoration plaster, applied in two buildings located in two very different climates: the interior of a not-heated church in the Netherlands (Brouwershaven, see chapter 4) and the façade of a building in Curaçao (NA) [Lub05c]. Due to the different drying conditions, the same plaster showed a completely different behaviour, even if applied on masonries with a comparable salt and moisture load. When the drying occurs slowly, as in the interior of the church in the Netherlands (the RH varies mostly between 60 and 80%, the temperature between 0 and 15 °C), the salts accumulate just beneath the outer surface of the plaster, causing sanding and scaling of the plaster layer (figure 3.21).



Figure 3.21 Sanding (left) and scaling (right) of the plaster (St. Nicholas church in Brouwershaven, the Netherlands)

⁴ Dew point is defined as the temperature to which a sample of moist air must be cooled at constant pressure and constant water vapour pressure in order to obtain saturation.

When the evaporation is enhanced by high temperatures and by strong wind, as in the façade of the building at Curaçao (yearly average temperature 27.5 °C, 77% RH and mean wind speed 7 m/s [Hee91]), the drying front remains deeper inside the material and the salts accumulate in the inner part of the plaster. It has been observed that damage to this plaster type in Curacao occurs mainly in two situations: if the plaster layer is not too thick (about 20 mm) or if rain, penetrating through the hair cracks (due to drying shrinkage) of the plaster, dissolves the salts accumulated in the inner layer and transports them to the surface.

The stability of the climate has a crucial effect on the development of the damage if hygroscopic salt are present just beneath the surface of the material. As already mentioned above and as shown in detail in chapter 4, changes in temperature and in RH of the air may produce dissolution/crystallization cycles of the salt and enhance the damage. Several examples are reported in the literature showing how RH changes may lead to serious damage when salts are present (among others [Kon01, Wat00])

In the specific case of NaCl temperature cycles are not harmful, since the solubility of this salt does not depend on temperature; however, RH cycles through the RH of crystallization of the salt (75%) may lead to serious damage (case study of Brouwershaven).

3.6 Evaluation of risk factors for salt damage

As shown in the previous sections, several factors (material properties, moisture/salt load and source, environmental conditions) contribute to the risk of occurrence of salt damage in buildings. These factors have a different importance for the damage and enhanced effects may occur when two or more factors act together.

Because of the complexity of the interaction between these factors, the study of several damage cases in practice is the best way to get information on the relative importance of these factors. This allows evaluating the risk of damage and helps choosing the most appropriate intervention.

For the present research work, the identification of the factors of risk helps selecting the parameters and conditions to be adopted in an effective weathering test (see chapter 5).

Primary factors of risk for the occurrence of salt damage are obviously moisture and salt load and sources. In order to have damage, the presence of both is necessary. A high salt load without any moisture will not cause any damage. On the other hand, even low salt amounts can become harmful in the presence of moisture sources causing their local accumulation and their repeated dissolution and crystallization.

The harmfulness of a moisture source is related to the following parameters:

- the moisture load it can carry (high, moderate or low): a high moisture content, enabling the dissolution and the transport of a large amount of (low soluble) salt, is considered more dangerous than a low moisture content;
- the frequency of its occurrence (continuous, recurrent or occasional): a continuous or recurrent source is generally regarded as more harmful, even if some occasional event (for example flooding) may have an enormous impact on the damage development;

- the amount of salt that it carries (high, moderate or low): some moisture sources (for example sea-salt spray) can carry with them a large amount of salt, increasing the risk of damage.

The result of this evaluation is that rising damp, leading to a high moisture content, being a continuous source and often transporting a relevant amount of salts, is a very risky moisture source. Other moisture sources are either leading to a lower moisture content, are less frequent, or may not increase the salt load in the material. For these reasons they may be considered less risky (table 3.1).

Table 3.1 Main factors contributing to the risk of different salt and moisture sources

	Rising damp	Rain penetration	Sea-salt spray	Leakage	RH air	sea-flooding
moisture load	high	moderate	low	moderate/ high	low/ moderate	high
frequency	continuous	recurrent	recurrent	occasional	recurrent	occasional
amount of salt carried	moderate/high	low	high	low	low	high

The evaluation of the risk due to the presence of the salt is even more complex than for moisture sources. It depends mainly on the following parameters:

- the amount and distribution of salt (high, moderate, low): a high salt amount is more dangerous than a low salt amount; salt accumulating in a local area may cause more damage than salt distributed in a large zone;
- the harmfulness of the salt (high, moderate and low): some salts, like Na_2SO_4 and MgSO_4 , are known to be more dangerous than others, like NaNO_3 , NaCl and CaSO_4 [Gou97];
- the salt supply (active, not active): a salt source that is still active keeps increasing the total salt content in the material and constitutes, therefore, a greater risk for damage than a source that is already extinguished.

When moisture is provided by the RH of the air, the following elements also play an important role:

- the salt type: highly hygroscopic salts (as for example NaCl), adsorbing moisture from the air, are more harmful than little hygroscopic salts. Salts having a RH of crystallization in a range that can be easily crossed by the air RH are more dangerous than salts that, because of their very high or very low RH of crystallization, remain always in crystallized form or in solution. Salts having more hydrated forms of different solubility (like Na_2SO_4 and MgSO_4) are more damaging than salts having only one anhydrous form (like NaCl); phase changes from one hydrated form to another may be accompanied by (large) volume changes which may result in severe damage;
- the distribution of salt (near the surface, in depth): salts crystallizing near the surface of the material have a fast response to RH changes, therefore even RH cycles of short duration may cause their dissolution and re-crystallization.

The material properties, as shown in section 3.2, are important for the occurrence of the damage. When a single material is considered, the following properties have to be taken into account to evaluate the risk of salt damage:

- pore size (fine or coarse): finer pores are more at risk than coarse pores;
- mechanical strength (low or high): a low mechanical strength constitutes a higher risk for the occurrence of damage; inhomogeneities in materials constitute weak points where the damage may start.

In case of masonry, the properties of the different components (brick, stone, mortar etc) have to be judged in relation to each other. In this perspective, the risk of damage will depend on the combination of materials. For example in a plastered wall, damage to the plaster is enhanced if a fine porous plaster is applied over a coarse porous substrate. The salt solution transport from the coarse substrate to the fine plaster is enhanced and the salt accumulates in the plaster layer increasing the risk of damage to the plaster [Pet04]. Whether damage to the plaster has to be preferred to damage to the existing substrate depends on the specific situation (see section 3.8).

The environmental conditions play also an important role in the damage development (see section 3.5). Two elements may influence the seriousness and the type of the damage:

- the drying speed, determined by the temperature, the RH and the air speed (fast or slow): generally speaking fast drying may be more damaging than slow drying. In the case of fast drying it is more probable that the evaporation rate dominates the rate of solution supply, leading to salt accumulation in depth in the material. This may result in scaling or spalling of the outer layer of the material, damage that is much more serious than powdering or sanding, which is usually observed when most of the salt crystallizes at the evaporation surface.

Furthermore, when a continuous moisture and salt source is present (as in case of rising damp), a fast drying keeps the material always dry enough to be enriched by new salt solution, leading to an increasing salt amount in the material. According to the crystallization theory, fast drying should produce more serious damage, since crystallization would occur at higher supersaturation levels. In addition, according to Scherer [Sch04], fast drying would make it possible that, during evaporation, the solution is trapped between the crystal and the pore walls whereas the free ends of the crystals are not in contact with the solution. In this situation, that according to Scherer is likely to happen during wet-dry cycles, formation of isolated pockets of salt is likely to occur and pressures of relevant magnitude might be developed even in large pores. This would mean that high crystallization pressures might be reached even in the absence of very small pores, which is the case in most traditional building materials.

- the stability of the climate i.e. the presence of temperature and RH changes (constant or variable): when hygroscopic salts are present and accumulate near the surface of the material, a variable climate (i.e. with RH and temperature changes) constitutes a factor of risk for salt damage to occur.

3.7 Input to the development of an effective weathering test

The analysis of the case studies gives input to the development of a laboratory weathering test, because it helps in selecting the most effective, but at the same time realistic, test conditions. Besides, it allows to check the reliability of the test, by comparing the types of damage obtained in the laboratory with those observed in practice.

In this chapter indications are given for the most effective test conditions and for the range of realistic values in which the selected parameters may vary. The evaluation of the reliability of the developed weathering test is done in chapter 5.

As discussed in the previous sections, the main parameters influencing the salt damage are:

1. moisture and salt sources, load, and distribution;
 2. material properties;
 3. environmental conditions.
-
1. Rising damp is the most harmful moisture and salt source. This can be simulated in the laboratory by partially immersing the specimen in water or salt solution.
A high moisture load is necessary to transport the salt to the surface of the material and should therefore be pursued in the laboratory test. Moisture content values up to 30% by mass have been occasionally measured (case study of Brouwershaven) and values of 20% by mass are quite common in brick masonry (case studies of Hensbroek, Domburg, Dreischor, Oostkapelle, Zoutelande). A high salt load enhances the damage and should therefore be preferred in a laboratory test. In practice a salt content of about 1% by mass Cl^- (1.6% NaCl) has often been found at the evaporation surface (1 cm thick layer); in some cases Cl^- contents up to 2% by mass (3.2% NaCl) have been measured. It should be remembered that, since the salts tend to accumulate at the evaporation surface, the measured percentage of salt will strongly depend on the thickness of the sampled layer: sampling either the outer 1 cm or the outer 2 cm layer will give two different percentages of salt content. This makes it difficult to compare the results of samplings performed using different procedures.
The salt distribution is important for simulating a damaging process due to RH or temperature changes. In this case a concentration of salt just beneath the outer surface of the material has to be obtained in order to achieve a fast response of the salt to the climate changes.
 2. If the susceptibility of a certain material to salt damage has to be evaluated, no choice can be obviously made with respect to its properties. However, there are situations in which an appropriate selection of materials may enhance the damage. For example, if the salt susceptibility of a material has to be tested in a system of two or more materials, the components of the system can be selected such to create the worst situation for the material to be evaluated. In case of a plaster to be tested on a substrate, a substrate with coarse and high porosity (leading to a high salt and moisture content and enhancing the extraction of salts from the substrate) has to be preferred above a substrate with a low volume of fine pores.

3. It is observed that fast drying may enhance the development of the damage, therefore a high temperature, a low RH and the presence of an air flow should be preferred in a laboratory test. On the other hand, the temperature, air RH and air-flow adopted in the laboratory should be kept within a realistic range. Temperatures higher than 60 °C or an RH lower than 30% are rarely measured in practice.

The presence of a variable climate, with RH and temperature changes, may also enhance the damage by causing dissolution and crystallization cycles of the salts in a relatively short period. The time necessary to dissolve and re-crystallize the salts depends on the salt type and location.

3.8 Discussion and conclusions

In this chapter, on the basis of the results of several case studies, the influence of material properties (e.g. pore size, mechanical strength, moisture transport behaviour) and boundary conditions (moisture supply, salt load and distribution, environmental conditions) on the severity and the type of salt damage has been evaluated.

Most of these factors cannot be considered as positive or negative on themselves, but the interactions among them determine the risk of damage. For example, a high moisture content may be very damaging even when a low salt load is present; on the other hand, even a large salt amount is not a problem if no water is present to activate the salt. This is just an example showing how the different parameters interact with each other; the possible combinations and consequences for the damage are countless.

Apart from determining the risk of damage, various parameters influence the decay pattern. Materials having good moisture transport properties will preferentially accumulate the salts near the external surface and will therefore suffer loss of cohesion of the outer layer. Materials inhibiting or preventing liquid moisture transport will accumulate the salt in depth; consequently, cracking will be a probable decay pattern. Homogeneous materials suffer usually sanding or powdering; non homogeneous materials or layered structures having an external layer hindering evaporation show more often spalling or loss of adhesion. However, depending on the environmental conditions, even the same material may show different decay patterns: the same plaster applied in two different climatic situations showed either salt accumulation in depth and no damage, or salt transport to the surface with consequent sanding and scaling.

From this discussion it is obvious that no general rule exists for performing a successful conservation intervention, but for each situation the priorities should be defined beforehand. These may be the preservation of the original materials, the esthetical aspect, the habitability of the space etc. Once the priorities have been established, the most suitable intervention can be defined, by taking into account the existing boundary conditions and the compatibility between the existing material and the new addition. For example, in case a valuable material has to be preserved, any further salt accumulation in that material should be avoided. Eventual integrations in contact with the existing material should be therefore performed using a

material having a more effective moisture transport than the existing one. The use of a “sacrificial” material may also be an option. In this way the salt will preferentially accumulate in the new material and the damage to the old valuable object will be limited. Partial substitutions of ancient lime-based plasters by salt-resistant plasters hindering evaporation have often caused new decay to the old material. However, the same salt-resistant plaster may be a satisfactory solution in cases where no compatibility issues are present, and a good aesthetical aspect (absence of efflorescences or moist spots) and the habitability of the space are the priorities.

Chapter 4

Effect of RH changes on NaCl damage: monitoring of a case study

4.1 Introduction

Most of the case studies investigated in this research are ancient buildings located in the province of Zeeland, in the southwest of the Netherlands. This region was flooded by the sea in 1953; as a consequence of this calamity many of the buildings are now still suffering of a serious sea-salts damage (see chapter 3).

This chapter reports the results of a series of investigations and monitoring, performed during a period of about four years, on an ancient church located in a small village in Zeeland (Brouwershaven). This building can be considered representative of many other brick-masonry buildings in the flooded areas in the Netherlands.

4.2 Notes on the history of the building and of the renovations

The construction of the church of St. Nicholas in Brouwershaven (figure 4.1) started probably in 1293 [Kam65] and went on until the 17th century. The nave dates back to the 14th century, the aisles and the choir to the beginning and to the end of the 15th century respectively. The first church-tower dated from 1667 and contained three bells; this tower was renewed in 1734 before being taken down during the French period. A new tower was built in 1883 and enlarged in 1932.

In 1953, due to the flooding, the church was submerged in the seawater up to the windowsills (about 2.5 m from the ground level) (figure 4.2). Because of the walls being saturated with seawater during the flooding, a serious decay developed when the masonry dried out. The church required an extensive restoration of the interior that was completed only in 1963: a tar-like layer was applied on the walls and on the top of this a plaster was applied. The aim of this intervention was to keep the salts inside the masonry, preventing them from reaching the plaster. Due to detachment of the plaster layer and salt appearing at the surface, a new restoration was necessary. This took place in 1991-1994: the plaster and the tar layer were removed and a new plaster was applied. This new plaster is a ready-to-use restoration plaster

for salt loaded substrates (Jahn M60) and, according to the producer description [<http://jahn-international.com/jahnbvm60algemeneinfo%20engels.htm>], should not limit the transport of the salt solution from the substrate to the plaster. When the monitoring started and the first investigations took place (July 2000), the plaster already showed a serious decay that considerably increased over the following years.



Figure 4.1 (left) Church of St. Nicholas in Brouwershaven

Figure 4.2 (right) Church of St. Nicholas in Brouwershaven during the flooding in 1953

4.3 Description of the damage

The church has a brick-masonry structure with some courses of stone, probably a Belgian limestone. The columns have a sandstone basement. The interior walls and the upper part of the columns are plastered.

The decay affects both the exterior and the interior of the church.

In the exterior few bricks show powdering (figure 4.3) and some of the stones show powdering and scaling of the outer surface (figure 4.4). In the interior the damage affects mainly the plaster layer. The sandstone constituting the basement of the columns shows often a white salt patina and sanding (figure 4.5). The damage to the plaster is mainly located up to 4 meters from the ground level, and is particularly severe on the walls (figure 4.6) and the plastered columns (figure 4.7) of the choir.



Figure 4.3 (left) Powdering of brick (exterior)

Figure 4.4 (right) Powdering and scaling of the stone (exterior)

The damage starts as peeling of the paint layer and formation of thin cracks and develops then with sanding, scaling and crumbling of the plaster (figure 4.8). These decay patterns have been observed in other occasions [Hee04] and seem to be typical of this plaster when applied in very severe conditions. At some spots in the church the plaster layer is completely weathered and the brick substrate starts decaying. Large amounts of efflorescences are visible on the plaster and on the substrate in the dry (low RH) periods.



Figure 4.5 (left) Stone basements of the column showing white salt patina and sanding

Figure 4.6 (middle) Plastered south wall of the choir showing serious damage

Figure 4.7 (right) Plastered part of a column in the choir showing sanding, scaling and crumbling of the plaster layer



Figure 4.8 Evolution of the damage: from peeling of the paint (left), to appearance of cracks in the plaster (middle) to sanding, scaling and crumbling of the plaster layer (right)

4.4 Sampling

Sampling campaigns were performed in the interior and in the exterior of the church, on several locations. The sampling campaigns took place in August 2000, July 2001 and March 2005. Different types of samples were collected, aiming to reach a complete analysis of the causes and processes of damage:

- powder samples: powder samples were drilled at different locations in the church. At each location, the drilling was performed along a vertical profile at several heights and depths. These samples were used to assess the moisture and salt distribution in the wall in order to define the moisture source (see appendix 3 for a complete description of the method). Chemical analyses were performed on some of the samples to assess the ion types and content.
- cores: cores of 5 cm diameter were drilled from the wall. The cores were used for determining the material properties (composition, total porosity and pore size distribution). The knowledge of the material properties, mainly of the pore size distribution, is fundamental for the understanding of the moisture and salt transport in layered systems like plastered walls [Pet04].
- efflorescences: salt efflorescences present on the stone and the plaster surface were collected to assess the type of salts present.

A complete mapping of the samplings is given in figure 4.9.

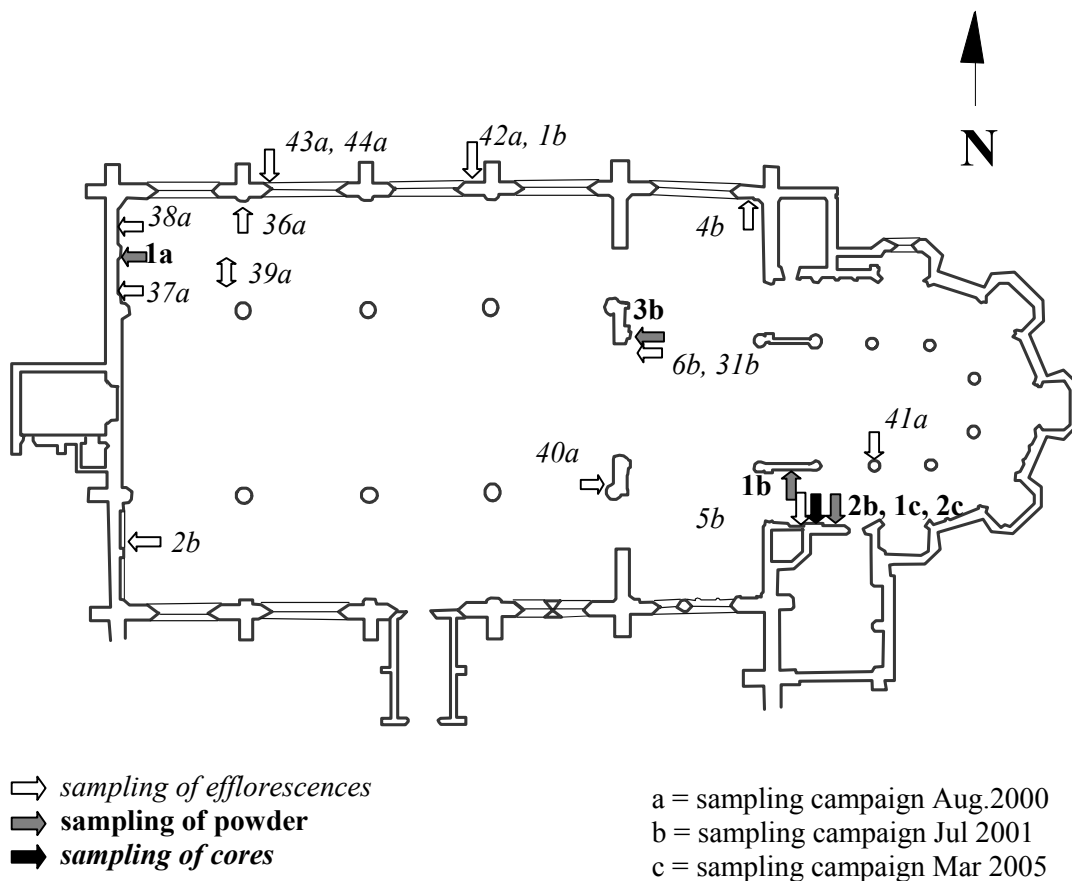


Figure 4.9 Plan of the church with indication of the location of the samplings

4.5 Laboratory investigation

4.5.1 Determination of moisture load and sources

The powder samples were dried in an oven at 60 °C until constant weight, and the actual moisture profile was gravimetrically determined. A common pattern is measured in most of the sampling locations: the moisture content decreases from the lower to the upper part of the wall and from inside to the surface of the wall (figure 4.10). This pattern indicates the presence of rising damp.

The height of the capillary rise varies in the different locations, also depending on the materials constituting the masonry (brick or stone). The lowest height of rising damp has been measured in the column (sampling 3b) due to the presence of the stone basement limiting the capillary rise. In the brick-masonry walls of the choir (samplings 1b, 2b, 1c and 2c) the rising damp reaches a much higher level. Comparing the moisture content and distribution measured in 2001 and 2005 at the same location (respectively sampling 2b and 1c) it seems that the masonry is slowly drying out: not only the height of the rising damp is lower but also the moisture content is reduced. It can be supposed that, due to the application of the tar layer limiting the evaporation in the restoration of 1963, both the height of the rising damp and the moisture content in the wall increased. The removal of the tar layer and the substitution of the plaster in 1991-1994 have allowed the masonry to slowly dry out: this has resulted in a lower moisture load in the wall.

4.5.2 Determination of salt type and distribution

The hygroscopic moisture content (HMC) of the powder samples at 96% RH was assessed. A complete description of the principles and the possibilities of this measuring method is given in Appendix 3. Here it is useful to remember that the HMC at a certain RH depends on the type and the quantity of salts. Therefore the HMC gives a first, indicative, evaluation of the amount of hygroscopic salts present in the material. From the HMC distribution it is clear that:

- the masonry has a high salt content;
- the hygroscopic salts accumulate near the surface of the plaster layer, due to the evaporation process;
- the hygroscopic salts accumulate at the upper fringe of the rising damp zone. In some cases (samplings 1c, 2c) a high salt content has been measured also at a level much higher than the height reached by the rising damp.

The sources of hygroscopic salts are both the ground, from which the salts are transported into the wall by rising damp, and the masonry itself, being saturated, up to the height of about 2.5 m from the ground level, with seawater during the flooding.

The HMC gives only an indication of the presence of hygroscopic salts in the wall. In order to define quantity and type of salt, chemical analyses (Cl^- and SO_4^{2-} anions) were performed on some of the powder samples and X-Ray Diffraction (XRD) analyses were carried out on efflorescences. The chemical analyses performed on three powder samples from location 1a showed the presence of Cl^- (content variable between 0.17 and 0.76% of the mass of the sample) and SO_4^{2-} (content of 1% of the mass of the sample).

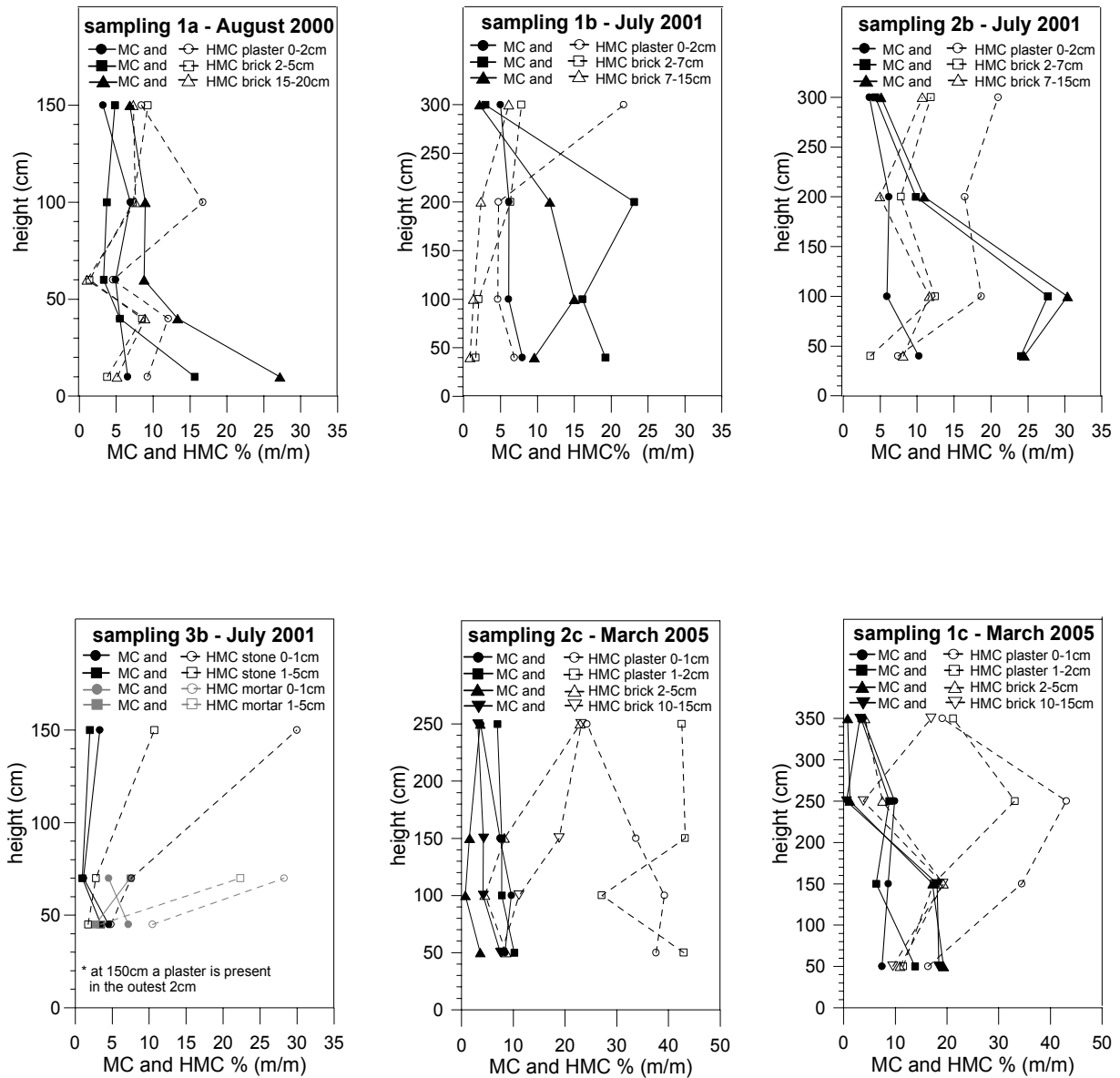


Figure 4.10 Moisture (MC) and hygroscopic moisture content (HMC) at different locations in the church as measured in the three sampling campaigns

The XRD analyses (table 4.1) showed the presence of halite (at the upper level of the south wall of the choir and of the plastered column), thenardite (on stone) and sodium carbonates (trona and thermonatrite).

The source of halite is the sea-flooding that enriched both the ground and the masonry with an enormous quantity of sea-salts. The origin of trona is probably the use of cement based plaster and re-pointing in the restoration interventions. The presence of this salt in concrete structures or cement-based mortars contaminated by sodium chloride has been often reported in literature [Fig76, Cha79, Col81, Nov89, Sar93].

Table 4.1 Results of the XRD analyses. The number of * indicates the quantity of salt present.

n.	material	location	height (cm)	Calcite	Trona	Thermo natrite	Thena rdite	Quartz	Halite
39a	pavement	inside	0	***				*****	
37a	effl. on plaster	inside	0	**	*	***		**	
36a	effl. on plaster	inside	25	**	*	***		**	
38a	effl. on plaster	inside	30	**	**	*		**	
5b	effl. on plaster	inside	250	**				**	***
6b	effl. on plaster	inside	200	**				**	***
40a	effl. on stone	inside	30-60	**			***	**	***
41a	effl. on stone	inside	90	**			*****	**	
31b	effl. on stone	inside	40	*	*		****	*	*
43a	under repoint.	outside	60	*		***		**	
44a	effl. on brick	outside	60	**	*	**		**	
42a	effl. on mortar	outside	150	***				*****	
1b	effl. on mortar	outside	160	***	*			***	

Environmental Scanning Electron Microscope (ESEM) investigations by means of Philips XL-FEG SEM were performed on plaster scales sampled at 350 cm from the ground level on the south wall of the choir. The ESEM photomicrographs show that salts grow preferentially at the aggregate-binder interface (figure 4.11); the crystals on the outer surface of the scales are often whisker like (figure 4.12), as expected in case of evaporation from dense substrate with low moisture content [Arn85b].

Energy Dispersive X-ray (EDX) analyses on the scales confirmed the presence of NaCl crystals in the plaster (figure 4.13).

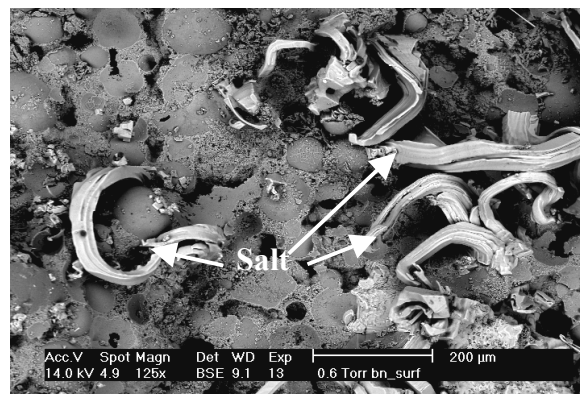
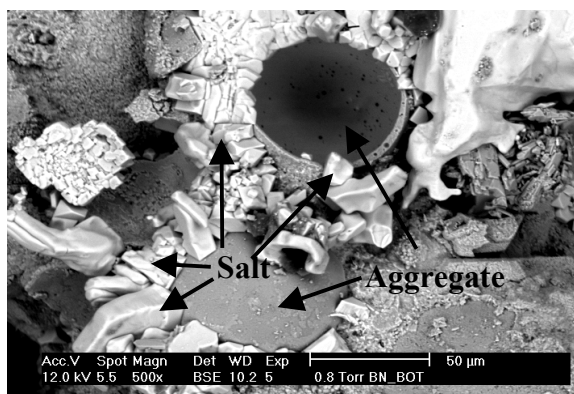


Figure 4.11 (left) ESEM photomicrograph showing salt crystals at the aggregate/binder interface

Figure 4.12 (right) ESEM photomicrograph showing whisker crystals on the surface of plaster scale

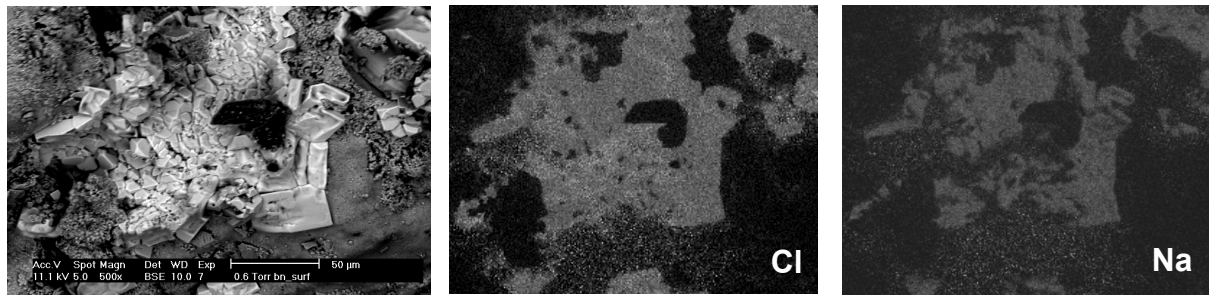


Figure 4.13 ESEM photomicrograph (left) and EDX mapping of Cl (middle) and Na (right) ions: the overlapping of the Cl and Na mappings indicates the presence of NaCl

4.5.3 Assessment of material properties

The properties of both plaster and substrate were studied by means of several techniques.

The properties of the plaster were studied on specimens prepared in laboratory by applying the same ready-to-use plaster on a fired-clay brick substrate. The structure of the plaster was studied by ESEM, on a broken section of the plaster, and by Polarized Fluorescent Microscopy (PFM) on a thin section impregnated with fluorescent resin.

Both the ESEM (figure 4.14) and the PFM photomicrographs (figure 4.15) show the presence of large voids, with the binder not filling completely the spaces between the aggregates.

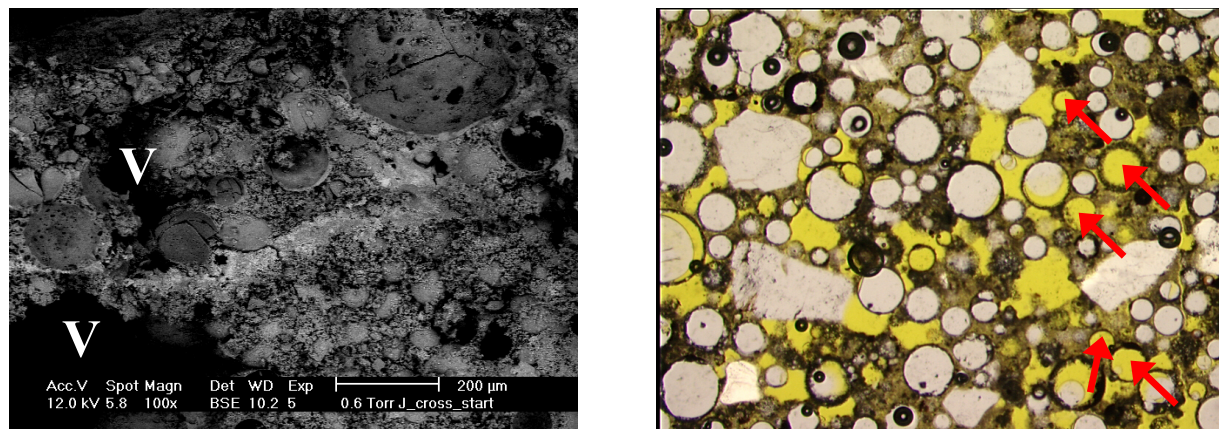


Figure 4.14 (left) ESEM photomicrograph of a broken section of the plaster: large voids (V) are visible

Figure 4.15 (right) PFM photomicrograph of a thin section of the plaster (size: 2.7 mm x 1.8 mm): the yellow area indicates the open porosity; the arrows indicate spheres filled with resin.

The composition of the plaster was investigated by means of PFM, EDX, XRD (X-ray diffraction) and FTIR (Fourier Transformed Infrared Spectroscopy) analyses. The plaster resulted to be composed of a cement binder and two types of aggregate: small quantities of siliceous aggregate and a large part of hollow spheres of different grain size. The XRD analyses showed the light aggregate to be constituted by mullite ($\text{Al}_6\text{Si}_2\text{O}_{13}$). The hollow

spheres have very thin porous walls (figure 4.16) and seem to be not accessible to moisture transport. However, ESEM photomicrographs of the light aggregate after its separation from the binder show that some of the hollow spheres may be broken and become therefore accessible to water (figure 4.17). Some broken spheres filled with fluorescent resin are also visible in the thin section (figure 4.15).

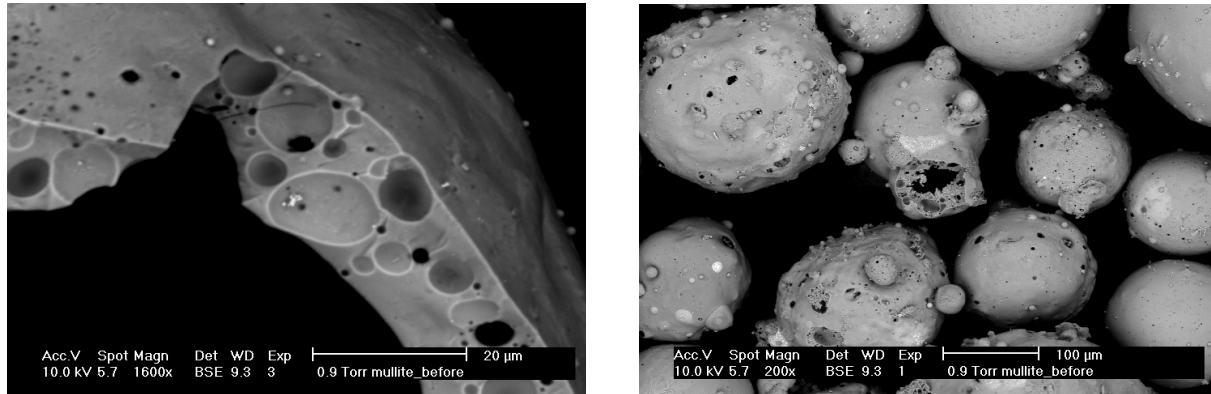


Figure 4.16 (left) ESEM photomicrograph of the porous wall of a mullite sphere

Figure 4.17 (right) ESEM photomicrograph of the mullite spheres after separation from the binder: some of the spheres are broken

FTIR analysis identified the presence of an additive, most likely modified cellulose, in the plaster. The additive was probably added to improve the curing process by retaining water and limiting shrinkage and crack formation during drying.

The porosity and the pore size distribution of the plaster were measured by water absorption method (according to the RILEM Recommendation CPC 11.3), Mercury Intrusion Porosimetry (MIP) and point counting. The open porosity of the restoration plaster resulted to be 58% V/V, measured by MIP as well as by immersion. The porosity is mainly constituted by large (>10 μm) and very small pores in the range of capillary condensation (< 0.1 μm) (figure 4.18). Some questions arise when considering the extremely high value of porosity measured for this plaster: either damage (the thin walls of hollow spheres may be broken due to the pressure) or deformation of the structure of the spheres may be supposed. Both hypotheses may explain the increase in the range of the smaller pores measured in the cumulative intrusion curve.

Point counting measurements were performed on a thin section in order to further investigate the porosity. These measurements allow defining both closed and open porosity; because of the detection limit of the optical microscope, only pores larger than 5 μm can be detected. The closed porosity (corresponding to the hollow spheres) constitutes 28% of the area; voids and large pores amount to about 19% of the surface. This last value is comparable to the porosity obtained by MIP when considering only pores larger than 5 μm.

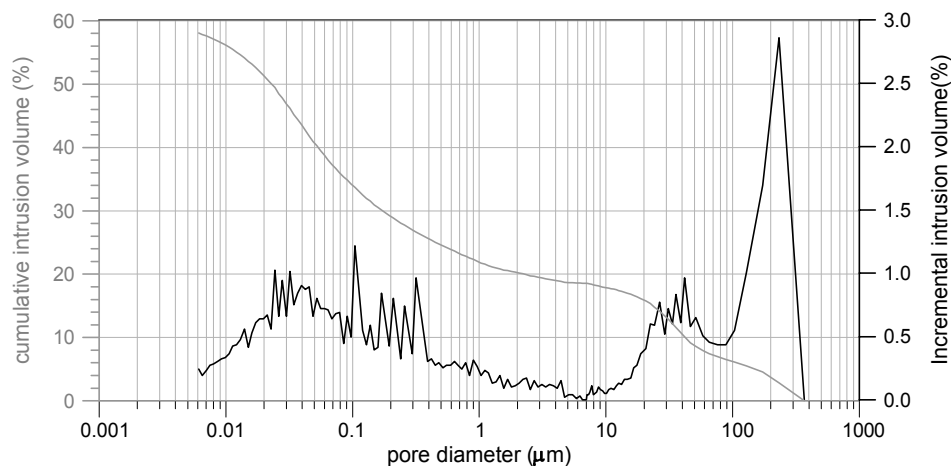


Figure 4.18 Open porosity and pore size distribution of the plaster as determined by Mercury Intrusion Porosimetry

The pore size distribution of the material strongly influences its absorbing and drying behaviour. Because of the presence of small pores, the plaster shows a slow absorption and drying in comparison, for example, to a lime-cement mortar (figure 4.19). Besides, the presence of the cellulose, which can retain water even in secondary moistening, contributes to explain the extremely slow drying of the restoration plaster.

The very slow transport of the salt solution to the surface determines the conditions for crystallization of the salts inside the plaster. The crystallization of the salt in the outer layer of the plaster, instead of on its surface, is confirmed by the in-situ monitoring: on the church wall mainly crypto-florescences are visible, pushing out scales few mm thick.

The properties of the brick substrate were measured on a core sampled from the south wall of the choir at 105 cm from the ground level.

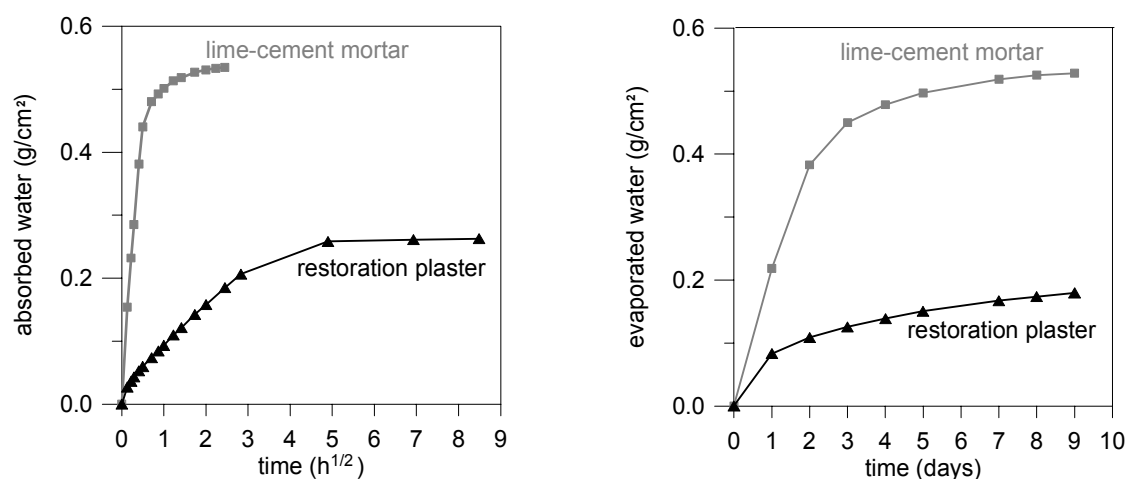


Figure 4.19 Water absorption by capillarity (left) and drying behaviour (right) of the restoration plaster in comparison to a lime-cement mortar

The total porosity and pore size distribution were measured by MIP on a desalinated brick sample. Figure 4.20 shows that the brick has a high total porosity (almost 40%), with a large percentage of pores with a radius of 5 μm . Considering the pore size distribution of the brick and of the plaster, knowing that the moisture transport occurs from large to small pores [Tam80], it can be concluded that in this case the transport of salt solution from the coarse porous substrate to the fine porous plaster is enhanced (figure 4.21). During drying, the salt solution will move from the substrate to the plaster where, due to evaporation, the salt will crystallize and accumulate in the plaster layer [Pet04]. It can be therefore concluded that a coarse substrate constitutes a risk for the occurrence of damage to the fine porous plaster applied on it.

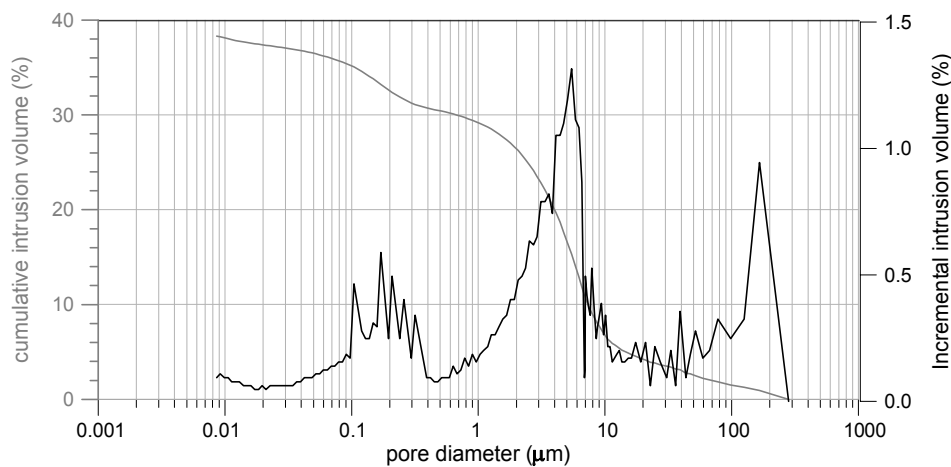


Figure 4.20 Open porosity and pore size distribution of the brick substrate as determined by MIP

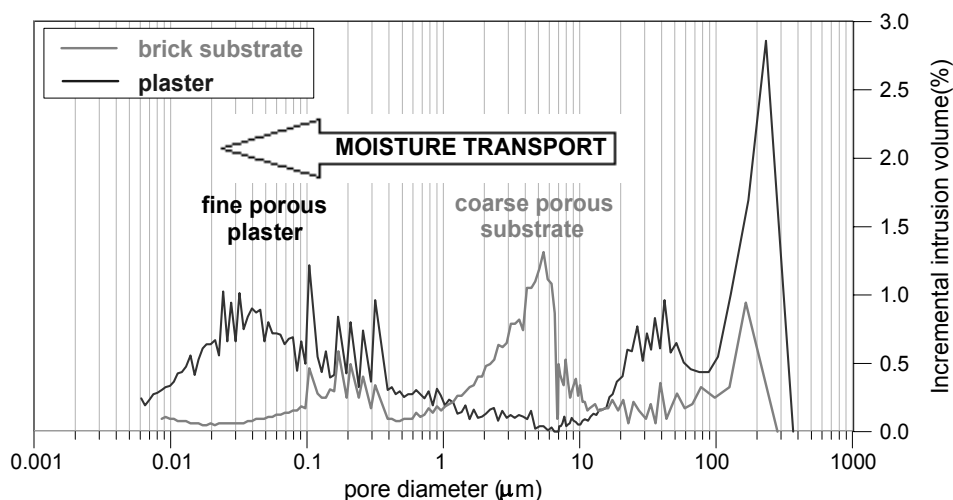


Figure 4.21 Pore size distribution of the brick substrate and of the plaster: the pore size distribution of the substrate/plaster combination determines the moisture transport from the coarse substrate to the fine plaster

4.6 Monitoring of the damage and of the environmental conditions

It is known that decay of porous material due to salt can only occur if dissolution-crystallization cycles of the salt happen, therefore both salt and moisture are necessary elements for the occurrence of the damage.

On the south wall of the choir rising damp is present up to 200-250 cm from the ground level (figure 4.10, sampling 2b and 1c), whereas a high salt load and a serious damage are present on the same wall up to 330 cm. It can be reasonably supposed that the tar layer, present on the wall for about 30 years, limited the evaporation and consequently increased the height of the rising damp. Salts have been therefore in the past transported to a level higher than the present fringe of the capillary rise (figure 4.22).

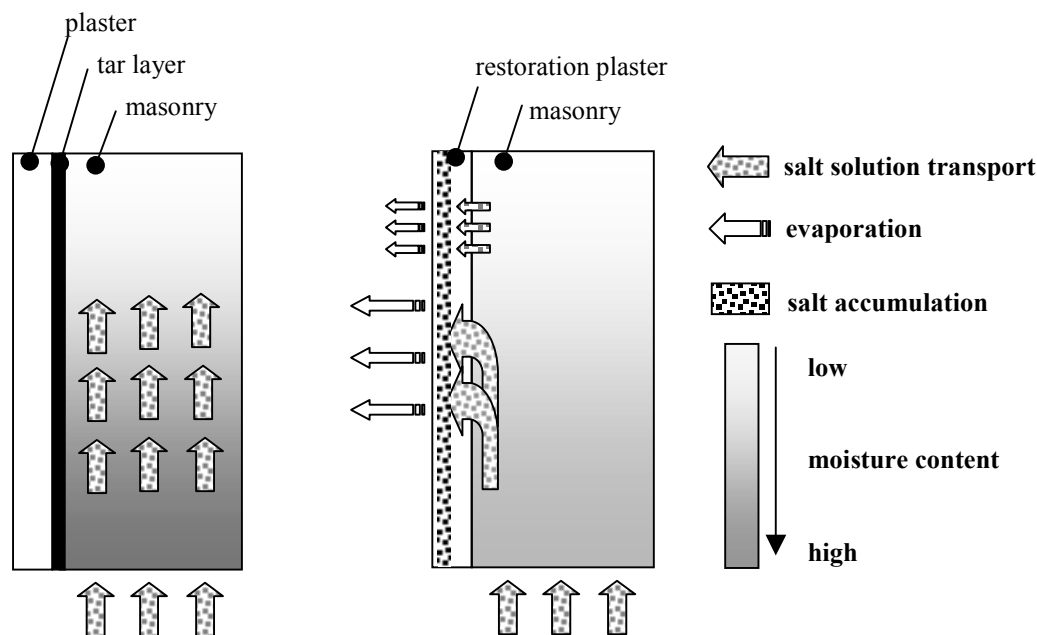


Figure 4.22 Sketch of the situation before (left) and after (right) the restoration of 1991-1994: the removal of the tar layer has allowed the drying out of the masonry and the transport of the salt from the substrate to the plaster

The moisture and salt distribution measured in the two most recent sampling campaigns on the same wall (locations 2b and 1c) supports this theory:

- the height of the rising damp and the moisture content decreased in the recent years due to the removal of the tar layer and to the application of the new plaster (compare sampling 2b and 1c in figure 4.10)
- the salt load in the upper part of the wall (location 1c, height 350 cm) is higher in depth than directly beneath the brick-plaster interface. This suggests that no moisture source is present anymore in depth in the wall, otherwise, due to the evaporation process, salts would be transported towards the surface. It is likely that the moisture present in the wall

at the moment of the application of the plaster and the water supplied by the fresh plaster have allowed the transport of the salt present in the outer layer of the brick into the plaster. Then, the absence of further moisture supply has inhibited the transport to the surface of the salt present in depth in the wall.

However, the presence of salt does not cause any damage in absence of moisture: a moisture source has to be found in order to explain the fast development of the decay in the area no longer reached by the rising damp (figure 4.23). Because of the high hygroscopicity of halite (the main salt present in the masonry) and of the plaster itself, it was supposed that RH changes could play a fundamental role in the damage, supplying the moisture necessary to activate the salts. A parallel monitoring of the environmental conditions and of the damage development was set up to prove this hypothesis.

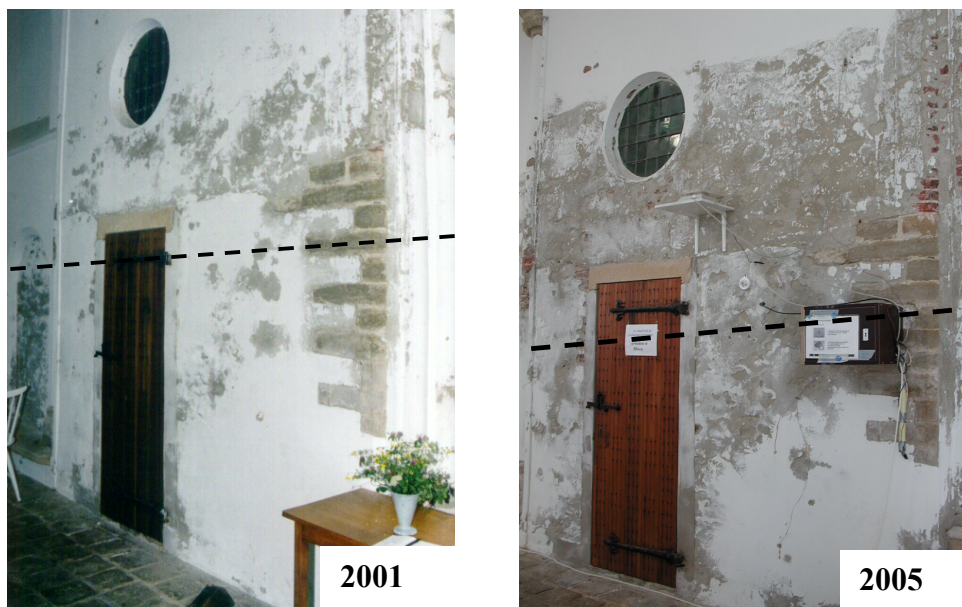


Figure 4.23 Evolution of the damage between 2001 and 2005; the dashed lines indicate the maximum height reached by the rising damp at the moment of the sampling

The monitoring of the environmental conditions in the choir started in year 2000. The data were obtained by two sensors measuring the temperature and RH of the air inside and outside the church, and by four thermocouples measuring the surface temperature of the south wall of the choir. A scheme of the monitoring system inside the church is reported in figure 4.24.

On the basis of the RH of the air and of the surface temperature of the wall, the RH at the wall surface can be calculated. The following procedure is used [Cas93].

The maximum concentration (c'_{air}) in g/cm^3 of moisture in air at a certain temperature of the air (T_{air}) is calculated:

$$c'_{\text{air}} = 6.18 \exp(T_{\text{air}}/18.2) - 1.32 \quad (4.1)$$

The actual moisture concentration in the air (c_{air}) in g/cm^3 is calculated:

$$c_{\text{air}} = c'_{\text{air}} * \text{RH} / 100 \quad (4.2)$$

The maximum moisture concentration at the surface (c'_{surf}) in g/cm^3 at a certain temperature (T_{surf}) is calculated:

$$c'_{\text{surf}} = 6.18 \exp(T_{\text{surf}}/18.2) - 1.32 \quad (4.3)$$

From the obtained data, the RH on the surface (RH_{surf}) in % is calculated:

$$\text{RH}_{\text{surf}} = (c_{\text{air}} / c'_{\text{surf}}) * 100 \quad (4.4)$$

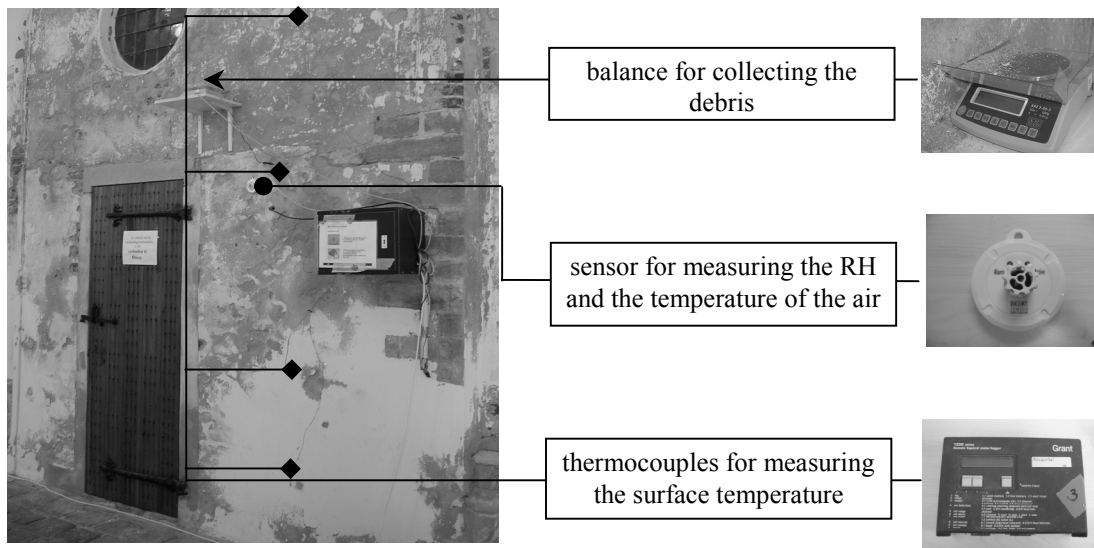


Fig 4.24 Monitoring system placed on the south wall of the choir

The obtained values show that the surface RH is not high enough for surface condensation to occur. However, the RH varies often across 75.5%, i.e. the equilibrium RH of NaCl, the main salt present in the wall (figure 4.25). This means that, when the RH increases over this value, the salt adsorbs moisture from the air and (partially) dissolves; when the RH decreases the water evaporates again and the salt crystallizes. These cycles, which occur several times in a month, lead to stresses and fatigue in the plaster, causing damage.

The monitoring of the damage has been performed photographically and, from April 2003 to March 2005, by continuously collecting and weighing the debris falling from the wall, with the use of a balance placed on the wall and connected to a laptop computer.

From the photographical monitoring it can be seen that the decay of the plaster has visibly increased (figure 4.23) during the last years. The damage has developed from peeling of the paint layer to sanding and crumbling of the plaster and, sometimes, of the substrate.

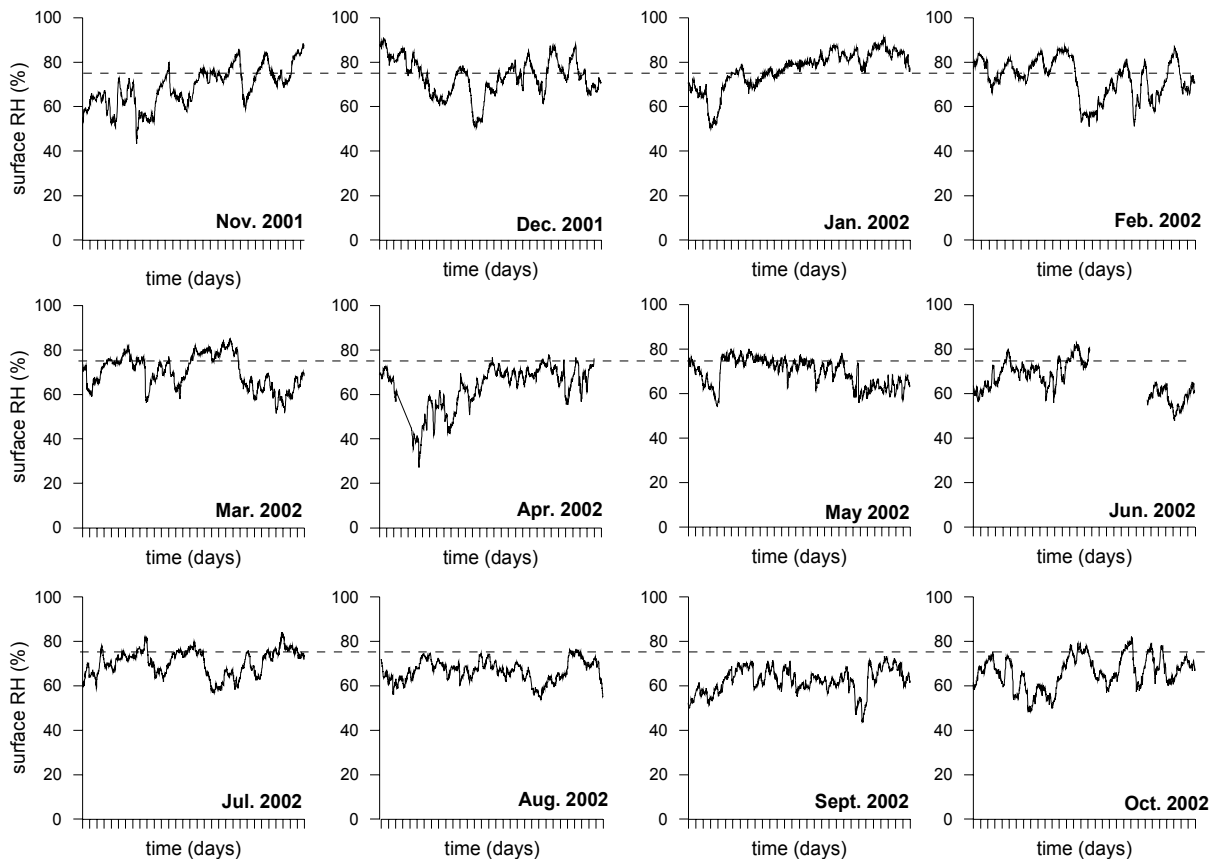


Figure 4.25 RH at the surface of the south wall of the choir wall at the height of 300 cm from the ground level in the period from November 2001 to October 2002. The dotted lines indicate the RH of crystallization of NaCl

The combined monitoring of the damage (measured as debris falling from the wall) and of the environmental conditions showed the relevance of the RH changes in the development of the decay affecting the plaster.

The monitoring pointed out that most of the debris is falling on the balance plate during the period of high RH (figure 4.26) (for precision, it has to be mentioned that the weight registered by the balance is both due to the debris falling from the wall and to the hygroscopic moisture uptake of the debris already present on the balance plate).

The appearance of damage during the period of high RH confirms what observed in other occasions [Kon01]. This is most probably due to the fact that the damage, occurring during the crystallization periods, becomes visible only when the halite, cementing together the de-cohesioned particles of the plaster [Gou74], goes into solution. The cementing effect of the NaCl has also been proved by experiments performed in the ESEM chamber under condition of changing RH through the RH of equilibrium of NaCl.

It is interesting to notice that not only the salt type but also the location of salt accumulation is relevant for the development of the damage. Salts accumulating on the surface have a fast response to RH changes but, being not in the pore spaces, cannot be damaging. Salts present in depth in the material are less sensitive to RH changes of the air; therefore, in absence of other moisture sources, they are not very harmful. Salts accumulating just beneath the surface of a material have a fast response to the RH changes of the air and dissolve and crystallize in the pores of the material causing damage. The salt distribution in the south wall of the choir supports this theory: in the upper part of the masonry (350 cm in sampling 1c and 250 cm in sampling 2c (figure 4.10)) the salt accumulates in the inner part of the plaster, instead of in the outer layer, and no damage is present yet.

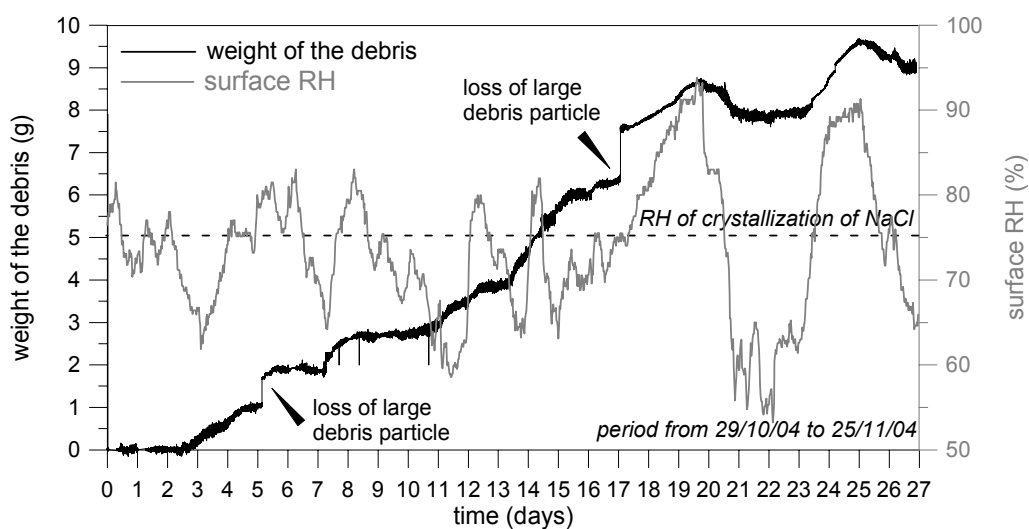


Figure 4.26 Surface RH and weight of the debris falling on the balance plate: the steep increase in the weight of the debris indicates that most of the debris is falling during the high RH periods

The occurrence of dissolution/crystallization cycles due to RH changes will depend, apart from the salt type, on the location of salt in the material (near or far from the surface) and on the length of the RH cycles. In order to cause dissolution or crystallization of salt located in depth in a material, longer periods of high or low RH will be necessary than for salt crystallized near the surface. From this it can be concluded that RH cycles of short duration will be risky for salt accumulating near the surface, whereas they will be not harmful for salt crystallizing in depth.

4.7 Discussion and conclusions

The research described in the present chapter shows that several factors may threaten the performance of a plaster in the field:

- The moisture load of the substrate: the presence of rising damp together with the high total porosity of the substrate lead to a permanently high moisture content. The lack of

any intervention against rising damp before the application of the plaster is one of the reasons of the unsatisfactory performance obtained.

- The salt load of the substrate: the salt load in the investigated case study is extraordinary high and it is still increasing due to the rising damp transporting salty water from the ground to the wall.
- The pore size distribution of the substrate/plaster combination: the substrate has a high total porosity, mainly constituted by coarse pores. The fine porous plaster can therefore easily extract, by capillary suction, the salt solution from the substrate. During drying the salt will therefore accumulate in the plaster. The very slow moisture transport of the restoration plaster causes the crystallization of the salt just beneath the surface of the plaster. This results in a serious damage consisting in scaling and spalling.
- The environmental conditions: serious damage may be caused by the mere presence of RH changes, even in absence of any other moisture source. This is likely to occur if salts, having a RH of crystallization in a range easily crossed by the air RH, accumulate just beneath the surface of the material. In presence of RH changes through the RH of crystallization, the salt dissolves and re-crystallizes in the pores of the material causing damage.

In the described situation, an intervention aiming at preventing a further development of the decay, may either consist of a strict control of the indoor climate or of interventions in the material and in the source of liquid water. In the context of this research project the interventions considered are limited to the material and the source of liquid water.

In order to slow down the development of the damage, stopping the rising damp, which constitutes a relevant source of moisture and sea-salts for the lower parts of the wall, should be considered. As far as the plaster is concerned, in the current situation the hygroscopic effect due to RH changes is clearly increased by the presence of the salt near the surface. A salt accumulating plaster, keeping the salt far from the surface, may offer a better solution; it will slow down the hygroscopic moisture uptake and probably work better in this situation where the RH changes are the main cause of the damage at the upper part of the wall.

Chapter 5

Towards an effective weathering test: effect of environmental conditions on damage

5.1 Introduction

Laboratory weathering tests are of primary importance in the field of restoration as they provide a means of estimating, in a relatively short time, the long-term performance of materials when applied in practice. Consequently, they are an important step in the process of formulating effective intervention methods.

Accelerated tests to simulate the damage caused to porous materials by soluble salts such as sodium sulfate are well known and highly effective. However, when using sodium chloride the existing test methods are not particularly successful, since, while this salt is known to cause serious damage to cultural property, this behaviour is usually not replicated in the laboratory.

One of the reasons for the discrepancy between laboratory results and in situ observations may be found in the different environmental conditions to which test samples and real objects are exposed. Many existing standards for laboratory weathering tests for sodium chloride (for example RILEM MS-A.1 and the WTA procedures) adopt mild temperature and stable RH conditions, whereas temperature and RH in practice may vary in a wide range. In practice drying is often faster than in the laboratory, due to the presence of high temperature, low RH and wind: this may cause crystallization at higher supersaturation and consequently higher crystallization pressure and more severe damage [Sch99]. Moreover, in the field, both the temperature and the RH may vary several times in a day resulting in repeated dissolution and crystallization of the salt in a short period.

In spite of the fact that several experiments on salt crystallization are reported in the literature, most of these researches aimed at either classifying different materials according to their susceptibility to salt decay or at ranking the harmfulness of different salts, rather than developing a more effective salt weathering test. The present research is undertaken with the specific aim of improving the effectiveness of salt weathering tests using NaCl.

In the preliminary phase of the research the environmental parameters to be considered have been selected on the basis of the literature data (section 5.2) and of the results from the case studies (section 3.7). Next the effect of the selected environmental parameters on NaCl decay has been studied:

- the influence of low RH, high temperature and air flow on the damage has been evaluated (section 5.4);
- the effectiveness of RH changes in causing damage has been assessed by comparing different lengths and ranges of RH cycles (section 5.5).

The obtained results have been combined to define an accelerated weathering test (section 5.6)

The research has not been limited to the development of an accelerated test, but the effects of the environmental conditions on the drying behaviour, the salt distribution in the material and the location of crystallization in the pores have also been investigated. Several methods and analysis techniques have been used: Hygroscopic Moisture Content (HMC) measurements (see appendix 3) and chemical analyses for the determination of the salt distribution, Mercury Intrusion Porosimetry (MIP), Environmental Scanning Electron Microscopy (ESEM) and Energy Dispersive X-ray Spectroscopy (EDX) microanalysis for the study of salt crystallization in pores, and XRay- diffraction for the investigation of possible chemical reactions occurring between the NaCl and the components of the materials.

The reliability of the proposed procedure has been assessed comparing the seriousness of the damage and the decay patterns obtained in the accelerated weathering tests with the situations observed in the field (section 5.6.3).

5.2 Literature overview on salt weathering tests

Several test procedures have been developed to assess, in the laboratory and in a short time, the susceptibility of building materials to salt decay. Some of these methods have resulted in codes and recommendations normally used for the evaluation of the durability of materials: examples are the Recommendation RILEM MS-A.1 and MS-A.2, WTA, ASTM C88-99a and EN 12370.

The present section does not aim to give an exhaustive overview of all the existing test methods (this can be found elsewhere [Gou97]), but to provide, on the basis of the experimental data reported in literature, indications on the most promising parameters to adopt for developing an effective weathering test in the specific case of NaCl.

Effect of temperature

The effect of temperature on the decay due to NaCl has been studied by Binda and co-authors [Bin85]: in their experiments NaCl damage is enhanced by the use of high temperatures (60 °C and 105 °C). Similar results are reported in [Riv97].

Effect of RH

The effect of RH on the NaCl damage has been addressed by Rodriguez-Navarro and Doehne [Rod99a]: the use of low RH seems to enhance the decay. According to the authors, the high

supersaturation, due to the enhanced evaporation, at which precipitation occurs, is the reason of the damage. At these conditions, sodium chloride crystallizes as prismatic or acicular crystals, more damaging than the cubic crystals precipitating at higher RH.

Effect of airflow

The use of airflow is not frequent in laboratory weathering tests, notwithstanding the fact that its influence on the evaporation speed may result in crystallization at higher supersaturation and therefore in increased damage. The effect of airflow on salt decay has been mainly studied in relation to the honeycomb weathering. In their laboratory simulation of the honeycomb weathering, Rodriguez-Navarro and co-authors [Rod99b] report an increased salt damage due to the presence of airflow. The authors explain the severe damage by the enhanced evaporation, leading to crystallization at high supersaturation and to precipitation of the salt inside the material (crypto-florescences) instead of at its surface (efflorescences).

Effect of RH cycles

All the experiments mentioned above address the effect of the enhanced evaporation on crystallization damage. Other laboratory researches have considered the influence of RH cycles, causing dissolution and crystallization of the salt, on the development of the decay. Experiments using RH cycles have been mainly performed on salts having more hydrated states, with the aim of verifying the relevance of the hydration mechanism for the occurrence of the damage [Bin85, Bin87]. In case of NaCl, which does not hydrate at ambient temperature, the effect of RH changes has not been often investigated.

Experiments on salt weathering using temperature and RH cycles have been performed by Goudie and are summarized in [Gou97]. The results of his experiment show that NaCl is not damaging, even in presence of RH and T cycles.

On the other hand, Faria Rodriguez [Far05] was able to obtain damage in sodium chloride contaminated mortars by applying RH cycles between 40 and 90% RH at the constant temperature of 20 °C.

Even RH cycles below the RH of equilibrium of the salt (mixture) present in the material have been shown to produce damage [Num01]. Besides, the effect of NaCl on the hygric dilation of clay containing sandstone [Wen92, Sne97] and brick [Wen02] underlines the relevance of RH changes in the damage due to NaCl.

In practice RH changes through the RH of equilibrium of the salt present in the wall have been proven to cause severe damage even in absence of any other moisture source [Kon01, chapter 4 of this thesis].

From this literature overview, it can be concluded that two main factors seem to enhance NaCl damage:

- a fast drying, obtained either by high temperature, low RH or air flow;
- variable RH conditions.

Notwithstanding the fact that these conclusions can be drawn from the literature, generally the focus of the described experiments was either ranking of different salts according to their

aggressiveness or defining the susceptibility of different materials to salt decay. The present research aims at investigating systematically the effect of each environmental factor on the NaCl damage and to combine the results obtained with the ultimate goal of defining an effective accelerated weathering test.

5.3 Materials

The tests described in the following sections have been performed on three types of materials: a lime-cement mortar, a fired-clay brick and a cement-based restoration plaster. These materials were selected for the following reasons:

- they are known from practice to suffer from salt damage;
- they are commonly used materials in the Netherlands, therefore the results of the test can be verified by comparison with practice;
- they are different in composition, mechanical strength and physical properties, offering a large range on which the effectiveness of the proposed test can be verified. The lime-cement mortar is expected to be easily damaged during the weathering test and it constitutes therefore a sort of reference material; the cement-based restoration plaster is a product developed to be resistant to salt damage and it is therefore expected to withstand salt decay better than the other two materials.

The properties of the selected materials have been investigated before starting the tests. This has been done not only because of the necessity of knowing their main properties, but also because changes in some of these properties (for example pore size distribution) after the test may provide information on the salt crystallization process.

5.3.1 Composition and preparation

Lime-cement mortar

The lime cement mortar was prepared by mixing hydrated lime, blast furnace slag cement and siliceous sand in the ratio 4:1:20 in volume. Aggregate of “gap graded” grain sizes, between 0.5 and 1 mm, was selected, in order to obtain a coarse porous mortar. The water content of the fresh mortar was about 20% m/m corresponding to a workability of 170-175 mm measured using a flow table according to the recommendation UNI 7044-72.

Since the physical properties of the mortar are greatly influenced by the liquid moisture uptake of the substrate on which it is applied [Gro93, Wij00], slabs of a size of 10x20x2 cm were prepared not in a mould but on a brick substrate, from which they were detached after one day. A filter paper was used between the substrate and the plaster to facilitate the detachment.

The lime-cement mortar specimens were stored at 20 °C / 65% RH for 2 weeks, and subsequently dried at 30 °C for 2 days and carbonated in a cabinet at 20 °C / 50% RH and 0.3% CO₂, according to a procedure defined in previous experiments [Lub03]. After 15 days the complete carbonation of the specimens was checked by spraying with phenolphthalein at freshly broken cross section.

Mortar specimens of size 4x4x16 cm were prepared in a mould, stored at 65% RH for 2 weeks and artificially carbonated in a cabinet at 20 °C / 50% RH and 0.3% CO₂. Completely carbonated specimens were tested for flexural and compressive strength according to the EN

1015-11. Because of the weakness of the mortar a loading rate of 5 N/sec and 50 N/sec was applied in the bending and compressive test, respectively. An average flexural strength of 0.1 N/mm^2 and a compressive strength of 0.3 N/mm^2 were measured, indicating that this mortar is a very weak material indeed.

Restoration plaster

The restoration plaster (Jahn M60, type Cura) was prepared in the laboratory adding water to the ready-to-use aggregate/binder mix provided by the producer until a workability of 170-175 mm was obtained. The same preparation procedure was followed as for the lime-cement mortar, but in this case the plaster was stored at 20°C 98% RH for 15 days in order to achieve the required mechanical strength. The composition of this ready-to-use plaster, apart from the presence of cement binder, was unknown. An in-depth study of the plaster composition was therefore carried out preliminarily, to define aggregate type and amount. Thin sections of the plaster were prepared and inspected by means of a Polarized Fluorescent Microscope (PFM), broken cross sections of the plaster were studied in the ESEM. The PFM photomicrographs of the thin section (figure 4.15) show the presence of two types of aggregate: a siliceous aggregate and a hollow aggregate. The hollow aggregate, shown by EDX analyses to be composed of Al and Si, has been defined by XRD to be constituted by mullite ($\text{Al}_4\text{Si}_2\text{O}_{10}$). The mullite spheres are generally closed (figures 5.1 and 5.2) and do not take part in the moisture transport. Only few of the spheres may be broken and accessible to water and salt solution. Therefore it can be concluded that salt cannot accumulate in the light aggregate.

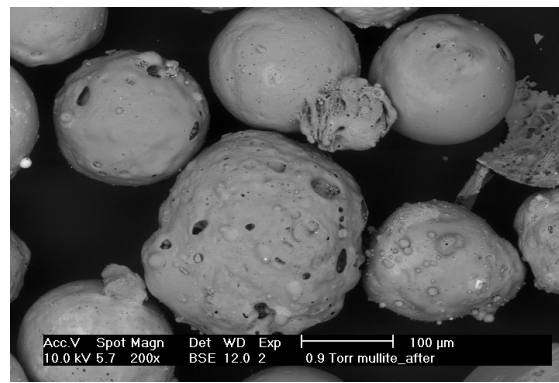
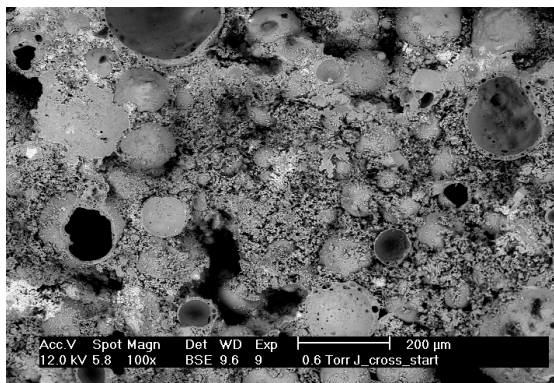


Figure 5.1 (left) ESEM photomicrograph of the mullite spheres in the plaster

Figure 5.2 (right) ESEM photomicrograph of a mullite sphere; the spheres look not accessible to water

Fourier Transformed Infrared Spectroscopy (FTIR) analyses have been performed by the Instituto Eduardo Torroja de Ciencias de la Construcción (Madrid, Spain). These have identified the presence of an additive, most probably cellulose, in the plaster. This additive has been probably mixed in the plaster to improve the curing process by retaining water and limiting shrinkage and crack formation during drying.

Fired-clay brick

The selected brick is a commercial product in the Netherlands, therefore its properties are certified to respect the code NEN 2489 for mechanical strength and salt (SO_4^{--}) content.

The mechanical tests performed on five brick specimens of a size of 4x4x16 cm give an average flexural strength of 3.1 N/mm² and an average compressive strength of 13 N/mm² (loading rate: 200 N/sec for the bending test and 50 N/sec for the compressive test).

5.3.2 Physical properties

Porosity and especially pore size distribution are of crucial importance for moisture/salt transport and for damage due to salt crystallization. For this reason the total porosity and the pore size distribution of the selected materials have been investigated and related to the measured water absorption and drying behaviour.

Lime-cement mortar

The properties of the lime-cement mortar are summarized in table 5.1. The difference between the total porosity measured by MIP and by immersion may be explained by the presence of large voids (larger than 130 μm) that are not measured by the MIP. The pore size distribution is bi-modal (figure 5.3), with peaks at 90 μm and 0.6 μm . Pores of size between 0.1 and 4 μm constitute almost 60% of the total porosity. No relevant amount of pores smaller than 0.1 μm is present.

Table 5.1 Physical properties of the selected materials

Properties	Method	Lime-cement plaster	Restoration plaster	Fired-clay brick
density [kg / m ³]	by saturation at atm pressure*	1795	1029	1691
open porosity [%V/V]		32.3	61.1	36.2
density [kg / m ³]	by vacuum saturation**	***	1003	1699
open porosity [%V/V]		***	59.5	36.7
density [g / ml]	by MIP	1.8-1.9	1.0	1.6-1.7
open porosity [%V/V]		27.4-27.8	58.0	22.0-27.6
open porosity [% of surface]	by point counting	-	19	-
closed porosity [% of surface]		-	28	-
WAC [Kg/(m ² h ^{0.5})]	capillary rise	6.4	0.8	18.2

* according to [Klu94]

** according to RILEM CP 11.3

*** for this type of materials the difference between porosity measured after saturation at atmospheric pressure and under vacuum is not relevant, therefore the measurement under vacuum was not performed

This pore size distribution results in a Water Absorption Coefficient of $6.4 \text{ kg}/(\text{m}^2\text{h}^{0.5})$ measured, according to the European Standard prEN 1015-18, on $5 \times 5 \times 2 \text{ cm}$ specimens. Thanks to its pore size distribution (absence of very fine pores and high percentage of pores effective in capillary rise [Men92]) the lime-cement mortar absorbs and dries out fast (figure 5.4 and figure 5.5).

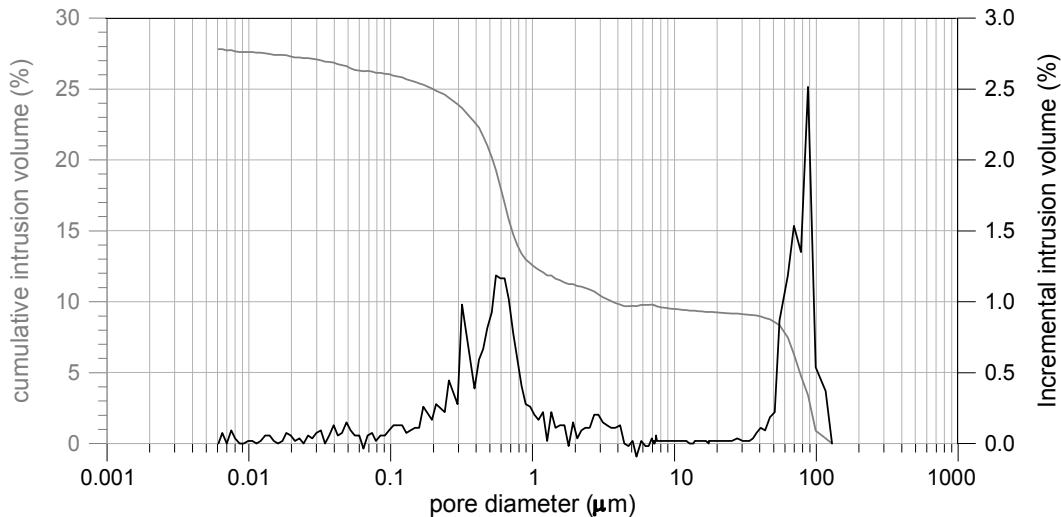


Figure 5.3 Pore size distribution and open porosity of lime-cement mortar measured by MIP

Restoration plaster

The properties of the restoration plaster are summarized in table 5.1. The open porosity of the restoration plaster measured by MIP (figure 5.6) and by immersion under vacuum resulted to be 58% V/V and 59% V/V respectively. The porosity is mainly constituted by large pores (pores larger than $10 \mu\text{m}$ constitute about 1/3 of the total porosity) and by very small pores in the range of capillary condensation.

Some questions arise with respect to the very high value of the open porosity of this material: either damage (the thin walls of hollow spheres may be broken due to the pressure) or deformation of the structure of the spheres may be supposed. Both hypotheses may explain the increase in the range of the smaller pores measured in the cumulative intrusion curve. The fine pores present on the mullite walls may also contribute to the amount of fine porosity.

To further investigate the pore size distribution, MIP measurements were performed on the mullite spheres only. The following procedure was used to separate the aggregate from the binder: the plaster powder was sieved and the fraction $<0.125 \mu\text{m}$ was discarded. The material was then dissolved in 5.5 M HCl solution and heated below the boiling point for 15 minutes. The solution obtained was filtered through a medium filter and washed till acid-free with hot water. The filter and the residue were then dissolved in a 100 ml 0.4 M Na_2CO_3 solution and boiled for 15 minutes. Then the solution was filtered through a medium filter using 1.6 M HCl solution and made acid free with hot water. In this procedure no force was applied for dissolving the binder, thus damage to the aggregate structure was avoided.

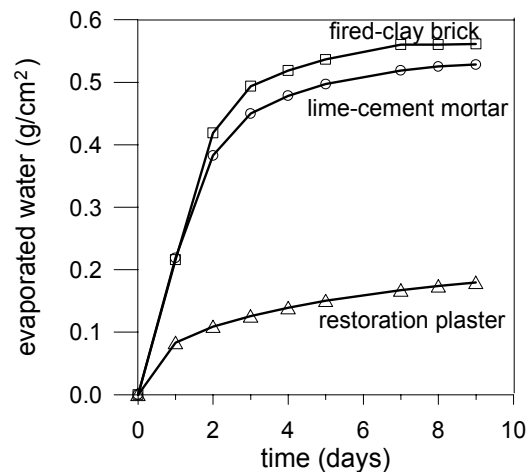
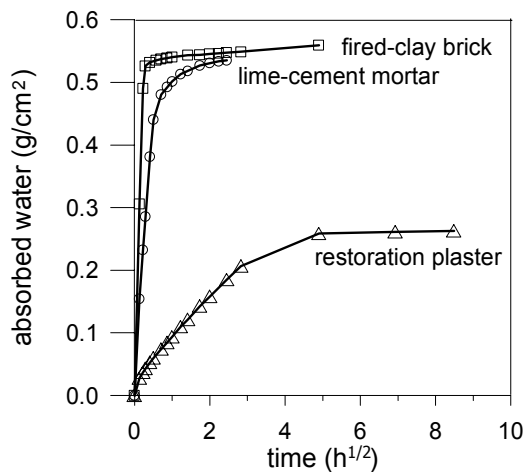


Figure 5.4 (left) Water absorption behaviour of the three materials measured on 5x5x2cm specimens at 20 °C / 50% RH

Figure 5.5 (right) Drying behaviour of the three materials measured on 5x5x2cm specimens at 20 °C / 50% RH

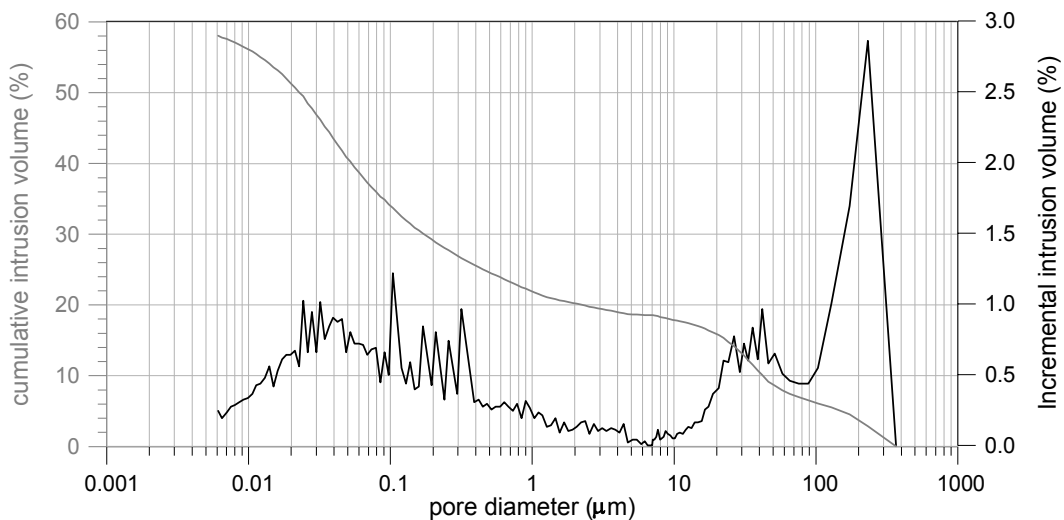


Figure 5.6 Pore size distribution and open porosity of restoration plaster measured by MIP

The MIP performed on the mullite spheres (figure 5.7) shows again an intrusion volume in the range of smaller pores, probably due to breaking and filling of the hollow spheres. The thin section of the plaster, showing some of the mullite spheres filled with resin, further supports this assumption (figure 5.2). It can therefore be concluded that the fine porosity measured in the plaster is due to both the cement binder and mullite spheres (due to breaking and filling of the hollow spheres and to filling up of the fine pores present in the mullite walls).

Point counting measurements by means of an optical microscope (at 100x magnification) were performed on a thin section of the restoration plaster in order to further investigate the

porosity. Using this technique it is possible to differentiate between the closed and open porosity; however, because of the detection limits of the instrument, only pores larger than 5 μm can be detected. The results showed that the closed porosity (corresponding to the hollow spheres) constitutes 28% of the surface of the thin section; while voids and large pores amount to about 19% of the surface. This last value is comparable to the porosity obtained by MIP when considering only pores larger than 5 μm .

The pore size distribution of the material strongly influences its absorbing and drying behaviour: because of the presence of very small pores, the plaster shows a slow absorption ($\text{WAC} = 0.77 \text{ kg}/(\text{m}^2\text{h}^{0.5})$) and drying (figure 5.4 and 5.5). Besides, the presence of the cellulose may further slow down the drying. The effect of the cellulose may be present even when the material, hardened and dried, is wetted and dried again.

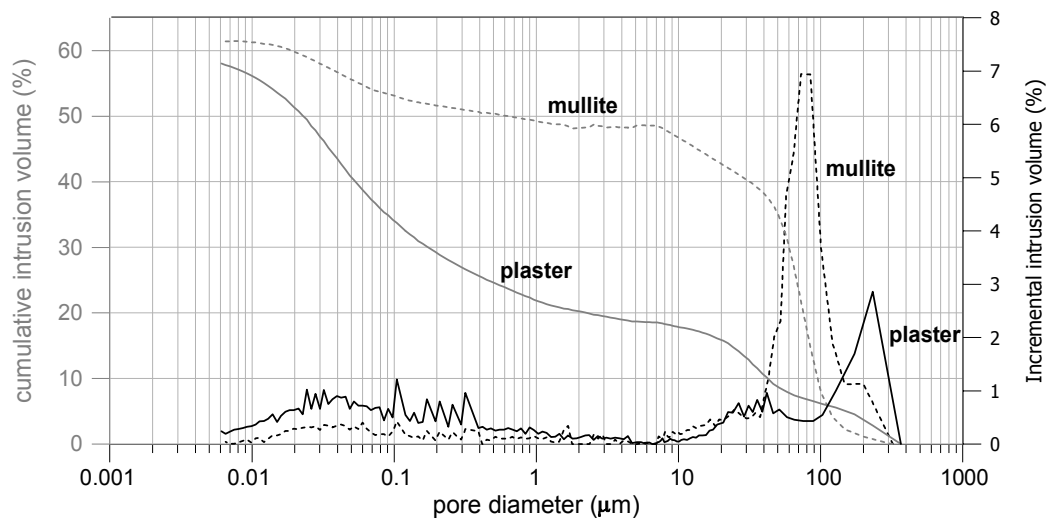


Figure 5.7 Pore size distribution and open porosity of mullite and restoration plaster measured by MIP

Fired-clay brick

The physical properties of the fired-clay brick are summarized in table 5.1. The total porosity measured by immersion at atmospheric pressure and under vacuum do not show significant differences: values ranging from 36 up to 37% V/V were measured in both cases. The total porosity measured by MIP (figure 5.8) is much lower (varying between 22% and 27.6% V/V): this can be due either to the inhomogeneity of the material (the MIP was performed on the surface layer of the brick, which is more dense than the core) and to the possible presence of pores and voids larger than the maximum pore size measured by the MIP (in this case about 300 μm). The pore size distribution shows a clear peak at 3 μm , with more than 50% of the pores in the range between 1 and 5 μm .

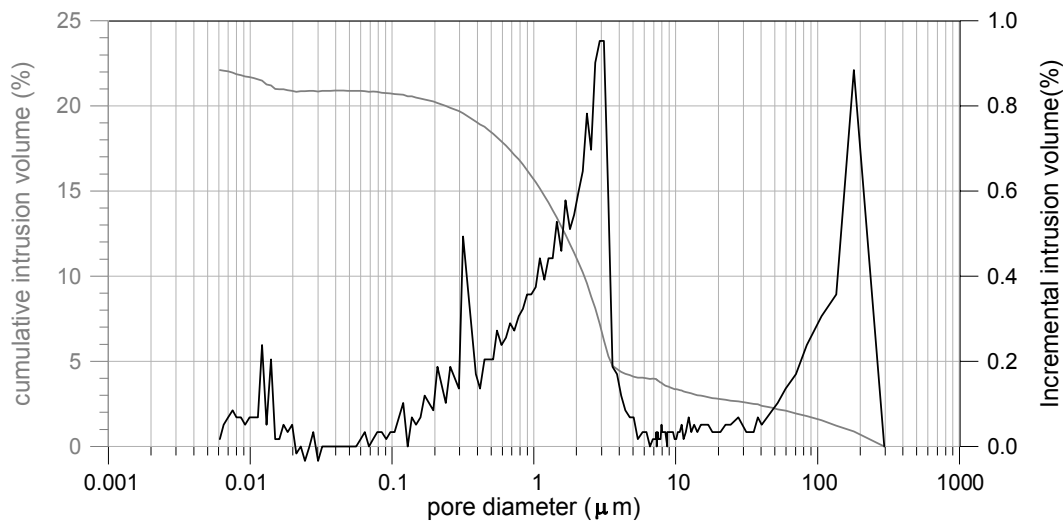


Figure 5.8 Pore size distribution and open porosity of fired-clay brick measured by MIP

5.4 Effect of accelerated drying on sodium chloride damage

In this first phase of the laboratory research the effect of low RH, high temperature and airflow on the drying behaviour and the damage due to NaCl crystallization was investigated. Each of these factors was considered and compared with the reference drying conditions (20 °C / 50% RH).

5.4.1 Test procedure

The specimens used in the weathering test were cut in pieces with dimensions of 5x5x2 cm and were sealed on the 4 lateral sides with epoxy resin. This small size reduces the test period (both saturation with water and drying need less time) and it provides at the same time sufficient surface for a sound evaluation of the damage. Besides, 2 cm is the usual thickness of plasters, a factor that was necessary to consider in the case of the restoration plaster in order to have a realistic test.

The specimens were dried in an oven at 60 °C until constant weight was reached and were allowed to cool down at room temperature before salt contamination. The specimens were contaminated with sodium chloride solution by capillary rise. In case of lime-cement mortar and brick, the quantity of absorbed solution was equal to the Capillary Moisture Content (C.M.C.), i.e. to the amount of water, absorbed by the specimen by capillary rise from the bottom, sufficient to wet the upper surface. In case of the restoration plaster, it was difficult to get the upper surface wet, so the moisture content after 24 h of capillary rise was adopted. The concentration of the solution was calculated in such a way that, for all the materials, a NaCl content of 2% of the dry mass of the specimen was obtained. This salt amount was selected on the basis of previous crystallization experiments [Hee01] and on the basis of the data obtained from the case studies (chapter 3). In table 5.2 the amount of salt solution, salt solution concentrations and salt amounts calculated for the three materials are given.

After contamination with salt solution by capillary rise, the bottom of the specimens was closed with removable tape and the specimens were dried under different environmental conditions. In this way the influence of the different environmental parameters on the moisture/salt transport and on the salt crystallization damage was assessed.

Table 5.2 Amount of salt solution, salt solution concentration and amount of salt calculated for the three materials

Material	amount of solution (w%)	solution concentration (w salt/w solution)	salt in the specimen (% w salt/w specimen)
Lime-cement mortar	7.6	26.3	2
restoration plaster	9	22	2
fired-clay brick	12.5	16	2

The following drying conditions were selected:

- 20 °C, 50% RH (reference)
- 21.5 °C⁵ low % RH (the low RH varied between 0% and a maximum of 20%)
- 21.5 °C⁴, 50% RH, air flow (1.5 m/sec)
- 60 °C, 0% RH

The 20 °C / 50% RH condition was obtained in a climatic room; the 21.5 °C / low RH condition was achieved using silica gel in a box placed in the 20 °C room; the 21.5 °C / 50% RH airflow condition was reached by placing the specimens on a rotating plate in the 20 °C / 50% room; the 60 °C / 0% RH condition was created in an oven using silica gel.

Three specimens were used for each material and drying condition.

The specimens were weighed every week and re-wetted with demineralized water when dry. Since the complete drying of the specimens would have taken a very long time, the specimens were rewetted when 80% of the water had evaporated: this allowed the crystallization of most of the salts and, at the same time, speeded up the test. The amount of water added in the re-wetting was equal to the amount of water added at the start of the experiment.

Any appearance of efflorescence and damage was visually monitored and photographically recorded. After one drying cycle and at the end of the testing period, the specimens were ground. The thickness of each layer was 1 mm in the outer centimetre of brick and restoration plaster and 2-3 mm in the case of the lime-cement mortar; the remaining 1 cm of the specimens was simply cut into 2 parts, each 5 mm thick.

The powder samples obtained were stored at 96% RH for four weeks. The Hygroscopic Moisture Content (HMC) was measured and used as an indication of the NaCl distribution [Lub04a, see appendix 3].

⁵ the increase of 1.5 °C is due to the motor of the ventilator

5.4.2 Results

5.4.2.1 Effect of the environmental conditions on the drying behaviour

The drying behaviour of blank (reference) and salt contaminated specimens at the different environmental conditions was monitored. The effect of the presence of salt and of the different environmental conditions on the drying is discussed in the following sections.

Effect of the presence of NaCl

As expected, a general reduction in the drying rate, in comparison with non contaminated specimens, was observed when salt was present. In figure 5.9 the curves measured at 20°C 50% RH are reported: the NaCl, because of its hygroscopicity, considerably slows down the drying of all materials.

Note that the restoration plaster that is not contaminated with salt does not dry completely even after several weeks, but retains a moisture content of 2.3% (m/m): this behaviour may be due to the presence of the cellulose (see section 5.3.1) or/and to capillary condensation. In fact, since no data are available that rule out the presence of pores smaller than 0.01 μm (allowing condensation at 50% RH [Tam80]), a contribution of capillary condensation cannot be excluded. The moisture content in the salt contaminated specimen is about twice that in the blank specimen after the same period of drying.

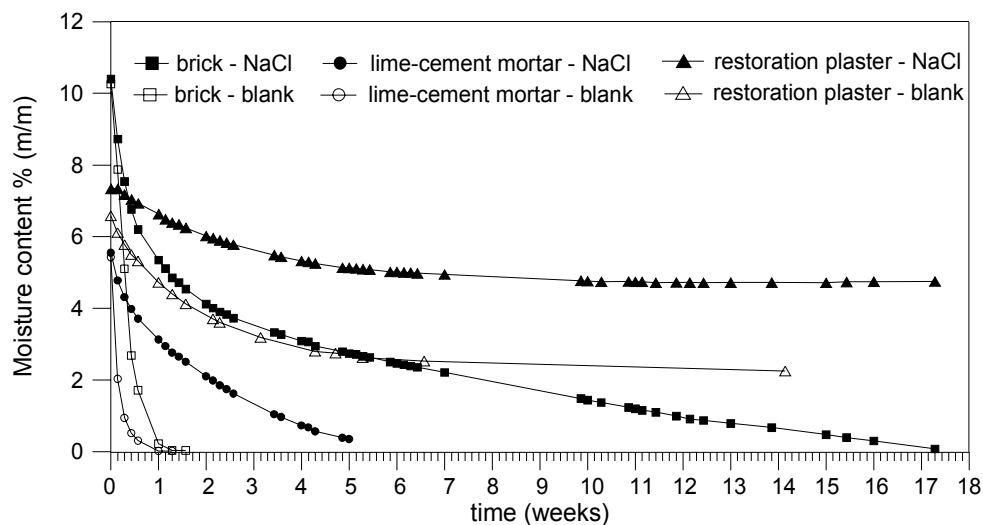


Figure 5.9 Drying curves at 20 °C 50% RH of the three materials, blank and contaminated with NaCl

Effect of the different environmental conditions

The drying rate of the materials depends not only on the material properties and on the presence of salts, but also on the environmental conditions. From the drying experiments performed on specimens contaminated with salt solution, it is clear that the use of a high temperature has the most important effect on the drying speed (figures 5.10-12). By using a high temperature (60 °C) it is possible to reduce the drying period of the lime-cement plaster and of the brick up to 20 times and it is the only way to dry completely the restoration plaster.

The use of low RH and an airflow (1.5 m/sec) has a similar effect in speeding up the drying: up to 3 times shorter drying periods are measured both in brick and lime-cement mortar. In the case of the hygroscopic restoration plaster, the moisture content at the end of the test depends on the temperature and on the RH during drying. The specimen dried at low RH shows a final moisture content that is lower than specimens dried at 50% RH (with or without air flow). This difference the final moisture content may be due both to the 1.5 °C difference in temperature and to the fact that the specimen stored at 20 °C / 50% RH has not reached equilibrium yet.

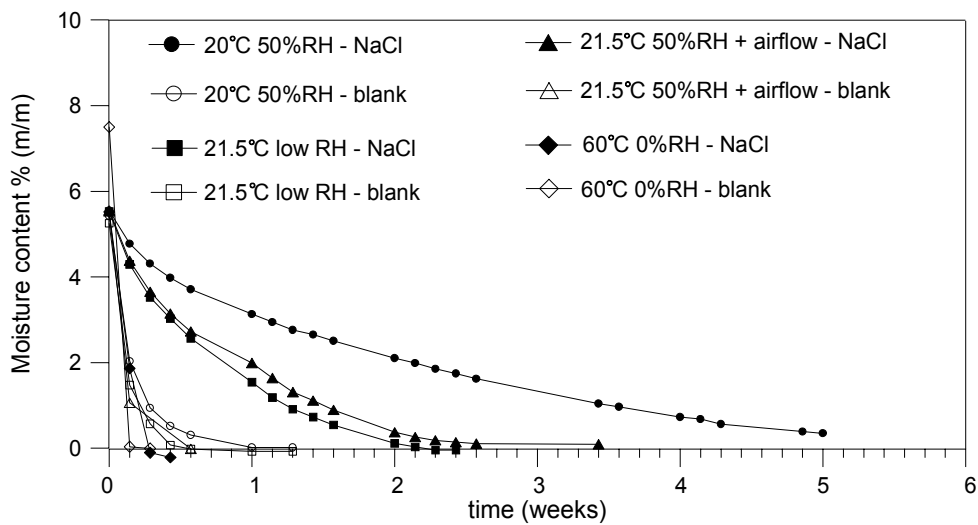


Figure 5.10 Drying curves at different environmental conditions of the lime-cement mortar, blank and contaminated with NaCl

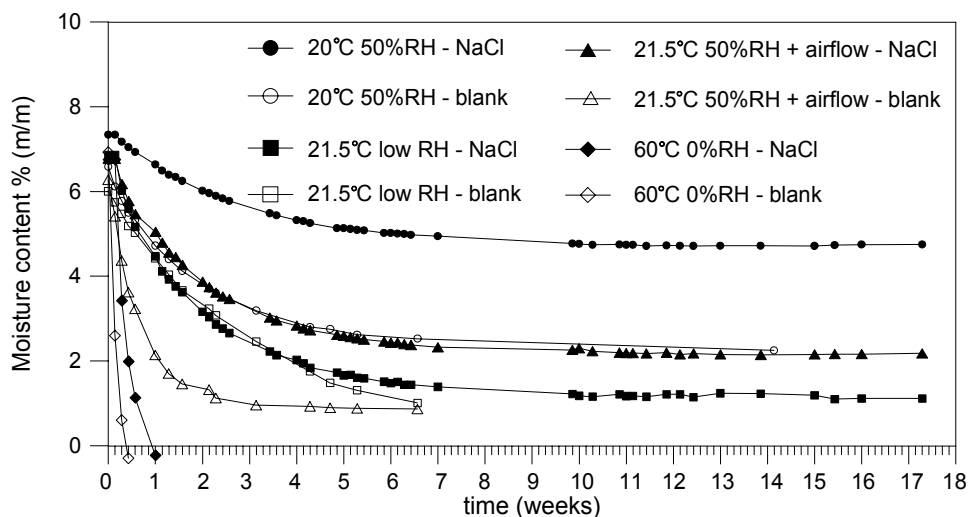


Figure 5.11 Drying curves at different environmental conditions of the restoration plaster, blank and contaminated with NaCl

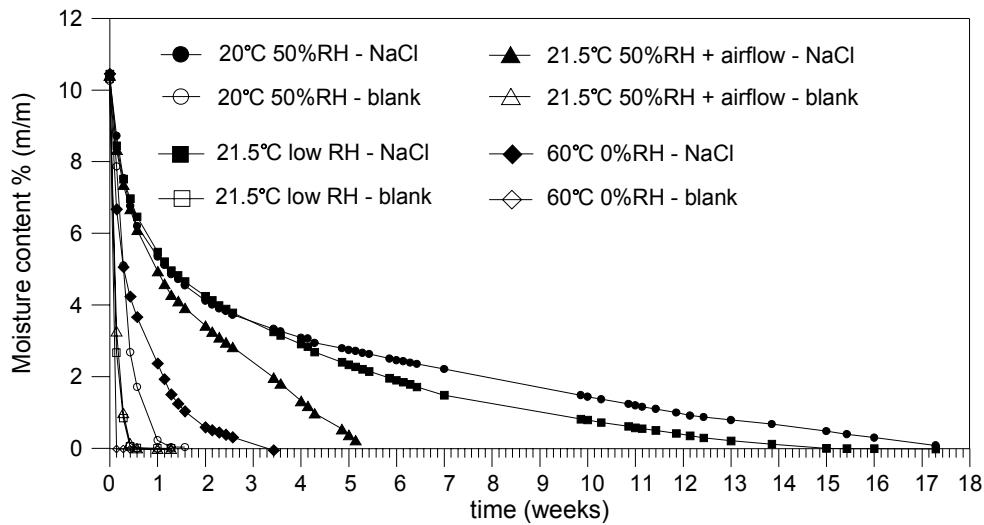


Figure 5.12 Drying curves at different environmental conditions of the fired-clay brick, blank and contaminated with NaCl

5.4.2.2 Effect of the environmental conditions on the salt distribution

The salt distribution in the specimens was measured for each combination of material and drying condition, after one drying cycle and at the end of the test period (after about four months). The number of the wet-dry cycles at the end of the test period varied between 1 and 6, depending on material type and environmental conditions. Figure 5.13 shows the HMC distribution at 96% RH measured after one drying cycle for lime-cement mortar, restoration plaster and brick.

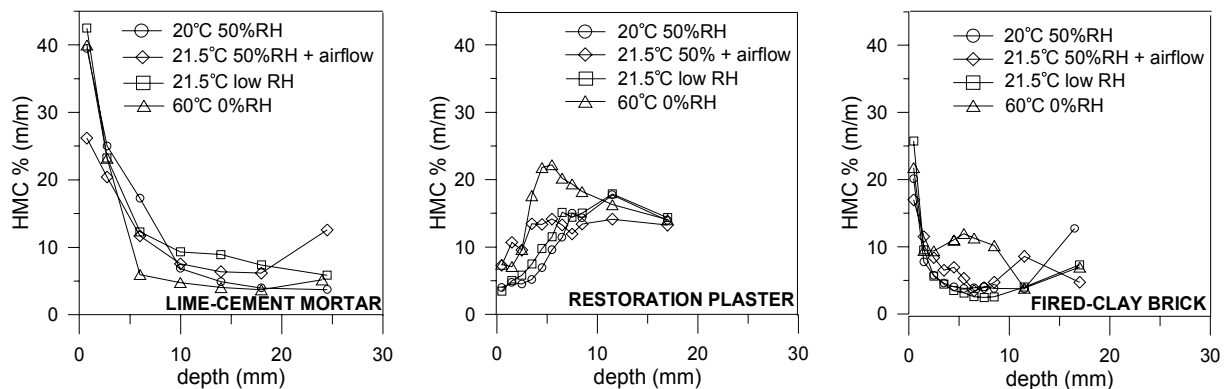


Figure 5.13 Hygroscopic Moisture Content (HMC) distribution measured at 96% RH in the three materials after one drying cycle at different environmental conditions

In the lime-cement mortar, the salt accumulates in the surface layer at all the drying regimes. Also in the brick most of the salt is present in the outer layer; a relevant amount of salt in

depth is measured only in the specimens dried at 60 °C / 0% RH. In the restoration plaster salt accumulation occurs inside the material and its distribution depends on the drying regime. In the following paragraphs the observed salt distribution is explained on the basis of the initial amount of solution, the material properties and the drying conditions.

In the lime-cement mortar and in the brick the amount of solution introduced was just enough to wet the upper surface; therefore, at the very beginning of the test, the surface of the specimens was wet. When the drying started, the salts were easily transported towards the evaporation surface. The salt crystallized either at the surface, as visible at 20 °C / 50% RH, or just beneath it, as in case of all the other drying regimes. The location of the crystallization may be explained by the drying process. In case of slow drying (20 °C / 50% RH) solution transport to the surface occurs and the evaporation front remains at the surface for a period long enough for the salt to reach the surface and crystallize on it. In case of fast drying, the drying front enters the material very soon; from this moment on no liquid transport to the surface is possible and the salt accumulates at the drying front, beneath the surface of the specimen. Since the moisture transport by capillarity in the lime-cement plaster and in the brick is quite fast, it may be reasonable to suppose that advection of the salt ions towards the drying front prevails over redistribution due to ion diffusion, and accumulation of salt near the surface results.

In the restoration plaster the amount of solution was not enough to wet the upper surface. When the drying started the surface was dry. The evaporation front remained inside the material in all cases and salt crystallization occurred inside. In this plaster drying at a high temperature leads to a clear peak in the salt distribution, whereas a flat profile is observed in case of slow drying. The drying process may explain the salt distribution: in case of fast drying, the rate of advection clearly dominates the rate of back diffusion, leading to a more pronounced salt accumulation. In case of slow drying the advection is partially compensated for by the diffusion, which is still possible because the moisture content remains high for a long time.

Repeating wet-dry cycles promotes the accumulation of salt near the surface, as shown in figure 5.14 in the case of the restoration plaster. This is due to more reasons. First of all the time scale has to be considered: the period during which the specimens are immersed in the solution is not long enough to allow the back diffusion of the ions and the attainment of equilibrium. Therefore, the drying following each subsequent re-wetting starts from a different situation, in which an increased amount of salt has accumulated near to the surface. Besides, the moisture content in the specimen increases with the number of cycles (when the specimens are re-wetted up to 20% of the introduced water is still present) and this favours the transport of the salt towards the surface.

5.4.2.3 Effect of the environmental conditions on the damage

The appearance of efflorescence and damage was monitored and photographically recorded.

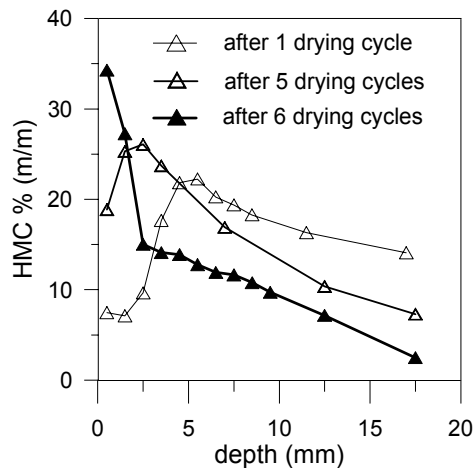


Figure 5.14 Hygroscopic Moisture Content (HMC) distribution measured at 96% RH in the restoration plaster after one, five and six drying cycles

On the lime-cement mortar the amount of efflorescences was significant only in the specimens dried at 20 °C / 50% RH: in this case the salt appeared on the surface after one day from the beginning of the test. In the specimens subjected to faster drying conditions (by the use of high temperature, low RH and air flow), the salts crystallized just under the surface and no efflorescences were visible. The presence of efflorescences shows that the evaporation front was maintained at the surface for a period long enough for the salt to reach the surface.

On the restoration plaster no efflorescences appeared on the surface because the drying front remained inside the material since the beginning of the test.

On the brick efflorescences appeared after one day of drying. Their amount was related to the drying conditions: the slower the drying, the higher the amount of salt that could be transported towards the surface and crystallize on it. No efflorescences were surveyed on brick dried at 60 °C. The amount of efflorescences increased after the rewetting of the specimens, when new liquid transport to the surface was possible.

Significant damage occurred only in brick and lime-cement specimens. No relevant damage was observed in the restoration plaster at the end of the test period. In the case of brick, damage appeared after a few wet-dry cycles, in case accelerated drying (low RH, air flow, and high temperature) was used. Decay occurred in the form of bulging of the surface layer; under the bulged layer no salt was visible (figure 5.15). The brick specimens dried at the reference conditions (20 °C / 50% RH), were not re-wetted (they were not dry yet after 4 months) and did not show any damage.

The mechanism causing the bulging in the lime-cement mortar was investigated using different methods. First the hypothesis of crypto-florescence pushing up the outer layer was checked by breaking the bulged layer. No crystals were visible in the void under the bulged layer, but powdered material was present (figure 5.18). The HMC and the chloride content of the bulged layer and of the powdered material directly beneath it was measured: the data showed that most of the salts were located in the bulged layer and not under it (figure 5.19).

These results allowed to reject the hypothesis of crypto-florescence pushing the outer layer up. The possibility of a chemical reaction in the outer layer, leading to compounds having a larger volume and therefore causing the bulging (for example Friedel's salt), was investigated by XRD analyses. Samples from the bulged layer and the bulk were analysed and compared with analogous samples from a non contaminated specimen (surface and bulk). The only difference between the damaged and the non contaminated plaster was the presence of NaCl, as visible in figure 5.20 in the peaks at $31.64^{\circ}2\theta$, $45.41^{\circ}2\theta$ and $56.44^{\circ}2\theta$. If a chemical reaction would have occurred the resulting compound would have been visible in the XRD analyses. It is therefore concluded that a chemical expansive reaction cannot be the cause of the bulging. The absence of any expansive reaction is also suggested by the fact that bulging of the outer layer occurred only after the first re-wetting and not already after the initial contamination with NaCl solution.

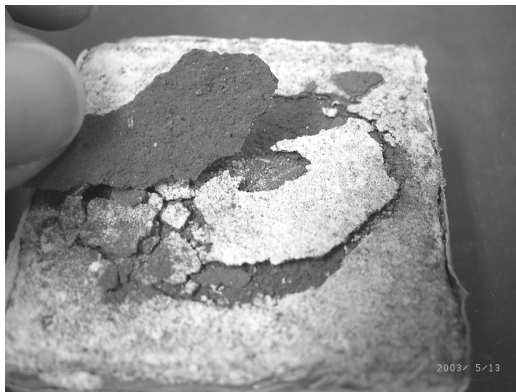


Figure 5.15 (left) Bulging and scaling of the outer layer of a brick specimen after 3 drying cycles at 21.5°C , 50% RH and airflow

Figure 5.16 (right) Scaling of the outer layer of a lime-cement mortar specimen after 2 drying cycles at 20°C / 50% RH



Figure 5.17 (left) Bulging of the outer layer of a lime-cement mortar specimen after 2 drying cycles at 60°C / 0% RH

Figure 5.18 (right) Bulging of the outer layer of a lime-cement mortar specimen after 2 drying cycles at 60°C / 0% RH: no salt efflorescences pushing out the outer layer are visible; the material under the bulged layer is reduced to sand

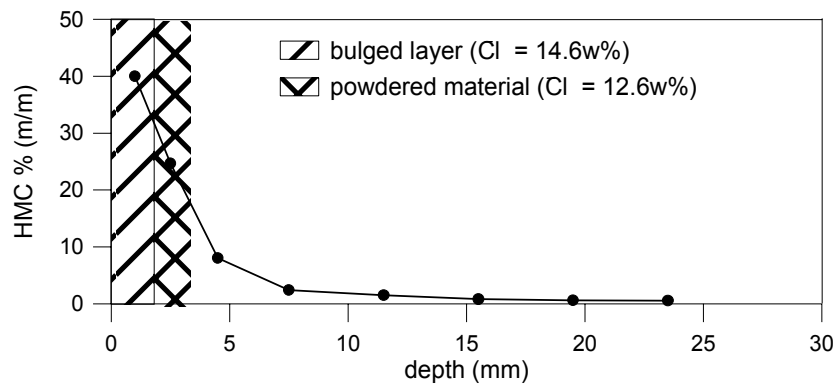


Figure 5.19 Hygroscopic moisture distribution in lime-cement mortar specimen after 2 drying cycles at 60 °C / 0% RH: most of the salt accumulates in the bulged layer

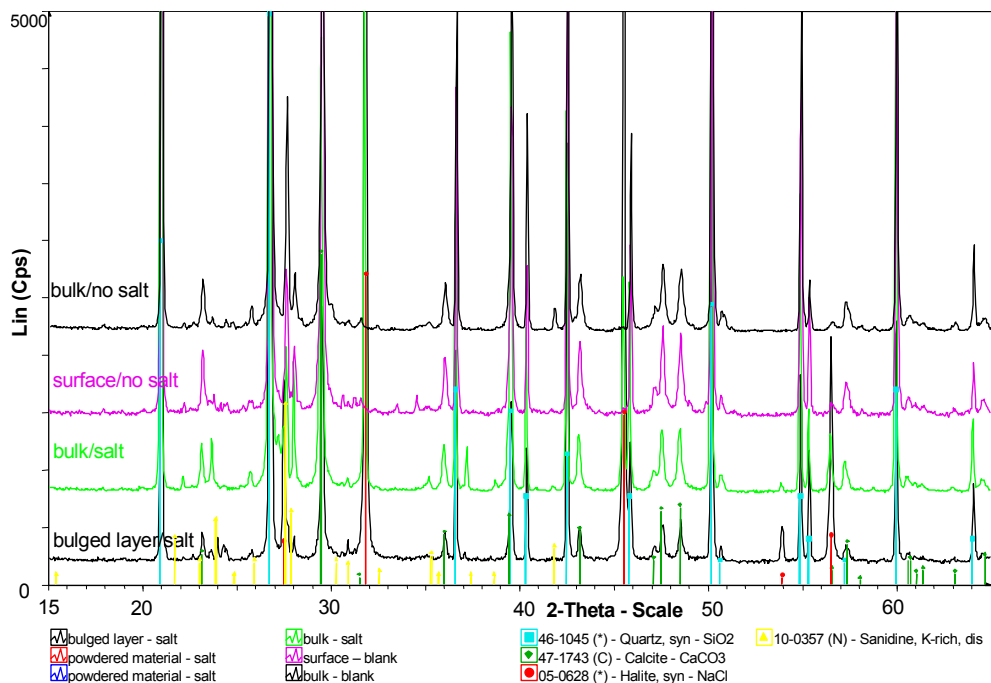


Figure 5.20 Results of the XRD analyses on samples from the NaCl contaminated (bulged layer, bulk) and blank (surface layer and bulk) lime-cement specimens

A final hypothesis with respect to the occurrence of the bulging concerns the different behaviour of contaminated and not contaminated material during wetting and drying [Wen02]. During wetting and drying, the changes in size of the outer layer, rich in salts, may have been different from changes in size occurring in the bulk of the mortar, where a much lower salt load is present. From observation of the damage development (bulging appeared during the drying period) it can be supposed that the outer layer (rich in salt) expanded more than the bulk of the specimen during drying. This differential dilation may have caused shear stresses

at the interface between the surface layer rich in salt and the less salt loaded bulk, leading to the loss of cohesion observed under the bulged layer. Furthermore, the dilation of the outer layer, prevented by the epoxy-resin sealing the lateral sides may have resulted in bulging. This hypothesis has been verified by a series of new experiments and has led to interesting conclusions (chapter 6).

In the restoration plaster, some damage, in the form of sanding, has been observed only in the specimens that were re-wetted six times (drying conditions: 60°C / 0%RH): in this case the NaCl had reached the surface and crystallized in the form of efflorescences and crypto-florescences. In all the other testing conditions no rewetting was performed (the specimens were not dry yet at the end of the test period), the salts remained in depth and no damage was observed.

5.4.2.4 Location of salt in pores

The Mercury Intrusion Porosimetry (MIP) technique was used to investigate the pore sizes involved in NaCl crystallization. MIP measurements were performed on the surface layer (thickness about 1 mm) of all materials. The presence of salt in the layer was first assessed by measuring the hygroscopic moisture content. In the case of the fired-clay brick and the restoration plaster, the MIP measurements were repeated after dissolving the salts by immersing the samples in demineralized water, to check whether the pores previously filled with salt would “reappear”. In the case of the lime-cement plaster, the pore size distribution was measured only before and after salt crystallization at 60 °C / 0% RH. Due to the weakness of the material, which fell apart during immersion in water, it was not possible to measure the salt distribution after desalination.

The pore size distribution of the lime-cement mortar, before and after salt crystallization test, is shown in figure 5.21. The MIP measurements were performed twice and the reproducibility of the results allows concluding that the decrease in the percentage of pores in the range between 0.2 and 1 µm is due to salt crystallizing in, and closing, this size of pore size. Changes in larger pore sizes, between 10 and 50 µm, are measured too. They may be related not only to crystallization of salt partially filling the larger pores (see section 5.4.2.5), but also to modifications in the porous structure of the material (cracking) due to damage development.

The pore size distribution of the restoration plaster, before and after crystallization at 60 °C / 0% RH and after desalination, is shown in figure 5.22. A decrease of porosity in the range between 20 and 100 µm is observed after the salt crystallization test. This may correspond to a partial filling of the pores. In the range of small pores a decrease in porosity for pore sizes smaller than 0.05 µm and an increase in porosity between 0.05 and 0.1 µm is measured after the salt crystallization test. Since the MIP curves before and after desalination are similar it is difficult to draw sound conclusions.

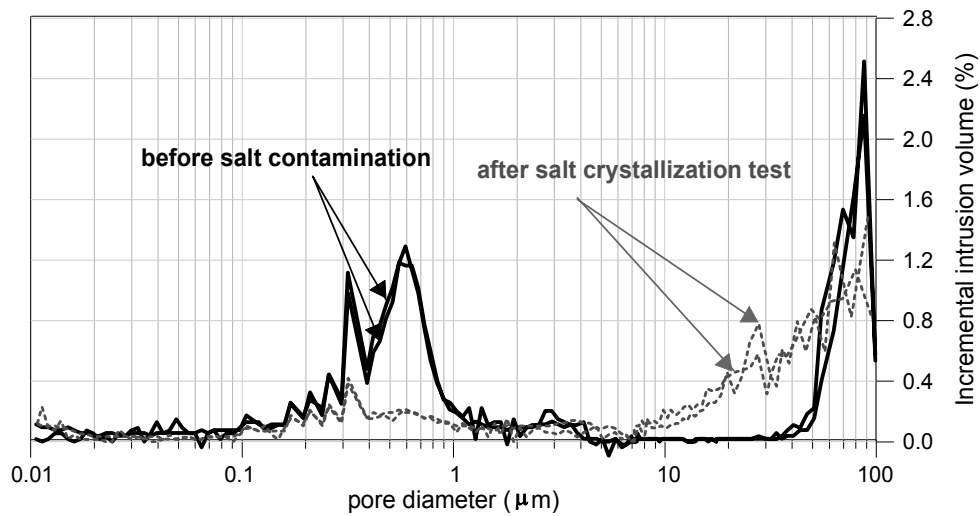


Figure 5.21 Pore size distribution of lime-cement mortar samples before salt contamination and after salt crystallization test (2 drying cycles at 60 °C / 0% RH)

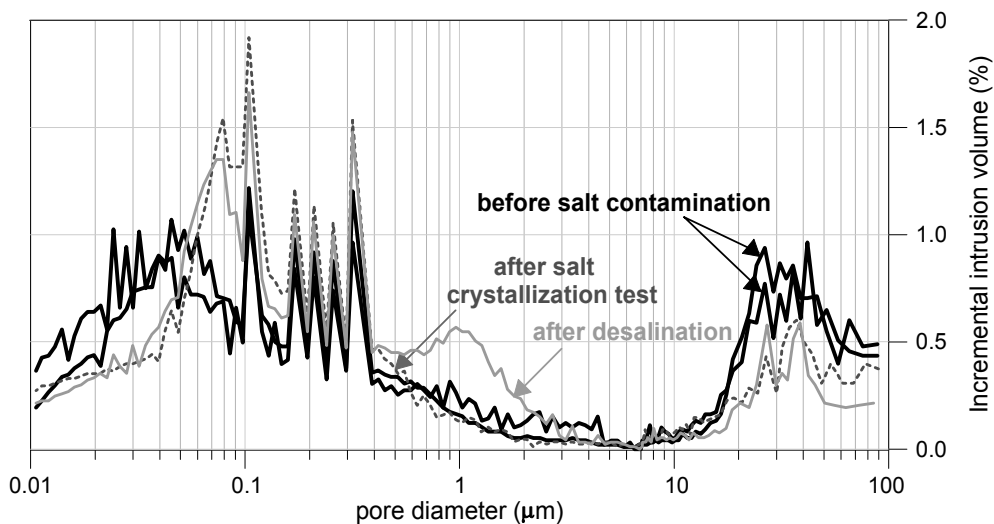


Figure 5.22 Pore size distribution of restoration plaster samples before salt contamination, after salt crystallization test (6 drying cycles at 60 °C / 0% RH) and after desalination

The pore size distribution of the brick (2 samples) before salt contamination, after the weathering test (3 samples) and after desalination (1 sample) is shown in figure 5.23. The variation of the obtained curves (see the 3 salt contaminated samples in figure 5.23) makes it difficult to make an assumption on the location of salt in pores. A shift towards large pore radii is registered in samples subjected to the crystallization test. This might be related to damage (cracks) development, but, due to the variation of the obtained data, a much larger number of measurements would be necessary to draw sound conclusions.

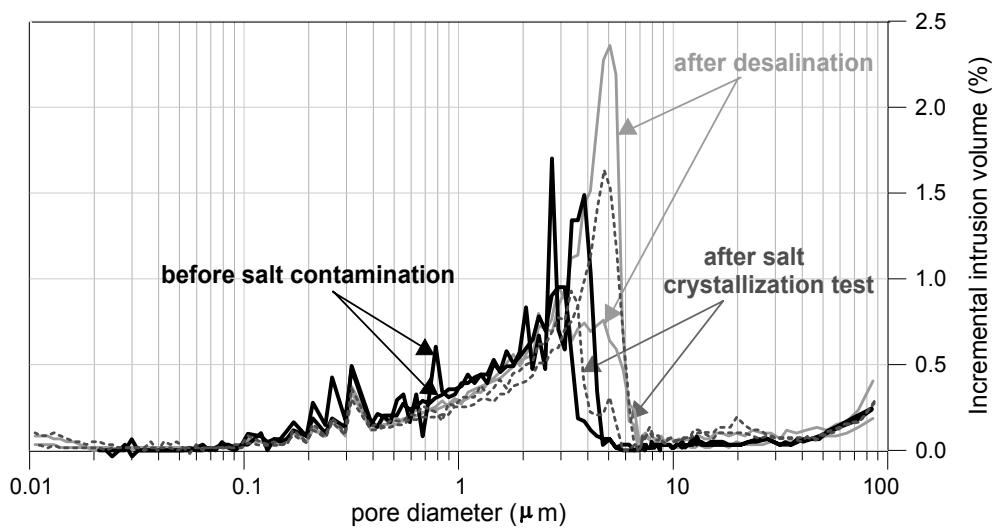


Figure 5.23 Pore size distribution of fired-clay brick samples before salt contamination, after salt crystallization test (one drying cycle at 20 °C / 50% RH) and after desalination

5.4.2.5 ESEM investigations

ESEM investigations, performed mainly by the use of a Back Scattered Electron (BSE) detector, were carried out on the materials damaged by the salt crystallization test. The ESEM was used to investigate the crystal patterns in relation to the material and the drying conditions. The preferential location of sodium chloride in pores and the effects of the crystallization on the structure of the substrate were also studied.

In general the crystal patterns vary from a salt layer covering the walls of wide pores, observed mainly in the bulk of the specimens (figure 5.24), to a salt crust, present over the surface of the lime-cement mortar and the brick (figure 5.25), and to whisker crystals visible over the surface of the restoration plaster (figure 5.26).

Only in a few cases regular cubic crystals are present on the surface of the lime-cement and of the brick specimens (figure 5.27). The mentioned crystal patterns confirm the large variety of crystal shapes reported in literature [Esw80, Obi89, Cha02].

As described by Arnold and Zehnder [Arn85], the shape of crystals precipitating in/on porous materials depends on: (i) material properties (thin crystals grow on a dense substrate, thicker crystals on a substrate having large pores), (ii) solution supply (very low solution supply gives place to whisker crystals, high supply to salt crust), (iii) evaporation rate and (iv) water content in the substrate (salt crust are formed on wet substrates, whisker like crystals on less humid material). This has been verified in the present research: whiskers have been mostly observed on the surface of the fine porous restoration plaster characterized by slow moisture transport, whereas thicker crystals have been found on the lime-cement mortar and in the brick having an initially wet surface and a fast moisture transport.

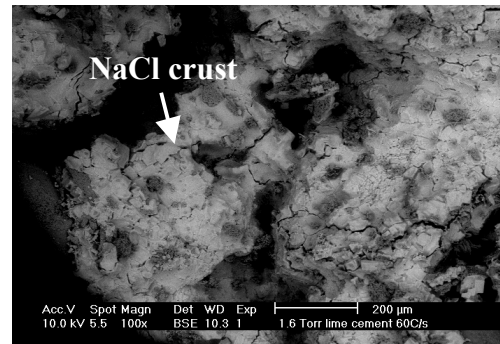
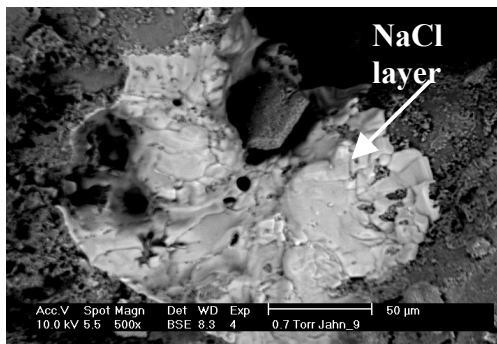


Figure 5.24 (left) ESEM photomicrograph (BSE mode) of the cross section of the restoration plaster after 1 drying cycle at 21.5 °C / 50% RH and air flow

Figure 5.25 (right) ESEM photomicrograph (BSE mode) of the surface of the lime-cement mortar after 2 drying cycles at 60 °C / 0% RH

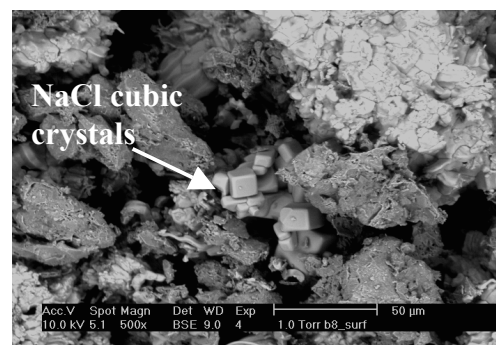
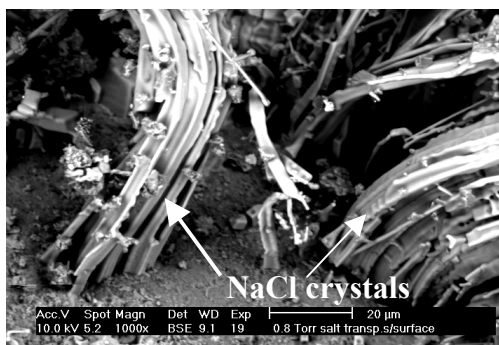


Figure 5.26 (left) ESEM photomicrograph (BSE mode) of the surface of the restoration plaster after 6 drying cycles at 60 °C / 0% RH

Figure 5.27 (right) ESEM photomicrograph (BSE mode) of the surface of fired-clay brick after 3 drying cycles at 21.5 °C / 50% RH and air flow

With respect to the damage, in the lime-cement mortar the salt crystallizes in the binder, disrupting it. The bulged layer of the lime-cement mortar dried at 60 °C / 0% RH appears, after 2 wet-dry cycles, as a structure of overlapping salt crystals and binder particles. The binder, that was compact before crystallization occurred, is now reduced to loose particles cemented by the sodium chloride (figure 5.28). In the restoration plaster crystallization at the binder/aggregate interface (figure 5.29) is observed and only little damage has occurred to the material.

In any of the investigated materials it was not possible to clearly distinguish pores filled with salt crystals.

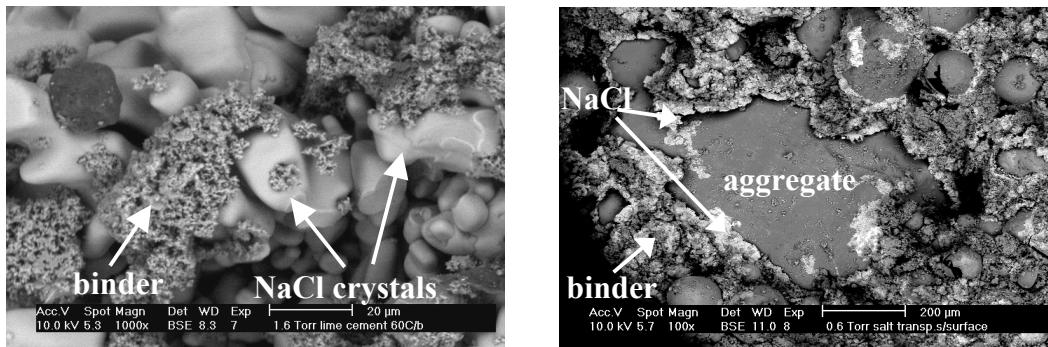


Figure 5.28 (left) ESEM photomicrograph (BSE mode) of the bottom of the bulged layer of the lime-cement mortar after 2 drying cycles at 60 °C, 0% RH

Figure 5.29 (right) ESEM photomicrograph (BSE mode) of the surface of restoration plaster after 6 drying cycles at 60 °C, 0% RH

5.4.3 Inputs to the development of an accelerated test

From the experiments performed during this first phase of the research the following conclusions were drawn, useful for a further development of the NaCl crystallization test:

- Visible damage only occurs after re-wetting of the specimens, i.e after dissolution and re-crystallization of the salts: this emphasises the necessity of introducing wet-dry cycles in a crystallization test. Because of the repeated wet-dry cycles, the salt accumulates in layers that become thinner and thinner. Therefore the generated pressures are exerted on smaller areas, leading to more important stresses that exceed the mechanical strength of the material and cause damage.
- Since damage appeared only after rewetting, the specimens that dried faster, i.e. at a higher temperature, were the first to be damaged. Moreover, in case of a slow drying material such as the investigated restoration plaster, the use of high temperature was the only way to dry the specimens and to repeat a number of wet-dry cycles sufficient to accumulate the salt and generate damage.
- The observed decay patterns are related to the salt distribution: crystallization at the surface, like it occurs at mild environmental conditions, causes sanding and scaling, while salt accumulating in an area directly beneath the surface can lead to bulging, scaling and spalling of the outer layer. This factor has to be taken into account when evaluating the behaviour of a material by means of an accelerated test: using laboratory conditions different from those in the field may lead to a different damage pattern.

From this first stage of the work it can therefore be concluded that a procedure combining the use of a high, but still realistic, temperature (60 °C) with repeated wet-dry cycles is recommended to accelerate NaCl crystallization tests.

5.5 Effect of RH cycles on sodium chloride damage

In a second phase of the research the effect of RH cycles through the RH of crystallization of NaCl (75.5% RH at 20 °C [Arn90]) was investigated. Several ranges and durations of RH cycles were applied and the damage obtained in the different cases compared.

The main aims of this phase of the research were:

- prove that RH changes alone (i.e. in the absence of any other moisture source) are able to cause damage to salt contaminated materials;
- verify whether the use of RH cycles leads to the acceleration of a weathering test;
- study the effect of repeated dissolution-crystallization cycles on the NaCl crystal shape.

5.5.1 Test procedure

The type and the size of the specimens and the salt contamination procedure used in this phase are the same as described in section 5.4.1.

Before starting the RH cycles, it was necessary to obtain a favourable salt distribution in the specimen: the salt has to accumulate near the surface of the specimens, without anyway efflorescing. This salt distribution is favourable since salts crystallizing near the surface are more sensitive to the RH changes of the air. Besides, salts can damage a material only if they crystallize as crypto-florescences in the pores.

In order to accumulate most of the salts in the outer layer of the specimens, the brick and lime-cement mortar were dried for 4 days at 20 °C / 50% RH and then moved into an oven at 60 °C / 0% RH until they reached a constant weight. The restoration plaster was subjected to 6 wet-dry cycles at 60 °C / 0% RH, since this procedure was able to accumulate salts at the surface of this slow transporting material (see section 5.4.2.2). Before starting the RH cycles the salt distribution in the three materials was checked by dry cutting specimens in 2 mm thick slices and by measuring the HMC of the slices after 4 weeks storage at 20 °C / 96% RH. The results showed that most of the salt was accumulated at the surface, so the RH cycles could start.

First two different RH cycles were tested:

- a. RH cycle type a: 1 day at 96% RH followed by 2.5 days at \approx 10% RH;
- b. RH cycle type b: 3 days at 80% RH followed by 4 days at \approx 10% RH

Then, on the basis of the results obtained (see section 5.5.2), the following RH cycle was set up:

- c. RH cycle type c: 2.5 days at 96% RH, followed by 1.5 days at 50% RH and 3 days at \approx 10% RH

In all the tested RH cycles, the temperature was kept constant at 20 °C. The tests lasted 70 days, corresponding to 20 cycles type a and to 10 cycles type b and c.

The 50%, 80% and 96% RH conditions were obtained in climatic rooms. The \approx 10% RH environment was reached in a closed box placed in a climatic room at 20 °C by the use of NaOH.

The mass change of the specimen, after each low and high RH period, was measured. The damage was evaluated by:

- monitoring (visually and photographically) the evolution of the efflorescences and the decay;
- weighing the debris brushed from the surface of the specimens after each low and high RH period;
- studying, by means of the ESEM, the surface and the cross section of the specimens at the beginning, halfway and at the end of the test.

Blank specimens were used as reference. Other specimens, contaminated with salt and subjected to the RH cycles but not brushed during the test, were used to check the evolution of the salt distribution and to study changes in crystal patterns and damage in the material structure at different time intervals during the test.

5.5.2 Results

5.5.2.1 Effect of RH cycles on the damage

After each low and high RH period, the specimens were brushed with a soft brush. About 200 ml of water were added to the brushed material in order to dissolve the salt and the solution was filtrated. The debris was then dried at 60 °C and weighed on a balance with an accuracy of 0.01 g. This procedure for the quantification of the damage and of its evolution in time has allowed comparing the susceptibility to salt damage of the tested materials and the effectiveness of the different types of RH cycles.

In figure 5.30 the material loss of lime-cement mortar, after each low and high RH period of the RH cycle type b, is reported. The graph indicates that the material loss mainly occurs at the end of the high RH period, when the salt, cementing the particles of the material together, dissolves and the debris can fall apart. Similar behaviour is registered for the other materials and for every RH cycle duration and range. These results confirm the observation from practice where the material loss is registered mainly at high RH (see chapter 4).

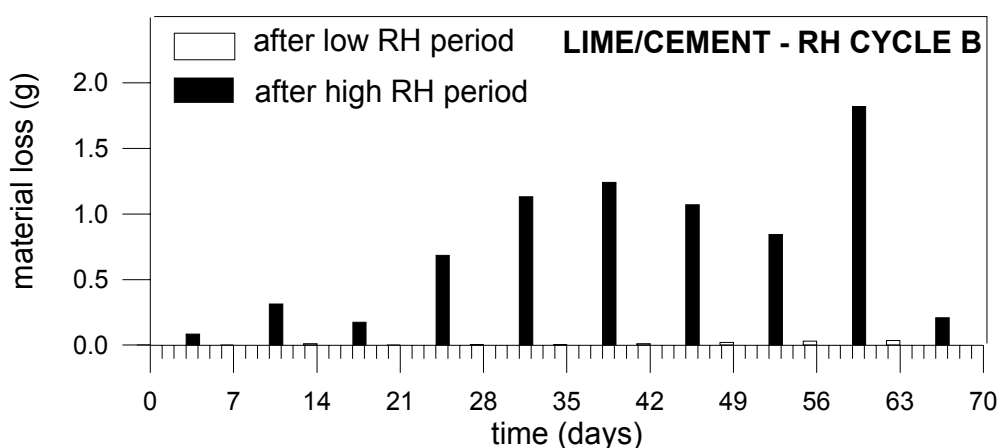


Figure 5.30 Material loss of lime-cement specimens after each low and high RH period during RH cycle type b

The cumulative material loss is reported in figures 5.31-33 for all the three different types of cycles. From these graphs it can be concluded that the RH cycles are effective in causing damage in the weak lime-cement mortar and in the brick. A mass loss of about 20% and 1% (mass of the debris/ mass of the specimen), respectively for lime-cement and brick specimens, is registered (RH cycle c). As expected, the lime-cement mortar is the most damaged material, because of its low strength. The restoration plaster shows only a limited sanding (0.15% mass loss in RH cycle c). The most effective test cycle is type c, the least effective is type a.

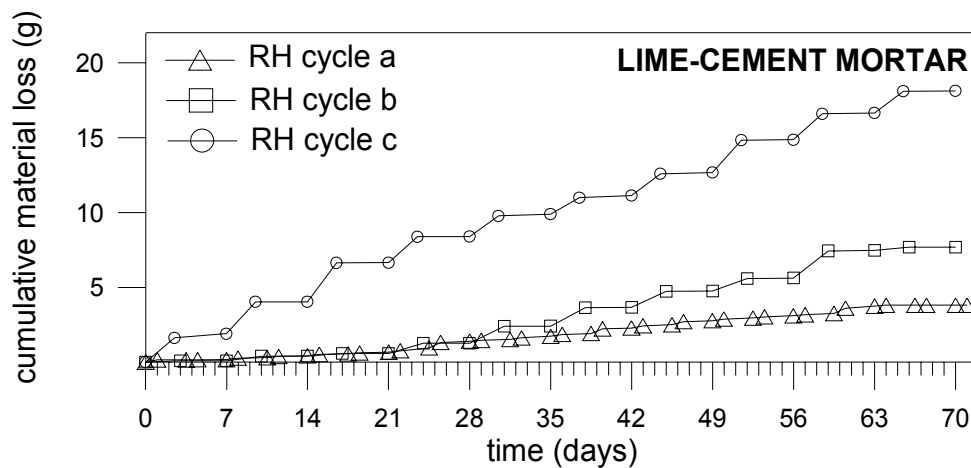


Figure 5.31 Cumulative material loss of lime-cement mortar specimens tested with different types of RH cycles

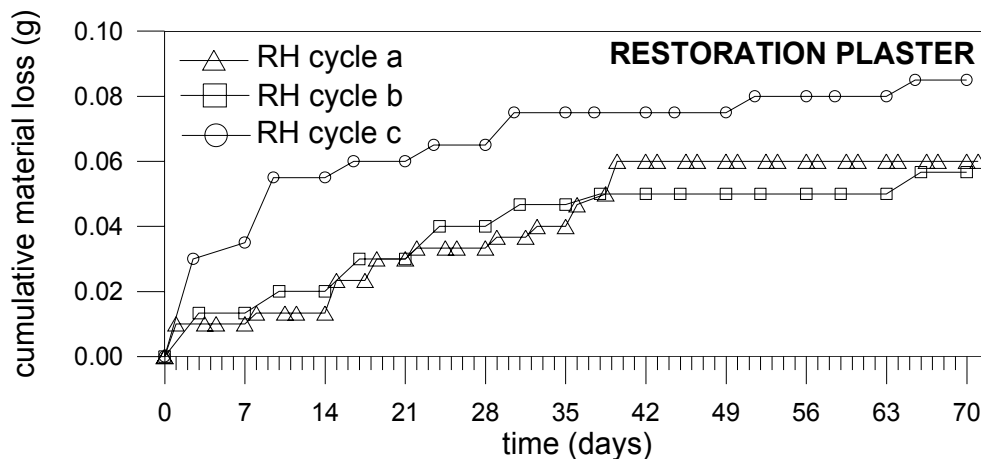


Figure 5.32 Cumulative material loss of restoration plaster specimens tested with different types of RH cycles

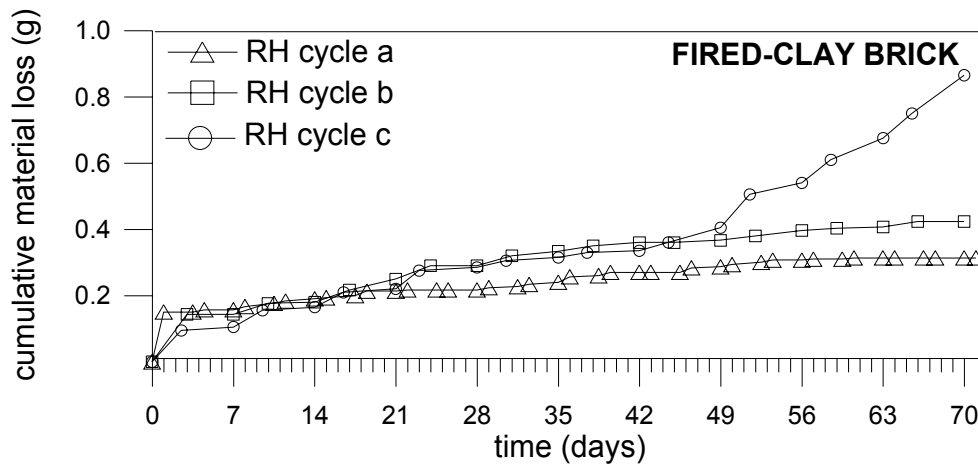


Figure 5.33 Cumulative material loss of fired-clay brick specimens tested with different types of RH cycles

The effectiveness of the test procedure is related to the amount of the adsorbed/evaporated water at each cycle and to the migration of salt in the specimens during the test. The most important material loss is registered when the amount of adsorbed/evaporated water at each cycle is higher (so for the cycle type c), because a larger salt amount undergoes dissolution and re-crystallization. This is clear by comparing the mass gain and loss at each cycle with the cumulative material loss at the end of the different RH cycle types (figure 5.34).

Also the migration of salts in the specimen during the RH cycles influences the material loss. RH cycles are most effective if a large amount of salt accumulates in a thin layer near the surface of the material; if the salt migrates in depth, the effectiveness of the test will decrease. This happened in the case of RH cycle type a and b in both lime-cement mortar and restoration plaster: the HMC distribution at the beginning and at the end of the test (figure 5.35) shows that the salts, dissolved and transported in depth during the high RH periods, could not accumulate again at the surface because of the fast drying (at $\approx 10\%$ RH) in the low RH period. This migration of the salts in depth is confirmed by the ESEM investigations (see section 5.5.2.2).

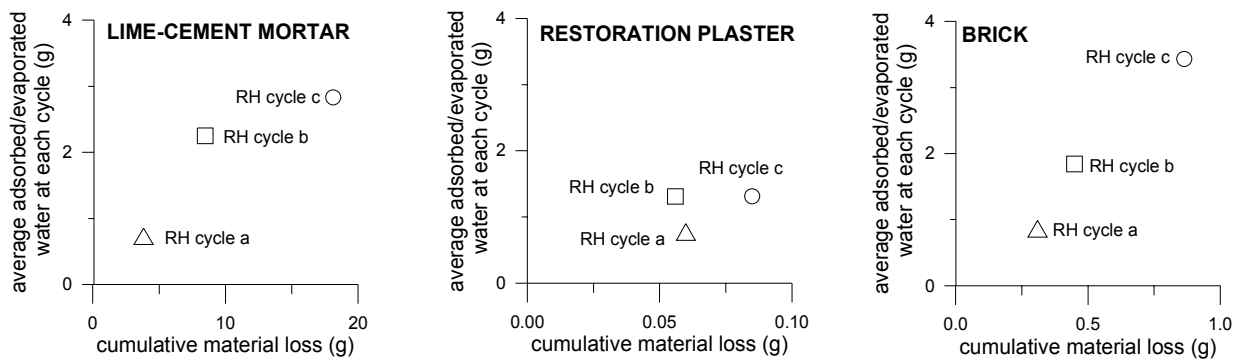


Figure 5.34 Average adsorbed/evaporated water at each cycle versus cumulative material loss

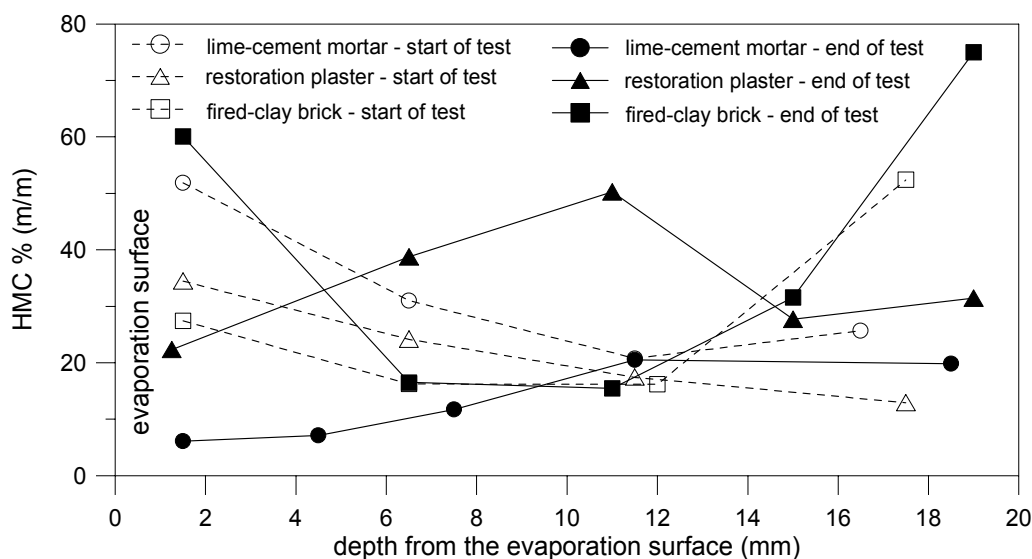


Figure 5.35 Hygroscopic Moisture Content distribution in lime-cement mortar, restoration plaster and fired-clay brick at the start and at the end of the test (RH cycle type b); evaporation surface on the left

To limit the migration of salt in depth, a period of drying at 50% RH following the 96% RH period was introduced in the RH cycle type c. In this way the surface of the specimens remained wet long enough to allow salt transport to the surface. The large amount of adsorbed water, able to dissolve up to 50% of the salt present on the specimens, together with the accumulation of salt near the surface, resulted in the improved effectiveness of the RH cycle type c.

The type of damage observed consists of de-cohesion of the surface layer in the form of powdering (brick) or sanding (lime-cement mortar and restoration plaster). This type of damage is related to salt accumulation in the outmost layer of the material and it is very similar to the decay pattern commonly observed in practice in case of sodium chloride weathering [Tsu03, Cha00b] (see chapter 3).

5.5.2.2 ESEM investigations

ESEM investigations were performed at the beginning, after 5 cycles and at the end of the RH tests to study changes eventually occurring in the crystal shape due to repeated dissolution/crystallization cycles. Both the surface and the broken cross section of the specimens were investigated. The BSE detector present in the ESEM was mainly used to identify the presence of salts; the salt composition was checked by means of the EDX analyses.

Lime-cement mortar

At the beginning of the test, after one drying cycle (see section 5.5.1), the salt forms a crust on the surface of the specimen; some cubic crystals are present identifying crystallization from solution (figure 5.36). After several RH cycles (test type a) only few small (about 1 μm) salt crystals are visible at the surface, confirming the migration of salt in depth (figure 5.37).

In the cross section, the salt is visible mainly as a layer on the walls of the large voids in the material (figure 5.38). The salt accumulates in areas delimited by a salt layer (figure 5.39). No evidence of salt filling the visible pores ($> 0.5 \mu\text{m}$) is present beneath the salt layer. No relevant damage to the mortar structure is detected.

After several RH cycles no significant changes in the crystallization patterns of the salt are visible; the salt still accumulates in areas delimited by a salt layer. The layer of salt covers the binder, and there is no evidence of salt filling the pores ($> 0.5 \mu\text{m}$) beneath the salt layer (figure 5.40). In some areas a structure of salt and de-cohesioned binder is present, denoting the occurrence of damage (figure 5.41).

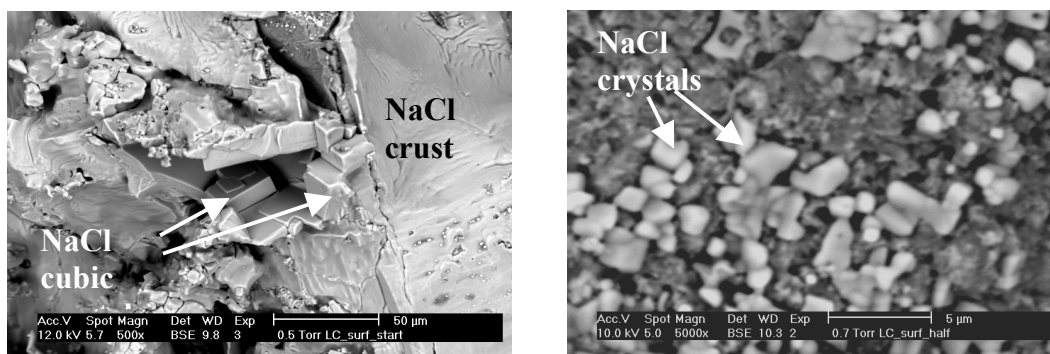


Figure 5.36 (left) ESEM photomicrograph (BSE mode) of salt crust at the surface of a lime-cement specimen at the beginning of the test; some cubic crystals are visible.

Figure 5.37 (right) ESEM photomicrograph (BSE mode) of salt crystals (white) at the surface of a lime-cement specimen after 10 RH cycles type a

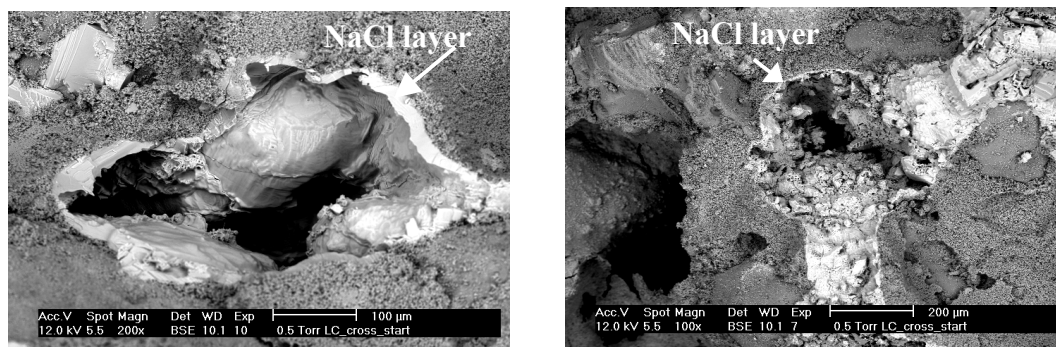


Figure 5.38 (left) ESEM photomicrograph (BSE mode) of salt layer covering a large void (cross section of lime-cement mortar specimen at the beginning of the test)

Figure 5.39 (right) ESEM photomicrograph (BSE mode) of salt crystallizing in areas delimited by a salt layer (cross section of lime-cement mortar specimen at the beginning of the test)

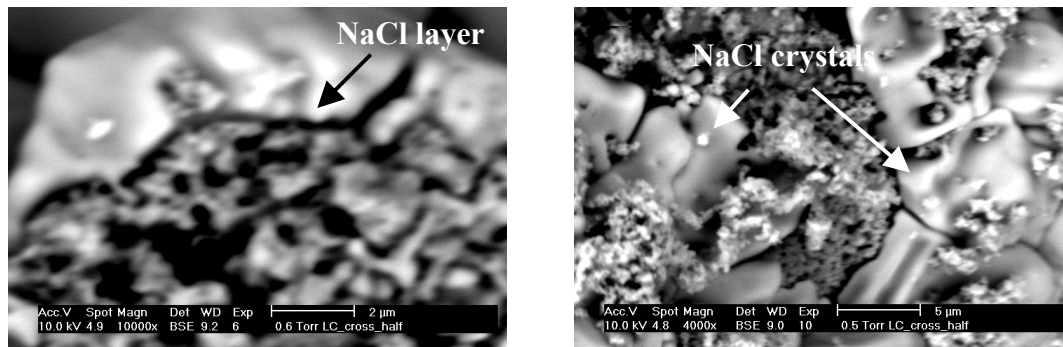


Figure 5.40 (left) ESEM photomicrograph (BSE mode) of the pore structure of the lime-cement beneath the salt layer: no evidence of salt filling pores (cross section of lime-cement mortar specimen after 10 RH cycles type a)

Figure 5.41 (right) ESEM photomicrograph (BSE mode) of the binder showing de-cohesion due to the salt crystallization (lime-cement after 10 RH cycles type a)

Restoration plaster

At the beginning of the RH test, i.e. after 5 wet-dry cycles at 60 °C / 0% RH (see section 5.5.1), the salts have crystallized mainly as hair-like crystals growing from the pores of the binder. After repeated RH cycles the crystallization patterns of the salt are not changed. The salts have crystallized, in the form of needles, preferentially at the binder/aggregate interface (figure 5.42), and they seem to have caused the detachment of the aggregate particles (figure 5.43). This preferential location of the crystallization may explain the sanding often observed on this plaster, in practice as well as in the laboratory experiments. In the cross section of the specimen the salt is mainly present, at the beginning as well as at the end of the test, in the form of a smooth salt layer adhering to the binder (figure 5.44). Beneath the salt layer there is no evidence of pores ($> 1 \mu\text{m}$) filled with salt (figure 5.45). No cracks or de-cohesion of the binder is detected in the cross section, confirming that no significant damage has occurred in depth.

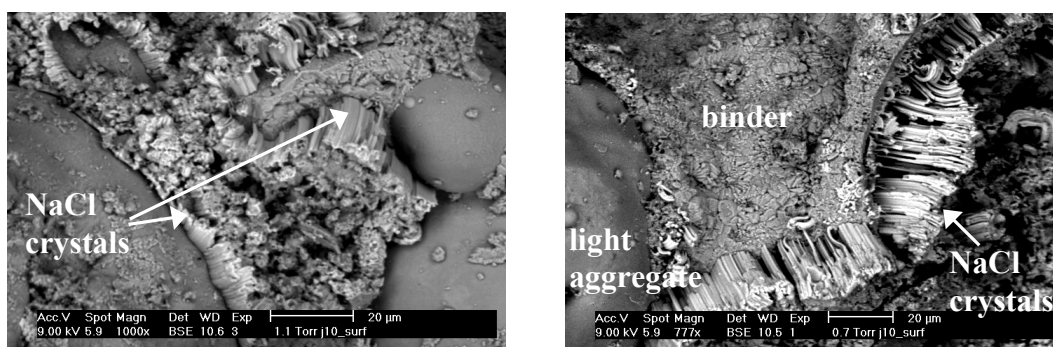


Figure 5.42 (left) ESEM photomicrograph (BSE mode) of salt crystallizing at the binder/hollow aggregate interface (surface of restoration plaster specimen after 10 RH cycles type a)

Figure 5.43 (right) ESEM photomicrograph (BSE mode) of salt growing from the binder. From the shape of the binder, it can be supposed that the growth of the salt has pushed away the round aggregate particles (surface of restoration plaster after 10 RH cycles type a)

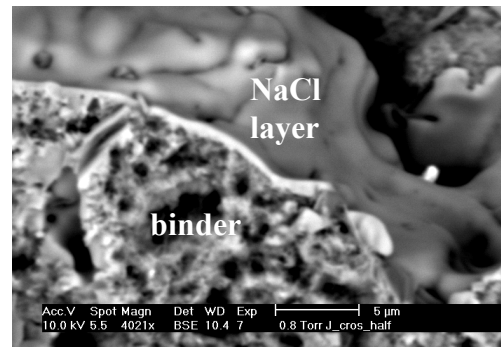
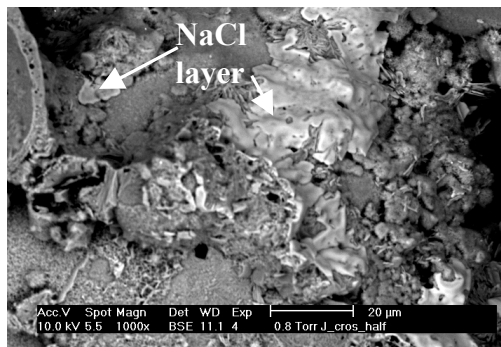


Figure 5.44 (left) ESEM photomicrograph (BSE mode) of salt crystallizing as a layer over the binder (cross section of restoration plaster specimen after 10 RH cycles type a)

Figure 5.45 (right) ESEM photomicrograph (BSE mode) of a salt layer over the binder; no evidence of pores filled with salt beneath the salt layer (cross section of restoration plaster after 10 RH cycles type a)

Fired-clay brick

At the beginning of the test, after one drying cycle (see section 5.5.1), agglomerations of salt crystals are present on the surface. After several RH cycles (type a) the amount of salt present on the surface is drastically decreased because of migration of salt in depth (in the case of test cycles a and b).

The cross section of the specimen at the beginning of the test shows the presence of salt in the outer 500 µm; NaCl has crystallized in the form of a layer covering the pore walls (figures 5.46-47). After several RH cycles, salt has migrated inside the specimen (accumulation is visible at about 1 mm from the surface) where it has precipitated mainly as small (1-5 µm) crystals. NaCl crystals growing in fissures between brick scales are detected (figures 5.48-49), denoting the occurrence of damage in the outer layer of the brick.

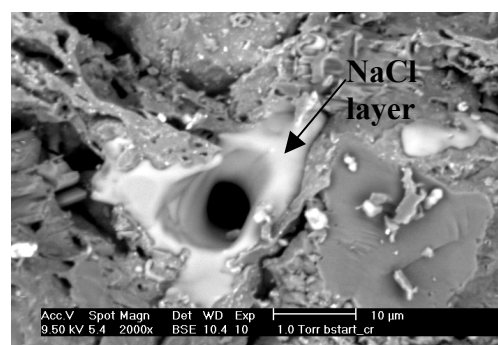
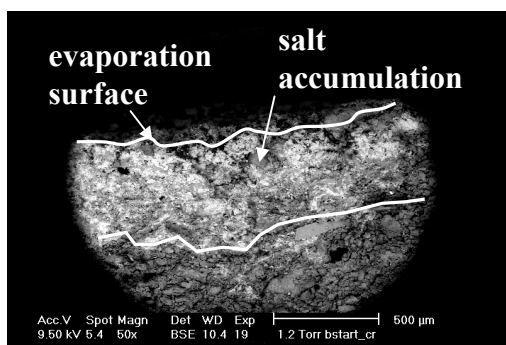


Figure 5.46 (left) ESEM photomicrograph (BSE mode) showing NaCl crystallization in the outer 500 µm of the specimen (cross section of fired-clay brick specimen at the start of the test)

Figure 5.47 (right) ESEM photomicrograph (BSE mode) of salt layer over the pore wall (cross-section of fired-clay brick specimen at the start of the test)

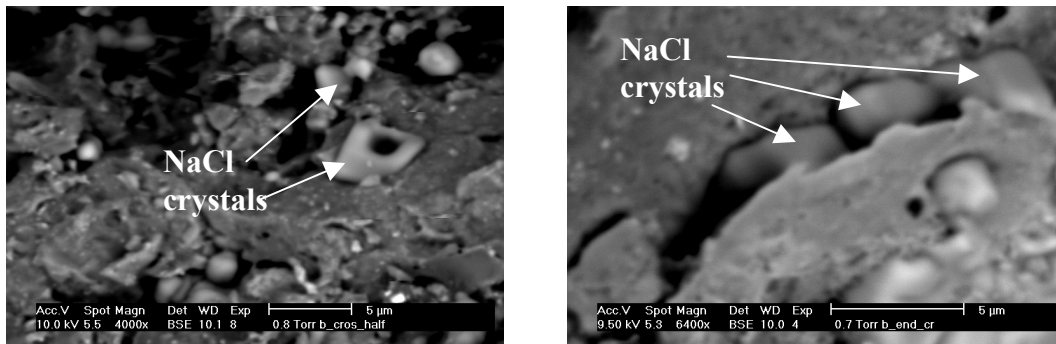


Figure 5.48 (left) ESEM photomicrograph (BSE mode) of salt crystals growing in the brick (cross section of fired-clay brick specimen after 10 RH cycles type a)

Figure 5.49 (right) ESEM photomicrograph (BSE mode) of salt crystal growing between scales of the brick (cross-section of fired-clay brick specimen after 20 RH cycles type a)

From the ESEM investigations performed on the three different materials the following general conclusions can be drawn:

- On the surface of the specimens NaCl crystallizes often as an agglomeration of crystals. The salt grows on the dense and slow transporting restoration plaster in the form of hair-like crystals, whereas it precipitates as a salt crust on the wet surface of the brick and of the lime-cement mortar. In the cross section of the specimens a salt layer, well adhering to the pore walls, is observed in all the materials at the beginning of the test. In the brick this layer evolves towards an agglomeration of small crystals after several RH cycles. In figure 5.50 the different patterns of the salt crystallizing in the material are schematically represented.
- No evidence has been found of pores filled with salts that would explain the observed damage. Immediately beneath the salt layer covering larger voids, the visible pores ($> 0.5 \mu\text{m}$) appear to be empty. However, because of the detection limit of the ESEM (pores smaller than $1 \mu\text{m}$ can not easily be detected on broken cross section) crystallization of salt filling pores of smaller sizes cannot be excluded.
- Salt migration in depth during the test (cycle type a and b) has been detected in all the materials: the amount of salt crystallizing on and immediately beneath the surface decreased when cycling the RH between 96% or 80% and 10% (cycle a and b). As already explained in 5.5.2.1, this is due to the migration of salt solution from the surface to the bulk of the specimens during the high RH period, followed by crystallization of salt in depth during the fast drying at low RH (10% RH). This effect is reduced in case of cycle c, thanks to the period of relatively slow drying ($20 \text{ }^\circ\text{C} / 50\% \text{ RH}$) following the high RH period.

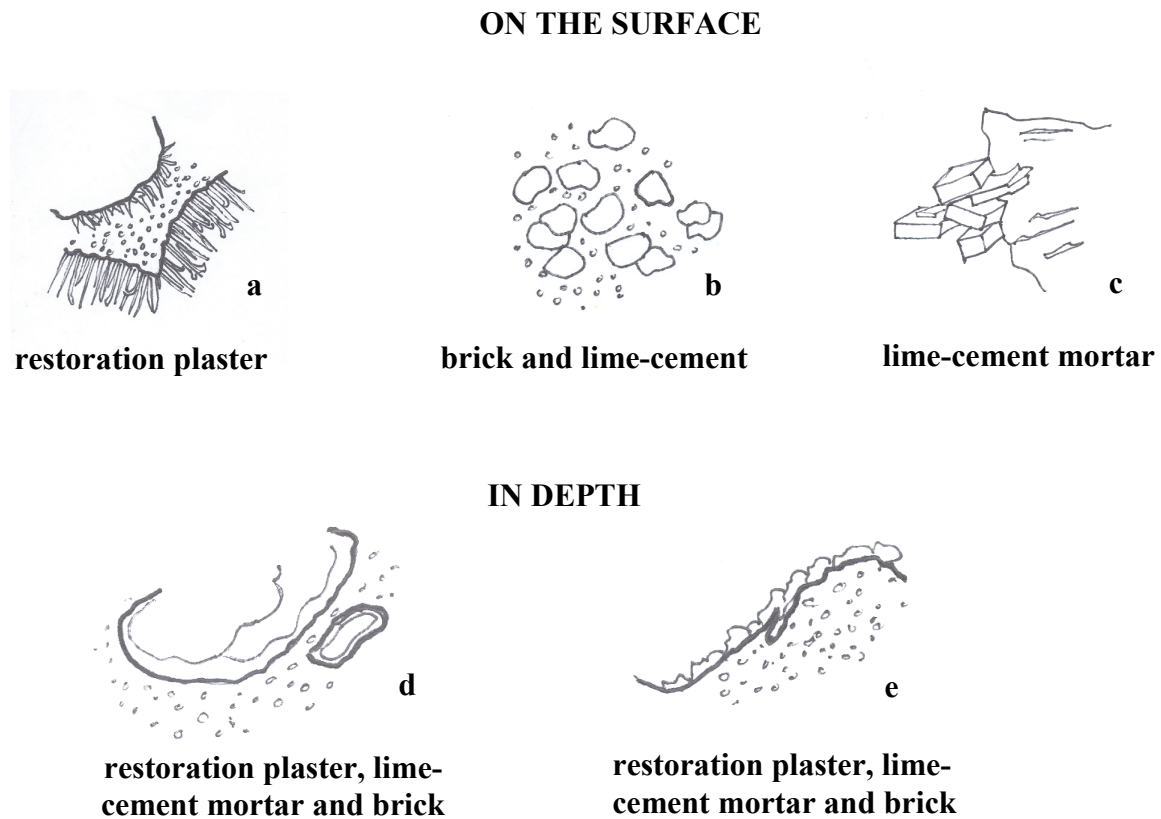


Figure 5.50 The salt crystallizes on the surface in the form of needle-like crystals (a), crystals agglomeration (b), cubic crystal and crust (c); in the cross section a layer of salt (d) or agglomeration of crystals well adhering to the pore wall (e) are observed

5.5.3 Inputs to the development of an accelerated test

From the three different RH cycles performed the following conclusions can be drawn, useful for a further development of a NaCl crystallization test:

- damage can be obtained by cycling the RH of the air through the RH equilibrium of NaCl, in absence of any other moisture source than the air RH;
- damage due to RH cycles is enhanced if the adsorbed/evaporated water is sufficient to dissolve and re-crystallize a relevant amount of salt;
- damage due to RH cycles is enhanced if the salts accumulate in the pores of a thin, outer layer of the material, however, without efflorescing. This has been obtained in the studied materials by an initial drying at 20 °C / 50% RH after absorption of salt solution;
- damage is enhanced if the salts do not migrate and crystallize in depth in the specimen during the RH cycle. This can be limited by an initial drying of the specimens at 20°C / 50% RH following the high RH period.

5.6 Accelerated weathering test

During this phase of the research, a weathering test procedure for sodium chloride has been defined on the basis of the results obtained during the previous two phases.

This procedure combines the elements that were found effective in the earlier experiments:

- use of wet-dry cycles obtained by re-wetting the specimens from the bottom by capillary rise;
- use of accelerated drying at high temperatures (60 °C);
- use of RH cycles through the RH of equilibrium of NaCl;
- use of high and low RH periods long enough to allow dissolution and complete re-crystallization of a relevant amount of salt;
- use of RH cycles favouring the accumulation of salt in a thin layer beneath the outer surface of the specimen, thus adsorption of moisture followed by an initial period of relatively slow drying (at 20 °C / 50% RH)

5.6.1 Test procedure

The type and the size of the specimens used in this test are the same as described in section 5.4.1. The specimens were sealed on the lateral sides with epoxy-resin and dried in an oven at 60 °C until constant mass was reached. The specimens were then left to equilibrate at room temperature before contaminating them with NaCl solution by capillary rise. A salt solution amount sufficient to wet the upper surface of the specimen and a salt amount of 1.5 g for each specimen was used. The salt solution concentration was calculated on the basis of the amount of solution and of the salt. Differently from the procedure described in the sections 5.4 and 5.5, a constant salt amount was used in all the materials, instead of 2% of their weight (see section 5.4.1). In this way a high salt content was obtained also in the restoration plaster in spite of its low density.

After salt contamination from the bottom, the specimens were sealed with removable tape and the weathering test started. In the case of the restoration plaster, preliminary wet-dry cycles were performed in order to transport and accumulate the salt near the surface. Salt accumulation at the surface is fundamental to guarantee the effectiveness of a weathering test including RH cycles.

The RH and the temperature during the test varied according to the cycle reported in figure 5.51. The use of a drying period of six hours at 20 °C / 50% RH following the 20 °C / 96% RH period is introduced to enhance salt transport to the surface (see section 5.5.3). The 20 °C / 50% RH and the 20 °C / 96% RH conditions were obtained in climatic rooms; the 60 °C / 0% RH condition was reached in an oven using a vessel with silica gel.

Each cycle (i.e period between two following re-wettings) comprised 3 low RH and 2 high RH periods and lasted 2 weeks. In total 6 cycles were performed in a period of about 3 months.

Every two weeks, at the end of the high RH period, the surface of the specimens was brushed with a soft brush. The debris was separated from the salt (see section 5.5.2.1), and its mass was recorded. Every two weeks, at the end of the high temperature period, the specimens were re-wetted with demineralized water by capillary rise from the bottom. The amount of water used for the re-wetting was equal to the amount of water added during salt contamination. The appearance of efflorescences and damage was visually and photographically monitored during the test. ESEM investigations on the cross section of the specimens were performed at the beginning and at the end of the weathering test.

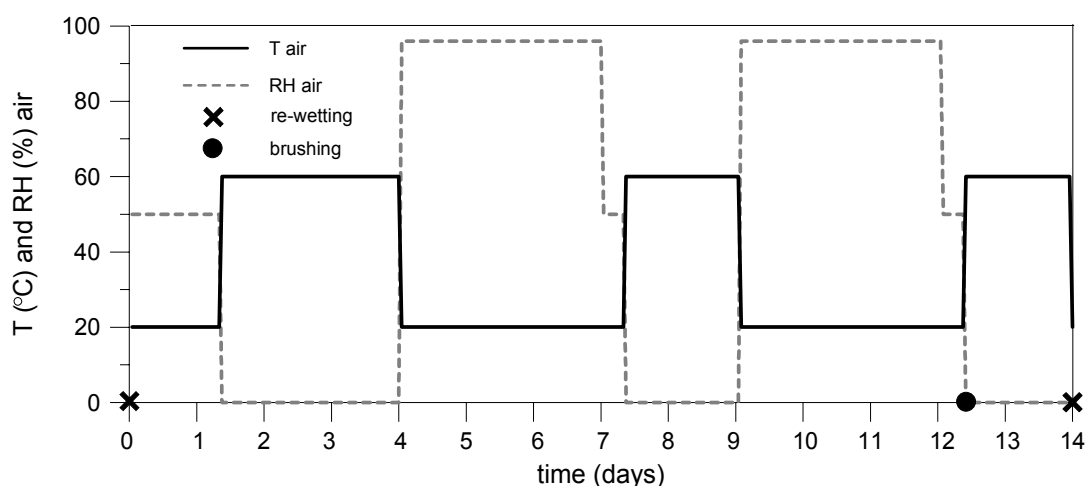


Figure 5.51 Temperature and RH cycle used in the weathering test

5.6.2 Results

5.6.2.1 Effect of the temperature and RH cycles on the damage

In table 5.3 the cumulative material loss at the end of the test is reported for each material.

Table 5.3 Cumulative material loss at the end of the weathering test

Material	Cumulative material loss (g)	Cumulative material loss (% of the initial mass)
lime-cement mortar	39.20	39.4
restoration plaster	0.12	0.27
fired-clay brick	0.18*	0.18*

* presence of cracks on the surface

It can be concluded that this test is very effective in the case of the lime-cement mortar in which an average mass loss of almost 40 g is recorded, corresponding to about 40% of the initial mass of the specimen. One of the three specimens was completely reduced to sand at the end of the test (figure 5.52).

Also the restoration plaster showed damage at the end of the test period, but to a less severe extent (the average material loss measured is about 0.3% of the initial mass of the specimen). The damage occurred in the form of sanding of the surface layer (figure 5.53).

The brick did not show any loss of cohesion of the surface but cracks appeared on the surface of the specimens contaminated with NaCl (figure 5.54). The reference specimen did not suffer any decay.

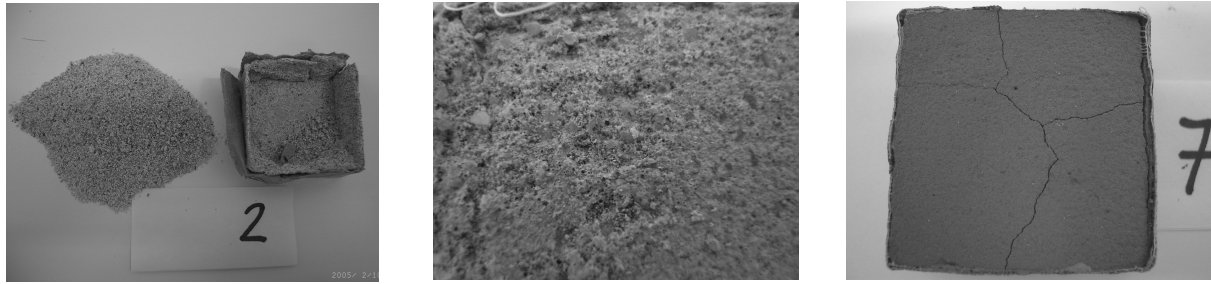


Figure 5.52 (left) Decay of the lime-cement mortar at the end of the weathering test: the specimen is completely reduced to sand

Figure 5.53 (middle) Decay of the restoration plaster at the end of the weathering test: the specimen shows sanding of the surface layer

Figure 5.54 (right) Decay of the brick at the end of the weathering test: the surface of the specimen is cracked

Investigations were carried out to explain this damage, since this was different from the powdering observed on the same brick in the previous weathering tests. It was found out that, by mistake, the outer layer (thickness about 2 mm) of the brick used in this experiment was originally impregnated with a water repellent.

The presence of the water repellent in the outer layer of the brick prevents the transport of the salt to the surface and causes salt crystallization at the untreated/treated interface. At the beginning of the test (after one drying cycle) salt accumulation is present at the treated-untreated interface but no damage has occurred yet (figure 5.55 - left). After 6 cycles a crack has developed at the interface (figure 5.55 - right), parallel to the surface; further cracks depart from the main crack and run perpendicular to the surface. The increasing accumulation of salt at the interface and the repeated dissolution-crystallization cycles are responsible for the observed cracks.

ESEM investigations were performed on cross sections of the brick specimens in order to investigate the origin of this damage pattern (section 5.6.2.2).

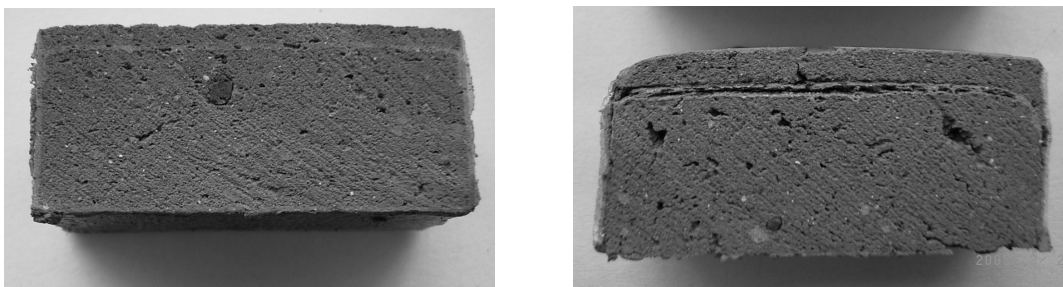


Figure 5.55 Cross section of brick specimens at the beginning (on the left) and at the end (on the right) of the weathering test

5.6.2.2 ESEM investigations

ESEM investigations were performed on the surface and on the cross section of the specimens at the beginning (after one drying cycle) and at the end of the weathering test.

The cross section of the lime-cement specimen shows, at the beginning of the test (i.e. after one drying cycle), the presence of agglomerations of crystals adhering to the binder and covering large voids (figures 5.56 and 5.57). At the end the test (i.e. after 6 wet-dry cycles), brighter zones are distinguishable in the binder (figure 5.58); in these areas the NaCl concentration measured by EDX is higher than in the other zones, but no individual salt crystal can be distinguished (figure 5.59).

The cross section of the restoration plaster shows, at the beginning as well as at the end of the weathering test, the presence of NaCl in the form of a smooth layer covering the pore walls. On the surface of the specimen, elongated, hair-like crystals are present.

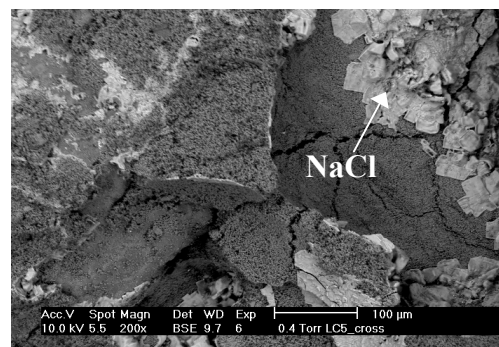
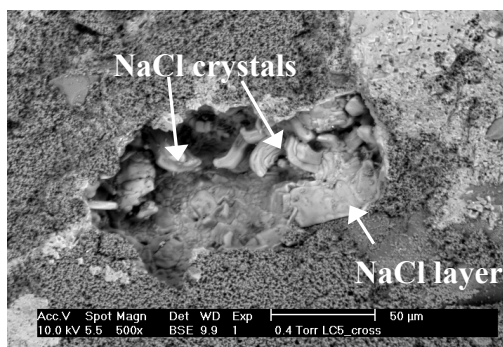


Figure 5.56 ESEM photomicrograph of NaCl layer covering a large void (cross section of lime-cement mortar specimen at the beginning of the test)

Figure 5.57 ESEM photomicrograph of NaCl crystallizing adhering to the binder (cross section of lime-cement mortar at the beginning of the test)

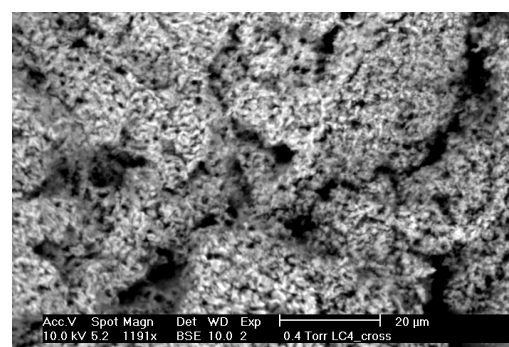
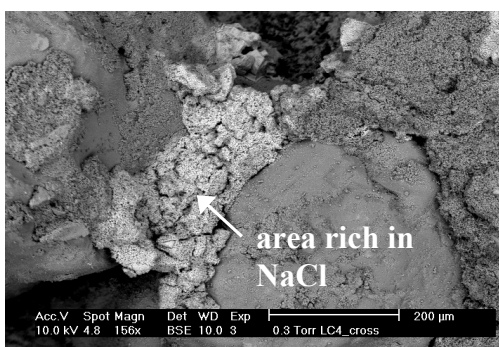


Figure 5.58 ESEM photomicrograph: the brighter areas indicate the presence of NaCl (cross section of lime-cement mortar specimen at the end of the test)

Figure 5.59 ESEM photomicrograph of the binder enriched in NaCl: no salt crystal is clearly distinguishable (cross section of lime-cement mortar specimen at the end of the test)

The brick specimen does not show any salt at the surface, neither at the beginning nor at the end of the test, because of the presence of the water repellent in the outer layer, precluding salt solution transport to the surface. At the end of the test a crack parallel to the evaporation surface is visible at the treated-untreated interface (figure 5.60). The average width of the crack is about 300 μm . Starting from this main crack, thinner cracks develop in the direction perpendicular to the evaporation surface. Most of the salt has accumulated in the area immediately above and beneath the crack (figure 5.61) whereas almost no salt is present in the crack. The salt has crystallized in the form of agglomerations of crystals adhering to the crack walls. No needle-like crystals are present in the crack, as often observed in case of scales lifted by salt crystals growing underneath them [Arn90].

Similar decay patterns (cracks not filled with salts) have been observed at other occasions in different materials [Roo05] in the presence of water repellent decreasing the drying rate and causing accumulation of salt in depth in the material.

In the present case the observed decay may be explained by supposing that:

- At first, salt accumulation at the treated/untreated interface is produced by the presence of a water repellent layer (inhibiting the liquid moisture transport to the surface) and by the repeated wet-dry cycles.
- Next, a differential dilation during wetting and drying between areas with high and low salt content leads to shear stresses and cracks (see section 5.4.2.3).
- Once the crack has appeared, moisture transport takes place preferentially through the pore system of the brick; therefore not much more salt grows in the crack.

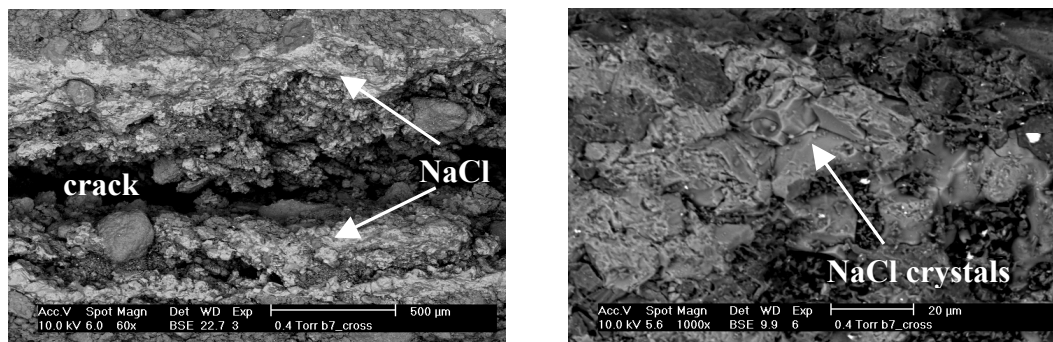


Figure 5.60 (left) ESEM photomicrograph of the crack parallel to the evaporation surface developed in the brick: salts have crystallized at both sides of the crack but not in it (cross section of brick specimen at the end of the weathering test)

Figure 5.61 (right) ESEM photomicrograph of NaCl crystallizing in the brick, at the border of the crack (cross section of brick specimen at the end of the weathering test)

5.6.3 Assessment of the test procedure

A weathering test can be considered effective if it is able to reproduce, in laboratory and in a short time, the damage occurring in practice during a much longer period. Therefore, a laboratory weathering test should be accelerated and, at the same time, realistic. The rate of

development of the damage and the reliability of the developed procedure are evaluated in the following sections.

5.6.3.1 Rate of development of the damage

The procedure developed in this research (see section 5.6.1) has been shown to cause damage within a period of about 3 months, even in salt resistant materials. The effectiveness of this procedure is based on the use of:

- re-wetting by capillary rise, leading to accumulation of salt in a thin outer layer of the material;
- RH cycles, producing repeated dissolution and re-crystallization of the salt;
- high temperature (60 °C) of drying, allowing repeated dissolution-crystallization cycles in a short period.

This procedure constitutes a step forward with respect to other weathering tests for NaCl. Previous experiments performed according to the RILEM MS-A.1 procedure (constant drying condition at 20°C / 50% RH) showed that in case of salt resistant materials like restoration plasters no damage was obtained even after several months [Wij97, Wij02].

Anyway, the newly developed procedure should be tested on a larger selection of materials in order to have a further proof of its effectiveness. The first results of the application of the weathering procedure on tuff stones [Bol05] suggest that higher salt contents may be used in order to speed up the damage. Re-wetting the specimens with salt solution instead of demineralized water is a way to increase the salt content. However, it should be considered that a too high salt content may result in a non realistic test.

Besides, the drying conditions in the period following the absorption of solution should be selected such to achieve the highest salt accumulation in the thinnest possible layer near the evaporation surface. As explained in [Pel03] salt distribution is the result of the competition between advection, accumulating the salt at the evaporation surface, and diffusion, which levels off any accumulation. The result of this competition, i.e. salt accumulation or homogeneous distribution, depends on the drying rate, the travel length of the salt solution, the moisture content and the diffusion coefficient of the ions in the solution. From this it is clear that several parameters should be known in order to predict the location of salt accumulation. This is obviously not realistic when performing a crystallization test on a large variety of materials.

In order to obtain salt accumulation near the surface the drying front should not enter the material. In order to reach this aim it can be suggested to perform a relatively slow drying of the specimens (for example at 20 °C / 50% RH) for a few days after the absorption of salt solution; next a higher temperature may be used to accelerate the complete drying. For slow transporting materials, like the restoration plaster tested in this research, repeated wet-dry cycles before starting the weathering test can constitute a faster way to obtain salt accumulation near the surface. The salt distribution should be checked anyway before starting the RH cycles.

Apart from assessing the increased rate of damage produced by the developed procedure with respect to other tests, it would be very useful defining a time scale between damage in laboratory and in practice. This would allow prediction of the service life of materials.

However, comparison between practice and laboratory is particularly difficult because of:

- the lack of quantitative data on the evolution of the damage in situ;
- the uncertainties in estimating the effect of differences, with respect to environmental conditions, salt and moisture load etc., between the real situations and the laboratory.

In the present work an attempt has been made to compare the evolution of the damage in practice and in laboratory. The monitoring of the damage in the church of St. Nicholas in Brouwershaven, in which the same restoration plaster as tested in the laboratory is present, provided the data on the in situ situation (see chapter 4). The results obtained in the newly developed test procedure (section 5.6.2) constituted the second term of the comparison.

This approach has inevitable limitations due to the differences between the laboratory and practice situation considered. Therefore, before discussing the results, some points should be emphasized:

- The quantification of the damage in the laboratory starts from a situation of undamaged plaster, whereas in reality damage was already present when the monitoring of the decay started. Since this type of decay has been observed to proceed much faster once it is initiated, this should be taken into account when comparing the results.
- The area from which the material falling from the plastered wall is collected comprises the whole zone from the debris collector to the ceiling. In the present research only the damaged area above the debris collector (about 25 x 100 cm) (figure 5.62) has been considered, since the presence of the salt, and therefore of the damaging mechanism, in the upper part of the wall has not been assessed.
- In practice, apart from sodium chloride, small quantities of other salts may be present

Because of these factors, the rate of the damage measured in practice is somewhat overestimated with respect to the damage measured in laboratory.

A decay index has been introduced in order to compare the material loss measured in situ and in the laboratory. The following decay index (D) has been defined:

$$D = \frac{m_i}{A \cdot t_i} \quad (5.1)$$

where:

m_i [g] = mass of the debris (falling from the wall or brushed from the surface) during a period i

A [cm²] = area of the surface (from which the debris falls or is brushed)

t_i [days] = time duration of the period i

For practical situations values between 0.3 and 0.7×10^{-4} g/(cm² day) are calculated, whereas in the laboratory for the same plaster the debris amounts to about 0.6×10^{-4} g/(cm² day). This means that, once the salts are deposited near the surface, the rate of decay in the laboratory is

about the same as in practice. However, it is clear that the new developed test shortens the time of appearance of the first damage: in practice it took about 6 years before the damage became visible whereas in laboratory this occurred after only a few weeks.

The defined procedure for the quantification and the comparison of the damage has proven to give the information necessary for a comparison. Monitoring of the damage, performed in the same ways as described in section 4.6, and starting from the very beginning of the decay process would help in relating the rate of decay in situ and in laboratory. The use of full-scale models (a hybrid situation between laboratory and practice, in which salt type, moisture source etc can be controlled but other environmental parameters are the same as in the field) has shown in the past to offer a good possibility for relating laboratory and practice [Bin96].

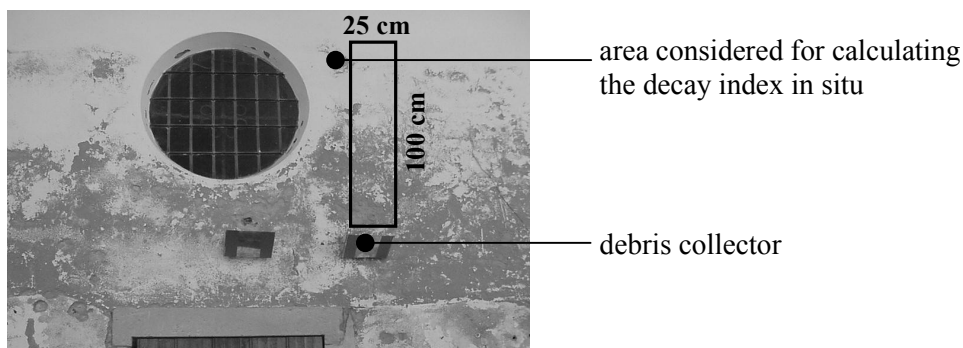


Figure 5.62 Debris collector on the decayed wall. The area considered for the calculation of the decay index in situ is indicated (church of Brouwershaven, The Netherlands)

5.6.3.2 Degree of realism

In order to be valid, the laboratory test, apart from being accelerated, has to offer a realistic simulation of the situation occurring in practice.

The reliability of the new developed test will now be evaluated with respect to the salt content and the environmental parameters, the simulated damage processes and the obtained decay patterns.

Salt content and distribution

The salt content in the specimens (2-3% NaCl m/m over a depth of 2 cm) has been defined also on the basis of the results of the case studies and it is therefore comparable to the salt content measured in practice (see section 3.7). The salt distribution obtained in the laboratory is similar to the one commonly observed in practice: in both cases most of the salt accumulates near the surface (provided that the material is homogeneous and no water repellent is present).

Environmental parameters

Temperature and RH values have been selected with the aim of speeding up both adsorption and drying. Nevertheless, the range of variation of the temperature between 20 and 60 °C is still realistic for our climates (a temperature of 60 °C can be measured on the surface of the wall in summer months).

Damage processes

The procedure is based on the combination of wet-dry cycles and RH cycles through the RH of equilibrium of NaCl. The rewetting of the specimens by capillary rise and the unidirectional drying through the surface simulate the processes of rising damp and evaporation in a wall much better than complete immersion and multidirectional drying (among others Gou74, Bin98 and the standard ASTM C88-99 and EN 12370).

The RH cycles reproduce the changes in the RH of the air that have been proven to cause serious damage in the field (chapter 4).

Decay pattern

As a consequence of the choice of parameters on the basis of the observation of the real cases, the type of damage obtained in the test is similar to the decay observed in practice. The loss of cohesion of the surface layer of the specimens in the form of powdering or sanding is the most common type of damage observed in presence of sodium chloride (see chapter 3) [Tsu03, Cha0b, Riv97].

5.6.3.3 Factors limiting the effectiveness of the test

From the evaluation given above it is possible to conclude that the new developed test is accelerated with respect to other existing procedures (see 5.6.3.1) and, at the same time, is a realistic simulation of the damage occurring in reality (see 5.6.3.2).

However, it should be reminded that the effectiveness of this test strongly depends on the salt accumulation near the evaporation surface. As discussed before (see 5.6.3.1), an initial drying at ambient conditions (20 °C / 50% RH) after salt contamination is usually sufficient to favour the accumulation of salts at the evaporation surface. In some slow transporting materials repeated wet-dry cycles may be necessary to accumulate most of the salt near the evaporation surface. The salt distribution before the start of the test should be checked in order to be sure that the weathering test will be effective.

The necessity of salt accumulation at the surface has as consequence that this test is not very suitable for materials containing a water repellent, either mixed in the mass (like some restoration plasters for salt loaded substrates) or applied on the surface. In these cases the salt crystallizes far from the surface and is not very sensitive to the RH changes of the air: a little salt amount undergoes dissolution and re-crystallization and the only effect of the high RH period (during which dissolution of the salt occurs) is delaying the drying. For these types of material, a different test procedure based on re-wetting and accelerated drying without any RH cycle, might therefore be more effective [Wij05].

5.7 Discussion and conclusions

The main aims of the research described in this chapter were the elucidation of the effect of the environmental conditions on NaCl damage and the development of an effective weathering test.

From the study of the effect of the environmental conditions on the NaCl damage, the following conclusions can be drawn:

- No evidence has been obtained that accelerated drying (by the use of high temperature, low RH or air flow) is as such more damaging than slow drying at ambient conditions. This conclusion may be related to the fact that, because of the very slow drying of the materials when contaminated with NaCl, only the situations after one drying cycle at different environmental conditions could be compared; at that point no damage had occurred yet for any of the drying conditions. In the tests performed, the main advantage of the enhanced drying is the possibility of repeating several dissolution-crystallization cycles in a short period.
- RH changes through the RH of equilibrium of the salt are very effective in enhancing the decay, provided that the salt accumulates just beneath the surface and that sufficient time is given for its dissolution and re-crystallization.
- The environmental conditions strongly influence the obtained decay pattern (see section 1.4.2.3); this should always be taken into account when evaluating the results of an accelerated test.
- The developed weathering test has proven to be effective for the investigated materials. This procedure is able to cause damage, even in a salt resistant plaster, in a period of about 3 months. The test shortens the time of appearance of the first damage with respect to situations in practice (from several years to a few weeks) and it constitutes an improvement of existing weathering tests (for example RILEM MS-A.1 test).

Recent results [Ver05] show that increasing the salt content in the specimen up to 4% m/m may enhance the damage. The possibility of further improving the test by re-wetting the specimens with salt solution instead of demineralized water might therefore be considered. However, a too high salt amount might be not realistic and lead to not reliable results.

For the test to be effective, salt accumulation near the evaporation surface is necessary. The difficulty of foreseeing the location of salt accumulation and therefore the necessity to check the salt distribution before starting the RH cycles may constitute a limit of the test. Usually an initial drying at ambient conditions (20 °C / 50% RH) and/or the use of repeated wet-dry cycles lead to salt accumulation near the surface in a reasonably short period of time.

The developed test is less suitable for materials containing water repellents (mixed in the mass or applied on the surface), since in these cases the necessary salt accumulation near the evaporation surface is inhibited. For these materials a weathering test based on re-wetting and

accelerated drying, without the use of RH cycles through the RH of equilibrium of the salt [Wij05], will probably give better results.

The procedure has been proven to be a realistic simulation of the damage in practice. The obtained decay patterns (sanding and powdering of untreated material and spalling of material having a water repellent layer) are in fact commonly observed in the field in NaCl contaminated materials.

For the future, the testing of the developed procedure on a larger selection of materials is recommended in order to have a further check of the results obtained until now. The possibility of improving the test by increasing the salt content should also be checked.

Interesting hypotheses on the damage mechanism in the presence of NaCl, based on the differential dilation of layers of material with different salt load, have emerged. These hypotheses constitute the starting point of the research described in chapter 6.

Chapter 6

Dilation due to NaCl crystallization: a hypothesis on the damage mechanism

6.1 Introduction

As extensively shown in chapter 2, the damage mechanism due to NaCl has not been unequivocally explained yet. According to the most accepted theory [Cor49, Win72, Sch99], salt crystallization damage occurs because salt fills the pores and creates pressure on the pore walls. This pressure is dependent on the supersaturation ratio. In an equilibrium situation, the degree of supersaturation that can be reached depends on the pore radius: the smaller the pores the higher the supersaturation. Following this theory, in order to produce crystallization pressures high enough to cause damage, NaCl should crystallize at high supersaturation, filling pore sizes in the range of a few nanometers [Fla02, Rij04].

Some objections have been raised to the possibility of NaCl to develop high pressures: NaCl has a low tendency to supersaturate [Pel02, Ste05], therefore it would perhaps not be able to produce high crystallization pressures. Besides, most traditional porous building materials do not have pores in the nanometer range. Nevertheless they may show serious damage in the presence of NaCl.

Recently the hypothesis of crystallization in a non equilibrium situation (e.g. in case of fast evaporation), and the possible development of high crystallization pressures even in larger pores, has been suggested by [Sch04, Ste05] (see chapter 2), but no experimental proof of this theory has been given yet.

The discussion reported above suggests that damage due to NaCl may not only be related to crystallization pressure as described in literature starting with Correns' work, but involves other mechanisms too. Some authors [Wen92, Sne97, Wen02] have observed that NaCl strongly affects the dilation behaviour of some materials (sandstone containing clay and brick) but no definitive explanation for this mechanism has been given yet. An important reason that hampers the clarification of this possible damage mechanism is the lack of systematic experimental investigations of the phenomenon. Until now, only few experiments have been carried out on a restricted number of materials.

The research reported in this chapter is aimed at studying the dilation phenomenon in detail and at verifying it for different salt types. The research was performed on lime-cement mortar specimens. The experiments were carried out in steps:

- the effect of NaCl on the hydric and hygric dilation behaviour of the lime-cement mortar was investigated (sections 6.3.1, 6.3.2, 6.3.3 and 6.3.7);
- the dilation in the presence of NaNO₃ and KCl was studied (section 6.4.2) in order to check whether the observed behaviour was limited to NaCl or common to more salts. These two salts were selected because they are both hygroscopic, they do not have hydrated forms and each of them has one ion in common with NaCl;
- the influence of the pH on the dilation was studied (section 6.3.4) since this parameter is known to have an effect on the creep of the salt [Puh83];
- the effect of a crystallization inhibitor, modifying the crystal habits of the salt, on the dilation behaviour of NaCl contaminated specimens was investigated (section 6.3.5);
- the dilation behaviour of specimens contaminated with Na₂SO₄ was studied (section 6.3.6)

An Environmental Scanning Electron Microscope (ESEM) was used in order to investigate the location and the crystallization habits of the salts in the specimens (section 6.4).

6.2 Materials and methods

A lime-cement mortar, whose properties have been described in section 5.3.2, has been selected for this study. This mortar has been shown to be extremely susceptible to damage due to sodium chloride (see chapter 5). Mortar specimens with a size of 20x10x2 cm were used for the study of the hydric and hygric behaviour. The mortar slabs were prepared and cured according to the description given in section 5.3.1.

Before measuring the hydric and hygric behaviour the specimens were contaminated with NaCl according to the following procedure: the mortar slabs were sealed on the four lateral sides by epoxy resin and a NaCl saturated solution (concentration 6M) was introduced from the bottom by capillary rise (figure 6.1). An amount of solution equal to the Capillary Moisture Content (C.M.C.) of the mortar (i.e. the moisture content high enough to wet the upper surface) and leading to 2% m/m of NaCl in the specimen was used.

This amount of salt has been proven to be enough to damage this material (see chapter 5). After contamination, the specimens were sealed at the bottom with removable tape and dried at 10% RH and 20 °C until a constant weight was reached. This drying process led to almost no efflorescences; salts accumulated just beneath the evaporation surface of the specimen. Since the crystallization inhibitor increases the tendency of the salt to efflorescence, the specimens contaminated with NaCl plus inhibitor were dried at 40 °C. By the use of a high temperature the drying front recedes fast in the material preventing the formation of efflorescences. Also the sodium sulphate contaminated specimens were dried at the temperature of 40 °C with the purpose of guaranteeing the precipitation of thenardite inside the material. Because of the limited solubility of Na₂SO₄ and the necessity of contaminating the specimen by a single wetting (to avoid repeated dissolution – crystallization cycles) 1% Na₂SO₄ (mass of salt / mass of the specimen) instead of 2% was used.

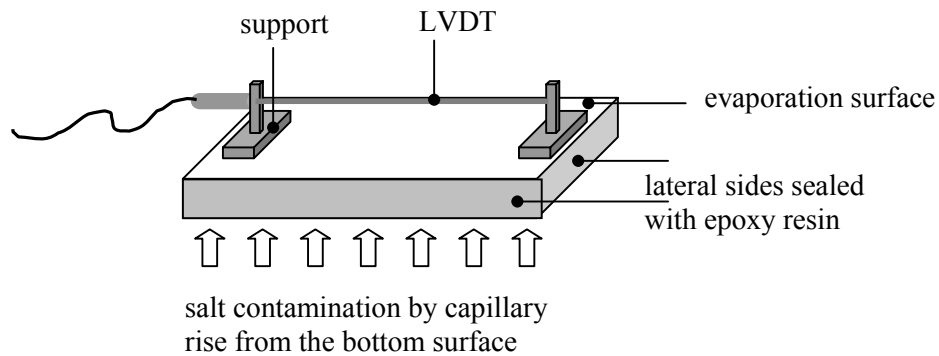


Figure 6.1 Salt contamination of the specimen

Once the specimens contaminated with salt had dried, metal supports for the Linear Variable Differential Transformer (LVDT) to be used in the measurement of the hydric and hygric behaviour were glued on the evaporation surface of the mortar slabs. The supports were glued, by means of a two-components glue, at a distance of 150 mm from each other (figure 6.1).

The hydric and the hygric behaviour of the specimens was monitored inside a climatic cabinet in which the temperature and RH of the air can be programmed and controlled. In order to reach a very low RH, dry air was blown into the cabinet.

The measuring apparatus (figure 6.2) was composed of:

- a balance with an accuracy of 0.1 g, connected to a PC, for monitoring the variation in specimen weight due to hygroscopic moisture uptake and release, connected to a PC; in some of the experiments two balances were used;
- a LVDT fixed to the supports glued on the mortar and connected, through the data acquisition system Labview, to a PC;
- two data loggers for a double check of the temperature and RH of the air in the climatic cabinet.

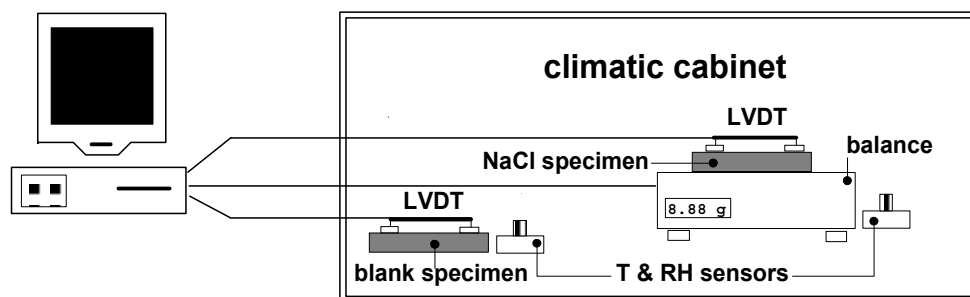


Figure 6.2 Test set up: the specimens, on which the LVDT's are mounted, are placed in a climatic cabinet. A PC collects the data on the dilation and on the mass changes. Temperature and RH sensors are used for an additional check of the environmental conditions

6.3 Results

6.3.1 Hydric behaviour of NaCl contaminated specimens

The hydric behaviour was studied both on NaCl contaminated and blank mortar slabs. The specimens were put in the climatic cabinet at 20 °C and 45% RH and they were allowed to absorb water by capillary rise from the bottom for a period of two days. Subsequently the bottom of the specimens was sealed with tape, the RH in the cabinet lowered to 0% RH and the drying started. After about 4 weeks, the wet-dry cycle was repeated.

Data on the temperature and RH of the air, as well as on the dimensional changes of the specimens at its surface, were collected continuously. Figure 6.3 shows the results of the experiment.

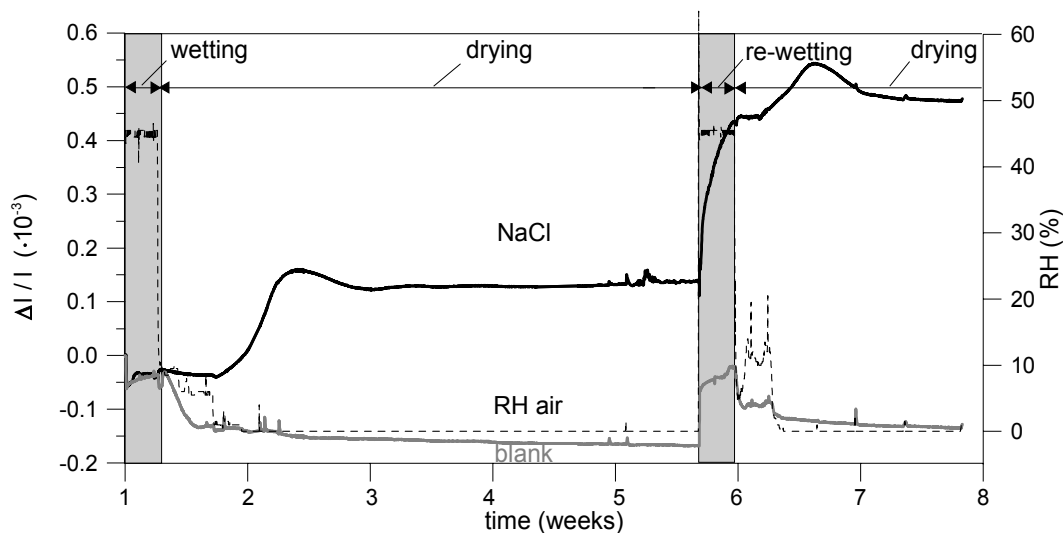


Figure 6.3 Change in length of blank and NaCl contaminated specimens during wetting at 20 °C/45% RH (grey areas) and drying at 20 °C/0% RH (white area) cycles

During wetting, the salt contaminated and the reference specimen have a similar behaviour, consisting of initial shrinkage (due probably to the wetting of the lower part of the sample) followed by dilation (corresponding to the migration of water to the surface of the sample). During drying, the blank specimen shrinks, while the salted specimen, after a period of about 4 days in which it does not show any change in length, starts dilating. It can be reasonably supposed that this dilation occurs when, because of evaporation of water, the salt starts crystallizing. The maximum dilation is about 0.13 $\mu\text{m}/\text{mm}$ and is reached in 5 days. During the re-wetting both specimens dilate, but the dilation is larger for the salt contaminated than for the blank specimen. During drying, the blank specimen shrinks while the salted specimen dilates further.

This experiment shows that the hydric behaviour of this material is strongly influenced by the presence of sodium chloride. The salt contaminated specimen undergoes an irreversible

dilation whereas the changes in lengths of the blank specimen, apart from being smaller, are reversible.

In the described experiment the effect of dissolution and crystallization of the salt on the shrinkage/dilation of the material cannot be followed in detail. In fact the amount of absorbed and evaporated water cannot be measured without handling of the specimen; besides, it is not known at which moment water, absorbed by capillarity from the bottom of the specimen, reaches the surface where most of the salt accumulates. For a better understanding of the dilation phenomenon, a slower and more controlled moisture absorption and release is necessary. The use of RH changes through the RH of equilibrium of NaCl (75%) allows to reach this aim.

In the following sections the study of the effect of RH changes on the dilation of salt contaminated specimens is described.

6.3.2 Hygric behaviour of NaCl contaminated specimens

The hygric behaviour of NaCl contaminated and blank (reference) mortar slabs was measured. The specimens, prepared as described in section 6.2, were placed in the climatic cabinet. The temperature was maintained constant at 20 °C and the RH was varied between about 10% RH and 90% RH every 48 hours. Six RH cycles were performed. During the test the NaCl contaminated specimen was put on a balance and its mass was continuously monitored.

The results, reported in figure 6.4, show that the blank specimen dilates during the high RH period and shrinks during the low RH period, as expected [Hil64], while the NaCl contaminated specimen behaves in the opposite way. The dimensional changes of the salt contaminated specimen are not only opposite but also much larger than for the blank specimen. When the cycles are repeated, the dilation increases while the shrinkage remains about the same magnitude: this leads to an increasing and irreversible dilation that reaches, at the end of the sixth cycle, 1.3 $\mu\text{m}/\text{mm}$. On the contrary, the dimensional changes are completely reversible for the blank specimen.

The dilation leads to a stress that is likely to exceed the low tensile strength of the plaster and in fact results, at the end of the test, in serious damage. The damage consists of sanding of the outer layer of the plaster (figure 6.5a-b); the material loss is about 7% of the initial mass of the specimen. The serious damage observed points out the importance of RH changes for the development of the salt decay in lime-cement mortars.

The results obtained in this work are in accordance with the data reported in the literature for clay containing sandstone and for brick [Wen92, Wen97, Wen02]. Moreover, the experiments on the lime-cement mortar clearly demonstrate that the presence of reactive clay is not a necessary factor for the dilation behaviour observed in NaCl contaminated materials.

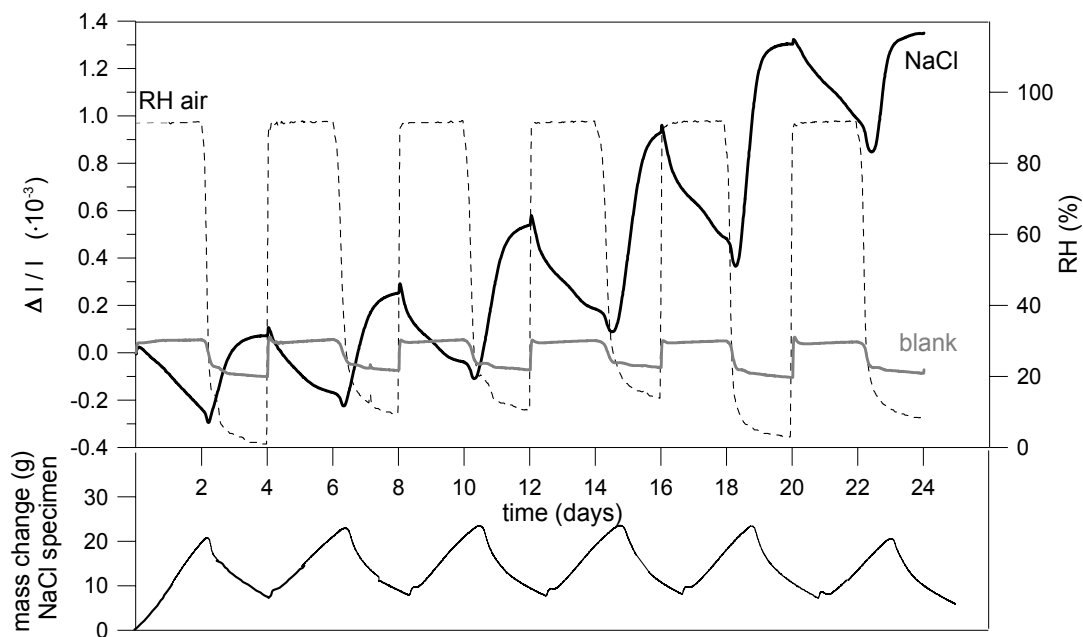


Figure 6.4 Dilation of blank and NaCl contaminated specimens (upper graph) and mass change of the NaCl contaminated specimen (lower graph) during RH cycles



Figure 6.5a (left) Sanding of the outer layer of the mortar in the presence of NaCl after 6 RH cycles
Fig.6.5b (right) Material brushed from the surface of the mortar after 6 RH cycles

Table 6.1 Hygric dilation in material contaminated with NaCl

Material	Hygric dilation
Lime/cement mortar without NaCl (this study)	0.13 $\mu\text{m}/\text{mm}$ (5-90% RH)
Lime/cement mortar with NaCl (this study)	1.3 $\mu\text{m}/\text{mm}$ (after 6 cycles 5-90% RH) 0.3 $\mu\text{m}/\text{mm}$ (after 1 cycle 5-90% RH)
Sandstone with clay without NaCl [Wen92]	0.2 $\mu\text{m}/\text{mm}$ (35-90%RH) (after 1 or 6cycles)
Sandstone with clay with NaCl [Wen92]	0.5 $\mu\text{m}/\text{mm}$ (after 6 cycles 35-90% RH)
Weathered 18 th century brick with NaCl [Wen02]	0.3-4 $\mu\text{m}/\text{mm}$ (after 9 cycles 40-85% RH)
Fresh 20 th century brick with NaCl [Wen02]	0.1-1 $\mu\text{m}/\text{mm}$ (after 9 cycles 40-85% RH)

In order to obtain a better understanding of the dilation mechanism, more detailed experiments were necessary. Performing a RH cycle slowly and with small increments would allow identifying the point at which dilation and shrinkage occur and relate these processes unequivocally to either salt crystallization or dissolution. A new experiment was set up in which the RH was varied stepwise between 30 and 96% RH. Each step in RH was done in 1 hour and was followed by 23 hours at constant RH. The experimental data (figure 6.6) clearly show that the blank specimen dilates while the RH increases and shrinks while the RH decreases. On the other hand, the NaCl contaminated specimen shrinks at RH values higher than 75% and considerably dilates when the RH drops below 75%.

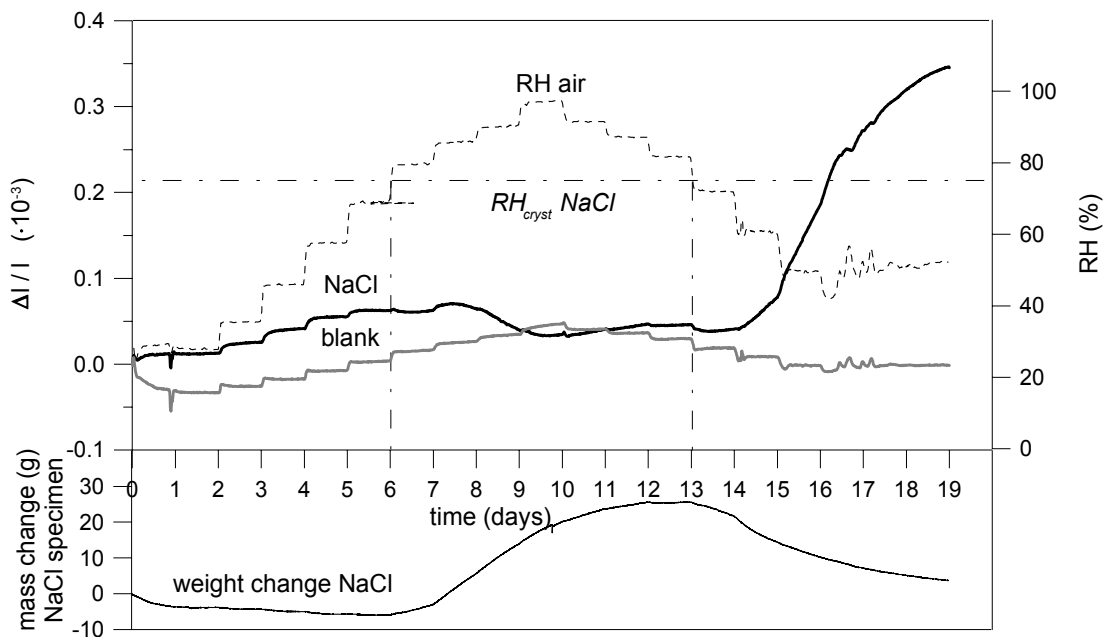


Figure 6.6 Dilation of blank and NaCl contaminated specimens (upper graph) and mass change of the NaCl contaminated specimen (lower graph) during a single RH cycle (max RH 95%)

Three parts can be distinguished in the curves:

1 Increasing the RH in a region below the RH of equilibrium of NaCl (30-75% RH)

In this RH range the behaviour of the blank and of the NaCl contaminated specimens is similar: both dilate when the RH increases. The dilation is due to water vapour adsorption [Hil64].

2 Increasing and decreasing the RH above the RH of equilibrium of NaCl (75-96-75% RH)

After crossing the value of 75%RH, the behaviour of the NaCl contaminated specimen starts to deviate from that of the specimen without salt: as soon as liquid water is present in the plaster (as shown by the mass change), the salt starts dissolving and some shrinkage is measured. The shrinkage of the salt contaminated specimen during salt dissolution is probably due to the release of the tension developed during the crystallization that occurred

during the initial contamination of the specimen. A definitive proof of this hypothesis is given in section 6.3.3.

3 Decreasing the RH (75%-45% RH) below the RH of equilibrium of NaCl

When the RH drops below 75%, the salt contaminated specimen starts drying (as shown by the mass loss) and dilates considerably. The curve becomes steeper with decreasing RH. At the end of the test, after 4 days of drying, the measured dilation is about $0.35 \mu\text{m}/\text{mm}$. The non contaminated specimen shrinks, as expected, when the RH is lowered; at the end of the cycle it has returned to its original length.

A further proof that the behaviour of a salt contaminated specimen is modified only if the equilibrium RH of the salt is crossed, is given by another experiment in which the RH was varied but kept below 75% (figure 6.7): in this case no irreversible dilation took place. The changes in length of the blank and of the NaCl contaminated specimen are similar, moderate and reversible.

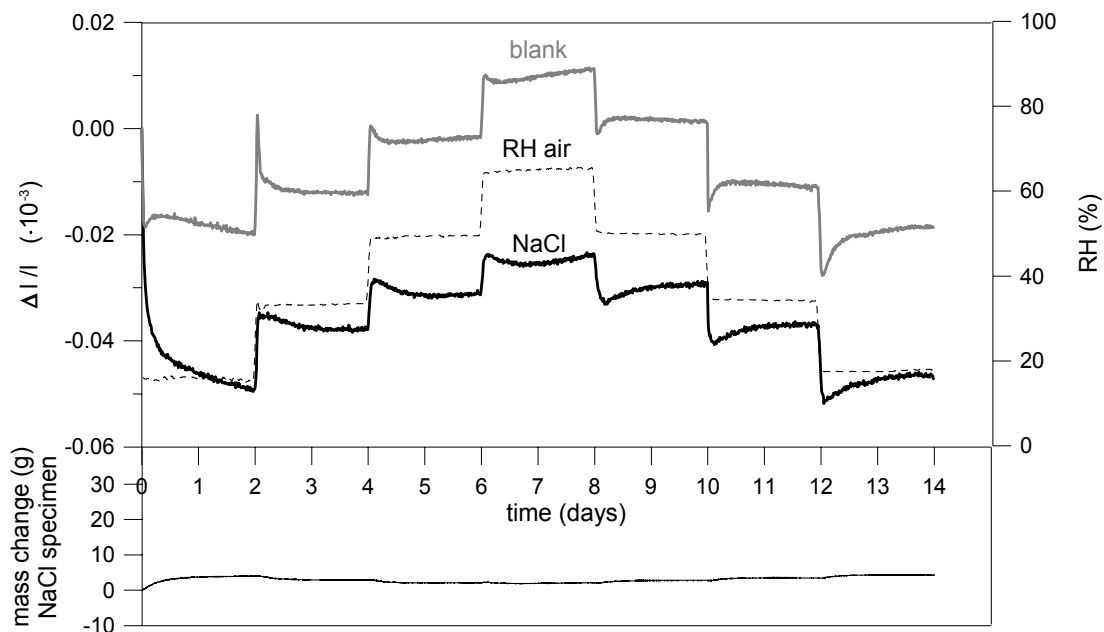


Figure 6.7 Dilation of blank and NaCl contaminated specimens (upper graph) and mass change of NaCl contaminated specimen (lower graph) during a RH cycle below 75% RH

6.3.3 Effect of absorption of NaCl solution on dilation

In order to prove that the shrinkage measured during dissolution of the sodium chloride (see section 6.3.2) is due to release of the stresses developed during the crystallization of the salt that occurred during the initial contamination of the specimen, the following experiment was set up. Solid NaCl (2% of the dry weight of the specimen) was distributed over the surface of a mortar slab not previously contaminated with salt. The specimen, with the LVDT attached to it, was placed in the climatic cabinet and the RH has increased over the RH of equilibrium of NaCl (75%). This caused the dissolution of the salt and the absorption of the salt solution in

the specimen. The absorption of the salt solution resulted first in dilation of the specimen (figure 6.8). Then the RH was lowered and the salt crystallized producing additional dilation. When the RH was increased again over the RH of equilibrium and the salt dissolved, the specimen shrank. This experiment clearly demonstrates that the shrinkage occurring during dissolution of the salt is due to the release of the stresses produced during crystallization. If dissolution of the salt takes place in specimens in which no crystallization event had occurred before, no shrinkage is measured.

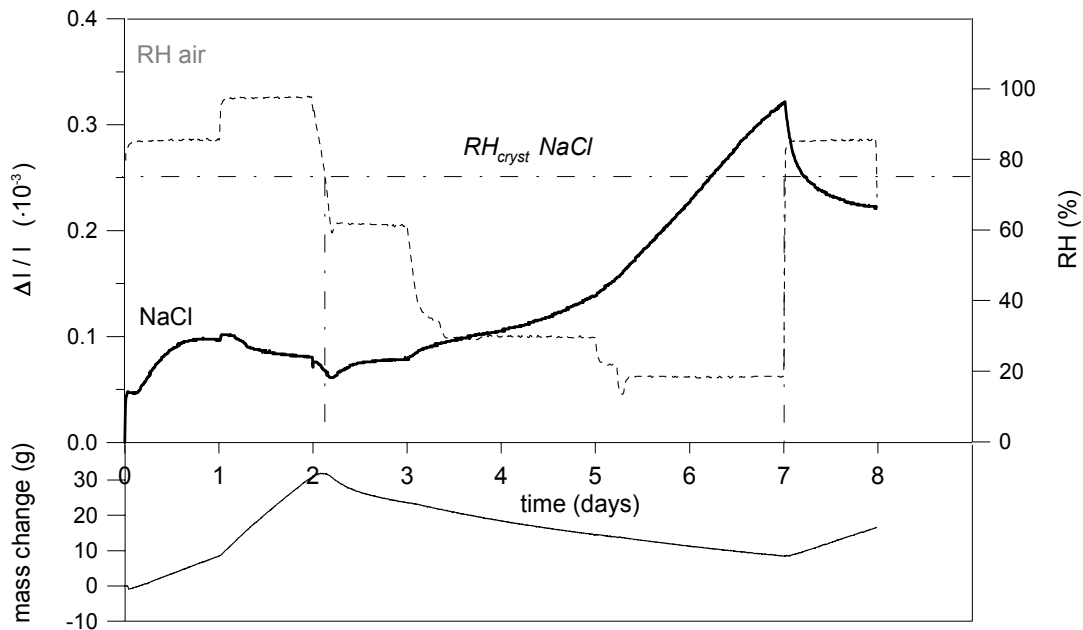


Figure 6.8 Change in length of a blank specimen during absorption of NaCl solution, subsequent crystallization and re-dissolution of the salt

6.3.4 Hygric behaviour of NaNO_3 and KCl contaminated specimens

The above-described experiments have shown that NaCl is able to produce irreversible dilation during crystallization. To check whether this behaviour is specific for NaCl or occurs also in the presence of other salts, further experiments were set up.

Two hygroscopic salts were selected having a cation or anion in common with NaCl, respectively, and no hydrated forms: NaNO_3 and KCl. The specimens were prepared in the same way as with NaCl. The same amount of solution was introduced in the mortar. The concentration of the solution was defined in such a way as to reach a salt content of 2% of the mass of the dry specimen in all cases. As shown in figures 6.9 and 6.10, in both cases shrinkage is observed when the RH exceeds the values where water starts to condensate and the salts dissolve in the water (at 20 °C this happens at 85% and 75% for KCl and NaNO_3 , respectively [Arn90]). When the RH decreases below these values the specimens start drying, the salts crystallize and dilation occurs. Therefore it can be concluded that this behaviour is not typical for NaCl but it is common to more salts.

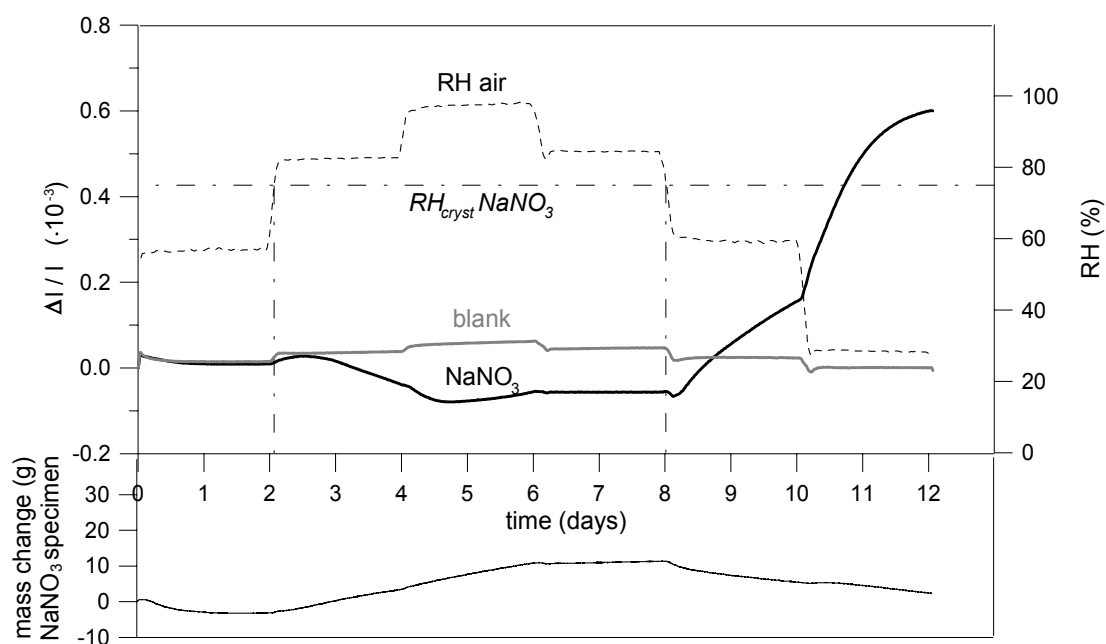


Figure 6.9 Dilation of blank and NaNO₃ contaminated specimens (upper graph) and change in mass of the NaNO₃ contaminated specimen (lower graph) during a RH cycle

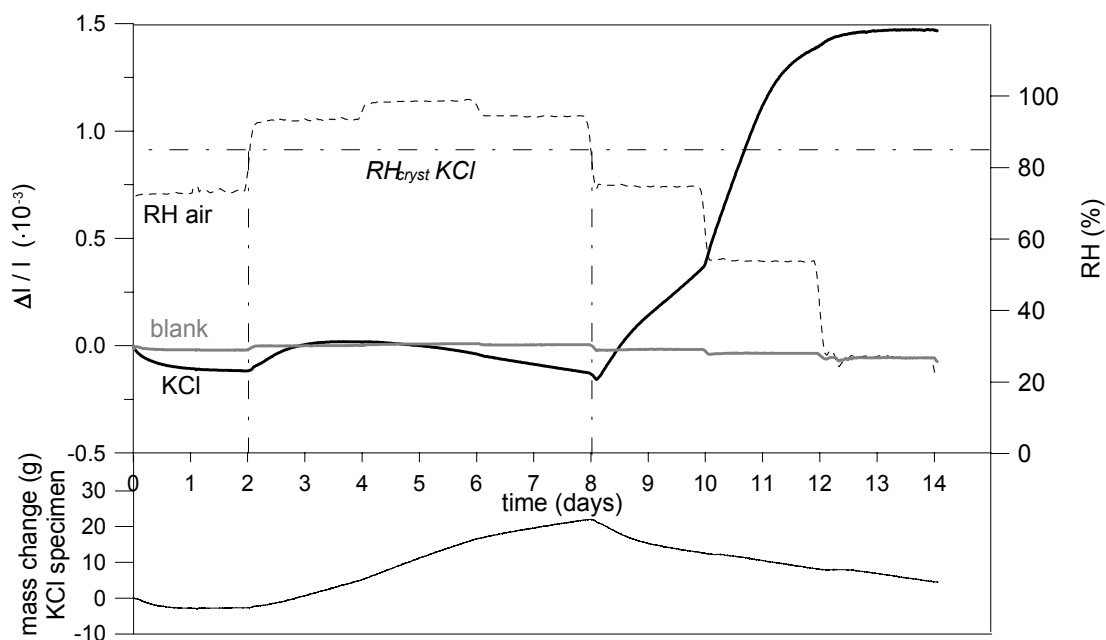


Figure 6.10 Dilation of blank and KCl contaminated specimens (upper graph) and change in mass of the KCl contaminated specimen (lower graph) during a RH cycle

6.3.5 Effect of pH on the dilation behaviour

It is known that the pH of the solution has an effect on the creep behaviour of the salt: alkaline solutions show a more pronounced creep [Puh83]. It was therefore interesting to investigate the effect of acidity or alkalinity of the NaCl solution on the dilation.

Two specimens were contaminated with NaCl solutions having a pH of 1.5 and 14 respectively. The acid and alkaline pH was reached by the use of HNO₃ and Na(OH), respectively. The response of the two specimens to the RH changes is similar and comparable to the one measured on NaCl contaminated specimens: shrinkage is measured during dissolution and expansion during drying (figure 6.11). Therefore our experiment suggests that the pH does not play an important role in the mechanism underlying the shrinkage and dilation. However, it should be mentioned that the acid pH of the solution might be neutralized in the alkaline environment of the mortar.

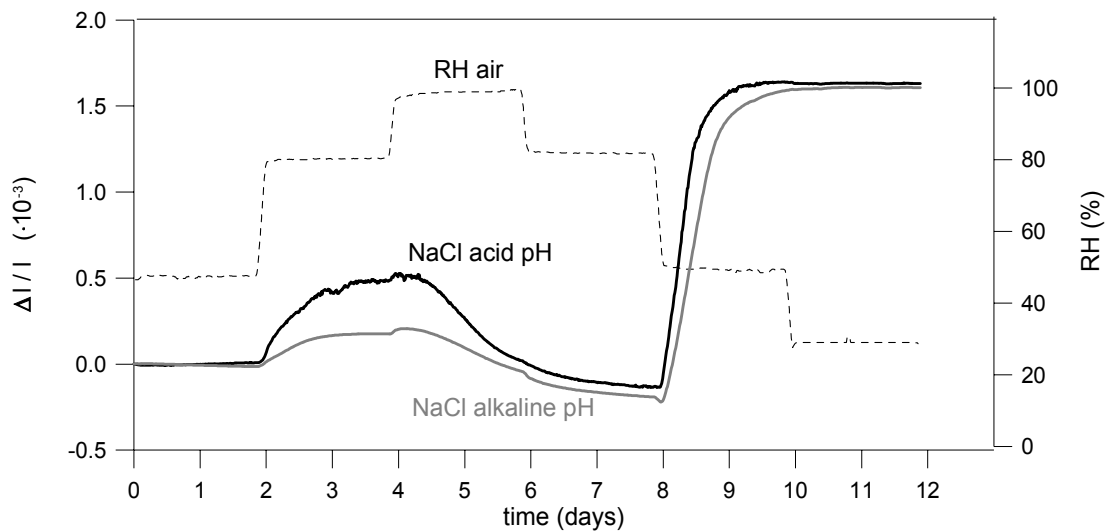


Figure 6.11 Dilation of specimens contaminated with acid and alkaline NaCl solution during a RH cycle

6.3.6 Hygric behaviour of NaCl contaminated specimens in the presence of a crystallization inhibitor

The use of crystallization inhibitors may also help answering some questions about the damage mechanism, because these products are supposed to increase the supersaturation level (and therefore the theoretical crystallization pressure) at which salt crystallization occurs and to modify the crystal habits [Rod02]. In the present study sodium ferrocyanide ($\text{Na}_4\text{Fe}(\text{CN})_6 \cdot 10\text{H}_2\text{O}$) has been chosen because it has been shown to be very effective in inhibiting NaCl crystallization [Rod02].

Two mortar specimens were contaminated with a NaCl saturated solution, with 0.1% (m/m) and without sodium ferrocyanide, $\text{Na}_4\text{Fe}(\text{CN})_6 \cdot 10\text{H}_2\text{O}$. In both specimens the same amount of NaCl was introduced.

The specimens were then placed in the climatic cabinet and the RH was varied step by step between 30% and 98% RH. In figure 6.12 the measured dilations are plotted as well as the mass change of the specimen containing the inhibitor. The specimen contaminated with NaCl solution shows, as expected, significant dilation during drying. The specimen with NaCl plus inhibitor displays, surprisingly, no change in length at all. The almost complete drying (and therefore the occurrence of salt crystallization) of the specimen containing the inhibitor can be checked by looking at its mass at the end of the experiment. The absence of significant shrinkage during dissolution of the salt in the presence of the inhibitor, suggests that hardly any tensions have been developed in this specimen during the crystallization of the salt following the initial contamination with salt solution.

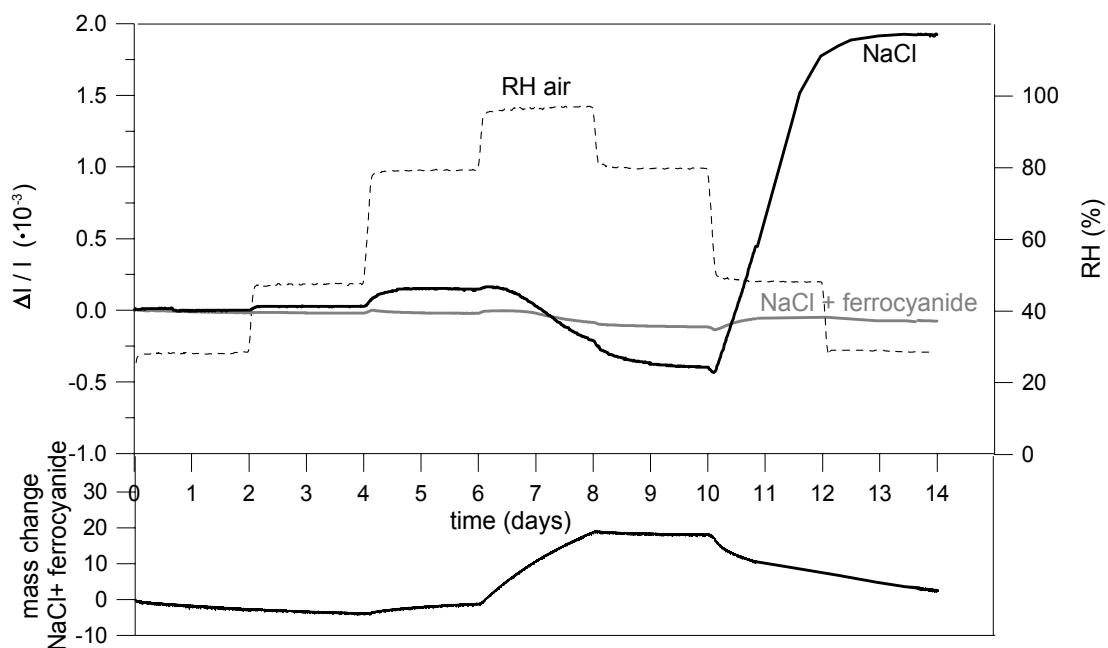


Figure 6.12 Dilatation of NaCl contaminated specimens with and without ferrocyanide inhibitor (upper graph) and mass change of the NaCl contaminated specimen with ferrocyanide (lower graph) during a RH cycle

In order to study the long-term effect and the consequences of the presence of the inhibitor on the damage, an experiment comprising repeated RH cycles between 20% and 88% RH was performed. The results are plotted in figure 6.13. The specimen containing the inhibitor dilates during the high RH periods and shrinks during the low RH periods. The changes in length slightly increase with cycling. However, at the end of the experiment no irreversible dilatation has occurred. The behaviour of the specimen contaminated with NaCl is completely consistent with the results reported before (section 6.3.2), showing an irreversible and increasing dilatation during subsequent crystallization cycles of the salts.

In spite of the similar amount of adsorbed/evaporated water in presence and absence of the inhibitor, strikingly different dilatation behaviour is observed. This corresponds to the damage

observed at the end of the experiment. The specimen contaminated with pure NaCl showed sanding of the surface layer. The specimen containing the inhibitor did not suffer any visible damage. This is surprising because, according to the theory relating crystallization pressure to the level of supersaturation, the higher level of supersaturation reached in the presence of the inhibitor should result in a higher crystallization pressure and, therefore, in more severe damage. However, for crystallization pressure to be developed, the salt should grow filling confined spaces [Cor49]. The question arises whether the latter is the case in the presence of the inhibitor.

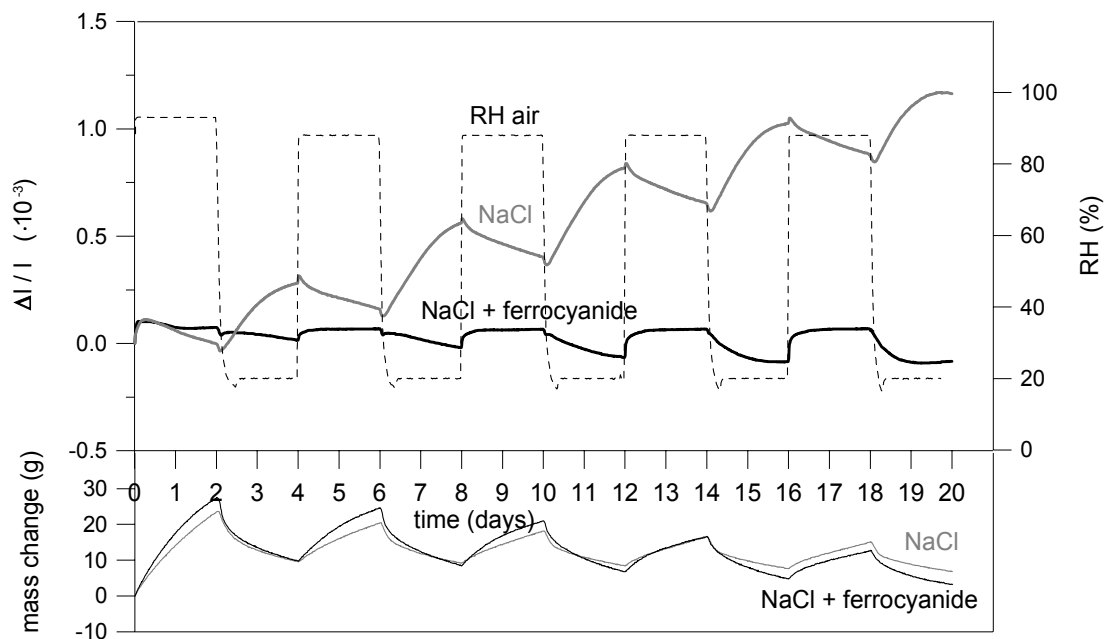


Figure 6.13 Dilation (upper graph) and mass change (lower graph) of NaCl contaminated specimens with and without crystallization inhibitor during several RH cycles

6.3.7 Hygric behaviour of Na_2SO_4 contaminated specimen

The hygric behaviour of a Na_2SO_4 contaminated specimen has been investigated. This salt has been selected because its crystallization behaviour differs from that of NaCl. NaCl tends to crystallize at the solution-air interface and at the surface of the pore (heterogeneous nucleation), showing a good interaction with the pore wall; Na_2SO_4 crystallizes mainly in solution (homogeneous nucleation) maintaining a layer of solution between the crystal nuclei and the pore wall [Rod99a, Ben04].

Sodium sulfate may crystallize in different hydrated forms, depending on temperature and RH [Ste96]. In order to allow only dissolution and re-crystallization of anhydrous sodium sulfate (thenardite) and no hydration/de-hydration processes, the dilation experiment was performed at a constant temperature of 40 °C. Before starting the measurements, the specimen, with the LVDT applied on it, was equilibrated at 40 °C. The RH was varied stepwise between 50% and 95% RH: each step was done in one hour and was followed by 23 hours of equilibration at

constant RH. The experimental data (figure 6.14) show that the specimen dilates when the RH increases. For RH lower than the RH of equilibrium (87% RH at 40 °C) the behaviour of the specimen is similar to that of NaCl contaminated (below 75% RH) and blank specimens: a dilation is observed, due to water vapour adsorption [Hil64].

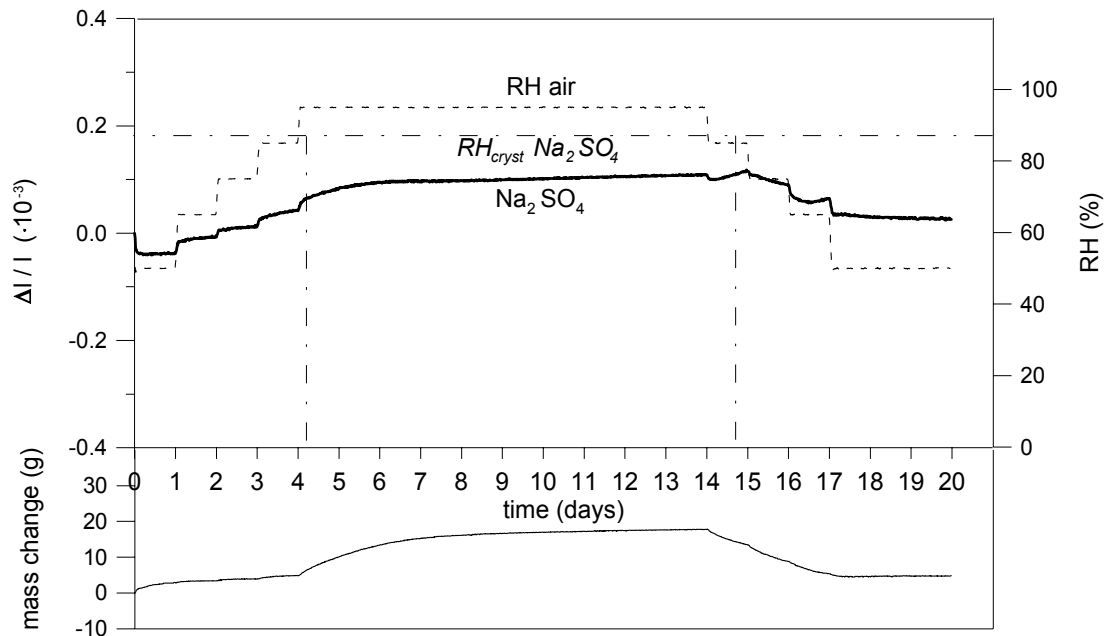


Figure 6.14 Dilation (upper graph) and mass change (lower graph) of a Na_2SO_4 contaminated specimen during a RH cycle at 40 °C

When the RH of equilibrium is crossed, the mass of the sample increases (due to hygroscopic moisture adsorption), but no abrupt changes are observed in the dilation. The dissolution of the salt (at the end of the 95% RH period the amount of adsorbed water is sufficient to dissolve about 70% of the salts present in the specimen) does not change the behaviour of the material.

When the RH of equilibrium is crossed again, and the specimen starts drying, an initial shrinkage followed by a slight dilation is measured at each RH step. This is probably the result of the competition between the shrinkage due to drying (as shown in section 6.3.8) and the (moderate) dilation due to crystallization of the salt. This results in an overall shrinkage of the specimen during drying. At the end of the test the specimen almost returns to its original length.

6.3.8 Hygric behaviour of blank and NaCl contaminated specimens at 40°C

In order to verify whether the different behaviour of Na_2SO_4 with respect to NaCl was related to the temperature, the dilation of blank and NaCl contaminated specimens at 40 °C was investigated.

In figure 6.15 the change in length of the blank specimen is reported. After an initial shrinkage, probably due to the fact that the specimen was not yet fully equilibrated at 40 °C

when the measurement started, dilation and shrinkage are observed at increasing and decreasing RH respectively, as expected.

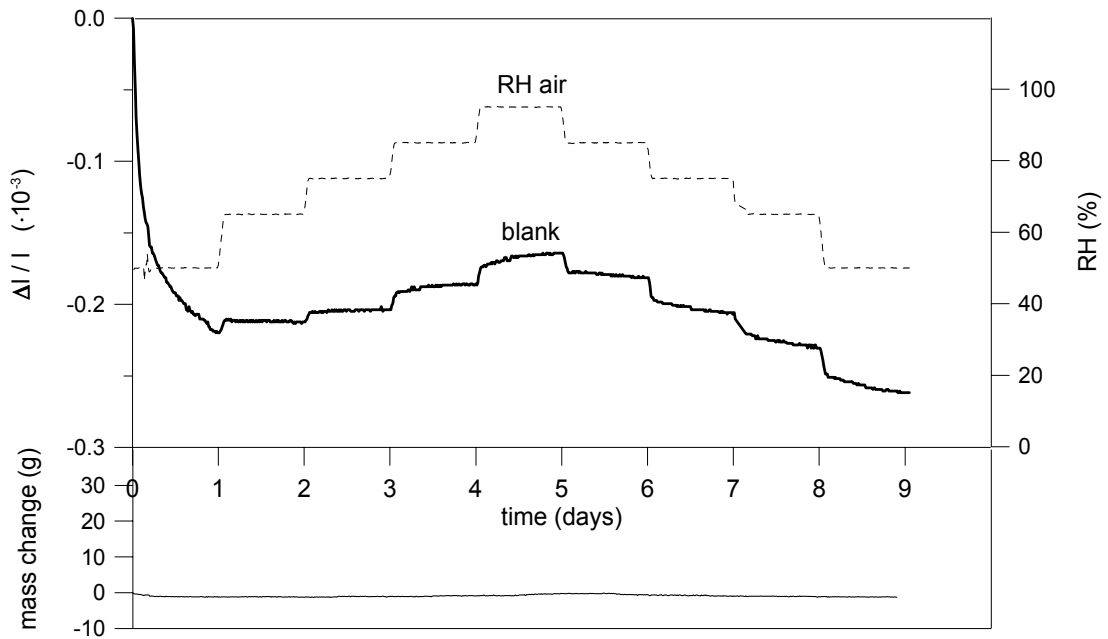


Figure 6.15 Dilation (upper graph) and mass change (lower graph) of a blank specimen during a RH cycle at 40 °C

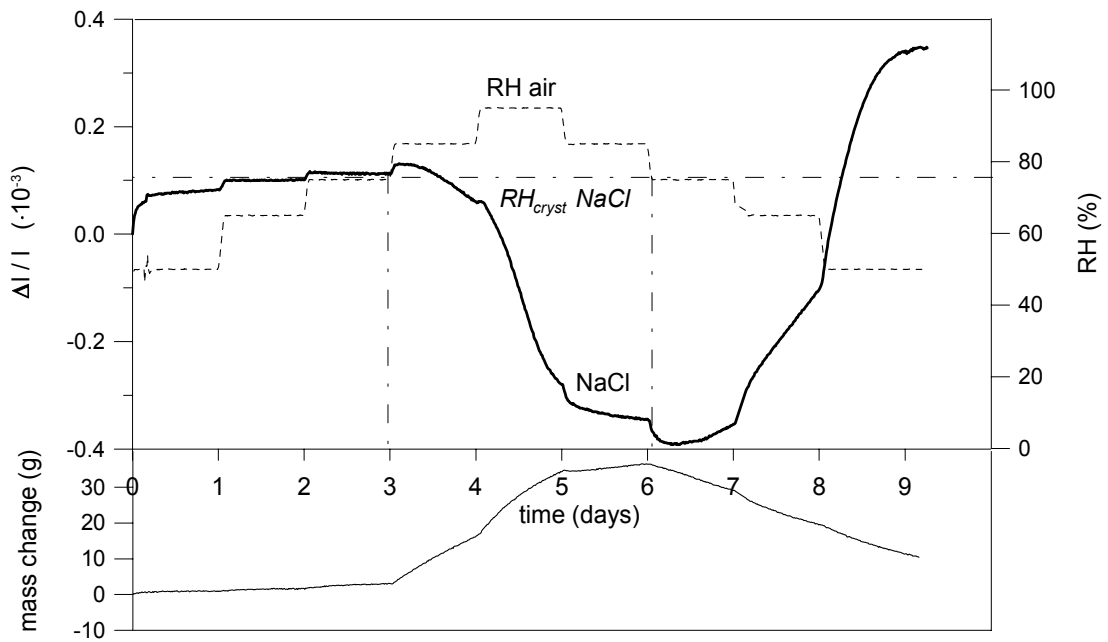


Figure 6.16 Dilation (upper graph) and mass change (lower graph) of a NaCl contaminated specimen during a RH cycle at 40 °C

The behaviour of the NaCl contaminated specimen at 40 °C (figure 6.16) is similar to that observed at 20 °C: shrinkage is measured during dissolution, and dilation during crystallization of the salt. This similarity may be explained by the fact that the temperature does not significantly affect both the solubility and the RH of equilibrium of NaCl.

In the light of these results it can be concluded that the different behaviour of Na₂SO₄ with respect to NaCl is not due to the temperature of 40 °C at which the experiment was performed, but it is related to the salt type.

6.4 ESEM investigations

Environmental Scanning Electron Microscopy (ESEM) observations have been performed on the specimens subjected to RH cycles, after their complete drying.

The cross sections of the outer layer (about 3 mm thick) of mortars specimens before and after the test described in the previous sections, were studied using a Back Scattered Electron (BSE) detector. The composition of the salt crystals was checked with Energy Dispersive Spectroscopy X-ray Microanalysis (EDX). The investigations aimed to study the crystallization pattern of the salt, i.e. the habits and the location in which the salt crystallizes in the pores.

In the ESEM picture of a broken cross section of lime-cement mortar contaminated with NaCl, the salt is visible in large pores, creating a layer over the pore walls (figures 6.17-6.19). It looks as if a good adhesion exists between the material and the salt crystals. This suggests that in this system the pore/crystal interfacial tension is lower than the pore/solution interfacial tension.

This behaviour of NaCl is in accordance with other recently reported observations [Ben04]. Below the salt, most of the distinguishable pores appear to be empty (figure 6.20).

In addition, when NaCl crystallization occurs at 40°C a salt layer is formed (figure 6.21a-b). Regular crystals are observed also in this case, suggesting that no relevant supersaturation was reached before crystallization took place.

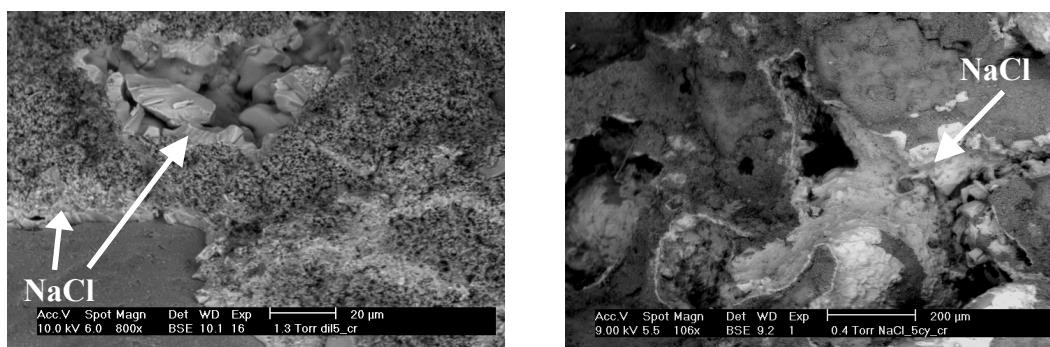


Figure 6.17 ESEM photomicrographs showing NaCl (lighter areas) crystallizing as a layer adhering to the binder and partly filling large pores (cross section of the specimen after 2 crystallization cycles, 1 mm from the evaporation surface)

Figure 6.18 ESEM photomicrographs showing NaCl (lighter areas) crystallizing as a layer on the pore walls (cross section of the specimen after several RH cycles, 5 mm from the evaporation surface)

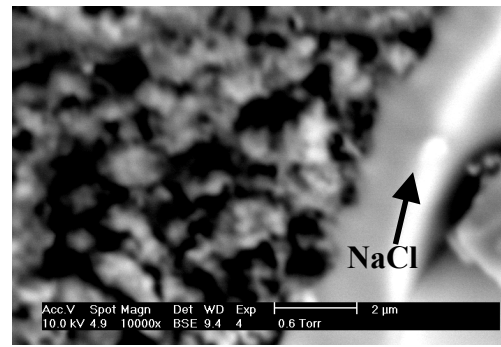
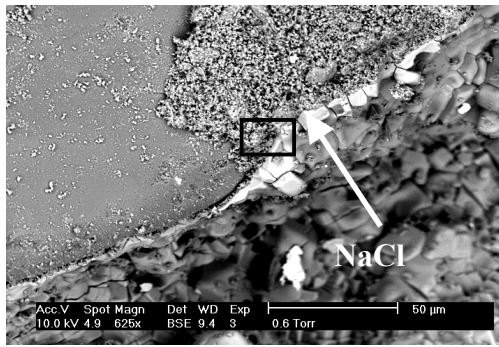


Figure 6.19 ESEM photomicrograph of NaCl crystallizing as a layer over the binder (cross section of the specimen after several RH cycles, 5 mm from the evaporation surface)

Figure 6.20 ESEM photomicrograph showing that, next to the salt layer (white area), there are pores not filled with salt (cross section of the specimen after several RH cycles, detail of figure 6.19)

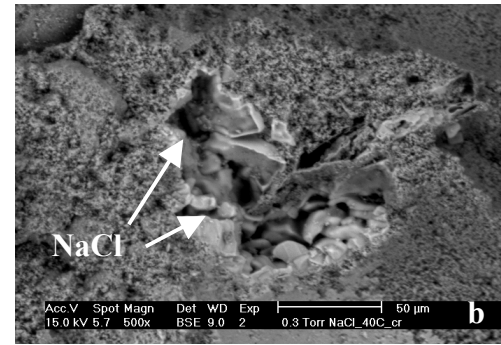
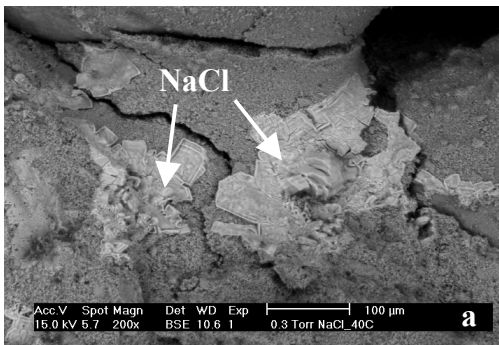


Figure 6.21a-b ESEM photomicrographs showing NaCl (lighter areas) crystallizing as a layer (cross section of specimen after two crystallization cycles at 40 °C, 2 mm from the evaporation surface)

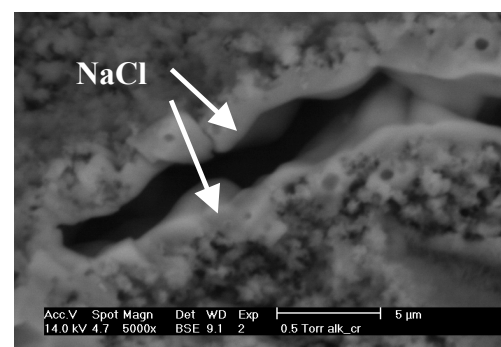
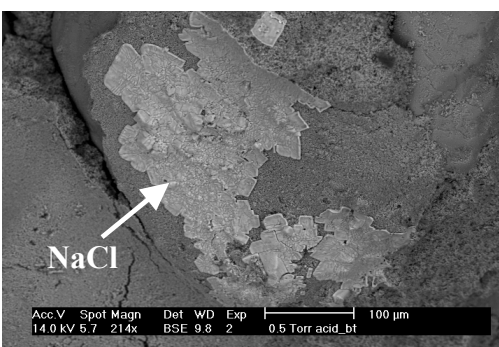


Figure 6.22 ESEM photomicrograph showing NaCl (lighter areas) crystallizing as a layer in a specimen contaminated with acid NaCl solution (cross section of the specimen after the one RH cycle, 2 mm from the evaporation surface)

Figure 6.23 ESEM photomicrographs showing NaCl (lighter areas) crystallizing as a layer covering pore walls in a specimen contaminated with alkaline NaCl solution (cross section of the test after one RH cycle, 2 mm from the evaporation surface)

The acid or alkaline pH of the salt solution does not affect the crystallization pattern of the sodium chloride (figures 6.22 and 6.23) in the studied lime-cement mortar. This may be related to the fact that the acid pH may be neutralized in the alkaline environment of the mortar.

The presence of a salt layer covering and partially filling large pores was also observed for NaNO_3 (figure 6.24) and KCl (figure 6.25).

The addition of ferrocyanide to the NaCl solution changes the crystallization pattern of the salt. The NaCl does not show a strong affinity to the substrate anymore: it does not cover the pore walls in the form of a layer, but crystallizes mainly as agglomerate of crystals, not attached to the material (figure 6.26a-b). The crystallization pattern does not change significantly after repeated RH cycles (figure 6.27a-b).

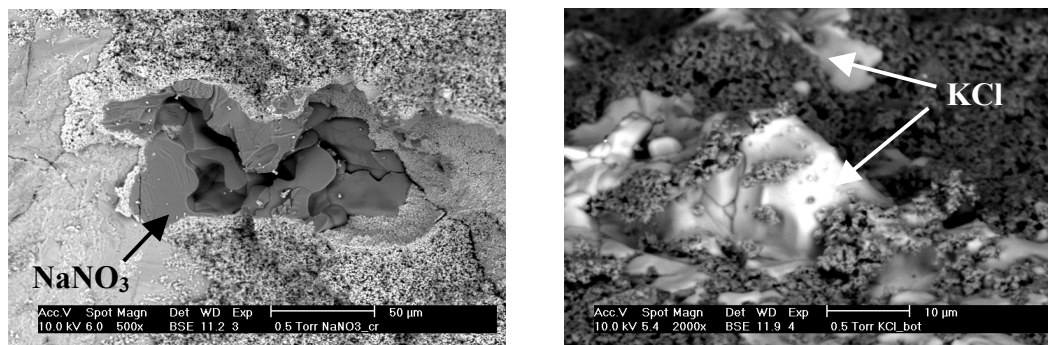


Figure 6.24 ESEM photomicrograph showing NaNO_3 (dark-grey area) crystallizing as a layer on the pore wall (cross section of the specimen after one RH cycle, 2 mm from the evaporation surface)

Figure 6.25 ESEM photomicrograph showing KCl (white area) crystallizing as a layer over the binder (cross section of the specimen after one RH cycle, 2 mm from the evaporation surface)

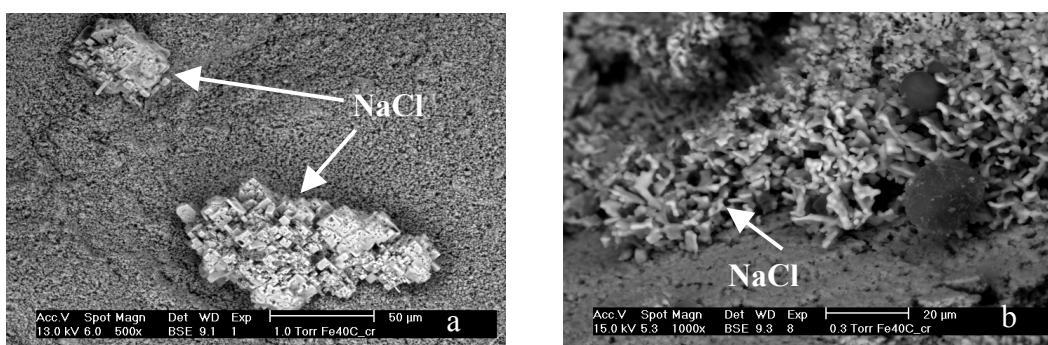


Figure 6.26 a-b ESEM photomicrograph showing NaCl crystallization in the presence of an inhibitor; crystal agglomerations (white areas) of cubic (a) or less regular crystals (b) are observed; (cross section of the specimen before the test)

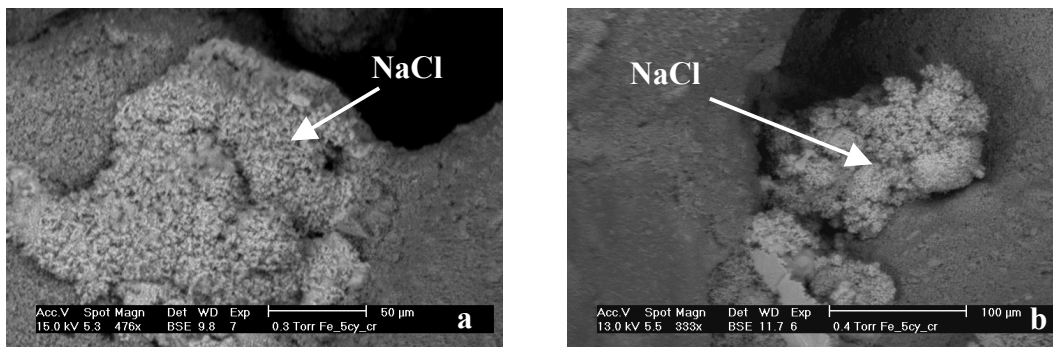


Figure 6.27 a-b: ESEM photomicrograph showing NaCl crystallization in the presence of inhibitor after repeated RH cycles. The crystal habit has not significantly changed: no salt layer is visible on the pore walls; (cross section of the specimen after several RH cycles)

XRD analyses were performed to check whether any change in crystal habits (as example preferential growth of certain crystal faces) was induced by the presence of the inhibitor. The outer layer of the specimens contaminated with NaCl solution and with NaCl solution plus inhibitor used in the dilation test were grinded and the binder was separated from the aggregate by sieving. The obtained samples were analysed by XRD. A sample constituted by NaCl crystallized in the presence of the inhibitor in a glass container was analysed too. As shown by the graphs (figure 6.28) no clear differences in the intensity peaks identifying the different faces of NaCl crystals could be found between NaCl and NaCl plus inhibitor when crystallizing in the mortar.

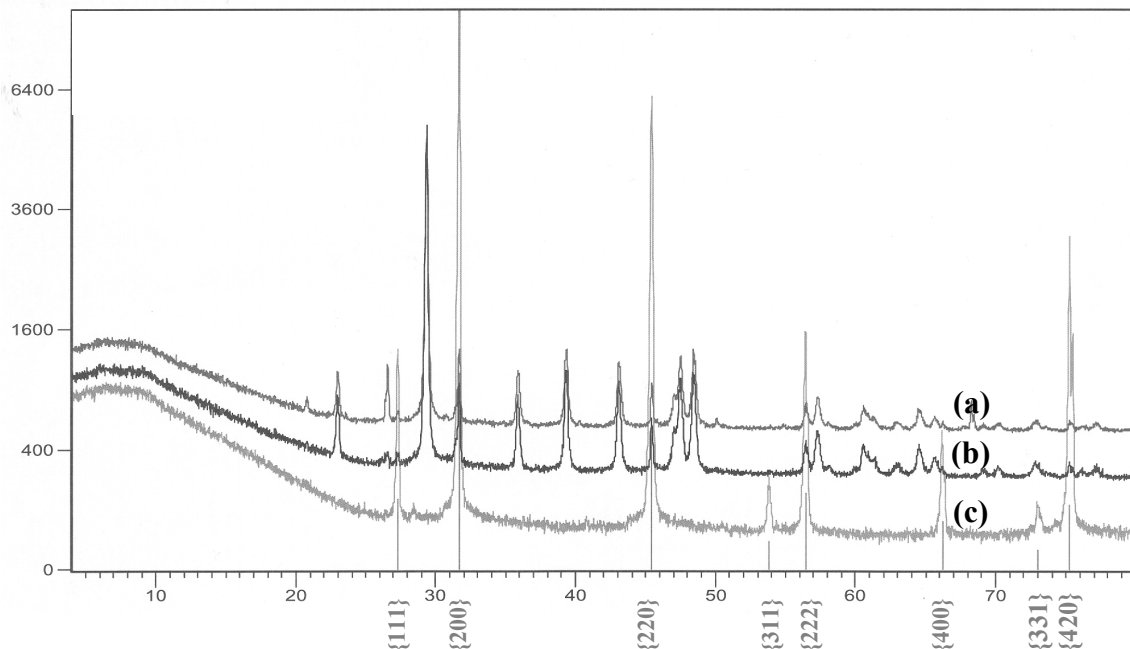


Figure 6.28 Results of the XRD analyses of: (a) the outer layer of the lime-cement mortar specimens contaminated with NaCl; (b) the outer layer of the lime-cement mortar specimens contaminated with NaCl plus inhibitor; (c) NaCl crystallized in a glass container in the presence of the inhibitor. The peaks identifying the different crystal faces of NaCl are similar.

The sample of NaCl plus inhibitor crystallizing in the glass container shows the presence of {311} face, absent in the other samples. Apparently, crystallization of halite in the presence of the inhibitor in free space is different from that in the presence of the inhibitor but in the mortar. Given the fact that powder diffractograms were obtained instead of single crystal XRD, it can not be excluded that grinding and different matrices affected the intensities in the diffraction pattern.

The Na_2SO_4 crystallizing at 40 °C shows a different crystallization pattern from NaCl, NaNO_3 and KCl: it does not adhere to the pore wall, but forms needle-like crystals (figure 6.29a-b). This may be related to the tendency of Na_2SO_4 to crystallize mainly in solution (homogeneous nucleation) [Rod99a, Ben04] instead of at the pore wall, like NaCl. We can attribute this different behaviour to the surface interfacial energies (see section 2.4.1): depending on the surface interfacial energies, in some systems deposition of crystals on the pore walls may occur (as in the case of NaCl), whereas in other systems (as in case of Na_2SO_4) the surface energies lead to minimal contact between crystals and the pore wall, thereby promoting the bridging of pores by the crystals.

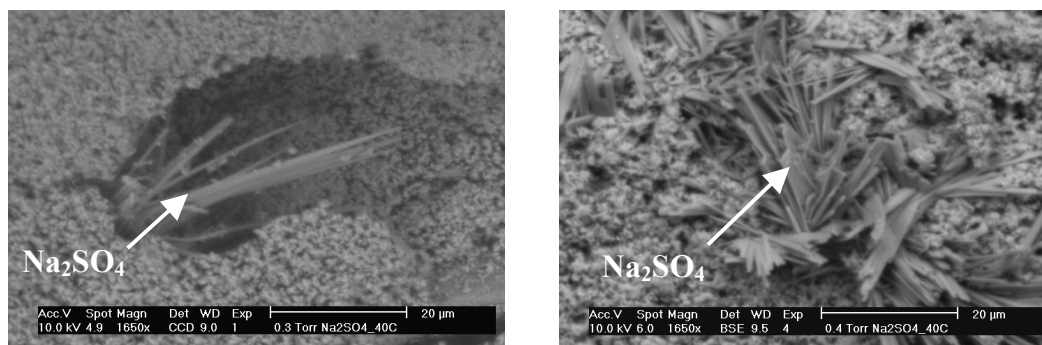


Figure 6.29 a-b ESEM photomicrograph showing Na_2SO_2 (white area) crystallizing as needle like crystals (cross section of the specimen after one RH cycle at 40 °C)

6.5 Discussion and conclusions

The experiments described in this chapter unambiguously prove that the presence of NaCl is able to modify the hydric and hygric behaviour of a material completely, even in absence of reactive clay. In a non contaminated lime-cement mortar, dilation occurs when the RH increases and shrinkage when the RH decreases. In lime-cement mortar contaminated with NaCl the opposite happens: dilation is measured during the drying phase of the RH cycle, when the salt crystallizes; shrinkage is observed during dissolution of the salt.

The use of step-by-step variations of the RH across the RH of crystallization of NaCl and the simultaneous monitoring of the changes in weight and in length of the specimens have allowed to demonstrate convincingly that the dilation is due to crystallization of NaCl. In fact it only occurs in the presence of the salt, when the RH of the air is low enough to cause the evaporation of water. The shrinkage measured during dissolution is most probably due to the

release of the stresses developed during crystallization, as shown by the fact that the absorption of salt solution itself does not result in any shrinkage.

The dilation occurring during crystallization is only partially recovered during dissolution of the salt and it increases with repeated RH cycles. The irreversibility of the dilation is probably related to the development of cracks in the binder and to the widening of the spaces between the aggregate grains. The dilation increases until damage appears and the material falls apart.

The different dilation behaviour observed between salt contaminated and blank specimens during the RH cycles suggests that shear stresses may develop in a salt contaminated material because of the differential dilation of areas containing different amounts of salt. This theory may explain those cases of damage in which there is no evidence of salt filling spaces under detached scales or layers (see sections 5.4.2.3, 5.6.2.2).

The dilation behaviour observed in NaCl contaminated lime-cement mortar has also been verified for other hygroscopic salts without hydrated forms (NaNO_3 and KCl), showing that this phenomenon is not restricted to NaCl but it is common to more salts.

The presence of a crystallization inhibitor definitely modifies the dilation behaviour of NaCl contaminated specimens: when the inhibitor is added, the crystallization of NaCl does not produce any irreversible dilation. This occurs in spite of the comparable amount of water adsorbed and released by the specimens with and without inhibitor during the RH cycles. The absence of any irreversible dilation in the specimen containing the inhibitor agrees with the absence of damage at the end of the test. This is interesting because, according to the theory that relates crystallization pressure to the level of supersaturation, the higher level of supersaturation reached in the presence of the inhibitor should result in a higher crystallization pressure and, therefore, in more severe damage. However, for crystallization pressure to be developed, the salt should grow filling confined spaces [Cor49]. The question arises whether the latter is the case in the presence of the inhibitor.

The ESEM investigations, performed on cross sections of the lime-cement mortar specimen after the experiment, appeared to be crucial for the study of the damage mechanism. The ESEM investigations showed that NaCl, as well as NaNO_3 and KCl , crystallize as a layer on the pore walls and that a good interaction between these salts and pore walls seems to be present. This suggests that in this system the pore/crystal interfacial tension is lower than the pore/solution interfacial tension. When the crystallization inhibitor is added to the NaCl solution, NaCl does not precipitate as a layer anymore but it forms agglomerate of crystals not adhering to the pore walls.

Combining the ESEM investigations with the dilation occurring during crystallization leads to a model of a damage mechanism based upon a mechanical interaction between salt and pore wall. Changes in the crystal structure due to variation in RH might result in stresses to the pore walls and finally lead to failure. Salts crystallizing in the form of a layer on the pore walls seem to be able to strongly affect the hygric dilation of the material producing relevant

expansion during drying of the specimen and crystallization of the salt. The observed salt layers appear able to transfer stresses to the pore walls and thereby to cause dilation and, at the long last, damage. A similar effect is, according to this model, not possible when the same salt (NaCl) crystallizes without adhering to the material. This was shown in the experiment in which the crystallization inhibitor was added.

In a last experiment the hygric behaviour and the related changes in length of a specimen contaminated with Na_2SO_4 were investigated. In spite of the known harmfulness of this salt, no significant dilation was measured during drying of the specimen and crystallization of the salt. Also the crystallization habit of the salt, precipitating in the form of needle-like crystals, looks different from the salt layer observed in the case of NaCl. Further experiments, studying the changes in length and the damage developed by thenardite crystallization during subsequent RH cycles, may help clarifying the relation between crystallization pattern, dilation and damage.

Chapter 7

Conclusions

7.1 Results of the research

This thesis has focused on the study of the damage due to sodium chloride (NaCl) crystallization in stone-like materials.

The research started with a critical study of the literature on salt damage (chapter 2).

The literature review clearly underlined the limits of the theory based on pore filling and supersaturation level to explain the damage due to NaCl crystallization. According to this “classic” theory, in equilibrium situation, significant pressures can only develop in pores of a few nanometers size. Therefore this theory cannot explain the damage observed in many traditional building materials (like brick, stone or lime-based mortars), in which this pore size is usually absent. Recently, the hypothesis that high, transient pressure may develop in a non equilibrium situation has been proposed to explain the occurrence of damage in materials with large pores.

From the literature review the possibility emerged that, apart from crystallization pressure due to pore filling, other mechanisms might contribute to the damage. In particular, the effect of NaCl on the hygric behaviour and the related dilation of material emerged as an interesting issue to be further studied, since both systematic experiments and definitive explanations of this phenomenon were missing.

A common limit of the models on crystallization damage is the gap between theory and practice. The situations in practice are much more complex than assumed in theoretical models. Different damage mechanisms may occur simultaneously, having a synergistic effect. Moreover, salt damage is rarely the result of a single crystallization event, but more often the consequence of repeated crystallization cycles creating gradients in the salt (and stress) distribution and gradually weakening the material.

From these considerations derives that the observation of damage evolution in practice is crucial for the understanding of the damage mechanism. The study of the practice situations should therefore constitute a starting point and, at the same time, a term of comparison of each

theory developed or laboratory result obtained. For this reason a research approach based on the combination of observations in the field (chapter 3 and 4) and laboratory experiments (chapter 5 and 6) was adopted in this work for the investigation of the mechanism of damage due to the crystallization of NaCl.

The investigation of several buildings (chapter 3) affected by damage due to NaCl clearly demonstrated that material properties (e.g. pore size, mechanical strength, moisture transport behaviour) and boundary conditions (moisture supply, salt load and distribution, environmental conditions) influence the seriousness of the damage and the decay patterns. Damage due to NaCl appears often as powdering or sanding of the outer layer where most of the salt accumulates; in non homogeneous materials, alveolization, delamination, scaling or spalling of thick layers may occur. Besides, the same material may show different decay patterns, depending on the boundary conditions (moisture supply and drying conditions).

The relevance of the environmental conditions, and in particular of RH changes, for the occurrence of salt damage, was demonstrated in situ (chapter 4). The combined monitoring of the debris falling from the wall and of the environmental conditions identified a clear relation between the RH and the decay: The damage, occurring in the low RH periods due to crystallization of the salt, became visible in the high RH periods when the salt dissolved and the debris particles, which were cemented by the salt, fell apart. Experiments in the ESEM chamber, reproducing the RH changes observed in practice, further established this process.

It is striking that sodium chloride, found to cause serious damage to building materials in practice, is usually ineffective in laboratory crystallization tests. From this consideration the necessity of improving the existing test procedures (chapter 5) emerged. The development of an effective salt crystallization test for NaCl has therefore constituted one of the main aims of this work.

The research on case studies suggested that the environmental conditions might play an important role enhancing the decay. Therefore, the study of the effect of environmental conditions (high temperature, low RH, air flow and RH changes) on the damage constituted a crucial step in the definition of an accelerated crystallization test.

The laboratory experiments showed that repeated wet-dry cycles and the use of RH changes enhance the decay. On the basis of these results, a weathering test was developed, specific for NaCl. The test consists of wetting by capillary rise, and drying at a relatively high temperature (60 °C). In addition to the dissolution/crystallization cycles produced by the re-wetting, the new developed procedure introduces also RH cycles. These determine additional dissolution/crystallization cycles of the salt and enhance therefore the damage.

The decay extents and patterns obtained in the laboratory test were compared with the ones observed in case studies. The comparison proved that the new procedure is an accelerated and reliable simulation of the damage occurring in practice.

Another part of the laboratory research concerned the study of the damage mechanism due to NaCl crystallization (chapter 6). Some of the decay patterns observed in laboratory (bulging of the outer layer without any evidence of crypto-florescence) suggested that the differential

dilation of more or less salt contaminated areas of a material during wet-dry cycles, might play a role in the damage. This mechanism, up to now never systematically investigated, was studied in detail on lime-cement mortar specimens.

The obtained results unambiguously prove that the presence of NaCl is able to completely modify the hygric behaviour and the related dilation of a material. In a not contaminated specimen dilation and shrinkage can be observed respectively when the RH increases and decreases. In NaCl contaminated specimens the opposite is observed: dilation occurs during the drying phase of the RH cycle, when the salt crystallizes, whereas shrinkage occurs during dissolution of the salt. The dilation is irreversible and it increases when repeating the RH cycles, until damage is observed.

The opposite behaviour of salt contaminated and blank specimens inevitably leads to the conclusion that shear stresses will develop in a salt contaminated material because of the differential dilation of more or less salt loaded areas. This theory may explain damage types like scaling, bulging or spalling where there is no evidence of salt pushing out the detached layers.

Experiments on NaNO₃ and KCl contaminated specimens showed that the observed dilation behaviour is not restricted to NaCl but it is a phenomenon common to more salts.

In the presence of a crystallization inhibitor, however, no dilation was registered during crystallization of NaCl and no damage occurred, despite of the fact that, theoretically, a higher crystallization pressure would have developed.

This discrepancy in the dilation behaviour corresponded to a different crystallization pattern of the salt. The ESEM observations performed on cross sections of the NaCl contaminated specimens, with and without inhibitor, illustrated that NaCl (as well as NaNO₃ and KCl) tends to crystallize as a layer showing a good interaction with the pore walls whereas in the presence of the inhibitor the salt preferentially forms agglomerations of crystals that are not adhering to the pore walls.

Combining the ESEM investigations with the dilation occurring during crystallization leads to the following model: the damage is based on a mechanical interaction between salt and pore wall. Changes in the crystal structure due to variation in RH might results in stresses to the pore wall. Salts crystallizing in the form of a layer on the pore walls seem to be able to strongly affect the hygric dilation of the material producing relevant expansion during drying of the specimen and crystallization of the salt. The observed salt layers appear able to transfer stresses to the pore walls and thereby to cause dilation and, at long last, damage. A similar effect would, in this model, not be possible when the same salt (NaCl) crystallizes without adhering to the material. This is shown in the case in which the crystallization inhibitor is added.

7.2 Practical application of the results

The research presented in this thesis provides useful suggestions for the treatment and the prevention of salt damage in practice.

The investigation of the case studies and the laboratory experiments have shown that both material properties and boundary conditions can not be considered positive or negative in

themselves but their interaction determines the risk of damage. For example, a high moisture content enhancing transport and accumulation of salt may be very damaging even in case a low salt load is present in the wall. On the other hand, even a high salt amount may be not risky in the absence of water activating the salt.

The environmental conditions are shown to play a crucial role in determining the risk of damage; they should therefore be considered when selecting a suitable restoration material. For example, in the presence of RH changes, a material accumulating the salts near the surface will have a high risk of decaying. In a stable environment, with high moisture supply and slow evaporation, the same material will most probably suffer only a limited damage.

From these few examples it already emerges that no general rule exists for performing a successful restoration intervention. For each specific situation the priorities should be beforehand identified. These may be the preservation of the original materials, the esthetical aspect, the habitability of the space, the available budget etc. Once the priorities have been identified, a suitable intervention can be defined, taking into account the boundary conditions and the compatibility between the existing and the new materials.

For example, if the priority is the preservation of a valuable object, any further salt accumulation in that object should be avoided. Eventual additions in contact with the existing material should be therefore performed using a material having a more effective moisture (and salt) transport than the existing one. The use of a “sacrificial” material might be an option. In this way the salt will preferentially accumulate in the new addition and the damage to the old valuable object will be limited. Partial substitutions of ancient lime-based plasters by salt-resistant plasters hindering evaporation may often worsen the decay of the material that should be preserved. However, the same salt-resistant plaster may be a satisfactory solution in case no compatibility issues are present, and a good aesthetical aspect (absence of efflorescences or moist spots) and the habitability of the space are the priorities.

In the decision process of a restoration intervention, the choice of the substitution material is an important step. Unfortunately, it is not always possible to forecast the susceptibility of (combinations of) materials to salt damage on the mere basis of their properties. Sometimes an accelerated crystallization test in laboratory is necessary. A procedure, like the one developed in this work, able to assess the durability of a material and to study its behaviour in a few months time is therefore a valuable help for architects and decision makers. Besides, an effective laboratory crystallization test may promote the development of salt-resistant materials and of products for the prevention of salt decay. In fact it offers the possibility of testing the effectiveness of new materials and products in a relatively short period and without risk for the existing building.

7.3 Outlook

On the basis of the results obtained in this work, some important research issues can be defined. These are described in the following paragraphs.

The developed crystallization test for NaCl has proven to be effective on the studied materials, but its efficacy should be verified on a larger number of substrates. The substrates should be selected in a wide range of porosity, pore size distribution and mechanical strength. These are in fact the most relevant material properties determining the susceptibility to salt decay. A high porosity allows the absorption of large quantities of salt solution and may result into relevant salt load in the material; the presence of small pores leads, when salts fill the pores, to high crystallization pressures; a low mechanical strength is easier overcome by the stresses produced by salt crystallization.

The procedure developed for the monitoring of the decay in-situ proved to give a reliable quantification of the evolution of the damage. Parallel monitoring, in practice and in laboratory, of the evolution of the damage would help to define a time relation between laboratory test and real situations. The use of test-walls built for this purpose and placed in a real environment may also provide useful results.

The research on the hygric behaviour proved that the irreversible dilation due to NaCl crystallization is able to produce damage in lime-cement specimens after repeated RH cycles. The ESEM observations suggested that a relation exists between the way in which the salt crystallizes (adhering or not to the material), the dilation behaviour and the subsequent damage mechanism. Further experiments on salts like sodium sulphate, known to have a different crystallization behaviour from NaCl and to be very damaging, may be helpful for explaining the relation between crystallization pattern, dilation and damage. This would clarify whether, depending on the salt type, different decay mechanisms (pressures due to salt filling the pores or shear stresses due to salt layers adhering to the pore walls) may explain the damage.

The investigation of the case studies has identified the factors influencing the occurrence of salt decay. The complex interaction between these factors may be further developed in matrixes evaluating the risk of damage. This may give an important contribution to the further development of “expert systems” providing help in the diagnosis of the damage occurring in buildings and in the intervention decision process [Hee05].

References

- [Arn82] A. Arnold, Rising damp and saline materials, in *Proceedings of the 4th International Congress on Deterioration and Preservation of Stone Objects*, 11-28 (1982)
- [Arn85a] A. Arnold, A. Küng, Crystallization and habits of salt efflorescences on walls. Part I: Methods of investigation and habits, in *Proceedings of the 5th International Congress on Deterioration and Conservation of Stone*, 255-267 (1985)
- [Arn85b] A. Arnold, K. Zehnder, Crystallization and habits of salt efflorescences on walls. Part II: Conditions of crystallization, in *Proceedings of the 5th International Congress on Deterioration and Conservation of Stone*, 269-277 (1985)
- [Arn90] A. Arnold, K. Zehnder, Salt weathering on monuments, in *The Conservation of Monuments in the Mediterranean Basin: The influence of coastal environment and salt spray on limestone and marble. Proceedings of the 1st International Symposium*, 31-58 (1990)
- [Atk78] P. Atkins, J. de Paula, *Atkins' Physical Chemistry*, 7th edition, Oxford University Press, Oxford, UK (2002)
- [Bal99] K. van Balen, J. Mateus, L. Binda, G. Baronio, R.P.J. van Hees, S. Naldini, L. van der Klugt, L. Franke, *Expert System for the evaluation of the deterioration of ancient brick structures*, Research report n.8, Vol. 1, Office for Official Publication of the European Communities, Luxemburg (1999)
- [Ben04] D. Benavente, M.A. Garcia del Cura, J. Garcia-Guinea, S. Sanchez-Moral, S. Ordonez, Role of pore structure in salt crystallization in unsaturated porous stone, *Journal of Crystal Growth* **260**, (3-4), 532-544 (2004)
- [Bin85] L. Binda, G. Baronio, A.E. Charola, Deterioration of porous materials due to salt crystallization under different thermohygro-metric conditions. I. Brick, in *Proceedings of the 5th International Congress on Deterioration and Conservation of Stone*, 279-288 (1985)
- [Bin87] L. Binda, G. Baronio, Mechanisms of masonry decay due to salt crystallization, *Durability of Building Materials* **4**, 227-240 (1987)

- [Bin96] L. Binda, G. Baronio, E.D. Ferrieri, P. Rocca, Full scale models for the calibration of laboratory ageing test, in *Proceedings of the 7th International Conference on Durability of Building Materials and Components*, Vol. 2, 968-978 (1996)
- [Bin98] L. Binda, G. Baronio, Crystallization test by total immersion of specimens, *Materials and Structures* **31**, 10-15 (1998)
- [Boc61] E. Bock, On the solubility of anhydrous calcium sulfate and of gypsum in concentrated solutions of sodium chloride at 25°C, 30°C, 40°C, 50°C, *Canadian Journal of Chemistry* **39**, 1746-1751 (1961)
- [Bol05] L. Bolondi, *Il tufo giallo napoletano*, Master Thesis, Polytechnic of Milan, Italy (2005)
- [Bro98] H.J.P. Brocken, *Moisture transport in brick masonry: the grey area between bricks*, PhD thesis, Eindhoven University of Technology, The Netherlands (1998)
- [Cab58] N. Cabrera, D.A. Vermilyea, The growth of crystals from solution, in *Growth and perfection of crystals. Proceedings of an International Conference on Crystal Growth*, 393-412 (1958)
- [Cam96] D. Camuffo, The role of the climate on stone weathering, in *Proceedings of the European research workshop: Origin, Mechanisms and Effects of Salts on Degradation of Monuments in Marine and Continental Environment*, 155-165 (1996)
- [Cam98] D. Camuffo, *Microclimate for Cultural Heritage*, Elsevier, Amsterdam, The Netherlands (1998)
- [Can98] E.N. Caner Saltik, I. Schumann, L. Franke, Stages of damage in the structure of brick due to salt crystallization, in *Conservation of Historic Brick Structures: Case Studies and Reports of Research*, (Eds. N.S. Baer, S. Fitz, and R.A. Livingston), Donhead Publishing, Shaftesbury, UK, 47-58 (1998)
- [Cas93] C.J.J. Castenmiller, J.C. van Es, *Maatregelen in kruipruimten – thermische en hygrische afscherming – Meet en beoordelingsrichtlijn*, Stichting Bouw Research, Rotterdam, The Netherlands, (1993)
- [Cha80] R.W. Chapman, Salt weathering by sodium chloride in the Saudi Arabian Desert, *American Journal of Science* **280**, 116-129 (1980)
- [Cha79] A.E. Charola, S.Z. Lewin, Efflorescences on building stones. SEM in the characterization and elucidation of the mechanism of formation, *Scanning Electron Microscopy* **1**, 379-386 (1979)
- [Cha92] A.E. Charola, J. Weber, The hydration-dehydration mechanism of sodium sulphate, in *Proceedings of the 7th International Congress on Deterioration and Conservation of Stone*, 581-590 (1992)
- [Cha00a] A.E. Charola, Salts in the deterioration of porous materials: An overview, *Journal of the American Institute for Conservation* **39**, (3), 327-343 (2000)

- [Cha00b] S. Chatterij, A discussion on the paper "crystallization in pores" by G.W. Scherer, *Cement and Concrete Research* **30**, (4) 669-671 (2000)
- [Cha02] A.E. Charola, J. Puhlinger, Salts in deterioration of porous materials: a call for the right questions, in *Proceeding of the Workshop ARCCHIP ARIADNE 13 - SALTeXPert* (2002) unpublished
- [Col81] W.F. Cole, C.J. Lancucky, M.J. Sandy, Products formed in an aged concrete, *Cement and Concrete Research* **11**, (3), 443-454 (1981)
- [Coo68] R.U. Cooke, I.J. Smalley, Salt weathering in deserts, *Nature* **220**, (5173), 1226-1227 (1968)
- [Coo94] R.U. Cooke, G.B. Gibbs, Crumbling Heritage - Studies of Stone Weathering in Polluted Atmospheres, *Atmospheric Environment* **8**, (7), 1355-1356 (1994)
- [Cor49] C.W. Correns, Growth and dissolution of crystal under linear pressure, *Discussion of the Faraday Society* **5**, 267-271 (1949)
- [Doe94] E. Doehne, In situ dynamics of sodium sulfate hydration and dehydration in stone pores: observation at high magnification using the environmental scanning electron Microscope, in *Proceeding of the III International Symposium on the Conservation of Monuments in the Mediterranean Basin*, 143-150 (1994)
- [Ele03] K. Elert, G. Cultrone, C. Rodriguez-Navarro, E. Sebastian Pardo, Durability of bricks used in the conservation of historic buildings - influence of composition and microstructure, *Journal of Cultural Heritage* **4**, 91-99 (2003)
- [Esw80] H. Eswaran, G. Stoops, A. Abathi, SEM morphology of halite (NaCl) in soil, *Journal of Microscopy* **120**, 343-352 (1980)
- [Eve61] D.H. Everett, The thermodynamics of frost damage to porous solids, *Transactions of the Faraday Society* **57**, 1541-1551 (1961)
- [Fab95] B. Fabbri, M. Dondi, *Caratteristiche e difetti del laterizio*, Gruppo Editoriale Faenza, Faenza, Italy (1995)
- [Far05] P. Faria-Rodriguez, Resistance to salts of lime and pozzolan mortars, in *Proceedings of the RILEM Workshop: Repair mortar for historic masonry*, (2005) unpublished
- [Fig76] J. Figg, E. Moore, W.A. Gutteridge, On the occurrence of the mineral trona ($\text{Na}_2\text{CO}_3 \cdot \text{NaHCO}_3 \cdot 2\text{H}_2\text{O}$) in concrete deterioration products, *Cement and Concrete research* **6**, (5) 691-696 (1976)
- [Fit82] B. Fitzner, R. Snelhage, Einfluss der porenradien verteilung auf das verwitterungsverhalten ausgewahlter sandsteine, *Bautenschutz und Bausanierung* **5**, (3), 97-103 (1982)

- [Fit97] B. Fitzner, K. Heinrichs, M. Volker, Model for salt weathering at maltese globigerina limestones, in *Proceedings of the European research workshop: Origin, Mechanisms and Effects of Salts on Degradation of Monuments in Marine and Continental Environment*, 333-344 (1996)
- [Fla02] R.J. Flatt, Salt damage in porous materials: how high supersaturations are generated, *Journal of Crystal Growth* **242**, (3-4), 435-454 (2002)
- [Fra98a] L. Franke, I. Schumann, Indoor brick damage in *Conservation of Historic Brick Structures* (Eds. N.S. Baer, S. Fitz, and R.A Livingston), Donhead, Shaftesbury, UK, 35-46 (1998)
- [Fra98b] L. Franke, I. Schumann, *Damage Atlas*, Fraunhofer IRB, Stuttgart (1998)
- [Fur68] E. Furby, E. Glueckauf, L.A. Mc Donald, The solubility of calcium sulphate in sodium chloride and sea-salt solutions, *Desalinisation* **4**, 264-276 (1968)
- [Gou74] A. Goudie, Further experimental investigation of rock weathering by salt and other mechanical processes, *Zeitschrift fur Geomorphologie Supplementband* **21**, 1-2 (1974)
- [Gou97] A.S. Goudie, H. Viles, *Salt Weathering Hazards*, John Wiley, Chichester, UK (1997)
- [Gou98] A.S. Goudie, A.G. Parker, Experimental simulation of rapid rock block disintegration by sodium chloride in a foggy coastal desert, *Journal of Arid Environments* **40**, (4), 347-355 (1998)
- [Gre82] J.P. Mc Greevy, 'Frost and salt' weathering: further experimental results, *Earth Surface Processes & Landforms* **7**, (5), 475-488 (1982)
- [Groo93] C.J.W.P. Groot, *Effect of water on mortar-brick bond*, PhD thesis, Delft University of Technology, The Netherlands (1993)
- [Hee91] R.P.J. van Hees, Damage caused by salts to Curacao Monuments, in *Structural repair and Maintenance of historical building II*, Vol. 1, 141-155 (1991)
- [Hee96] R.P.J. van Hees, J.A.G. Koek, Treatment of rising damp. Evaluation of six chemical products, in *Proceedings of the 8th International Congress on Deterioration and Conservation of Stone*, 1435-1446 (1996)
- [Hee01] R.P.J. van Hees, H.J.P. Brocken, Interaction of the SBW treatment with Na₂SO₄, NaCl and NaNO₃ in *Salt Compatibility of Surface treatment*, Final report EU Contract no. ENV4-CT98-0710, (Ed. E. de Witte) 109-119 (2001)
- [Hee02] R.P.J. van Hees, L. Pel, B. Lubelli, Towards compatible repair mortars for masonry in monuments, in *Proceedings of the 5th Int. Symp. on the Conservation of Monuments in the Mediterranean Basin*, 371-375 (2002)
- [Hee03] R.P.J. van Hees, B. Lubelli, H. Brocken, Hydrofoberen van windmolens – Effectieve behandeling of vragen om ellende, *Praktijkboek Instandhouding Monumenten* **14**, 2-11 (2003)

- [Hee04] R.P.J. van Hees, B. Lubelli, L. Pel, H. Huinink, C.J.W.P. Groot, M. de Rooij, Transport and crystallization of salts in masonry and plasters, in *Proceedings of the 13th International Brick and Block Masonry Conference*, 711-720 (2004)
- [Hee05] R.P.J. van Hees, S. Naldini, M. Sanders, An expert system for analysis of damage to plasters due to salt and moisture, in *Proceedings Seminar 'Soluble salts in the walls of old buildings. Damages, processes and solutions'*, 16.1-16.11 (2005)
- [Hon58] D.B. Honeyborne, P.B.Harris, The structure of porous building stone and its relation to weathering behaviour, in *Proceedings of the Tenth Symposium of the Colston Research Society*, 342-365 (1958)
- [Hui05] H. Huinink, J. Petkovic, L. Pel, K. Kopinga, Water and salt transport, in *Compatibility of plasters and renders with salt loaded substrates in historic buildings*, Final report EU Contract no. EVK4-CT-2001-0047-DGXII, (Ed. R.P.J. van Hees), 94-112 (2005)
- [Klu94] L.J.A.R. van der Klugt., Koek J.A.G., De kwaliteit van voegen in metselwerk, *SBR-publication* **299**, 80-81 (1994)
- [Joh82] C.L. Johannessen, J.J. Feiereisen, A.N. Wells, Weathering of Ocean Cliffs by Salt Expansion in a Mid-Latitude Coastal Environment, *Shore and Beach* **50**, 26-34 (1982)
- [Jon80] D.K.C. Jones, British applied Geomorphology: an appraisal, *Zeitschrift für Geomorphologie* **36**, 48-73 (1980)
- [Kam65] P.N. van Kampen, *Kunst-reisboek voor Nederland*, Amsterdam, The Netherlands (1965)
- [Kau71] D.W. Kaufmann, *Sodium chloride - The production and properties of salt and brine*, Hafner, New York, USA (1971)
- [Klu93] L.J.A.R. van der Klugt, Technological factors influencing the frost susceptibility of clay building materials, *ZI annual*, 24-33 (1993)
- [Klu05] L.J.A.R. van der Klugt, personal communication
- [Kon01] T. von Konow, Mechanisms of brick deterioration due to salts: new results on salt behaviour from in situ studies at the Suomenlinna fortress in Finland, *Internationale Zeitschrift für Bauinstandsetzen und Baudenkmalpflege* **7**, (6), 675-688
- [Lar90] K.P. Larsen, C.B. Nielsen, Decay of bricks due to salt, *Materials and Structures* **23**, 16-25 (1990)
- [Lar98] K.P. Larsen, *Desalination of painted brick vaults*, PhD thesis, Technical University of Denmark, Denmark (1999)
- [Lau27] A.P. Laurie, J. Milne, The evaporation of water and salt solutions from surfaces of stone, brick and mortar, in *Proceedings of the Royal Society of Edinburgh* **47**, 86-92 (1927)

- [Lew82] S.Z. Lewin, The mechanism of masonry decay through crystallization, in *Conservation of historic stone buildings and monuments*, National Academy of Sciences, Washington, D.C., USA, 120-144 (1982)
- [Lie60] J.A. van Lierde, P.L. Bruin, J.Th.G. Overbeck, The solubility of quartz, *The journal of physical chemistry* **64**, 1675-1682 (1960)
- [Lub01] B. Lubelli, R.P.J. van Hees, L. Pel, The role of the pointing mortar in the damage due to salt crystallisation, in *Structural Studies, Repairs and Maintenance of Historical Buildings VII*, 537-547 (2001)
- [Lub03] B. Lubelli, T.J. Wijffels, *Experimental research on the carbonation of hydrated and hydraulic lime mortar*, TNO report 2003-BS-R0050, (2003)
- [Lub04a] B. Lubelli, R.P.J. van Hees, H.J.P. Brocken, Experimental research on hygroscopic behaviour of porous specimens contaminated with salts, *Construction and Building Materials* **18**, (5), 339-348 (2004)
- [Lub04b] B. Lubelli, R.P.J. van Hees, C.J.W.P. Groot, The role of sea-salts in the occurrence of different damage mechanisms and decay patterns of brick masonry, *Construction and Building Materials* **18**, (2), 119-124 (2004)
- [Lub05a] B. Lubelli, R.P.J. van Hees, J. Larbi, Influence of brick properties on salt crystallization damage, *Restoration of Building and Monuments* **11**, (2), 1-10 (2005)
- [Lub05b] B. Lubelli, R.P.J. van Hees, C.J.W.P. Groot, R. Investigation on the behaviour of a restoration plaster applied on heavy salt loaded masonry, *Construction and Building Materials*, in press
- [Lub05c] B. Lubelli, R.P.J. van Hees, C.J.W.P. Groot, Sodium chloride crystallization in a restoration plaster, *Proceedings of the 10th EMABM*, (2005)
- [Lub05d] B. Lubelli, R.P.J. van Hees, H.P. Huinink, C.J.W.P. Groot, Irreversible dilation of NaCl contaminated lime-cement mortar due to crystallization cycles, *Cement and Concrete Research*, in press
- [Men92] B. Meng, Moisture-transport-relevant characterization of pore structure, in *Proceedings of the 7th International Congress on Deterioration and Conservation of Stone*, 387-396 (1992)
- [Nov89] G.A. Novak, A.A. Colville, Efflorescent mineral assemblages associated with cracked and degraded residential concrete foundations in southern California, *Cement and Concrete Research* **19**, (1), 1-6 (1989)
- [Num01] S. Nunberg, A.E. Charola, Salts in Ceramic Bodies II: Deterioration due to minimal changes in Relative Humidity, *Internationalke Zeitschrift fur Bauinstandsetzen un Baudenkmalpflege* **2**, 131-145 (2001)

- [Obi89] B. Obika, R.J. Freer-Hewish, P.G. Fookes, Soluble salt damage to thin bituminous road and runway surfaces, *Quarterly Journal of Engineering Geology* **22**, 59-73 (1989)
- [Pel02] L. Pel, H. Huinink, K. Kopinga, Ion transport and crystallization in inorganic building materials as studied by NMR, *Applied Physics Letters* **81**, (15), (2002)
- [Pel03] L. Pel, H. Huinink, K. Kopinga, Salt transport and crystallization in porous building materials, *Magnetic Resonance Imaging* **21**, 317-320 (2003)
- [Pel04] L. Pel, H. Huinink, K. Kopinga, R.P.J. van Hees, F. Zezza, Ion transport and crystallization in fired-clay brick: a NMR study, in *Proceedings of 13th International Brick and Block Masonry Conference*, 735-739 (2004)
- [Pet04] J. Petkovic, L. Pel, H. Huinink, K. Kopinga, R.P.J. van Hees, Salt transport in plaster/substrate layers: a nuclear magnetic resonance study, in *Proceedings of the 13th International Brick and Block Masonry Conference*, 727-734 (2004)
- [Pet05] J. Petkovic, *Moisture and ion transport in layered porous building materials: a Nuclear Magnetic Resonance study*, PhD thesis, Eindhoven University of Technology, The Netherlands (2005)
- [Pol00] R.B. Polder, A. Hug, Penetration of chloride from de-icing salt into concrete from a 30 years old bridge, *Heron* **45**, (2), 109-124 (2000)
- [Pre67] M. M. Prebble, Cavernous weathering in the Taylor Dry Valley, Victoria Land, Antarctica, *Nature* **216** 1194-1195(1967)
- [Puh83] J. Puhlinger, *Salt disintegration*, Swedish Council for Building Research, Stockholm, Sweden (1983)
- [Puh96] J. Puhlinger, Deterioration of materials by hydraulic pressure in salt water systems - an outline model, in *Proceedings of the 8th International Congress on Deterioration and Conservation of Stone*, 545-556 (1996)
- [Sun81] I. Sunagawa, Characteristics of crystal growth in nature as seen from the morphology of mineral crystals, *Bulletin de Mineralogie* **104**, 81-87 (1981)
- [Rie94] E. Riecke, Ueber das Gleichgewicht zwischen einem festen, homogen deformirten Korper und einer flussigen Phase, insbesondere uber die depression des Schmelzpunktes durch eiseitige Spannung, *Nachrichten von der (koniglichen) gesellschaft der wissens*, 278-284 (1894)
- [Riv97] T. Rivas, B. Prieto, B. Silva, The effect of crystallization of Na₂SO₄ and NaCl on the weathering of various granites, in *Proceedings of the 4th International Symposium on the Conservation of Monuments in the Mediterranean*, 271-180 (1997)
- [Rij04] L. Rijniens, *Salt crystallization in porous materials: an NMR study*, PhD thesis, Eindhoven University of Technology, The Netherlands (2004)

- [Rob59] R.A. Robinson, R.H. Stokes, *Electrolyte solutions - The measurement and interpretation of conductance, chemical potential and diffusion in solutions of simple electrolytes*, Butterworth, London, UK (1959)
- [Rod99a] C. Rodriguez-Navarro, E. Doehne, Salt weathering: influence of evaporation rate, supersaturation and crystallization pattern, *Earth Surface Processes and Landforms* **24**, (3), 191-209 (1999)
- [Rod99b] C. Rodriguez Navarro, E. Doehne, E. Sebastian, Origin of honeycomb weathering: the role of salts and wind, *Bulletin of the Geological Society of America* **111**, (8), 1250-1255
- [Rod00] C. Rodriguez Navarro, E. Doehne, E. Sebastian, How does sodium sulfate crystallize? Implications for the decay and testing of building materials, *Cement and Concrete Research* **30**, 1527-1534 (2000)
- [Rod02] C. Rodriguez-Navarro, L. Linares-Fernandez, E. Doehne, E. Sebastian, Effects of ferrocyanide ions on NaCl crystallization in porous stone, *Journal of Crystal Growth* **243** (2-4), 503-516 (2002)
- [Roo05] M. de Rooij, C.J.W.P. Groot, A closer look at salt loaded microstructures, in *Compatibility of plasters and renders with salt loaded substrates in historic buildings*, Final report EU Contract no. EVK4-CT-2001-0047-DGXII, (Ed. R.P.J. van Hees), 129-137 (2005)
- [Ros91] R. Rossi Menaresi, A. Tucci, Pore structure and disruptive or cementing effect in salt crystallization in various types of stone, *Studies in Conservation* **36**, (1), 53-58 (1991)
- [Sar93] L.S. Sarkar, J. Beaulieu, Microstructural evaluation of a concrete overpass system during rehabilitation, *Cement and Concrete Research* **23**, (4), 874-884 (1993)
- [Sch99] G. Scherer, Crystallization in pores, *Cement and Concrete Research* **29**, (8), 1347-1358 (1999)
- [Sch00] G. Scherer, Reply to discussion by S. Chatterij of the paper "Crystallization in pores", *Cement and Concrete Research* **30**, (4), 673-675 (2000)
- [Sch04] G. Scherer, Stresses from crystallization of salt, *Cement and Concrete Research*, **34**, (9), 1613-1624 (2004)
- [Sne97] R. Snethlage, E. Wendler, Moisture cycles and sandstone degradation, in *Saving our architectural heritage: the conservation of historic stone structures*, (Eds. N.S. Baer and R. Snethlage), J. Wiley & Son, Chichester, UK, 7-24 (1997)
- [Ste96] M. Steiger, A. Zeunert, Crystallization properties of salt mixtures: comparison of experimental results and model calculations, in *Proceedings of the 8th Int. Congr. On Deterioration and Conservation of Stone*, 535-544 (1996)
- [Tah98] A. Taheri, *Durability of Reinforced Concrete Structures in Aggressive Marine Environment*, PhD thesis, Delft University of Technology, The Netherlands (1998)

- [Tam80] E. Tammes, B.H. Vos, *Warmte- en vochttransport in bouwconstructies*, Kluwer Technische Boeken B.V. - Deventer-Antwerpen, Belgium (1980)
- [The97] P. Theoulakis, A. Moropoulo, Microstructural and mechanical parameters determining the susceptibility of porous building stones to salt decay, *Construction and Building Materials* **11**, (1), 65-71 (1997)
- [Tho62] J. Thomson, On crystallization and liquefaction, as influenced by stresses tending to change of forms in crystals, *Philosophical Magazine* **24**, (162), 395-401 (1862)
- [Tsu03] N. Tsui, R.J. Flatt, G.W. Scherer, Crystallization damage by sodium sulfate, *Journal of Cultural Heritage* **4**, (2), 109-115 (2003)
- [Ver05] V. Vergès-Belmin, T.J. Wijffels, T. Gonçalves, M. Nasraoui, The Compass salt crystallisation test (compass-test) as a way to figure out how salts migrate and accumulate in renovation plasters, in *Compatibility of plasters and renders with salt loaded substrates in historic buildings*, Final report EU Contract no. EVK4-CT-2001-0047-DGXII, (Ed. R.P.J. van Hees), 157-168 (2005)
- [War00] P.A. Warke, B.J. Smith, Salt distribution in clay-rich weathered sandstone, *Earth Surface Processes and Landforms* **25**, (12), 1333-1342
- [Wat00] D.S. Watt, B.J. Colston, Investigating the effect of humidity and salt crystallization on medieval masonry, *Building and Environment* **35**, (8) 737-749 (2000)
- [Wel65] H. W. Wellman, A. T. Wilson, Salt weathering, a neglected geological erosive agent in coastal and arid environments, *Nature* **205**, (4976), 1097-1098 (1965)
- [Wel68] H.W. Wellman, A.T. Wilson, Salt weathering or fretting, in *Encyclopedia of geomorphology*, Dowden, Hutchinson & Ross, Stroudsburg, Pennsylvania, Vol. 3, 968-970 (1968)
- [Wen92] E. Wendler, R. Ruckert-Thumling, Gefügezerstörendes Verformungsverhalten bei salzbefrachteten sandstein unter hygrischer Wechselbelastung, in *Proceedings of the third International Colloquium on Materials Science and Restoration*, Vol. 3, 1818-1830 (1992)
- [Wen02] E. Wendler, Laboratory measurement on salt-loaded brick samples in periodically changing climate conditions, in *The study of Salt Deterioration Mechanisms*, (Ed. T. von Konow), Helsinki, Finland, 81-87 (2002)
- [Wey59] P.K. Weyl, Pressure solution and the force of crystallization: A phenomenological theory, *Journal of Geophysical Research* **64**, (11), 2001-2025 (1959)
- [Wij97] T.J. Wijffels, C.J.W.P. Groot, R.P.J. van Hees, Performance of restoration plasters, in *Proceedings 11th International Brick/Block Masonry Conference*, Vol. 2, 1050-1062 (1997)
- [Wij00] T.J. Wijffels, R.P.J. van Hees, The influence of the loss of water of the fresh mortar to the substrate on the hygric characteristics of so-called restoration plaster, in *Proceedings International Workshop on Urban Heritage and Building Maintenance VII*, 49-54 (2000)

- [Wij02] T.J. Wijffels, R.P.J. van Hees, *Salt transportation in restoration plaster*, TNO report 2001-BS-R0400 (2002)
- [Wij05] T.J. Wijffels, B. Lubelli, Development of a new accelerated crystallization test, in *Compatibility of plasters and renders with salt loaded substrates in historic buildings*, Final report EU Contract no. EVK4-CT-2001-0047-DGXII, (Ed. R.P.J.van Hees), 142-156 (2005)
- [Wil81] R.B.G. Williams, D.A. Robinson, Weathering of sandstone by the combined action of frost and salt, *Earth Surfaces Process and Landforms*.**6**, (1), 1-9 (1981)
- [Win72] E.M. Winkler, P.C. Singer, Crystallization pressure of salts in stone and concrete, *Geological Society of America Bulletin* **83**, (11), 3509-3514 (1972)
- [Win94] E.M. Winckler, *Stone in architecture*, Springer-Verlang, Berlin, Germany (1994)
- [Zeh93] K. Zehnder, New aspects of decay caused by crystallisation of gypsum, in *Proceedings of the Int. RILEM/UNESCO Congress: Conservation of stone and other materials: research-industry-media*, Vol. 1, 107-114 (1993)

Standards

- ASTM C88-99a, Standard Test method for Soundness of Aggregate by Use of Sodium Sulfate or Magnesium Sulfate (1999)
- EN 1015-11, Methods of test for mortar for masonry- Part 11: Determination of flexural and compressive strength of hardened mortar (1999)
- EN 1015-18, Methods of test for mortar for masonry, Determination of water absorption coefficient due to capillary action of hardened rendering mortar, Draft version (1996)
- EN 12370, Natural stone test method- Determination of resistance to salt crystallization, (1999)
- NEN 2489, Metselbaksteen (1976)
- RILEM Recommendation CPC 11.3, Absorption of water by immersion under vacuum, *Material and Structures* **12**, 391-394 (1979)
- RILEM Recommendation MS-A1, Determination of the resistance of wallettes against sulphates and chlorides, *Materials and Structure* **31**, 2-19 (1998)
- RILEM Recommendation MS-A2, Unidirectional salt crystallization test for masonry units, *Materials and Structure* **31**, 10-11 (1998)
- UNI 7044-72, Determinazione della consistenza delle malte cementizie mediante l'impiego di tavola a scosse (1972)
- WTA Merkblatt 2-2-91, Sanieputzsysteme, *Bautenschutz+Bausanierung* **15**, 59-63 (1992)

Appendix 1

Properties of NaCl solution

Table A1.1 Water activities and osmotic coefficients for NaCl solution at different molality at 25°C [Rob59]

m	Water Activity a_w	Osmotic Coeff. ϕ	m	Water Activity a_w	Osmotic Coeff. ϕ
0.1	0.996646	0.9324	2.8	0.9011	1.0321
0.2	0.993360	0.9245	3.0	0.8932	1.0453
0.3	0.99009	0.9215	3.2	0.8851	1.0587
0.4	0.98682	0.9203	3.4	0.8769	1.0725
0.5	0.98355	0.9209	3.6	0.8686	1.0867
0.6	0.98025	0.9230	3.8	0.8600	1.1013
0.7	0.97692	0.9257	4.0	0.8515	1.1158
0.8	0.97359	0.9288	4.2	0.8428	1.1306
0.9	0.97023	0.9320	4.4	0.8339	1.1456
1	0.96686	0.9355	4.6	0.8250	1.1608
1.2	0.9601	0.9428	4.8	0.8160	1.1761
1.4	0.9532	0.9513	5.0	0.8068	1.1916
1.6	0.9461	0.9616	5.2	0.7976	1.2072
1.8	0.9389	0.9723	5.4	0.7883	1.2229
2.0	0.9316	0.9833	5.6	0.7788	1.2389
2.2	0.9242	0.9948	5.8	0.7693	1.2548
2.4	0.9166	1.0068	6.0	0.7598	1.2706
2.6	0.9089	1.0192			

Table A1.2 Effect of pressure on NaCl solubility [Kau71]

Pressure (atm)	Grams NaCl per 100 g solution	Grams NaCl per 100 g water
0	26.42	35.91
250	26.59	36.22
500	26.74	36.50
750	26.88	36.76
1000	27.01	36.99
1250	27.11	37.18
1500	27.20	37.37

Table A1.3 Increase of surface tension in air at 20 °C of NaCl solutions at different concentrations

moles NaCl per 100g water	$\Delta\gamma$ (air) (dynes/cm)
0.025	0.055
0.05	0.09
0.1	0.17
0.25	0.42
0.5	0.82
1.0	1.64
2.0	3.28
3.0	4.90
4.0	6.54
5.0	8.17
6.0	9.80

Table A1.4 Density of NaCl solutions at different concentrations at 20 °C [Kau71]


Per Cent NaCl by weight in solution	Density Kg/m ³
1	1.00534
2	1.01246
4	1.02680
6	1.04127
8	1.05589
10	1.07068
12	1.08566
14	1.10085
16	1.11621
18	1.13190
20	1.14779
22	1.16395
24	1.18040
26	1.19717


Table A1.5 Viscosity (in centipoises) of NaCl solutions at different concentrations at 20 °C [Kau71]


Per cent NaCl by weight in solution	Viscosity (centipoises)
0.9	1.006
1.9	1.013
2.9	1.023
3.9	1.035
4.9	1.049
5.9	1.062
7.0	1.078
8.0	1.098
9.1	1.117
10.2	1.137
11.3	1.162
12.3	1.191
13.4	1.225
14.5	1.260
15.6	1.301
16.7	1.342
17.9	1.387
19.0	1.437
20.1	1.491
21.2	1.550
22.3	1.622
22.4	1.624
23.5	1.699
24.7	1.787
25.9	1.895
26.3	1.933


Appendix 2


List of case studies


Building and location	Type of damage and material concerned	Test performed	Diagnosis
Mill (Alkmaar) 	Push out of the re-pointing (exterior) Biological growth: algae and mosses (exterior) Spalling of the brick (interior) Crumbling and layering (parallel to the joint) of the mortar (interior) Efflorescences and cryptoflorescences on mortar and brick (interior)	MC profiles on 3 locations (N, W, and E) HMC profiles on 3 locations (N, W, and E) Chemical analyses PFM on thin section of a brick/mortar core XRD on efflorescences sampled on the mortar (interior) Karsten tube on the treated surface Measurements of total porosity of brick	The damage is due to the presence of moisture and salts. In the interior of the mill the main source of moisture is rain penetration. The main sources of salt are sea-salt spray and the brick itself since it contains sulfates. The application of a water repellent on the exterior, limiting the drying out of the masonry, has worsened the situation.


Building and location	Type of damage and material concerned	Test performed	Diagnosis
Church (Brouwersahven) 	Push out of the re-pointing (exterior) Scaling of the brick (exterior) Sanding of the stone (interior and exterior) Crypto-florescences and efflorescences (interior and exterior) Peeling of the paint layer of the plaster (interior) Sanding and crumbling of the plaster (interior)	MC profiles (several locations, 3 sampling campaigns) HMC profiles (several locations, 3 sampling campaigns) RH and T (air and wall surface) monitoring Photographical monitoring of the damage Debris collection Ion chromatography on powder samples XRD on efflorescences MIP of the brick substrate and of the plaster Physical and petrographical characterization of the plaster ESEM observations on plaster scales	The damage is due to salt (mainly NaCl) and moisture. In the interior of the church the main sources of moisture are the rising damp and the RH of the air. The main source of salt is the sea-flooding occurred in 1953. The damage in the upper part of the interior walls is due to RH cycles.


Building and location	Type of damage and material concerned	Test performed	Diagnosis
Church (Domburg) 	Push out of the re-pointing (exterior) Brick blistering (exterior) Powdering of the brick (exterior)	MC profiles HMC profiles Ion chromatography on the powder samples Measurements of total porosity of brick (immersion method) MIP of the brick XRD on brick samples and on scales	The damage is due to salt (mainly NaCl) and moisture. In the exterior of the church the main sources of moisture are rising damp and rain. The main sources of salts are the ground (because of the flooding in 1953) and the sea-salt spray.


Building and location	Type of damage and material concerned	Test performed	Diagnosis
Church (Dreischor) 	Powdering of the brick (exterior) Efflorescences and cryptoflorescences (interior) Loss of bond of the plaster layer (interior) Peeling of the paint layer of the plaster (interior)	MC profiles HMC profiles Chemical analyses on powder samples XRD analyses on efflorescences	The damage is due to salt (mainly NaCl) and moisture. In the interior of the church the main moisture source is rising damp. The application of a new plaster inhibiting evaporation in the lower part of the interior walls has increased the height reached by the rising damp and has caused the appearance of the damage in the old plaster.

Building and location	Type of damage and material concerned	Test performed	Diagnosis
Church (Hensbroek) 	Efflorescences on the brick (exterior) Push out of the pointing (exterior) Efflorescences and cryptoflorescences on the plaster (interior) Peeling of the paint layer (interior) Sanding and crumbling of the plaster (interior)	MC profiles HMC profiles Salt crystallization test on two brick/plaster cores	The damage is caused by the presence of moisture and salts. Moisture is due both to rainwater penetration (on the south side) and to presence of hygroscopic salts (on the north side).

Building and location	Type of damage and material concerned	Test performed	Diagnosis
Church (Oostkapelle) 	<p>Powdering of the brick (exterior)</p> <p>Erosion of the re-pointing mortar (exterior)</p> <p>Complete erosion of the mortar joints (exterior)</p> <p>Biological growth (exterior)</p> <p>Peeling of the paint (interior)</p> <p>Moisture stains (interior)</p>	<p>MC profiles</p> <p>HMC profiles</p> <p>MIP on bricks</p> <p>Measurements of total porosity of bricks (immersion method)</p> <p>PFM on thin sections of bricks</p>	<p>The damage is due to presence of moisture and sea-salts. In the exterior of the church the main moisture source is rain and the salt source is sea-salt spray. The quality of the bricks (mainly their pore size distribution) influences the severity of the damage.</p>

Building and location	Type of damage and material concerned	Test performed	Diagnosis
Church (de Rijp) 	<p>Efflorescences on brick (exterior)</p> <p>Efflorescences and cryptoflorescences on plaster (interior)</p> <p>Peeling of the paint layer (interior)</p> <p>Sanding and crumbling of the plaster (interior)</p> <p>Loss of bond between the different layers of the plaster and between the plaster and the masonry (interior)</p>	<p>MC of damaged and undamaged areas</p> <p>HMC of damaged and undamaged areas</p>	<p>Damage is related to presence of moisture and salt. The main moisture source is rain penetration. The damage interest mainly the south wall, exposed to rain and wind. The north wall shows low moisture content and only little damage, in spite of the presence of a considerable amount of salts.</p>

Type of building and location	Type of damage and material concerned	Test performed	Diagnosis
Church (Velsen) 	Algae (exterior) Powdering of the brick (exterior) Cracks in the bricks and pointing (exterior) Voids in the pointing (exterior) Moist spots (exterior) Peeling of the paint layer (interior) Sanding, scaling and crumbling of the plaster (interior)	MC profiles HMC profiles HMC on brick/mortar/plaster cores	Damage is related to presence of moisture and salt. The main sources of moisture in the interior of the church are rising damp and rain penetration.

Building and location	Type of damage and material concerned	Test performed	Diagnosis
Church (Zoutelande) 	Sanding of the re-pointing (exterior) Efflorescences (interior and exterior) Powdering of the brick (interior and exterior) Peeling of the paint (interior) Sanding of the bedding mortar (interior)	MC profiles HMC profiles Cl and SO ₄ analyses Ion chromatography	Damage is related to presence of moisture and salt (chlorides and sulfates). In the tower rising damp is the main moisture source.

Appendix 3

Method for the assessment of moisture and salt distribution

In the investigation of the case studies reported in this thesis a standard method for the determination of the moisture and salt distribution in a wall, has been followed. The procedure, including sampling and a measuring technique, has been developed in the framework of the European Project COMPASS⁶, also on the basis of previous experiences. This procedure has been tested on several case studies and it proved to lead to a fair assessment of moisture and (hygroscopic) salt distribution and to help identifying the source(s) of the moisture.

Aims and limits of the method

Main aim of the method is to determine the quantity and distribution of moisture in a wall and to obtain information on the presence and distribution of hygroscopic salts.

The actual moisture content gives quantitative information on the moisture load and distribution.

The hygroscopic moisture content (HMC) gives only qualitative information on the salt quantity and type(s).

The method is a little destructive and therefore repair of the damage is necessary.

Principle

The method for the determination of the Moisture Content (MC) is based on the difference between the mass of the sample before and after drying (gravimetric method)

The method for the determination of the Hygroscopic Moisture Content (HMC) is based on the fact that hygroscopic salt (mixture) adsorbs moisture from the air, when the RH of the air is higher than the RH of equilibrium of the salt (mixture). The difference between mass of the sample dry and after conditioning at a certain RH gives indications on the amount and on the

⁶ EU Contract no.EVK4-CT-2001-0047-DGXII (www.compass-salt.org)

type of salt present. In this procedure 20 °C 96% RH conditions are used, in order to include most of the hygroscopic salts present in the walls [Arn99].

When it is not necessary to exactly determine the quantity of salt present in the material, the hygroscopic moisture uptake of the material represents an easy to perform method, giving a good indication of the quantity and the distribution of salts. Besides, when chemical analyses are wanted, the hygroscopic moisture content forms the basis for selecting the most interesting or representative samples to be used.

Symbols

m_b = mass of the empty bottles, in g

m_i = initial mass of the sample (bottle + powder), in g

m_d = the oven dry mass of the sample (bottle + powder), in g

$m_{96\%}$ = the mass of the sample (bottle + powder) after conditioning at 20 °C 96% RH, in g

Apparatus

Hammer drill

Glass (or any other material resistant to 105 °C) bottles with lid

Scale, accurate to 0.01g.

Climatic room or box in which the temperature and the RH can be controlled and maintained at 20 °C/96% RH

Well ventilated oven, thermostatically controlled to maintain a temperature of 40±5 °C, 80±5 °C and 105±5 °C

Procedure

In situ

The sampling consists in the extraction of material from the wall by means of dry powder drilling. A hammer drill at a low number of revolutions is used.

The powder drilling needs to be performed at different locations; if possible, at least two locations per wall. The sampling should be done at different heights along the same vertical profile, for example at 10, 50, 100, 150, 200, 300 cm from the ground level. The heights of the sampling may differ depending on the situation, but at least three heights should be selected to carry out the measurements.

The depth of the drilling at each height depends on the aims of the sampling and on the type of masonry. If only a definition of the distribution and source of moisture is needed, two depths, depending on the wall thickness, (for example from the surface to 5 cm depth and from 10 cm to the middle of the wall) are sufficient. If also the salt type and distribution need to be investigated, the following depths from the surface are suggested: 0-1 cm, 1-2 cm, 2-5 cm, 5-10 cm, 10-20 cm.

If a plaster is present, this should be sampled separately from the substrate.

The powder samples collected have to be stored in glass (or other material resistant to temperature of 105 °C) bottles, which are hermetically closed immediately after sampling. The bottle should be numbered and the weight of the empty bottles (m_b) should be known.

It is recommended to report, together with height and depth of the sampling, also information on the type (and color) of material sampled and on the presence of damage in order to correctly interpret the results.

In laboratory

The bottles containing the powder samples are opened and the mass of the sample (bottle + powder) is recorded (m_i). The samples are then dried in an oven until constant weight at 40 ± 5 °C (in case of gypsum based materials), 60 ± 5 °C or 105 ± 5 °C, depending on the type of material. The mass of the dry samples (bottle + powder) is recorded (m_d).

The actual moisture content (MC) is derived from the difference between the mass of the sample before and after drying, and is expressed in % m/m.

$$\text{MC \% [m/m]} = 100 * (m_i - m_d) / (m_d - m_b)$$

After determination of the MC, the samples are stored at 20 °C / 96% RH, until equilibrium is reached. The mass of the sample (bottle + powder) at equilibrium is recorded ($m_{96\%}$).

Because reaching the equilibrium may take a long time, the use of small samples is suggested (for example 1 g). A good indication of the HMC can be generally obtained after a minimum period of 4 weeks.

The Hygroscopic Moisture Content (HMC) is calculated by the following formula and is expressed in % m/m:

$$\text{HMC \% [m/m]} = 100 * (m_{96\%} - m_d) / (m_d - m_b)$$

Report

The report should include the following information:

- place, date and time of the sampling
- identification of the samples (material type, height and depth of sampling)
- detail on the samples (presence of damage, other useful information)
- results of the MC and HMC measurements
- remarks

Remarks

The MC and HMC should provide indication of moisture and salt distribution in the walls. To correctly apply this procedure and to obtain reliable results, some precautions are needed:

- the sampling should concern the representative materials in a wall. If, as usual, two or more materials compose the wall the sampling should take this into account;
- the influence of a very dry or very wet period should be taken into account when planning the measurements.

Regarding the interpretation of the results:

- the presence of a source of moisture not anymore active, may explain the salt accumulation at a certain location in the wall;
- when substitutions of materials have taken place, the moisture transport properties of the new materials with respect to the old ones may explain the moisture and salt distribution.

Summary

Sodium chloride damage to porous building materials

Salt crystallization in porous materials constitutes one of the most frequent causes of decay of buildings, in a wide range of environments. Among salts commonly found in walls, sodium chloride (NaCl) is one of the most abundant and ubiquitous. In spite of the several theories developed to explain salt crystallization damage, no unanimous opinion exists yet on the mechanism causing the decay. This matter is particularly controversial in the case of sodium chloride, since the most accepted models on crystallization pressure can hardly explain the damage occurring in porous building materials having no pores of nanometer size. Moreover, the severe damage caused by NaCl observed in-situ is not easily reproduced in laboratory: in fact NaCl is usually one of the less harmful salts in accelerated crystallization tests.

The present work is concerned with the study of the decay due to NaCl in porous building materials. The reported research aimed at gaining a better understanding of the damage process and at developing an effective laboratory crystallization test. In order to reach these objectives an approach combining investigation of the damage in practice and experimental research in laboratory was adopted.

The survey of several case studies affected by damage due to NaCl showed that the interaction between material properties (e.g. pore size, mechanical strength, moisture transport behaviour) and boundary conditions (moisture supply, salt load and distribution, environmental conditions) determines the risk of salt damage and the type of decay pattern.

On the basis of the obtained results, criteria for the evaluation of the risk of salt damage have been formulated. From these criteria, guidelines for suitable restoration interventions have been derived.

The importance of the environmental conditions and, in particular, of RH cycles for the development of damage has been demonstrated in-situ. The combined monitoring of the damage (quantified as debris falling from the wall) and of the air and surface RH and temperature showed that most of the debris falls in the high RH period, when the salt dissolves and the debris particles, cemented together by the salt, can fall apart. This damage process was further shown in experiments performed in the ESEM chamber, reproducing the RH cycles observed in practice.

The survey of the case studies provided the input to the development of an effective crystallization test by identifying the most aggressive boundary conditions and their realistic range of variation. Series of crystallization experiments, each considering the effect of a single variable (air temperature, air RH, air flow, moisture supply, RH changes), were performed in order to define the most effective boundary conditions. On the basis of the obtained results a weathering test consisting of wetting by capillary rise and drying comprising temperature and RH cycles has been defined. The developed procedure was applied on three types of materials; it was able to cause damage, even in a salt resistant plaster, in a period of about 3 months.

Another part of the laboratory investigation was devoted to the study of the damage mechanism occurring in NaCl contaminated materials. The hypothesis that damage may develop from the differential dilation of salt contaminated and not salt-contaminated areas of a material was investigated. Systematic experiments were performed studying the hygric behaviour and the related dilation of a lime-cement mortar in the presence of NaCl.

The obtained results definitely prove that the presence of NaCl modifies the hygric behaviour and the related dilation of a material completely. In a not contaminated specimen dilation and shrinkage can be observed respectively when the RH increases and decreases. In NaCl contaminated specimens the opposite is observed: dilation occurs during the drying phase of the RH cycle, when the salt crystallizes, whereas shrinkage occurs during dissolution of the salt. The dilation is irreversible and it increases when repeating the RH cycles, until damage is observed. These results prove that damage in a salt contaminated material may originate from shear stresses developed between areas containing different amounts of salt. This theory may explain those decay patterns in which there is no evidence of crypto-florescences under detached scales or layers of the material.

Experiments performed on KCl and NaNO₃ contaminated specimens have shown that the described dilation behaviour is not limited to NaCl but common to more salts. If a crystallization inhibitor was added to the NaCl solution, no dilation was observed during NaCl crystallization. This absence of dilation corresponded to a different crystallization pattern of the salt: NaCl, which is observed to crystallize as a layer on the pore walls of the mortar, forms, in the presence of the crystallization inhibitor, agglomerations of crystals not adhering to the substrate.

Combining the ESEM investigations with the dilation occurring during crystallization forms the basis for a model on a damage mechanism based on a mechanical interaction between salt and pore wall. Changes in the crystal structure due to variation in RH might result in stresses to the pore wall. Salts crystallizing in the form of a layer on the pore walls are able to strongly affect the hygric dilation of the material, producing relevant expansion during drying of the specimen and crystallization of the salt. The observed salt layers appear able to transfer stresses to the pore walls and thereby to cause dilation and, at long last, damage. A similar effect would according to this model not be possible when the same salt (NaCl) crystallizes without adhering to the material. This is shown in the case in which the crystallization inhibitor is added.

Barbara Lubelli

Samenvatting

Natriumchlorideschade aan poreuze bouwmaterialen

Zoutkristallisatie in poreuze materialen vormt één van de belangrijkste oorzaken van degradatie van gebouwen in een groot aantal verschillende klimaten. Van de zouten die in muren worden aangetroffen is natriumchloride (NaCl) één van de meest voorkomende.

Hoewel diverse theorieën zijn opgesteld om schade door zoutkristallisatie te verklaren, bestaat er nog geen eensgezindheid ten aanzien van het mechanisme dat de degradatie veroorzaakt. De controverse doet zich met name voor in het geval van natriumchloride, aangezien de meest geaccepteerde modellen van de beschrijving van de kristallisatiedruk eigenlijk niet in staat zijn de schade te verklaren die optreedt in poreuze bouwmaterialen die geen poriën op nanometerschaal hebben. Bovendien kan de aanzienlijke schade die in de praktijk door NaCl wordt veroorzaakt niet eenvoudig worden gereproduceerd onder laboratoriumcondities: NaCl is doorgaans één van de minder schadelijke zouten in versnelde kristallisatietests.

In het voorliggende werk wordt de degradatie bestudeerd die NaCl in poreuze bouwmaterialen veroorzaakt. Het onderzoek heeft zich gericht op het vergroten van het begrip van het schadeproces en op het ontwikkelen van een effectieve versnelde kristallisatietest. Om deze doelstellingen te bereiken is gekozen voor een benadering waarbij onderzoek naar schade in de praktijk werd gecombineerd met experimenteel onderzoek in het laboratorium.

Een inventarisatie van diverse case-study's waarbij sprake was van schade door NaCl maakte duidelijk dat de interactie tussen materiaaleigenschappen (afmetingen van de poriën, sterkte-eigenschappen, gedrag met betrekking tot vochttransport) en randcondities (vochtbron, zoutbelasting en -verdeling, omgevingsgebonden omstandigheden) de kans op zoutschade alsmede het soort degradatie bepaalt.

Op basis van de verkregen resultaten zijn criteria geformuleerd voor de bepaling van het risico op zoutschade. Uit deze criteria zijn richtlijnen herleid voor geschikte restauratietechnieken.

Het belang van de omgevingsgebonden omstandigheden en, meer in het bijzonder, cycli van diverse luchtvochtigheden, is in situ aangetoond. Gecombineerde waarnemingen van de schade (gekwantificeerd door van de muur losgeraakt materiaal) en de lucht- en oppervlaktetemperatuur en -vochtigheid maakten duidelijk dat het meeste materiaal losraakt in

een periode van hoge luchtvochtigheid, wanneer het aanwezige zout oplost en de brokstukjes, aanvankelijk bijeengehouden door het zout, uiteen vallen. Dit schadeproces is tevens aangetoond in experimenten die zijn uitgevoerd in de ESEM-kamer, waarbij de in de praktijk waargenomen cycli van luchtvochtigheden werden nagebootst.

De inventarisatie van de case-study's legde de basis voor de ontwikkeling van een effectieve kristallisatietest, doordat werd vastgesteld welke randcondities het agressiefst waren en in welke mate zij in de praktijk varieerden. Om de effectiefste randcondities te kunnen vinden, zijn kristallisatietests uitgevoerd waarbij steeds de invloed van één variabele (luchttemperatuur, relatieve luchtvochtigheid, luchtsnelheid, vochtbron, variaties in de relatieve luchtvochtigheid) werd beschouwd. Op basis van de verkregen resultaten is een versnelde kristallisatieproef ontwikkeld, bestaande uit bevochtiging door capillaire zuiging en droging tijdens cycli van temperatuur en relatieve luchtvochtigheid. De ontwikkelde procedure is toegepast op drie soorten materiaal. Ze bleek in staat om in een tijdsbestek van ongeveer 3 maanden schade te veroorzaken, zelfs in een speciale pleister, die als beter zoutbestendig op de markt wordt gebracht..

Een ander gedeelte van het laboratoriumonderzoek was gewijd aan de studie van het schademechanisme dat optrad in door NaCl aangetaste materialen. De hypothese dat schade kan ontstaan door het verschil in uitzetting tussen al dan niet door zout belaste gedeelten van een materiaal is getoetst. Er zijn systematisch experimenten uitgevoerd waarbij het hygrisch gedrag en de daaraan gerelateerde uitzetting van een kalkcementpleister in de aanwezigheid van NaCl zijn bestudeerd.

De verkregen resultaten tonen onmiskenbaar aan dat de aanwezigheid van NaCl het hygrisch gedrag en de daaraan gerelateerde uitzetting van het materiaal volledig verandert. In een onbelast proefstuk wordt uitzetting en krimp waargenomen wanneer de relatieve luchtvochtigheid respectievelijk toe- en afneemt. In door NaCl belaste proefstukken doet zich precies het omgekeerde voor: uitzetting treedt op tijdens uitdroging, wanneer het zout kristalliseert, terwijl krimp optreedt tijdens het oplossen van het zout. De uitzetting blijkt daarbij onomkeerbaar en neemt toe bij herhaalde cycli van relatieve luchtvochtigheden, totdat zich schade manifesteert.

Deze resultaten bewijzen dat schade aan een door zout belast materiaal kan voortkomen uit schuifspanningen die ontstaan tussen gebieden die verschillende hoeveelheden zout bevatten. Deze theorie kan de degradatiepatronen verklaren waarbij zich geen aanwijsbare cryptoflorescentie voordoet onder los geraakte schilfers of lagen van het materiaal.

Experimenten met proefstukken die waren belast door KCl en NaNO₃ hebben laten zien dat het beschreven vervormingsgedrag zich niet beperkt tot NaCl, maar dat het bij meerdere zouten voorkomt.

Als een kristallisatie-inhibitor wordt toegevoegd, wordt geen uitzetting waargenomen tijdens de kristallisatie van NaCl. Dit achterwege blijven van uitzetting correspondeert met een afwijkend kristallisatiepatroon van het zout: NaCl, dat als een laag blijkt te kristalliseren op de wanden van de poriën van de mortel, vormt in de aanwezigheid van de kristallisatie-inhibitor conglomeraten van kristallen die zich niet aan de ondergrond hechten.

De waarnemingen die zijn gedaan met behulp van ESEM vormen, in combinatie met de uitzetting die tijdens de kristallisatie optreedt, de aanzet tot een model van het schademechanisme, gebaseerd op een mechanische interactie tussen het zout en de poriënwand. Veranderingen in de kristalstructuur ten gevolge van variaties in de relatieve luchtvochtigheid kunnen resulteren in spanningen in de poriënwand. Zouten die als een laag op de poriënwand kristalliseren, kunnen de hygrische uitzetting van het materiaal sterk beïnvloeden, waardoor zich een aanzienlijke expansie voordoet tijdens het uitdrogen van het materiaal en de kristallisatie van het zout. Een vergelijkbaar effect kan volgens dit model niet optreden als hetzelfde zout (NaCl) kristalliseert zonder aan het materiaal te hechten, zoals in het geval waarbij de kristallisatie-inhibitor wordt toegevoegd.

Barbara Lubelli

Acknowledgements

I would like to thank those who have helped me to complete this research. First of all, I thank my supervisor Rob van Hees for his continuous support during these years. I am grateful to him for being available whenever I needed his assistance, for placing confidence in me, and for transmitting to me his knowledge and enthusiasm for the research.

I am grateful to Klaas van Breugel, whose experience in a different field has brought valuable inputs and points of view into my research.

Another person has helped me since the beginning of this project: Caspar Groot. I thank him for his useful suggestions, for his constant support and for encouraging me whenever I attempted to speak (*babbelen*) Dutch.

I thank all the members of the panel for carefully reviewing and commenting this thesis.

I am grateful to Mario de Rooij for introducing me into the secrets of those techniques that have been essential for my research and to Rinus van Maasakkers for helping me out with the ESEM.

As every PhD student knows, an experimental research requires numerous attempts to optimize the set-up of the tests. In all these trials Gerrit van der Ende has been very helpful: for that I thank him from the heart.

In these years I have had the pleasure to collaborate with several persons of Eindhoven University of Technology. In particular, I would like to thank Leo Pel for his challenging attitude and his straightforward opinions, and Henk Huinink for his considerable help in pointing out problems, asking myself (and him!) the right questions, and systematically proceeding towards the answers.

Using the TNO laboratories I got help from many persons, and I thank them all. I am especially grateful to Sacha Hermanns for carrying on my experiments during my absence, thus allowing me to attend various conferences and enjoy a whole week of summer holidays!

To work as a PhD student is a lonely job, so chatting (unless about the PhD research) can give some relief. For this I thank my colleagues at TNO.

I am particularly grateful to Timo Nijland, Joe Larbi and Loek van der Klugt who taught me a lot during these years, and to Tomas Wijffels, Harold Brocken and Michèle Sanders with whom I collaborated on several projects.

Sometimes it happens that work and friendship mix, making the first more pleasant and the second rich of common interests. I have experienced this with Silvia, whom I thank for the innumerable translations of German articles, for the lovely days spent in Zeeland monitoring

monuments, for the weekends of shopping and culinary experiments, and, above all, for her contagious optimism.

Two persons who played an important role in my choice to remain in the Netherlands are Jan and Lucia: they gave me a warm welcome and did not make me feel too homesick. I thank them for their constant and unconditional support, and for being the model of love, strength and courage they still are to me.

In these Dutch years some friendships have survived time and distance. I thank Mara for the support she gave me during the endless telephone calls, and Fabiana, who came to visit me several times during these years.

I thank Mark, who experienced more than others the mood changes that sometimes this work carries with it.

Ringrazio infine la mia famiglia tutta, in particolare Caty e Fra, e soprattutto mia madre che, nonostante per lei sia stato difficile, mi ha sempre sostenuta nelle mie scelte.

Curriculum vitae

Born in 1971 in Milan (Italy), Barbara Lubelli obtained her scientific high school degree in 1990. She graduated cum laude in Architecture at the Polytechnic of Milan in 1997 with a thesis on the effectiveness of surface treatments for the conservation of decayed materials. From 1997 till 1999 she worked at the Department of Structural Engineering of the Polytechnic of Milan, in the group co-ordinated by Prof. Binda, collaborating on several European projects in the field of conservation of historical buildings. Within the same group, she collaborated on the survey of the structural damage caused by earthquakes, studying the collapse mechanisms and the effectiveness of the strengthening techniques.

In 1998-1999 she co-tutored a course on “Architectural restoration” at the Faculty of Architecture of the Polytechnic of Milan and worked part-time at the architectural studio Architettura/Ambiente in Milan.

In October 1999 she won a postgraduate research grant from the University of Padova (Italy) to be spent in a research centre abroad. She chose to work at TNO Building and Construction Research in Delft (the Netherlands) where she remained, working as employee after the expiry date of her grant, till February 2001. In this period she collaborated on research projects related to decay of materials and structures due to moisture and salts.

In March 2001 she started her PhD on sodium chloride damage to porous building materials at the Delft University of Technology. Part of her PhD research was developed in the framework of the following EU projects, in which she participated always in close collaboration with TNO Building and Construction Research:

- EU Project EVK4-2000-00572, *ASSET Assessment of suitable products for the conservative treatment of salt decay*
- EU project EVK4-CT-2001-0047 - DG XII, *COMPASS Compatibility of plasters and renders with salt loaded substrates in historic buildings*

In December 2002 she spent a month at the Getty Conservation Institute (GCI) at L.A. (U.S.A.), studying the crystallization of NaCl in restoration plasters by the use of the Environmental Scanning Electron Microscopy.

At the moment she is working as researcher at the group [®] MIT, at the Faculty of Architecture of the Delft University of Technology, and collaborating with TNO. Her expertise is mainly related to the diagnosis and the advice in case of damage to materials and structures due to the presence of moisture and salts. She is taking part in the European Project SALT CONTROL on the use of crystallization inhibitors for limiting the damage due to salt crystallization.

